

Applied Sonochemistry: Uses of Power Ultrasound in Chemistry and Processing.

Timothy J. Mason, John Philip Lorimer

Copyright © 2002 Wiley-VCH Verlag GmbH & Co. KGaA

ISBNs: 3-527-30205-0 (Hardback); 3-527-60054-X (Electronic)

T. J. Mason and J. P. Lorimer

Applied Sonochemistry

Timothy J. Mason and John P. Lorimer

Applied Sonochemistry

The Uses of Power Ultrasound
in Chemistry and Processing

Professor Timothy J. Mason
Professor John P. Lorimer
Coventry University
Priory Street
Coventry CV1 5FB
U.K.

This book was carefully produced. Nevertheless, authors and publisher do not warrant the information contained therein to be free of errors. Readers are advised to keep in mind that statements, data, illustrations, procedural details or other items may inadvertently be inaccurate.

Library of Congress Card No.: Applied for.

British Library Cataloguing-in-Publication Data:

A catalogue record for this book is available from the British Library.

Die Deutsche Bibliothek – CIP Cataloguing-in-Publication Data:

A catalogue record for this publication is available from Die Deutsche Bibliothek.

© Wiley-VCH Verlag GmbH, Weinheim 2002

All rights reserved (including those of translation in other languages). No part of this book may be reproduced in any form – by photoprinting, microfilm, or any other means – nor transmitted or translated into machine language without written permission from the publishers.

In this publication, even without specific indication, use of registered names, trademarks, etc., and reference to patents or utility models does not imply that such names or any such information are exempt from the relevant protective laws and regulations and, therefore, free for general use, nor does mention of suppliers or of particular commercial products constitute endorsement or recommendation for use.

Printed on acid-free paper.

Printed in the Federal Republic of Germany.

Composition Mitterweger & Partner
Kommunikationsgesellschaft mbH, Plankstadt
Printing betz-druck GmbH, Darmstadt
Bookbinding Großbuchbinderei J. Schäffer
GmbH & Co. KG, Grünstadt

ISBN 3-527-30205-0

Contents

1	Introduction to Applied Ultrasonics	1
1.1	Background	1
1.2	Sound Frequency Ranges	3
1.3	Some Current Industrial Uses of Ultrasound	4
1.3.1	Ultrasonic Welding	5
1.3.2	Ultrasonic Cleaning and the Decontamination of Surfaces	7
1.3.3	Ultrasound in Biology and Medicine	9
1.3.4	Engineering Applications	12
1.3.5	Processing Applications	17
1.4	Ultrasound in Chemistry	20
1.4.1	Reactions Involving Metal or Solid Surfaces	21
1.4.2	Reactions Involving Powders or Other Particulate Matter	21
1.4.3	Emulsion Reactions	22
1.4.4	Homogeneous Reactions	22
2	General Principles	25
2.1	Introduction	25
2.2	Intensity and Pressure Amplitude	31
2.3	Sound Absorption	33
2.4	Bubble Formation and the Factors Affecting Cavitation Threshold	36
2.4.1	Effect of Gas and Particulate Matter	36
2.4.2	Effect of Viscosity	39
2.4.3	Effect of Applied Frequency	39
2.4.4	Effect of Temperature	42
2.5	Motion of the Bubble in the Applied Acoustic Field	45
2.5.1	Transient Cavitation	53
2.5.2	Stable Cavitation	55
2.6	Summary	56
2.6.1	Frequency	56
2.6.2	Solvent	57
2.6.3	Temperature	57
2.6.4	Gas Type and Content	58
2.6.5	External Applied Pressure	59

2.6.6	Intensity	59
	Appendix 1: Relationship Between Particle Velocity (v) and Acoustic Pressure (P_a)	61
	Appendix 2: Critical Pressure (P_K) and Bubble Radius Relationship	62
	Appendix 3: Time of Bubble Collapse	65
	Appendix 4: Motion of Cavity Wall	68
	Appendix 5: Maximum Bubble Temperature (T_{max}) and Pressure (P_{max})	69
	Appendix 6 Bubble Dynamics	72
	Operation of the Programme	72
3	Synthesis	75
3.1	Introduction	75
3.2	The Various Sites for Sonochemical Reactions	78
3.3	An Attempt to Define the Laws of Sonochemistry	81
3.4	Homogeneous Reactions	83
3.5	Heterogeneous Sonochemistry	93
3.5.1	Heterogeneous Reactions Involving a Metal as a Reagent	93
3.5.1.1	Preparation of Active Metals from Metals their Salts and Complexes	93
3.5.1.2	<i>In situ</i> Sonochemical Activation of Metals	97
3.5.2	Heterogeneous Reactions Involving Non-Metallic Reagents	110
3.5.2.1	Addition Reactions	110
3.5.2.2	C Alkylation Reactions	113
3.5.2.3	O and N Alkylation Reactions	115
3.5.2.4	Reduction and oxidation Reactions	117
3.6	Sonochemical Preparation of Ultrafine Powders and Nanostructured Materials	120
3.6.1	Metal Powders	121
3.6.2	Metal Oxide and Other Powders	123
3.6.3	Supported Nanopowders	124
4	Sonochemistry in Environmental Protection and Remediation	131
4.1	Introduction	131
4.2	Water Purification	132
4.2.1	Biological Decontamination	132
4.2.1.1	The Mechanisms of Ultrasonic Action on Cellular Material	132
4.2.1.2	Ultrasonic Destruction of Biological Contaminants in Water	134
4.2.2	Chemical Decontamination	137
4.2.2.1	The Sonication of Water	137
4.2.2.2	The Effect of Ultrasound Alone	138
4.2.2.3	Combined Application of Ultrasound with Ozone	141
4.2.2.4	Combined Application of Ultrasound with Ultraviolet Light	142
4.2.2.5	Combined Application of Ultrasound with Electrochemistry	142
4.3	Surface Decontamination	144
4.4	Decontamination of Soil	145
4.4.1	Surface Cleaning of Particles	146
4.4.2	Leaching of Pollutants from within Particles	147

4.5	The Control of Air-Borne Contamination	149
4.6	Treatment of Sewage Sludge	152
4.6.1	Ultrasonically Assisted Digestion	152
4.6.2	Ultrasonically Assisted Dewatering	153
5	Polymers	157
5.1	Introduction	157
5.2	Degradation of Polymers	161
5.3	Factors Affecting Polymer Degradation	170
5.3.1	Frequency	170
5.3.2	Solvent	172
5.3.3	Temperature	174
5.3.4	Nature of the Gas	175
5.3.5	Intensity	179
5.3.6	External Pressure	185
5.3.7	R.M.M. and Concentration	188
5.3.8	Nature of the Polymer	190
5.4	Degradation Mechanisms	191
5.5	Polymer Synthesis	196
5.6	Ultrasonic Processing of Polymers	214
5.6.1	Treatment of Plastics	214
6	Sonoelectrochemistry	225
6.1	Introduction	225
6.2	Electrolytic Discharge	231
6.3	Electroplating in the Presence of Ultrasound	234
6.3.1	Chromium Plating	235
6.3.2	Zinc Electroplating	243
6.3.3	Iron Electroplating	244
6.3.4	Copper Electroplating	245
6.3.5	Electrolytic Removal of Silver	246
6.3.6	Nickel Electroplating	247
6.4	Sonoelectroorganic Synthesis	249
6.4.1	Electrooxidative Syntheses	250
6.4.2	Electroreductive Syntheses	255
6.4.3	Organometallic Systems	257
6.4.4	Electroinitiated Polymerisations	258
6.5	Summary	263
7	Ultrasonic Equipment and Chemical Reactor Design	267
7.1	Methods for the Generation of Power Ultrasound	267
7.1.1	Gas-Driven Transducers	268
7.1.2	Liquid-Driven Transducers	269
7.1.3	Electromechanical Transducers	269
7.2	Ultrasonic Apparatus	275

7.2.1	Whistle Reactor	276
7.2.2	Ultrasonic Cleaning Bath	276
7.2.3	Laboratory Equipment Based on the Ultrasonic Cleaning Bath	278
7.2.4	Direct Immersion Sonic Horn	279
7.2.4.1	Horn Design	280
7.2.5	Laboratory Scale Reactors Involving Probe Systems	283
7.3	Large Scale Applications	286
7.3.1	Whistle Systems	286
7.3.2	Low Intensity Systems	287
7.3.3	High Intensity Systems	288

Subject Index	295
----------------------	-----

Preface

When Phil Lorimer and I had completed the book for Ellis Horwood over ten years ago we really did feel as though we were contributing to a solid foundation for our chosen field of research in sonochemistry, and so it has proven to be.

Sonochemistry has moved on substantially since those days. Most of the major international acoustics meetings now include a component of relating to the applications of power ultrasound in chemistry and processing. Indeed a biennial conference with this title was first launched in Toulouse in 1997 and the European Society of Sonochemistry has had seven major meetings to date. On the one hand research into sonochemistry has expanded in terms of groups involved but on the other there is a tendency to concentrate on areas of particular interest such as sonoluminescence, food technology, nanoparticle synthesis, electrochemistry, environmental protection and, of course, chemistry and chemical processing. The first two of these have seen the publication of edited texts [1, 2] which have concentrated these specialist topics. In our book we have revised and expanded a number of chapters from the original text and added two others: environmental protection and electrochemistry.

It is our hope that this book will present the reader with an appreciation of current trends in the applications of sonochemistry. The theoretical aspects of the subject are, once again, included but not emphasised. It is our intention to concentrate on the uses of sonochemistry and to leave the interested reader to find the more complex mathematical aspects from other sources.

- *Ultrasound in Food Processing*, M. Povey and T. J. Mason (eds.), Blackie Academic and Professional, pp 282, 1998, ISBN 0-7514-0429-2.
- *Sonochemistry and Sonoluminescence*, NATO ASI Series, L. A. Crum, T. J. Mason, J. L. Reisse and K. S. Suslick (eds.), Kluwer Academic Publishers, pp 404, 1999, ISBN 0-7923-5549-0.

Coventry, 2001

Tim Mason



Speakers at the first international symposium on Sonochemistry organised by T. J. Mason. Held as part of the Royal Society of Chemistry Annual Congress, Warwick University, April 1986. The affiliations of the speakers are those which were current at the time of the conference.

Front Row (left to right)

R. Verrall
Department of Chemistry
University of Saskatchewan
Saskatoon
Canada

A. Henglein
Bereich Strahlenchemie
Hahn-Meitner-Institut
Berlin
Germany

T. J. Mason
School of Chemistry
Coventry Polytechnic
Coventry
United Kingdom

P. Boudjouk
Department of Chemistry
North Dakota State University
North Dakota
USA

K. S. Suslick
School of Chemical Sciences
University of Illinois at Urbana
Champaign
Illinois
USA

C. Dupuy
Chimie Recherche
Universite Scientifique et Medical
de Grenoble
Grenoble
France

Second Row (left to right)

J. Lindley
School of Chemistry
Coventry Polytechnic
Coventry
United Kingdom

P. Riesz
National Institutes of Health
Bethesda
Maryland
USA

T. J. Lewis
Department of Electronic
Engineering
University College of North Wales
Bangor
United Kingdom

J. Perkins
Sonic Systems
Marlborough
Wiltshire
United Kingdom

E. J. Einhorn
Chimie Recherche
Universite Scientifique et Medical
de Grenoble
Grenoble
France

P. Kruus
Department of Chemistry
Carleton University
Ottawa
Canada

Back Row (left to right)

R. S. Davidson
Dept of Chemistry
City University
London
United Kingdom

J.-L. Luche
Chimie Recherche
Universite Scientifique et Medical
de Grenoble
Grenoble
France

B. Pugin
Ciba-Geigy
Basle
Switzerland

J. P. Lorimer
School of Chemistry
Coventry Polytechnic
Coventry
United Kingdom

Subject Index

a

acoustic

- motion of the bubble in the applied acoustic field (*see there*) 45–56

- pressure 37, 61

- wave theory 25

air-borne contamination control,

- water purification 149–152

- acoustic standing waves 149

- defoaming liquids 151

- dust suppression 149

- emission in coal combustion 150

- mist suppression 151

alcohols, oxidation 119

alkali metals 98

- *Barbier* reaction 99

- *Bouveault* reaction 100

- lithium diisopropylamide 100

- magnesium 98

- *Wurtz* coupling 99

alkylation

- C alkylation reactions (*see there*) 113–114

- N alkylation reactions (*see there*) 115–117

- O alkylation reactions (*see there*) 115–117

amino acids 112

amorphous

- catalysis 123

- iron 121

- magnetic metals 122

- MoS₂ 124

- nickel 121

anti-algae 135

apparatus

- laboratory 275–285

- – cleaning bath 275–279

- – cup-horn 275, 286

- – dimple cell 284

- – flow cell 285

- – probe (or horn) system (*see there*) 275, 279–282

- – simple pressure cell 284

- – whistle reactor 276

- large scale applications 286–290

- – cross-section shapes for flow processors 290

- – high intensity system 288

- – low intensity system 287–288

- – *Nearfield* acoustic processor (NAP) 291

- – radial ultrasonic emitters 292

- – reaction tube with externally bonded transducers 292

- – reaction tube with probe inserts 289

- – reaction tube with transduce inserts 289

- – submersible transducer assembly 288

- – whistle systems 286–287

- for organo-zinc reagents 106

aqueous polyethylene oxide,

- intensity effect of 184

aromatic

- carbon-halogen bond, cleavage of 117

- nitro group, reduction of 117

ASDIC echo-sounder 2

atomisation 15–16

aziridine 111

b

bacterial

- biofilms 145

- removal 144

Barbier reaction 99

benzaldehyde, electroreduction of 255

benzoic acid, electroreduction 256

benzyl / benzylic

- bromide, electroreduction 256

- position, oxidation at 118

biological cell disruption 9

block, polymer synthesis 196–197

- cellulose 196

- graft polymers 196

- polymethyl methacrylate 196
- poly(methyl phenyl silane) 197
- polystyrene 196
- Bouveault* reaction 100
- bubble
 - collapse time 46, 65
 - dynamics 73
 - formation (*see also* cavitation threshold) 36–45
 - motion of the bubble in the applied acoustic field (*see there*) 45–56, 65
 - radius 62
 - temperature (T_{\max}) 70
- butadiene sulfone, polymerisation 259

C

- C alkylation reactions 113–115
 - Wittig reactions 114–115
- Cannizzaro* reaction 119
- carbene 87
- carbonisation 88
- cavitation (threshold effects) 36–45
 - frequency 56
 - – applied 39–40
 - gas 36
 - – gas type and content 58–59
 - hydrodynamic (*see there*) 3
 - intensity 59
 - particulate matter 36
 - pressure 44
 - – external (applied) 59
 - solvent 40, 57
 - – of solvent viscosity 43
 - surface tension 43
 - temperature 42, 57
 - transient 53–54
 - viscosity 39
- cell disruption, biological 9
- cellulose, polymer synthesis 196
- chain polymerisation 258–259
 - butadiene sulfone, polymerisation 259
 - copolymer composition 259
 - copolymerisation of isoprene with α -methyl styrene 259
 - homopolymerisation 259
 - styrene, polymerisation 259
- chemical applications (general) 20–23
 - emulsion reactions 22
 - homogenous reactions 22
 - reactions involving
 - metal or solid surfaces 21
 - powders or other particulate matter 21

- chlorinated hydrocarbons 140
- m*-chloroperbenzoic acid (MCPBA) 111
- 4-chlorophenol, decomposition of 139
- chromium, electroplating 235–242
 - chrome mist suppression 239
 - control of emissions 240
 - Cr(III) system 235–238
 - CR(VI) system 235
 - current density, effect of 237, 239
 - discharge rate 242
 - efficiency 236, 241
 - hardness of deposit 241
 - pH dependence 238
 - stabiliser, effect of 238
- cleaning, ultrasonic 7–8
- cobalt nanoclusters 122
- concentration, polymer degradation 188–189
 - aqueous dextran 189
 - aqueous poly(ethylene oxide) 188
 - polystyrene 189
- condensation (step growth) polymerisation 157, 212–213
 - polyformal 213
 - poly(organosilanes) 213
- copolymer composition, polymerisation 259
 - copolymerisation of isoprene with α -methyl styrene 259
- copper 108–109, 123, 245
 - electroplating 245
 - – diffusion layer 245
 - – rate of deposition 245
 - nanoparticles 123
 - Ullmann coupling 108
- coupling reactions, polymer synthesis 212, 214
 - Ziegler-Natta polymerisation 214
- Cr_2O_3 123
- cryptosporidium parvum 136
- crystallisation 19–20
- cutting, ultrasound in 13–14
- cyanohydrin 112
- cyclohexanecarboxylate, electrolysis of 251
- cyclopropanation, large scale, zinc 104
- cysts for water decontamination 135

d

- Daniell* cell 230
- decontamination of surfaces 7–8
- degradation, polymer (*see there*) 161–170
- dentistry, ultrasound in 11–12
- dewatering, ultrasonically assisted 153
- dextran, polymer degradation 167

diagnostic medicine, ultrasound in 9–10
 dichlorocarbene 110
 dimethyl maleate, electroreduction of 256

e

echo-sounder 2
 – ASDIC 2
 – *Langévin* 2
 – SONAR 2
 electrically-conducting polymers 261–263
 – poly *N*-vinyl carbazole 262
 – polypyrrole 261
 – polythiophene 262
 electrochemical cell 228–230
 – *Daniell* cell 230
 – electrolytic cell 229
 – galvanic cells 229
 – lead accumulator 230
 electrochemistry (*see* sonoelectrochemistry)
 97, 142–144, 225–263
 electroinitiated polymerisations, sono-
 electroorganic synthesis 258–263
 – chain polymerisation (*see there*)
 258–259
 – copolymerisation (*see there*) 259
 – electrically-conducting polymers
 (*see there*) 261–263
 electroless nickel plating 248
 electrolysis of cyclohexanecarboxylate 251
 electrolytic cell 229
 electrolytic
 – discharge 231–234
 – removal of silver 246–247
 electrooxidation 250–251
 – cyclohexanecarboxylate, electrolysis of
 251
 – frequency, effect of 253
 – pentamethylbenzene 253–254
 – phenylacetate, electrolysis of 251
 electroorganic synthesis (*see* sonoelectro-
 organic synthesis) 249–263
 electroplating 234–248
 – advantages of ultrasound 234
 – chromium (*see there*) 235–242
 – copper (*see there*) 245
 – iron (*see there*) 244–245
 – nickel (*see there*) 247–248
 – silver (*see there*) 246–247
 – zinc (*see there*) 243–244
 electroreduction, sonoelectroorganic
 synthesis 255–256
 – benzaldehyde 255
 – benzoic acid 256
 – benzyl bromide 256

– dimethyl maleate 256
 – frequency, effect of 256
 – methyl iodide 256
 emulsification 17–18
 emulsion
 – polymer synthesis 200
 – – styrene 200
 – reactions 22
 environmental protection 131–153
 epoxidation 111
 etard reagents, oxidation 118

f

ferrilactones 89
 filtration 19
Flory Huggins constants 194
 food sterilisation 136
 frequency, effect of
 – electrooxidation 253
 – electroreduction 256
 – polymer degradation 164, 170–172
 – – polymethyl methacrylate 171
 – polymer synthesis 202
 fullerene 92

g

Galton whistle 2
 – transducers 268
 galvanic cells 229
 gas
 – effect of, polymer degradation 175–178,
 192
 – – degradation of polystyrene 176
 – – solubility of gas 178
 – effect of, polymer synthesis 202
 gas-driven transducers 268–269
 graft polymers, polymer synthesis 196
Grignard reagents, magnesium 98

h

heterogeneous sonochemistry / medium
 79, 93–120
 – alkali metals 98
 – copper (*see there*) 108–109
 – magnesium 96, 98
 – metal as a reagent (*see also* metal) 93
 – non-metallic reagents (*see there*) 110–120
 – organosilicon compounds 95
 – preparation of active metals 93
 – radical sonochemistry 97
 – zinc (*see there*) 95, 97, 101–107
HMS Daring, hydrodynamic cavitation 3
 homogenous reactions 22, 83–92
 – β -lactones 91

- carbene 87
 - carbonisation 88
 - decompensation of iron carbonyls 88
 - ferrilactones 89
 - fullerene 92
 - hydroboration 92
 - hydrolysis reactions 84
 - non-aqueous 86
 - organotin 91
 - pyrolyses 88
 - radicals 86
 - solvent effect 85
 - solvolysis 85
 - sonochemical switching 90
 - temperature effect 85
 - water decomposition 86
 - homopolymerisation 259
 - hydroboration 92
 - hydrodynamic cavitation 3, 124
 - HMS *Daring* 3
 - Lord *Rayleigh* 3
 - hydrolysis reactions 84
 - hydroxycellulose, intensity effect of 181
 - hydroxyethyl cellulose, intensity effect of 183
- i**
- impregnation 18–19
 - industrial uses of ultrasound 4–20
 - atomisation 15–16
 - biological cell disruption 9
 - cutting 13–14
 - decontamination of surfaces 7–8
 - machining 13
 - metal casting, melt treatment 16–17
 - metal tube drawing 14
 - processing applications 17–20
 - crystallisation 19–20
 - extraction 18
 - filtration 19
 - impregnation 18–19
 - mixing and emulsification 17–18
 - ultrasonic cleaning 7–8
 - ultrasound in medicine 9–12
 - dentistry 11–12
 - diagnostic 9–10
 - therapeutic 10–11
 - ultrasound surface treatment 14–15
 - ultrasound welding (*see also* welding) 5–7
 - intensity 31–33
 - cavitation 59
 - effect of, polymer degradation 179–185
 - aqueous polyethylene oxide 184
 - hydroxycellulose 181
 - hydroxyethyl cellulose 183
 - limiting molar mass 181
 - PMMA 183
 - polystyrene 182
 - effect of, polymer synthesis 202–203, 209
 - cavitation 203
 - inverse Arrhenius 205, 207
 - iron
 - carbonyls, decompensation of 88
 - electroplating 244–245
 - composition of deposit 245
 - hardness 244
 - silica-supported 124
 - irradiation time, effect of, polymer degradation 168, 193
 - isoprene with α -methylstyrene 211
- k**
- Kolbe*
- electrolysis 249
 - reaction 250
- l**
- β -lactones 91
 - γ -lactones 112
 - Langévin* echo-sounder 2
 - laws of sonochemistry 81
 - sonochemical switching 81
 - liquid
 - heterogeneous medium 79
 - homogeneous liquid phase 78
 - liquid-liquid interface 79
 - longitudinal waves 30
 - liquid-driven transducers 269
 - lithium 98
 - alkyl 98
 - aryl 98
 - diisopropylamide 100
 - longitudinal waves 25–29
 - in air 27
 - compression 28
 - displacement 29
 - in liquid 30
 - reaction 28
 - Lord *Rayleigh*, hydrodynamic cavitation 3
- m**
- machining with slurry, ultrasound in 13
 - magnesium 96, 98
 - *Grignard* reagents 98
 - monoperoxyphthalate (MMPP) 111
 - magnetic field, external 124
 - magnetostrictive transducer 272–273
 - MCPBA (*m*-chloroperbenzoic acid) 111

- mechanism
 - polymer degradation 162, 191, 194
 - – *Flory Huggins* constants 194
 - polymer synthesis 199
- medicine, ultrasound in 9–12
 - dentistry 11–12
 - diagnostic 9–10
 - therapeutic 10–11
- mercury metal 93
- metal
 - active metals 93
 - – magnesium 96, 98
 - – mercury 93
 - – nickel 94
 - – palladium 95
 - – platinum 95
 - – potassium 94
 - – preparation of 93
 - – rhodium 95
 - – *Rieke* powder 95
 - – in situ activation 97
 - – sonoelectrochemistry 97
 - – zinc (*see there*) 95, 97, 101–107
 - alkali metals 98
 - – *Barbier* reaction 99
 - – *Bouveault* reaction 100
 - – lithium diisopropylamide 100
 - – magnesium 98
 - – *Wurtz* coupling 99
 - melt treatment in metal casting 16–17
 - oxide and other powders 123–124
 - – amorphous MoS_2 124
 - – Cr_2O_3 123
 - – delaminated zeolites 123
 - – external magnetic field 124
 - – hydrodynamic cavitation 124
 - – Mn_2O_3 123
 - – NiFe_2O_4 123
 - powders 121–123
 - – amorphous catalysis 123
 - – amorphous iron 121
 - – amorphous magnetic metals 122
 - – amorphous nickel 121
 - – cobalt nanoclusters 122
 - – copper nanoparticles 123
 - – noble metal nanoparticles 122
 - – palladium clusters 122
 - as a reagent 93
 - or solid surfaces, chemical application 21
 - tube drawing 14
- methyl
 - iodide, electroreduction 256
 - methacrylate (MMA) 202
 - – effect of intensity 202
 - – effect of temperature 202
- mixing 17–18
- MMPP (magnesium monoperoxyphthalate) 111
- Mn_2O_3 123
- molar mass, limiting 181
- motion of the bubble in the applied acoustic field 45–56
 - bubble collapse time 46, 65
 - bubble dynamics 73
 - cavity wall 68
 - frequency dependent 49
 - resonance frequency 48
 - stable
 - – bubble 47, 50
 - – cavitation 55–56
 - – resonance with the applied acoustic field 55
 - transient cavitation 53–54
 - – polytropic index of gas 54
 - transient collapse 50
- n**
- N* alkylation reactions 115–117
 - hindered phenols 115
- nanostuctured materials and ultrafine powders (*see* ultrafine...) 120–125
- NAP (*Nearfield* acoustic processor) 291
- Nearfield* acoustic processor (NAP) 291
- nickel 94
 - on alumina 125
 - amorphous 121
 - electroplating 247–248
 - – efficiency 248
 - – electroless 248
 - – hardness 247–248
- NiFe_2O_4 123
- nitrene 111
- non-aqueous 86
- non-metallic reagents 110–120
 - addition reactions 110–113
 - – amino acids 112
 - – aziridine 111
 - – cyanohydrin 112
 - – dichlorocarbene 110
 - – epoxidation 111
 - – γ -lactones 112
 - – *m*-chloroperbenzoic acid (MCPBA) 111
 - – magnesium monoperoxyphthalate (MMPP) 111
 - – nitrene 111
 - – *Strecker* synthesis 113
 - C alkylation reactions 113–115

- N alkylation reactions 115–117
- O alkylation reactions 115–117
- phase transfer catalysis 110
- reduction oxidation reaction (*see* oxidation reaction) 117–120
- ultrafine powders and nanostructured materials (*see there*) 120–125

O

- O alkylation reactions 115–117
- hindered phenols 115
- organometallic systems, sonoelectroorganic synthesis 257–258
- germanium 258
- selenium 257
- silicon 258
- tellurium 257
- organosilicon compounds 95
- organotin 91
- organo-zinc reagents, apparatus for 106
- oxidation reaction 117–120
- alcohols, oxidation 119
- benzylic position, oxidation at 118
- Cannizzaro reaction 119
- cleavage of aromatic carbon-halogen bond 117
- etard reagents, oxidation 118
- reduction of the aromatic nitro group 117
- SET mechanism 120
- ozone, application of ultrasound with 141–142
- decolourisation of dyes 141
- sources of OH 141

P

- palladium 95
- on alumina 125
- clusters 122
- particle
- movement 26
- velocity 61
- pentamethylbenzene, electrooxidation 253–254
- perfluoroalkyl substitution, zinc 104
- permeability of the cell walls 133
- peroxide formation of water 140
- phenol
- decomposition of 140
- destruction of 143
- phenylacetate, electrolysis of 251
- photocatalysis, ultraviolet light 142
- piezoelectric
- effect 1
- transducers 270–271

- sandwich transducer 271
- x-cut quartz 270
- platinum 95
- PMMA, intensity effect of 183
- PNVK, polymer degradation of 195
- pollutants, leaching of 147
- poly N-vinyl carbazole 262
- polychlorobiphenyls, ultraviolet light 142
- polymer
- degradation 161–170
- cavitation effects 170
- concentration, effect of (*see there*) 188–189
- degradation curves 195
- dextran 167
- external pressure, effect of (*see* pressure) 185–187
- factors which influence 190
- frequency, effect of (*see there*) 164, 170–172
- frictional forces 164
- furadene time 195
- gas, effect of (*see there*) 175–178, 192
- intensity, effect of (*see there*) 179–185
- irradiation time, effect of 168, 193
- limiting R.M.M. 167
- mechanism (*see there*) 162, 191, 194
- nature of polymer, effect of 191
- PNVK, degradation of 195
- polymer, effect of 190
- polymethyl methacrylate 171
- polystyrene 163, 189
- rate, degradation of styrene 165
- solvent, effect of 172–174
- temperature, effect of 174
- viscosity reduction 162
- synthesis 157–161, 196–214
- addition chain 157
- block (*see there*) 196–197
- condensation (step growth) polymerisation (*see there*) 157, 212–213
- coupling reactions (*see there*) 212, 214
- electroinitiated polymerisation 211
- emulsion (*see there*) 200
- frequency, effect of 202
- H bonding, effect of 210
- gas effect of 202
- graft co-polymers 196
- initiator, effect of 206, 208–209
- intensity, effect of (*see there*) 202, 203, 209
- isoprene with α -methylstyrene 211
- macroradical 198
- mass average molar mass (Mw) 160

- – mechanisms 157, 199
- – number average molar mass (Mn) 160
- – polymers 196
- – pulsed ultrasound 211
- – radical production 206
- – radical scavenger 204
- – rate of bond scission 198
- – ring opening (*see there*) 212
- – suspension 200
- – temperature, effect of (*see there*) 202, 204, 205
- – thiophene 211
- polymerisations, electroinitiated (*see there*) 258–263
- polymethyl methacrylate, polymer synthesis 196
- polypyrrole 261
- polystyrene
 - polymer degradation 163, 176, 182, 186–187
 - – external effect of 186–187
 - – intensity effect of 182
 - – temperature, effect of 176
 - polymer synthesis 196–198
 - – block 196
 - – rate of bond scission 198
- polythiophene 262
- polyvinylcarbazole, effect of temperature 176
- potassium 94
- pressure (P_{\max}) 70
 - acoustic 37, 61
 - amplitude 31–33
 - critical 62
 - effect of external, polymer degradation 185–187
 - – limiting R.M.M. 187
 - – polystyrene 186
- probe (or horn) system 275, 279–282
 - horn design 280–282
- processing applications 17–20
 - crystallisation 19–20
 - extraction 18
 - filtration 19
 - impregnation 18–19
 - injection molding 216, 217
 - mixing and emulsification 17–18
 - polymer blending 221
 - powder coating 221
 - ultrasound / ultrasonic
 - – atomisation 219
 - – insertion 216–217
 - – spot welding 216
 - – staking 216

- – vulcanisation 221
- – welding 215
- viscosity reduction 218
- pulse length 41
- pyrolyses 88

r

- radicals 86
 - radical scavenger, polymer synthesis 204
- reaction tube
 - with externally bonded transducers 292
 - with probe inserts 289
 - with transduce inserts 289
- reactions involving
 - metal or solid surfaces 21
 - powders or other particulate matter 21
- reduction and oxidation reaction (*see* oxidation reaction) 117–120
- Reformatsky reaction, zinc 101
- rhodium 95
- Rieke powder 95
- ring opening, polymer synthesis 212
 - nylon 6 212
 - polycarbonates 212
 - poly(dimethylsiloxane) 212
- R.M.M., limiting, degradation of polystyrene 187–188
- ruthenium on alumina 125

s

- SET mechanism 120
- sewage sludge, treatment of 152–153
 - assisted digestion 152
- silica-supported iron 124
- silver, electroplating 246–247
 - electrolytic removal 246–247
- Simmons-Smith reaction, zinc 103
- soil, decontamination of, water purification 145–148
 - cleaning of particles 146
 - leaching of pollutants 147
- solvent effect 85
 - polymer degradation 172–174
 - – vapour pressure 172
 - – viscosity 172
- solvolysis 85
- SONAR echo-sounder 2
- sonication of water 137–138
- sonochemical
 - reactions, synthesis 78–81
 - switching 81, 90
- sonochemistry, laws of 81–83
- sonoelectrochemistry 97, 142–144, 225–263

- advantages, use of ultrasound in electro-chemistry 234
- application of ultrasound with 142–144
- dyes, destruction of 143
- phenol, destruction of 143
- diffusion layer 232
- disturbance of 232
- electrochemical cell (*see there*) 228–230
- electrolytic discharge 231–234
- sonoelectroorganic synthesis 249–263
- electroinitiated polymerisations (*see there*) 258–263
- electrooxidation (*see there*) 250–251
- electroreduction (*see there*) 255–256
- Kolbe
- electrolysis 249
- reaction 250
- organometallic systems (*see there*) 257–258
- sound
- absorption 33–34
- attenuation 34
- classical absorption 34
- thermal conductivity 34
- viscosity 34
- echo-sounder (*see there*) 2
- frequencies 3
- spores or cysts for water decontamination 135
- Strecker synthesis 113
- styrene
- degradation of 165
- polystyrene 163
- polymerisation 259
- submersible transducer assembly 288
- surface
- decontamination 144–145
- bacterial biofilms 145
- removal of bacteria 144
- treatment, ultrasound 14–15
- synthesis 75–125
- frequency effect 76
- polymer (*see there*) 157–161, 196–214
- power effect 77–78
- sites for sonochemical reactions 78–81
- heterogeneous medium 79
- homogeneous liquid phase 78
- liquid-liquid interface 79

t

- temperature, effect of 85
- polymer degradation 174–176
- polyvinylcarbazole 176
- polystyrene 176

- polymer synthesis 202, 204, 205
- inverse Arrhenius 205, 207
- therapeutic medicine 10–11
- thermoplastic components 5
- thermosonication 136
- thiophene 211
- transducers 267–272
- 1–3 composite transducer 272
- electromechanical 269
- Galton whistle 268
- gas-driven 268–269
- liquid-driven whistle 269
- magnetostrictive transducer 272–273
- piezoelectric (*see there*) 270–271
- vibrating bar 274

u

- Ullmann coupling 107
- copper 108
- zinc 107
- ultrafine powders and nanostructured materials 120–125
- metal powders 121–123
- amorphous catalysis 123
- amorphous iron 121
- amorphous magnetic metals 122
- amorphous nickel 121
- cobalt nanoclusters 122
- copper nanoparticles 123
- noble metal nanoparticles 122
- palladium clusters 122
- metal oxide and other powders 123–124
- amorphous MoS₂ 124
- Cr₂O₃ 123
- delaminated zeolites 123
- external magnetic field 124
- hydrodynamic cavitation 124
- Mn₂O₃ 123
- NiFe₂O₄ 123
- supported nanopowders 124–125
- nickel on alumina 125
- palladium on alumina 125
- ruthenium on alumina 125
- silica-supported iron 124
- ultrasonic plastic welding machine 6
- ultrasound, industrial uses (*see there*) 4–20
- ultraviolet light, application of ultrasound with (*see there*) 142
- photocatalysis 142
- polychlorobiphenyls 142

v

- vibrating bar, transducer 274
- viscosity reduction 162

W

water

- decomposition 86
- purification, decontamination
- - air-borne contamination control 149–152
 - - - acoustic standing waves 149
 - - - defoaming liquids 151
 - - - dust suppression 149
 - - - emission in coal combustion 150
 - - - mist suppression 151
- - biological 132–137
 - - - anti-algae 135
 - - - cryptosporidium parvum 136
 - - - food sterilisation 136
 - - - permeability of the cell walls 133
 - - - spores or cysts 135
 - - - thermosonication 136
- - ultrasonic action on cellular material 132
 - - - chemical 137–144
 - - - chlorinated hydrocarbons 140
 - - - 4-chlorophenol, decomposition of 139
 - - - - electrochemistry, application of ultrasound with (*see there*) 142–144
 - - - - ozone, application of ultrasound with (*see there*) 141–142
 - - - - peroxide formation 140
 - - - - phenol, decomposition of 140
 - - - - sonication of water 137–138
 - - - - ultrasound alone 138
 - - - - ultraviolet light, application of ultrasound with (*see there*) 142
 - - - soil, decontamination of 145–148
 - - - - cleaning of particles 146
 - - - - leaching of pollutants 147

- - surface decontamination 144–145
 - - - bacterial biofilms 145
 - - - removal of bacteria 144
 - treatment of sewage sludge 152–153
 - - assisted digestion 152
 - ultrasonically assisted dewatering 153
- wave
- acoustic wave theory 25
 - longitudinal waves (*see there*) 25–29
 - particle movement 26
- welding 5–7
- ultrasonic plastic welding machine 6
- whistle systems 286–287
- Wittig reactions, C alkylation reactions 114–115
- Wurtz coupling 99

X

- xylylene intermediate, zinc 101

Z

- zeolites, delaminated 123
- Ziegler-Natta polymerisation 214
- zinc 95, 97, 101–107
 - apparatus for organo-zinc reagents 106
 - cycloaddition 102
 - electroplating 243–244
 - - diffusion layer 243
 - efficiency 243
 - porosity 244
 - large scale cyclopropanation 104
 - methylenation 102
 - perfluoroalkyl substitution 104
 - Reformatsky reaction 101
 - Simmons-Smith reaction 103
 - Ullmann coupling 107
 - xylylene intermediate 101

1

Introduction to Applied Ultrasonics

1.1

Background

If you were asked what you knew about ultrasound you would almost certainly start with the fact that it is used in animal communications (e.g. bat navigation and dog whistles). You might then recall that ultrasound is used in medicine for foetal imaging, in underwater range finding (SONAR) or in the non-destructive testing of metals for flaws. For a chemist however sound would probably not be the first form of energy that would be considered for the excitation of a chemical reaction. Indeed up to a few years ago the use of ultrasound in chemistry was something of a curiosity and the practising chemist could have been forgiven for not having met the concept. To increase chemical reactivity one would probably turn towards heat, pressure, light or the use of a catalyst. And yet, if one stops for a second to consider what is involved in the transmission of a sound wave through a medium it is perhaps surprising that for so many years sound was not considered as a potential source of enhancement of chemical reactivity. The only exception to this being the green fingered chemist who, in the privacy of his own laboratory, talks, sings or even shouts at his reaction. After all, sound is transmitted through a medium as a pressure wave and the mere act of transmission must cause some excitation in the medium in the form of enhanced molecular motion. However, as we will see later, in order to produce real effects the sound energy must be generated within the liquid itself. This is because the transfer of sound energy from the air into a liquid is not an efficient process.

The basis for the present-day generation of ultrasound was established as far back as 1880 with the discovery of the piezoelectric effect by the Curies [1–3]. Most modern ultrasonic devices rely on transducers (energy converters) which are composed of piezoelectric material. Such materials respond to the application of an electrical potential across opposite faces with a small change in dimension. This is the inverse of the piezoelectric effect and will be dealt with in detail later (Chapter 7). If the potential is alternated at high frequencies the crystal converts the electrical energy to mechanical

vibration (sound) energy – rather like a loudspeaker. At sufficiently high alternating potential high frequency sound (ultrasound) will be generated.

The earliest form of an ultrasonic transducer was a whistle developed by Francis Galton (1822–1911) in 1883 to investigate the threshold frequency of human hearing (see Chapter 7) [4]. Galton himself was a remarkable man. As well as inventing the whistle that carries his name he explored and helped map a portion of the African interior, invented the weather map and developed the first workable system for classifying and identifying fingerprints. His whistle was part of his study of sensory perception, in this case to determine the limits of hearing in terms of sound frequencies in both humans and animals.

The first commercial application of ultrasonics appeared around 1917 and was the first “echo-sounder” invented and developed by Paul Langévin (1872–1946). He was born in Paris and was a contemporary to Marie Curie, Albert Einstein and Hendrik Lorentz. He was noted for his work on the molecular structure of gases, analysis of secondary emission of X-rays from metals exposed to radiation and for his theory of magnetism. However Langévin is more generally remembered for important work on piezoelectricity and on piezoceramics. The original “echo-sounder” eventually became underwater SONAR for submarine detection during World War 2. The transducer was a mosaic of thin quartz crystals glued between two steel plates (the composite having a resonant frequency of about 50 kHz), mounted in a housing suitable for submersion. The early “echo sounder” simply sent a pulse of ultrasound from the keel of a boat to the bottom of the sea from which it was reflected back to a detector also on the keel. For sound waves, since the distance traveled through a medium = $1/2 \times \text{time} \times \text{velocity}$ (and the velocity of sound in seawater is accurately known) the distance to the bottom could be gauged from the time taken for the signal to return to the boat. If some foreign object (e.g. a submarine) were to come between the boat and the bottom of the seabed an echo would be produced from this in advance of the bottom echo. In the UK this system was very important to the Allied Submarine Detection Investigation Committee during the war and became popularly known by the acronym ASDIC. Later developments resulted in a change in the name of the system to SONAR (**SO**und **N**avigation **A**nd **R**anging) which allowed the surrounding sea to be scanned. The original ASDIC system predated the corresponding **R**adio **D**etection **A**nd **R**anging system (RADAR) by 30 years.

Essentially all imaging from medical ultrasound to non-destructive testing relies upon the same pulse-echo type of approach but with considerably refined electronic hardware. The refinements enable the equipment not only to detect reflections of the sound wave from the hard, metallic surface of a submarine in water but also much more subtle changes in the media through which sound passes (e.g. those between different tissue structures in the body). It is high frequency ultrasound (in the range 2 to 10 MHz) which is used primarily in this type of application because by using these

much shorter wavelengths it is possible to detect much smaller areas of phase change i. e. give better 'definition'. The chemical applications of high frequency ultrasound are concerned essentially with measurements of either the velocity of sound through a medium or the degree to which the sound is absorbed as it passes through it. These applications are diagnostic in nature and do not effect the chemistry of the system under study.

When more powerful ultrasound at a lower frequency is applied to a system it is possible to produce chemical changes as a result of acoustically generated cavitation (see below). Cavitation as a phenomenon was first identified and reported in 1895 by Sir John Thornycroft and Sidney Barnaby [5]. This discovery was the result of investigations into the inexplicably poor performance of a newly built destroyer HMS Daring. Her top speed was well below specifications and the problem was traced to the propeller blades that were incorrectly set and therefore not generating sufficient thrust. The rapid motion of the blades through water was found to tear the water structure apart by virtue of simple mechanical action. The result of this was the production of what are now called cavitation bubbles. The solution to this problem lies in using very wide blades covering about two-thirds of the disc area of the propeller, so as to present a very large surface contact with the water. This helps to prevent disruption under the force necessary to propel the vessel. As ship speeds increased, however, this became a serious concern and the Royal Navy commissioned Lord Rayleigh to investigate. He produced a seminal work in the field of cavitation which confirmed that the effects were due to the enormous turbulence, heat, and pressure produced when cavitation bubbles imploded on or near to the propeller surface [6]. In the same work, he also observed that cavitation and bubble collapse was also the origin of the noise made when water is heated towards boiling point.

Since 1945 an increasing understanding of the phenomenon of cavitation has developed coupled with significant developments in electronic circuitry and transducer design (i. e. devices which convert electrical to mechanical signals and *vice versa*). As a result of this there has been a rapid expansion in the application of power ultrasound to chemical processes, a subject which has become known as "*Sonochemistry*".

1.2

Sound Frequency Ranges

Sound frequencies are recorded in units of Hertz (1 Hertz = 1 cycle per second). The range of human hearing for a young person is from about 20 Hz to 20 kHz (the upper limit reduces with age). Within this range lies middle C at 256 Hz. Other species have a wider hearing range e. g. dogs 40 Hz to around 45 kHz and bats 1 kHz to 150 kHz. Bats use high frequency sound (20–100 kHz in air) for echo location as do whales

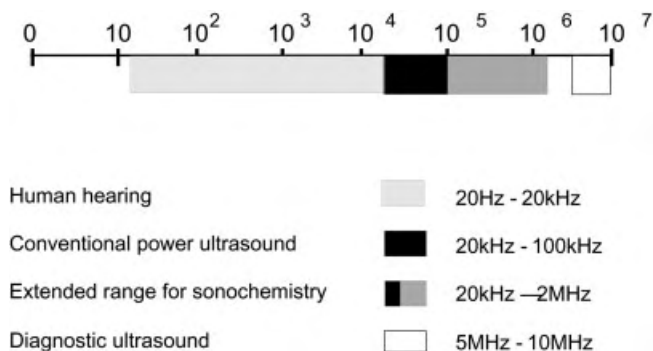


Fig. 1.1. Sound frequency ranges.

(50–200 kHz in water). Ultrasound itself is defined in terms of human hearing and is sound having a frequency higher than that to which the human ear can respond (i. e. > 20 kHz). The upper limit of ultrasonic frequency is one that is not sharply defined but is usually taken to be 5 MHz for gases and 500 MHz for liquids and solids. The uses of ultrasound within this large frequency range may be divided broadly into two areas.

The first area involves low amplitude (higher frequency) sound and is concerned with the physical effect of the medium on the wave and is commonly referred to as “low power” or “high frequency ultrasound”. Typically, low amplitude waves are used for analytical purposes to measure the velocity and absorption coefficient of the wave in a medium in the 2 to 10 MHz range. Information from such measurements can be used in medical imaging, chemical analysis and the study of relaxation phenomena and this will be dealt with later.

The second area involving high energy (low frequency) waves, known as “power ultrasound”, lies between 20 and 100 kHz. It is used for cleaning, plastic welding and, more recently, for sonochemistry (see Fig. 1.1). In fact the range available for sonochemistry has been extended to 2 MHz with the development of high power equipment capable of generating cavitation within liquid systems at these higher frequencies.

1.3

Some Current Industrial Uses of Ultrasound

Before we discuss how sound energy can affect chemistry and chemical processing it would be instructive to explore some of the broader applications of the uses of ultrasound in industry [7–9]. Some of these have been in existence for many years and a range of such are shown in Tab. 1.1. A few of these are explored in more detail in later chapters.

Tab. 1.1. Some industrial uses of ultrasound.

Field	Application
Biology, Biochemistry	Homogenisation and cell disruption: Power ultrasound is used to rupture cell walls in order to release contents for further studies.
Engineering	Ultrasound has been used to assist drilling, grinding and cutting. It is particularly useful for processing hard brittle materials e.g. glass, ceramics. Other uses of power ultrasound are welding (both plastics and metals) and metal tube drawing.
Dentistry	Cleaning and drilling of teeth, also for curing glass ionomer fillings.
Geography, Geology	Pulse/echo techniques are used in the location of mineral and oil deposits and in depth gauges for seas and oceans. Echo ranging at sea has been used for many years (SONAR).
Industrial	Pigments and solids can be easily dispersed in paint, inks and resins. Engineering articles are often cleaned and degreased by immersion in ultrasonic baths. Two less widely used applications are in acoustic filtration and metal casting.
Medicine	Ultrasonic imaging (2–10 MHz) is used, particularly in obstetrics, for observing the foetus and for guiding subcutaneous surgical implements. In physiotherapy lower frequencies (20–50 kHz) are used in the treatment of muscle strains, dissolution of blood clots and cancer treatment.

Two of these applications have provided the direct antecedents of the types of equipment now commonly used for sonochemistry namely ultrasonic welders and cleaning baths.

1.3.1

Ultrasonic Welding

A large proportion of ultrasonic equipment currently in industry is used for welding together thermoplastic components for the consumer market [10]. A simple form of ultrasonic welding equipment is shown in Fig. 1.2. It consists of a generator producing an alternating frequency of around 20 kHz which drives a transducer assembly in a housing that contains controls for both the amplitude and duration of ultrasonic pulse required. This assembly also provides the pneumatic pressure required during the welding process. A shaped tool is attached to the horn and together these comprise a resonating unit that is the basic instrument to provide ultrasonic vibrations. With this tool two thermoplastic parts of compatible material may be joined together quickly and efficiently. The mechanical vibration of the horn contact face (the vibrational amplitude employed is typically 50–100 μm) is passed to the upper component which is correspondingly vibrated against the lower part at 20 000 times per second. The small initial contact area is where energy is most readily dissipated in the form of frictional

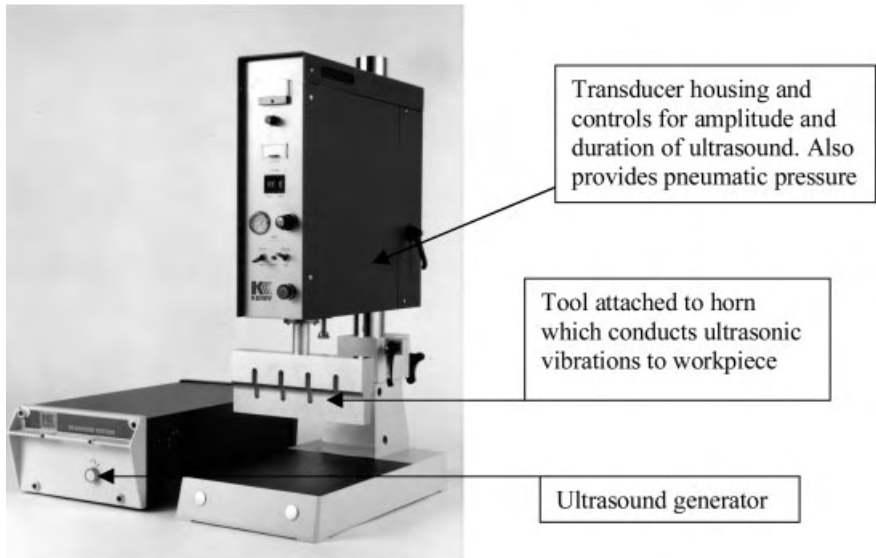


Fig. 1.2. Ultrasonic plastic welding machine (photo courtesy of Kerry Ultrasonics, UK).

heat. The rise in temperature causes localised melting of the material. The parts are continuously held together under pneumatic pressure thus maintaining the melting process until the vibrations are stopped. Pressure is further maintained for a fraction of a second until the liquid material has set. The strength of the finished weld is primarily dependent upon correct choice of materials and component design.

Ultrasonic welding is generally used for the more rigid amorphous types of thermoplastic. These are most suitable for welding because the ultrasonic vibration can travel through the bulk plastic of the component to the joint. The more flexible and crystalline the plastic material, the more readily it will absorb the vibration energy as it travels through the material i.e. the “sound” is attenuated (or deadened) rapidly as it passes through. This type of plastic is generally only welded in the form of thin sections of sheet or film. For plastic welding it is particularly important that the vibrational energy is transmitted only to the joint and not the body of the material, since any warming of the bulk material may lead to a release of internal molding stresses and produce distortion.

Thermoplastics have two properties which make them particularly suited to ultrasonic welding (a) low thermal conductivity and (b) melting or softening temperatures of between 100 and 200 °C. As soon as the ultrasonic power is switched off the substrate or bulk material becomes a heat sink, giving rapid cooling of the welded joint. When more traditional conductive heating is used for welding however the thermal

gradient developed must be reversed before cooling occurs, leading to long heating/cooling process cycles. Another major advantage of the use of ultrasound is the high joint strength of the weld, reaching 90–98 % of the material strength. Indeed test samples usually break in the body of the material and not at the weld itself.

To emphasise the advantages of ultrasonic welding compared with the more traditional approach several examples can be quoted. For aesthetic reasons it is important to avoid distortions in spectacle frames and this has been achieved by ultrasonically welding the metal hinge joint into the plastic frame. Other examples are to be found in the automotive industry where, for example, the car rear reflector cluster will normally have its plastic lens welded into place and the threaded brass insert may well have been inserted by ultrasound. In the UK the 13A mains plug often has the brass threaded nut ultrasonically inserted into the lid; the outer knurling is trapped in place by the plastic melted by the vibrational energy. Emulsion paint cans rust and discolour the paint, consequently several firms now use plastic cans to avoid this problem. The rim, which takes the snap-on lid, is welded ultrasonically to the body in an automated high-speed canning line.

Ultrasonic welding is not only restricted to plastics but can also be used for metals. In this case the ultrasonic motion must be lateral rather than vertical so that frictional heating is induced between the surfaces. One typical application is in the welding of aluminium which is difficult by normal methods because of its tenacious surface oxide. With ultrasonic metal welding – a form of low temperature diffusion welding – the oxide layer is easily broken up and adsorbed within the metal surrounding the weld. Welding by lateral vibrational movement is readily achieved using this technique without the formation of brittle intermetallic compounds. Ultrasonic metal welding, like plastic welding, permits the very delicate joining of components. In flute manufacture it is clearly important to avoid distortion when attaching pillars to the flute body. The well known musical instrument makers Boosey and Hawkes largely eliminated the problem by using an ultrasonic stud-welder for the process thus avoiding the heat normally associated with hard soldering.

1.3.2

Ultrasonic Cleaning and the Decontamination of Surfaces

Ultrasonic cleaning is another major application for power ultrasound. It is now such a well-established technique that laboratories without access to an ultrasonic cleaning bath are in a minority. It is important to recognise the historical significance of the development of ultrasonic cleaning technology on the growth of sonochemistry because, in the early years, the humble laboratory cleaner was almost certainly the first ultrasonic apparatus used by chemists.

Ultrasound is particularly useful in surface decontamination since cavitation bubble collapse near a solid is non-symmetric (see Fig. 3.4) and produces a powerful jet which will dislodge dirt and bacteria. The particular advantage of ultrasonic cleaning in this context is that it can reach crevices that are not easily accessible using conventional cleaning methods. Objects that can be cleaned range from large crates used for food packaging and transportation to delicate surgical implements such as endoscopes. This breadth of application was recognised some years ago in a general patent that relates to the use of ultrasound as a method of pasteurisation, sterilisation and decontamination of instruments and surfaces used within the medical, surgical, dental and food processing industries [11]. The use of ultrasound allows the destruction of a variety of fungi, bacteria and viruses in a much reduced processing time when compared to thermal treatment at similar temperatures. The removal of bacteria from various surfaces is of great importance to the food industry and can be efficiently accomplished with the combined use of sonicated hot water containing biocidal detergent [12].

A good example of the use of ultrasonic technology was the raising of the Tudor warship the “Mary Rose” from the sea-bed of the Solent in England in 1982. The ship had lain buried by preserving silt, for 437 years and ultrasound was used in two ways to assist in this historic “rescue” [13]. The initial location of the wreck was greatly assisted by SONAR. Subsequently, following her recovery, strenuous efforts were made by the ‘Mary Rose’ Trust to preserve the 17 000 or so artifacts recovered from the wreck. These included hundreds of bows, arrows, musical instruments and personal objects such as clothes, footwear, coins and so forth. The prospect of cleaning and preserving this vast amount of material by laborious soaking and rinsing had proved daunting even before the ‘Mary Rose’ itself broke the surface of the waves. A large ultrasonic cleaning bath (donated by the UK company Kerry Ultrasonics) was used to clean items as bulky as wooden gun carriages but could as easily be used for smaller items. One of the major problems in preserving artifacts constructed of organic materials – wood and leather – is that they often have become impregnated with iron deposits. These deposits have to be removed to prevent further deterioration, since iron staining and rust block the pores of the organic materials, preventing effective penetration of the chemical preservatives. Ultrasonic cleaning is very effective in removing such deposits and can, at a later stage, be used to improve the penetration of preservatives into the material.

Many complex (and expensive) automated multibath cleaning, rinsing and drying systems can be found in high volume production lines. For the chemical laboratory however a single small cleaning bath can be obtained at a very reasonable cost.

1.3.3

Ultrasound in Biology and Medicine**Biological cell disruption**

One of the first uses of power ultrasound in biology was the disruption of cell walls to release the contents for in vitro studies. The type of apparatus used for this purpose is a direct descendent of the welding equipment described above. A horn resonating at 20 kHz is dipped into a suspension of biological cellular material. The vibrating tip generates cavitation within the liquid immediately below the tip and the resulting forces and turbulence can cause cell disruption. The process depends upon the efficiency with which the cell wall can be broken to release the cellular contents without at the same time destroying them. This is much more difficult than it would appear. The problem is that most simple one-cell organisms have an exceedingly tough cell wall which is only a few microns in diameter, and similar in density to the medium that surrounds it. On the other hand the protein and nucleic acid components contained within the cell are large macromolecules, easily denatured by extreme conditions of temperature or oxidation.

Maximum disruption is obtained in a zone close to the probe tip and the biological cells must be kept here for sufficient time to allow disruption to take place. A delicate balance must therefore be struck between the power of the probe and the disruption rate since power ultrasound, with its associated cavitation collapse energy and bulk heating effect, can denature the contents of the cell once released. Indeed for this type of usage it is important to keep the cell sample cool during sonication. The method is very effective and continues to be an important tool in microbiology and biochemistry research.

Ultrasound in diagnostic medicine

Unlike the echo-sounding applications referred to above diagnostic medical scanners (and NDT equipment) work at very low power levels (milliwatts) on a pulsed echo system. As its name suggests diagnostic (or high frequency) ultrasound provides a non-invasive technique for scanning the human body and can be considered to be complementary to X-ray and magnetic resonance methods. One of the most publicised uses of diagnostic ultrasound has been in foetal imaging [14]. Another major usage is as a continuous and non-hazardous method of visualising the position of needles and other surgical implements as they are used within the body.

The origins of acoustic sensing in medical diagnosis go back a long way. Physicians have always used the direct approach of listening for the sounds generated from the heart and lungs but in the 18th century a new technique was introduced known as “percussion”. This involved the physician tapping on the surface of the skin of a patient and listening for the resonant note emitted by the air-filled or liquid filled spaces

within the body. Practice in the method allows diagnosis of a range of medical conditions.

In the medical use of diagnostic ultrasound, high-frequency acoustic pulses of short duration are propagated from a source placed on the outer skin of the patient. The source is both a sender of pulses and a receiver of echoes and a gel is used to ensure good acoustic contact with the skin. The pulses proceed in more or less straight lines and are scattered as they encounter various physical gradients or boundaries within tissues. “Back-scatter”, in which the pulses are reflected 180° , results in a series of echoes which can be detected at the skin surface. The lapse of time between launching and receiving a pulse is proportional to the depth of the reflecting tissue (the average sound velocity in body tissues is about 1.54 km s^{-1}). Likewise, the time lapse between echoes corresponds to the space between structures which are reflecting the pulses. Signals can also vary in strength, or amplitude, depending on the specific features of the reflecting structures, such as their composition, compressibility, and density.

An ultrasound image is synthesised line by line, each line of the image representing the echo pattern of an individual acoustic pulse. The result is a spatial map of phase boundaries within the tissues. Signal amplitude is portrayed in a gray scale of tonal gradations, with the strongest reflected signals shown as intense white and the absence of a signal as black. Today’s devices use acoustic pulses with an average frequency in the range of 3–10 MHz; pulse wavelengths and the corresponding resolution features of the image are equal to or less than 1 mm.

Medical scanners have an array of transducers in each probe and are capable of providing thousands of measurements of the small changes in the velocity of sound as it passes through various phase changes within the body. This information is fed to computers that create a television picture of the internal tissues of the human body.

Ultrasound in therapeutic medicine

One of the first applications of ultrasound in medicine was the so-called ultrasonic massage introduced in Germany before the Second World War. This was introduced as a substitute for the hands of the masseur in patients who had suffered from fractures and similar injuries. Rubbing movements are capable of improving the circulation very considerably and help also to break down adhesions between muscles and their sheaths that limit the range of movement. The use of ultrasound for the treatment of sporting injuries, particularly strains and “tennis elbow” is now commonplace as equipment for this purpose is readily commercially available to the physiotherapist. This is one of the first uses of ultrasound in the treatment of medical problems and is part of a new field of medicine called therapeutic ultrasound [15].

One recent medical application is for the destruction of blood clots where a miniaturised ultrasonic device (1 MHz) is attached to the end of a catheter so that it can be

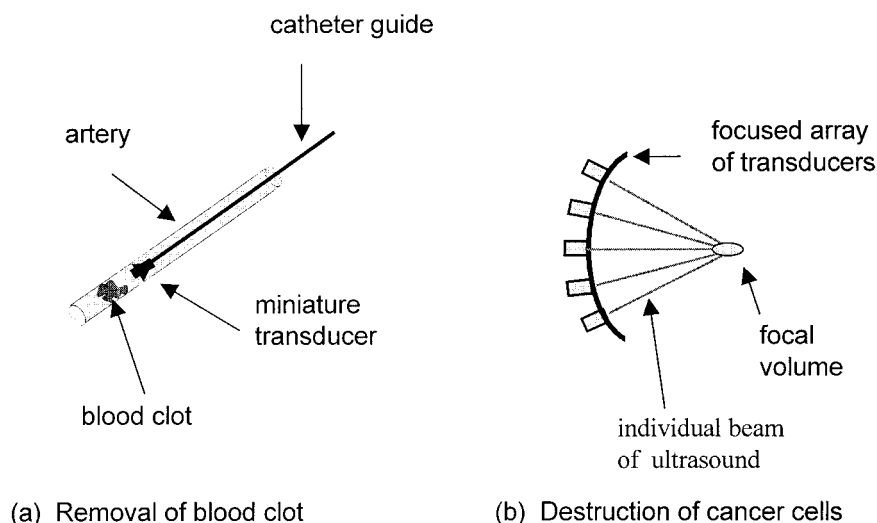


Fig. 1.3. Therapeutic uses of ultrasound.

inserted into the blood vessel. The device is brought close to the clot at which point a fibrolytic enzyme is released (Fig. 1.3a). When the transducer is activated the acoustic energy accelerates the enzymatic dissolution of the clot.

Another use involves a technique known as High Intensity Focused Ultrasound (HIFU) is used in the treatment of cancer (Fig. 1.3b). In this methodology an array of transducers is constructed to produce a focus in the shape of a rugby football only a millimeter or so in cross section and a few millimeters long. When applied to the skin of a patient the focus can be targeted accurately on cancerous tissue within the body and thermally destroy it. In a sequence of exposures the focus can be moved to cover the whole of the infected region. At lower powers the focused ultrasound can also be used to enhance the action of a chemotherapy agent such as a porphyrin which is known to become localised in a region of cancerous cells. The ultrasound is again targeted in the affected region and is thought to promote the types of radical reaction which are generally considered to be involved in chemotherapy.

Ultrasound in dentistry

The connection between the use of ultrasound for the machining and drilling of hard materials (see below) and dentistry is clear since tooth enamel is a very hard material. In the dentist's surgery a new instrument has been introduced which is essentially a small ultrasonic probe operating at 25 kHz with a variety of attachments. Although

these instruments were first produced back in the late 1950's, technical improvements have seen their adaptation for an increasingly wide range of dental applications including cleaning and polishing teeth, descaling, drilling and even root canal work. For simple cleaning the dentist will use the instrument in a mode such that the vibrating tip is used to sonicate a fine spray of air, water and specially prepared sodium carbonate. Such a spray when precisely projected against the tooth surface has been found to have a cleaning/polishing effect which is far less abrasive towards tooth enamel than the more traditional grinding with pumice stone.

With a selection of different hook-shaped metal tools the same implement can be used for de-scaling making use of the 25 000 times per second push-pull motion of the resonating tip. If a straight diamond tipped drill attachment is used in conjunction with abrasive slurry containing alumina powder then the same motion gives efficient drilling. For root-canal work the use of the drill can be augmented by the use of a file and, as a bonus, the ultrasonic vibrations produced in the sterilising aqueous irrigation fluid gives a very efficient cleansing action.

A somewhat more recent application is in the curing of glass ionomer (white) dental filling material. This is normally accomplished by mixing two components (a base material and an accelerator) in a ratio that governs the setting time. A dentist can then work within this time to place the filling material, while still mobile, in the drilled cavity. A preferred approach would be to have a non-limited time to arrange the filling material and then cause it to set (so-called "command set"). At the moment uv curing is the method of choice for command set but it requires that the filling material is built up in layers and each layer is set before the next is applied (uv light does not penetrate very far into opaque materials). Power ultrasound provided through the dental tool can be used to cause setting of glass ionomer cement and, since ultrasound is not impeded by opacity, it can be used to set the material at the end of the operation [16].

1.3.4

Engineering Applications

A number of applications of power ultrasound are to be found in heavy industry both in metalworking and processing [17]. The machining of modern materials requires tools that can deal with unusual properties, complex shapes of work-pieces, and accuracy in working. Basic ultrasonic machining processes become of importance when dealing with carbides, stainless steels, ceramics and glass. Four main types of application are of industrial relevance:

- machining of hard and brittle materials with a vibrated tool and free abrasive particles
- cutting with vibrating tools alone

- metal tube drawing
- final surface-hardening treatment.

Machining with slurry

Ultrasonic machining of materials with abrasive particles lies in the feeding of abrasive slurry *into* a gap between vibrated horn tool (normally operating around 20 kHz) and the workpiece surface. Abrasive slurry particles subject to ultrasonic vibrations knock out tiny pieces of material from the workpiece surface, producing a depression which has a profile of the horn end. Abrasive particles (containing silicon carbide, boron carbide or alumina) gradually degrade (wear out) and so new portions of abrasive slurry must be fed into the process zone, which simultaneously assists in the removal of particles detached from the worked material. Another use is in the production of three-dimensional engraved glass that can easily be produced by a shaped ultrasonic tool using abrasive slurry.

Cutting

Ultrasonic cutting has been available to industry since the early 1950's specifically for accurate profile cutting of brittle materials such as ceramics and glass. It has also been extensively used in the aerospace industry since the 1970's for glass and carbon fibre composites. In recent years ultrasonic cutting has been introduced into the food processing industry where it would appear to have far wider application than the laser and water (oil) jet cutting technologies introduced in the 1980's [18, 19].

Ultrasonic cutting uses a knife type blade attached through a shaft to an ultrasonic source. Essentially the shaft with its blade behaves as an ultrasonic horn driven normally at 20 kHz and with a generator similar to that of a welder operating at around 2 kW. The cutting action is a combination of the pressure applied to the sharp cutting edge surface and the mechanical longitudinal vibration of the blade. Typically the tip movement will be in the range 50 to 100 microns peak to peak. Several advantages arise from this technology:

- The ultrasonic vibration of 20 kHz applies an intermittent force to the material to be cut and generates a crack (cut) at the tip, controlling its propagation or growth thereby minimising the stress on the bulk material.
- The repeated application of the cutting tip to the product applies a local fatiguing effect that reduces significantly the overall force required to break the bonds of the bulk material.
- In conventional cutting the blade has to compress the bulk material to allow a gap the width of the blade to pass through and this applies a tensile rupturing force at

the crack tip. With ultrasonic cutting the whole blade moves or vibrates continuously as it stretches and contracts. This very high frequency movement effectively reduces the co-efficient of friction to a very low level, enabling the blade to slide more easily through the bulk material.

Metal tube drawing

In the 1950's an investigation into the effect of ultrasonic vibrations on the mechanical properties of metals showed that superimposing an alternating stress on a workpiece greatly affected the process rate and considerably reduced the force necessary for workpiece deformation [20].

One of the consequences of this is that improvements in the cold drawing of metal tubing can be achieved when the die to be used is subjected to radial ultrasonic vibrations. There are several advantages obtained from drawing round products through a die ultrasonically vibrating in a radial mode, these include:

- reductions of area per single pass approaching or exceeding 50 %
- much reduced draw force as a result of ultrasonically reduced friction
- greatly improved surface textures of the order of 0.12 μ .

Commercial drawing of tube in 'difficult-to-draw' alloys through such a die subjected to 20 kHz was originally established in the 1960's for tubes in the diameter range 5 mm to 35 mm. Further developments of the technique have expanded the ranges to the drawing of tubes having diameters as large as 60 mm and rods in the diameter range 5 mm to 15 mm. The method also allows cups and cans having diameters between 5 mm and about 55 mm to be draw-ironed [21].

Ultrasonic surface treatment

Surface deformation is a widespread and effective method for hardening metallic materials. With this method, the surface layer of a material is a subject of high compressive stresses, which results in a better product strength, durability, and reliability. Many surface deformation techniques have been employed including rolling, ball treatment, and shot blasting (peening). Ultrasonic surface hardening provides an efficient alternative. Applied ultrasonic vibrations relieve residual stresses and improve surface finish and hardness, thereby providing a better wear resistance of products.

The ultrasonic rolling or ball treatment process is similar to conventional ball deformation methods, in which a roller (or a ball) is pressed onto the surface of a workpiece moving specifically with respect to the tool. The only difference between ultrasonic and conventional processes is that in the former the pressure applied is also subjected to ultrasonic vibrations.

Shot peening of metallic materials is an effective procedure for increasing the fatigue limit of alloys, as well as preventing tensile and corrosion cracks of structural parts. A conventional approach to surface treatment is the use of shot peening a process whereby small metal shots are agitated and impact onto a surface. This strengthens the surface layers due to the introduction of inherent compression stresses into the surface region. Through shot peening some of the problems associated with production e.g. edge decarbonisation, roughness and inherent tensile stresses are relieved. Shot peening results in considerable increase of the operating and service life of constructions affected by dynamic loads.

Recently an ultrasonic surface treatment, similar to shot peening, has been developed. In this process a powerful ultrasonic field is generated to transfer high kinetic energy to steel balls that hit the surface of the workpiece being treated. The energy transferred to the workpiece during a one-ball impingement event is small. The required surface strain is achieved through repeated action on the surface of the workpiece. The process creates homogeneous residual stress simultaneously on each side of the parts to be treated. The process will act on hardness, corrosion fatigue, friction coefficient and improvement of the surface of the material.

Atomisation

The conventional method of producing an atomised spray from a liquid is to force it at high velocity through a small aperture. A typical domestic example is a spray mist bottle used for perfume. The disadvantage in the design of conventional equipment is that the requirement for a high liquid velocity and a small orifice restricts its usage to low viscosity liquids and these atomisers are often subject to blockage at the orifice.

Fig. 1.4 shows a schematic diagram of a whistle atomiser. The system comprises of an air or gas jet which is forced into an orifice where it expands and produces a shock wave. The result is an intense field of sonic energy focused between the nozzle body and

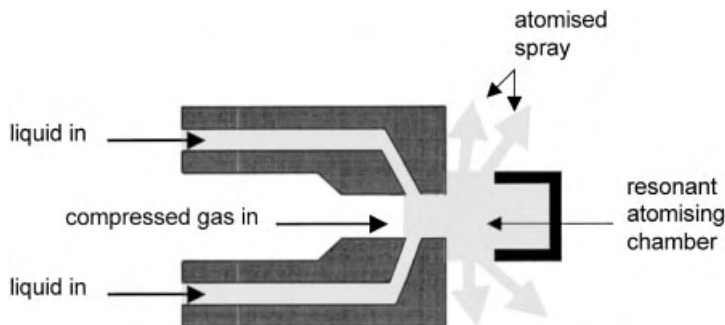


Fig. 1.4. Schematic diagram of a whistle atomiser.

the resonator gap. When liquid is introduced into this region it is vigorously sheared into droplets by the acoustic field. Air by-passing the resonator carries the atomised droplets downstream in a fine soft plume shaped spray. The droplets produced are small and have a low forward velocity. Atomised water sprays have many uses including dust suppression in industry and humidifiers for horticultural use under glass.

There are several different types of ultrasonic atomiser based on a sonic horn in which the liquid is pumped through a central tube and emerges at the vibrating tip [22]. Although this type of atomiser is usually restricted to fairly low viscosity material the ultrasonic vibration itself does help to reduce the shear viscosity of the liquid. When using sonic atomisation, it is the tip motion that causes atomisation and not the velocity of ejection through the orifice. Since the “nozzle” is under constant agitation there is less risk of blockage with this design. In the coating industry, apart from the obvious advantages of being able to use higher viscosity material with no jet blockage, sonic spraying has another great advantage over conventional methodology. Normal jet atomisation ejects particles at high velocity and some of these would collide with a surface with such high energy that “bounce-back” might occur, particularly if there was no strong adhesion between the ejected spray and the surface. Although electrostatic methods have been employed in conventional spraying in order to reduce “bounce-back”, sonic atomisation does not produce high particle velocity and so impact adhesion is much less of a problem. Either the ultrasonic power or the frequency of tool vibration can accurately control the particle size of sonically atomised sprays such that greater control of coating is possible. Ultrasonic atomisation has also been used to produce finely particulate sprays from such materials as molten glass and metal.

Ultrasonic sprays produced *via* horns are also finding use in spray drying installations where there are clear advantages in producing minimal particle velocity with a controlled particle size through a non-clogging nozzle.

Ultrasonic melt treatment in metal casting

The final quality of a cast metal product is broadly dependent upon any factors which will have an effect on the metal solidification. The mechanical properties of the casting will largely be determined by the cast structure. Any structural defects occurring in the cast product may be transferred to the final product. Thus any process which would reduce defects and improve the metal structure of a cast product would clearly be of benefit to the foundry industry.

One major problem associated with aluminium and light alloy castings is the inability to completely eliminate the various production defects in their structure, such as gas cavities, porosity and intermetallic inclusions. The All-Russia Institute

of Light Alloys (VILS) has been involved in basic and applied research concerning the effects of power ultrasound on the metallurgical processes of refining and solidification of aluminium and magnesium alloys for many years [23, 24]. These investigations have shown that the major role of acoustic cavitation is in degassing, filtration and grain refinement.

Ultrasonic degassing has been shown to be very efficient for both aluminium and magnesium based alloys. Hydrogen filled bubbles easily form during the negative pressure phase of a sound wave and coalesce to become large enough to migrate to the surface. The generation of pressure pulses and cumulative jets during the cavitation bubble collapse also facilitates melt penetration through the fine filters used to remove solid impurities from the melt.

When ultrasonic vibrations are coupled to the solidifying metal structural changes occur including grain refinement, suppression of columnar grain structure, increased homogeneity and reduced segregation. Ultrasonic waves also decrease the viscosity of the molten metal. Additionally, mechanical mixing of the melt due to cavitation collapse and acoustic streaming results in a much reduced temperature gradient across the solidifying charge, and, an increase in the transfer of fine solid particles. In large-scale tests, commercial aluminium alloys have been ultrasonically treated either during continuous casting or in shaped casting processes. It was found that ultrasound had little effect on the structure of commercially pure grade aluminium. However, on addition of 0.1 wt% titanium, zirconium and boron carbide, ultrasonic irradiation of the solidifying aluminium resulted in the formation of ultrafine non-dendritic structure of light alloys that improved the plasticity without strength loss. This is very important for crack-free production and processing of large-scale ingots from structural light alloys. Extruded, rolled and forged metal produced from non-dendritic ingots demonstrated an improved plasticity without strength loss and improved service characteristics, i. e. low- and multi-cycle fatigue endurance, fracture toughness and corrosion resistance.

1.3.5

Processing Applications

Mixing and emulsification

There are a large number of industrial processes which employ cavitation as an energy source for the generation of fine emulsions and dispersions. One of the earliest devices which was developed for this purpose was the so-called liquid whistle (see Chapter 7) and this continues to be used widely. Typical examples of the uses of such whistles include the preparation of emulsion bases for soups, sauces or gravies which consist of a premix of water, milk powder, edible oil and fat together with flour or starch

as thickening agent. After passing through the homogeniser a fine particle size emulsion is generated with a smooth texture. Another example is the production of ketchup as a smooth product with increased thickness and improved taste compared with conventional mixers as a result of the complete dispersion of any clumps of tomato pulp.

In the textile industry poor quality dyeing of fabrics usually can be attributed to the mechanical mixing used. Agglomerates of non-dispersed dye can produce a speckled appearance and uneven mixing may change the shade. By passing the mixture through an ultrasonic homogeniser before use these problems can be overcome.

Extraction

When cavitation bubble collapse occurs near a porous material the jet that is generated is able to force liquid to penetrate the surface. This effect can be utilised to enhance any process that involves either extraction or impregnation of a liquid in a solid.

The classical techniques for the solvent extraction of chemical compounds from vegetable material are based upon the correct choice of solvent and conditions e.g. heating or agitation. A range of commercially important pharmaceuticals, flavours and colourants are now derived from vegetable sources. It has been shown that the solvent extraction of organic compounds contained within the body of plants and seeds is significantly improved by the use of power ultrasound [25].

Impregnation

The benefits of sonochemically forced impregnation of porous materials can be found in a wide variety of technologies. One of these is in the preparation of catalysts of the type often termed “egg shell” where a catalytically active material is supported on the outside of an inert support material. Thus a catalyst comprising of 1 % (w/w) ruthenium on the surface of 4 mm grain size alumina can be made by adsorbing RuCl_3 from aqueous solution onto the alumina followed by reducing the Ru^{3+} to Ru metal using hydrazine. The resulting catalyst prepared under sonochemical conditions was very different from that prepared conventionally in that there was a greater penetration of the metal into the support with no metal close to the surface [26]. Similar results have been obtained by the same group using catalytic palladium supported on carbon.

The same process of sonochemically forced impregnation can be used to enhance the dyeing of leather. Normal vat dyeing process involves steeping the leather in an aqueous solution of the dye for a period of time. In the presence of 20 kHz ultrasound (approx. 5 W cm^{-2}) the dye impregnation can be substantially increased [27]. Ultrasonically enhanced dyeing offers the commercially attractive possibilities of attaining a more rapid turnover and savings on the quantities of dye used. Since most of the

processes in leather technology involve liquid treatments and surface penetration there are a number of tanning processes which may be helped by sonication.

Filtration

The requirement to remove suspensions of solids from liquids is common to many industries. This separation can be either for the production of solids-free liquid or to isolate the solid from its mother liquors. Conventionally membranes of various sorts have been employed for these processes ranging from the simple filter pad through semi-permeable osmotic type membranes to those which are used on a size-exclusion principle for the purification of polymeric materials. Unfortunately the conventional methodologies often lead to “clogged” filters and, as a consequence, there will always be the need to either replace filters or stop the operation and clean them on a regular basis. The application of ultrasound enables the filtration system to operate more efficiently and for much longer periods without maintenance through two specific effects. Sonication will cause an agglomeration of the fine particles and will supply sufficient vibrational energy to the system to keep the particles partly suspended and therefore leave more free “channels” for solvent elution. Studies of acoustic filtration and separation processes continue to be an important area of applied acoustics research [28].

Crystallisation

In conventional crystallisation techniques (e.g. in penicillin production), a solution containing materials to be crystallised is super-saturated either by cooling or by evaporation and is then seeded. The problem with seeding is that it may be initiated non-uniformly and this can result in crystal growth proceeding at different rates at different nuclei sites. The resulting crystals may then show a very broad and uneven crystal size distribution. It is also of considerable practical importance to be able to control the onset of crystallisation in a large-scale production process. Often it occurs in an uncontrolled manner simply due to a slight change in external factors such as a temperature or pressure fluctuation.

Ultrasound has proved to be extremely useful in crystallisation processes since it can initiate seeding and control subsequent crystal growth in a saturated or super-cooled medium. This is thought to be due to cavitation bubbles themselves acting as nuclei for crystal growth and to the disruption of seeds/nuclei already present within the medium thus increasing the number of nuclei present in the medium. Through the correct choice of sonication conditions it is possible to produce crystals of a uniform and designated size which is of great importance in pharmaceutical preparations [29].

Power ultrasound also has an additional property which is particularly beneficial in crystallisation operations namely that the cleaning action of the cavitation effectively stops the encrustation of crystals on cooling elements in the crystallisation vat and thereby ensures continuous efficient heat transfer.

1.4

Ultrasound in Chemistry

Perhaps somewhat surprisingly sonochemistry is not a particularly new subject – it was under active investigation in the first half of the 20th century. There are literature references to applications in polymer and chemical processes in the 1940's [30, 31]. Despite the fact that a book dealing with sonochemistry was translated from Russian and published in 1964 [32] the major renaissance in the subject has occurred only over the last two decades of the century. This is undoubtedly due to the more general availability of commercial ultrasonic equipment nowadays. In the 1960's the ultrasonic cleaning bath began to make its appearance in metallurgy and chemical laboratories. Having seen the way in which these baths cleaned soiled glassware and dispersed immiscible organic solvents in aqueous detergent it was not surprising that chemists began to consider using them to enhance chemical reactivity – as indeed we ourselves did in the early 70's. A chapter will be devoted to sonochemistry later in this book.

For the majority of chemists an interest in power ultrasound springs from the fact that it provides a form of energy for the modification of chemical reactivity which is different from that normally used e. g. heat, light and pressure. Power ultrasound produces its effects *via* cavitation bubbles. These bubbles are generated during the rarefaction cycle of the wave when the liquid structure is literally torn apart to form tiny voids which collapse in the compression cycle. It has been calculated that pressures of hundreds of atmospheres and temperatures of thousands of degrees are generated on collapse of these bubbles. The physical background for the generation and collapse of such bubbles will be discussed in detail in Chapter 2.

Chemical activation for sonochemistry is provided through the energy of collapse of the cavitation bubbles. The most popular view of this process is incorporated in the so-called Hot-Spot theory. This involves the concept that the cavitation bubble collapses rapidly and violently and, in doing so, generates temperatures of many thousand Kelvin and pressures of several thousand atmospheres. Certainly the whole subject of what actually happens during cavitation bubble collapse is still under active discussion and provides the basis for a range of research projects for chemists, engineers, mathematicians and physicists. Whatever the true nature of the collapse the mechanical and chemical effects of cavitation occur in three distinct regions:

- within the bubble itself which can be thought of as a microreactor
- in the liquid region immediately adjacent to the bubble where the temperatures are not so great and
- in the immediate vicinity of the bubble where the shockwave produced on collapse will create enormous shear forces.

The synthetic chemist will be mainly concerned with reactions in solution and the effects of ultrasound in such cases are best summarised in terms of four different reaction types.

1.4.1

Reactions Involving Metal or Solid Surfaces

There are two types of reaction involving metals (1) in which the metal is a reagent and is consumed in the process and (2) in which the metal functions as a catalyst. While it is certainly true that any cleansing of metallic surfaces will enhance their chemical reactivity, in many cases it would seem that this effect alone is not sufficient to explain the extent of the sonochemically enhanced reactivity. In such cases it is thought that sonication serves to sweep reactive intermediates, or products, clear of the metal surface and thus present renewed clean surfaces for reaction. Other ideas include the possibility of enhanced single electron transfer (SET) reactions at the surface.

1.4.2

Reactions Involving Powders or Other Particulate Matter

Just as with the metal surface reactions described above, the efficiency of heterogeneous reactions involving solids dispersed in liquids will depend upon the available reactive surface area and mass transfer.

Conventional technology involves agitating and stirring with rotating devices and baffled pipes as the processors of fluids when mixing, reacting or dissolving small and submicron sized particles on an industrial scale. This can take many hours, days or even weeks until the desired properties are obtained. The basic problem with conventional rotational mixing techniques, when trying to disperse solid particles of 10 microns in diameter or smaller in a liquid is that the rate of mixing and mass transfer of these particles through the medium reaches a maximum. In fact the mass transfer coefficient K reaches a constant value of about 0.015 cm s^{-1} in water, and liquids of similar viscosity, and cannot be increased any further by increasing the speed of rotational agitation, no matter how large this increase may be. Sonication provides a solution to this problem in that power ultrasound will give greatly enhanced mixing.

1.4.3

Emulsion Reactions

Ultrasound is known to generate extremely fine emulsions from mixtures of immiscible liquids. Ultrasonic homogenisation has been used for many years in the food industry for the production of tomato sauce, mayonnaise and other similar blended items. In chemistry such extremely fine emulsions provide enormous interfacial contact areas between immiscible liquids and thus the potential for greater reaction between the phases. This can be particularly beneficial in phase transfer catalysis.

1.4.4

Homogeneous Reactions

From the above one might be tempted to attribute ultrasonically enhanced chemical reactivity mainly to the mechanical effects of sonication. However this cannot be the whole reason for the effect of ultrasound on reactivity because there are a variety of homogeneous reactions which are also affected by ultrasonic irradiation. How, for example, can we explain the way in which power ultrasound can cause the emission of light from sonicated water (sonoluminescence), the fragmentation of liquid alkanes, the liberation of iodine from aqueous potassium iodide or the acceleration of homogeneous solvolysis reactions?

The answer to these questions lies in the actual process of cavitation collapse. The microbubble is not enclosing a vacuum – it contains vapour from the solvent and any volatile reagents so that, on collapse, these vapours are subjected to the enormous increases in both temperature and pressure referred to above. Under such extremes the solvent and/or reagent suffers fragmentation to generate reactive species of the radical or carbene type some of which would be high enough in energy to fluoresce. In addition the shock wave produced by bubble collapse or even by the propagating ultrasonic wave itself, could act to disrupt solvent structure which could influence reactivity by altering solvation of the reactive species present.

Tab. 1.2. Possible benefits from the use of power ultrasound in chemistry.

-
- A reaction may be accelerated or less forcing conditions may be required if sonication is applied.
 - Induction periods are often significantly reduced as are the exotherms normally associated with such reactions.
 - Sonochemical reactions often make use of cruder reagents than conventional techniques.
 - Reactions are often initiated by ultrasound without the need for additives.
 - The number of steps that are normally required in a synthetic route can sometimes be reduced.
 - In some situations a reaction can be directed to an alternative pathway.
-

The practicing chemist might thus expect to use ultrasound for a range of applications and perhaps achieve one or more of a number of the beneficial effects that are listed in Tab. 1.2.

References

1. A.P. Cracknell, *Ultrasonics*, Wykenham Publishers, 1980, Ch. 6, 92–105.
2. J. Curie and P. Curie, *Compt. Rend.*, 1880, **91**, 294.
3. J. Curie and P. Curie, *Compt. Rend.*, 1881, **93**, 1137.
4. F. Galton, *Inquiries Into Human Faculty and Development*, MacMillan, London, 1883.
5. J. Thornycroft and S.W. Barnaby, Torpedo boat destroyers, *Proc. Inst. Civil. Engineers*, 1895, **122**, 51.
6. Lord Rayleigh, On the pressure developed in a liquid during the collapse of a spherical cavity, *Phil. Mag.*, 1917, **34**, 94–8.
7. T.J. Mason and E.D. Cordemans, Ultrasonic intensification of chemical processing and related operations – a review, *Trans. I. Chem. E.*, 1996, **74**, 511–516.
8. T.J. Mason, A sound investment, *Chemistry and Industry*, 1998, 878–882.
9. L.A. Crum, T.J. Mason, J.L. Reisse, and K.S. Suslick (eds.), *Industrial applications of sonochemistry and power ultrasonics, Sonochemistry and Sonoluminescence*, NATO ASI Series, Kluwer Academic Publishers, 1999, 377–390, ISBN 0-7923-5549-0.
10. F.F. Rawson, *Phys. Bull.*, 1987, **38**, 255.
11. R.M.G. Boucher, US Patent 4 211 744 (1980).
12. T. Quartly-Watson, The importance of power ultrasound in cleaning and disinfection in the poultry industry – a case study, *Ultrasound in Food Processing*, M. Povey and T.J. Mason (eds.), Blackie Academic and Professional, 1998, ISBN 0-7514-0429-2.
13. M. Rule, *The Mary Rose*, Conway Maritime Press, 1982.
14. J.C. Birnholtz and E.E. Farrell, *American Scientist*, 1984, **72**, 608.
15. L. Crum and K. Hynynen, Sound Therapy, *Physics World*, 1996, 28.
16. Research at Coventry University sponsored by Advanced Health Care, Tonbridge, Kent, U.K., 1990.
17. O.V. Abramov, *High-Intensity Ultrasound: Theory and Industrial Applications*, Gordon and Breach, London, 1998.
18. F.F. Rawson, *Phys. Bull.*, 1987, **38**, 255.
19. F.F. Rawson, An introduction to ultrasonic food cutting, *Ultrasound in Food Processing*, M.J.W. Povey and T.J. Mason (eds.), Thomson Science, London, 1997, 193.
20. F. Blaha and B. Langenecker, *Z. Naturwiss.*, 1955, **20**, 556.
21. G.R. Dawson, C.F. Winsper, and D.H. Sansome, A complete appraisal of oscillatory metal working, *Journal of Metal Working*, Aug./Sept. 1970, Part I, 234–238, Part II, 254–261.
22. A. Morgan, Ultrasonic atomisation, *Advances in Sonochemistry*, T.J. Mason (ed.), JAI Press, London, 1993, **3**, 145–164.
23. G.I. Eskin, *Ultrasonic Treatment of Light Alloy Melts*, Gordon&Breach Science Publishers, Amsterdam, 1998, 4.
24. G.I. Eskin, Degassing, filtration, and grain refinement processes of light alloys in a field of acoustic cavitation, *Advances in Sonochemistry*, T.J. Mason (ed.), JAI Press, London, 1996, **4**, 101–159.
25. M. Vinatoru, M. Toma and T.J. Mason, Ultrasonically assisted extraction of bio-active principles from plants and their constituents, *Advances in Sonochemistry*, T.J. Mason (ed.), JAI Press, London, 1999, **5**, 209–248.

26. C.L. Bianchi, E. Gotti, L. Toscano, and V. Ragaini, *Ultrasonics Sonochemistry*, 1997, **4**, 317.
27. J.-P. Xie Dyeing, J.F. Ding, T.J. Mason, and G.E. Attenburrow, Influence of power ultrasound on leather processing. Part 1, *Journal of the American Leather Chemists Association*, 1999, **94**, 146–157.
28. E.S. Tarleton and R.J. Wakeman, Ultrasonically assisted separation processes, *Ultrasound in Food Processing*, M.J.W. Povey and T.J. Mason (ed.), Blackie Academic and Professional, London, 1998, 193–218.
29. C. Price, *Pharmaceutical Technology Europe*, 1997, October Issue.
30. A. Weissler, *J. Chem. Educ.*, 1948, 28.
31. H. Mark, *J. Acoust. Soc. Amer.*, 1945, **16**, 183.
32. I.E. El'Piner, Ultrasound physical, *Chemical and Biological Effects*, Consultants Bureau, New York, 1964.

2

General Principles

2.1

Introduction

In this chapter we will deal with those parts of acoustic wave theory which are relevant to chemists in the understanding of how they may best apply ultrasound to their reaction system. Such discussions will of necessity involve the use of mathematical concepts to support the qualitative arguments. Wherever possible the rigour necessary for the derivation of the basic mathematical equations has been kept to a minimum within the text. An expanded treatment of some of the derivations of key equations is provided in the appendices. For those readers who would like to delve more deeply into the physics and mathematics of acoustic cavitation numerous texts are available dealing with bubble dynamics [1–3]. Others have combined an extensive treatment of theory with the chemical and physical effects of cavitation [4–6].

A summary of the major physical factors influencing sonochemical events has also been included at the end of the chapter for those more interested in the practical applications than the theoretical considerations of ultrasound. Since the vast majority of chemical systems, whether they are homogeneous or heterogeneous, are studied in the solution phase, the discussions here will be restricted to liquid systems.

Being a sound wave, ultrasound is transmitted through any substance, solid, liquid or gas, which possesses elastic properties. The movement of the vibrating body (i. e. sound source) is communicated to the molecules of the medium, each of which transmits the motion to an adjoining molecule before returning to approximately its original position. For liquids and gases, particle oscillation takes place in the direction of the wave and produces *longitudinal* waves (Fig. 2.1a). Solids, however, since they also possess shear elasticity, can also support tangential stresses giving rise to *transverse* waves, in which particle movement takes place perpendicular to the direction of the wave (Fig. 2.1b).

An easily visualised example of a transverse wave is that obtained when a stone is dropped into a pool of water. The disturbance, or water wave, can be seen spreading across the surface in the form of circular crests of increasing radius. Any objects in the pool (e. g.

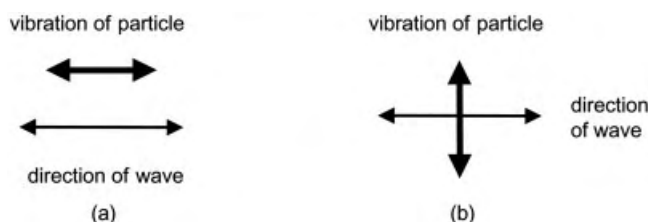


Fig. 2.1. Wave particle movement; (a) longitudinal waves; (b) transverse waves.

cork or wood) move up and down when the wave reaches them but they do not move forward in the direction of the wave. In other words, if the motion of particles was considered to be equivalent to the motion of the cork or wood, the particles would move up and down in a direction perpendicular to the horizontal movement of the wave.

A good example of a longitudinal wave can be seen when a coiled spring, anchored at one end, is given a sharp push from the other end. The action causes a disturbance in the spring (Fig. 2.2) which can be seen to “run” through the whole length.

If an individual coil is identified, (e. g. by painting it white), as the wave passes the coil it will be seen firstly to move forward in the direction of the wave and subsequently to return to its original position. For a series of consecutive waves, the motion will be one of oscillation. The physical aspect of this motion is best understood by examining the action of a tuning fork vibrating in air (Fig. 2.3). Movement of the prong, *R*, to the right causes the air layer closest to it to be displaced to the right, the disturbed layer pushing the next layer to it etc. (Fig. 2.3a) – i. e. the layers are compressed.

Movement of prong *R* to the left (Fig. 2.3c) causes displacement of the air to the left and hence there is a deficiency of layers to the right of the fork. This is the rarefaction region. The return of *R* to the right will now begin a new cycle and the wave will proceed with a series of compression and rarefaction portions. It is important to note that the disturbance does not cause the layer to move bodily but to vibrate about

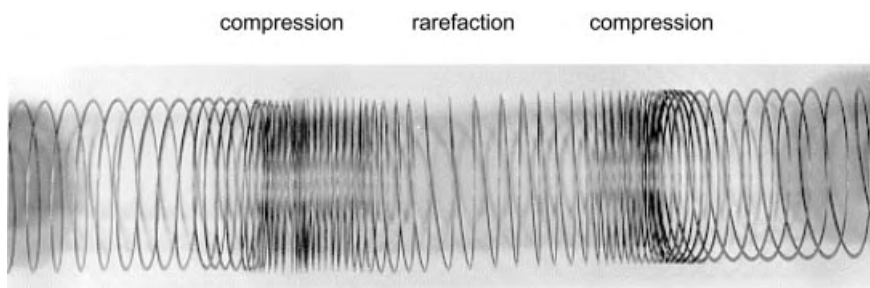


Fig. 2.2. Illustration of wave motion in a spring.

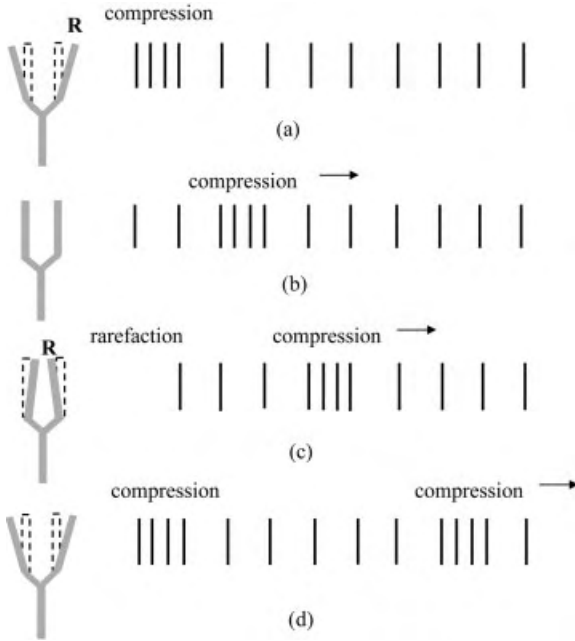


Fig. 2.3. Longitudinal waves in air; (a) first outstroke of prongs; (b) prongs in normal position; (c) first instroke of prongs; (d) second outstroke of prongs.

a mean rest position – just like the coil of the spring. At any time (t) the displacement (x) of an individual air molecule from its mean rest position is given by Eq. 2.1.

$$x = x_0 \sin 2\pi ft \quad (2.1)$$

where x_0 is the displacement amplitude, or maximum displacement of the particle, and f is the frequency of the sound wave (Fig. 2.4).

Differentiation of the above leads to an expression for the particle velocity (Eq. 2.2)

$$v = dx/dt = v_0 \cos 2\pi ft \quad (2.2)$$

where v_0 ($= 2fx_0$) is the maximum velocity of the particle.

Besides the variation in the molecules' position when the sound wave travels through the air, there is a variation in pressure (Fig. 2.5). At the point where the layers are crowded together (i. e. where the molecules are compressed) the pressure is higher

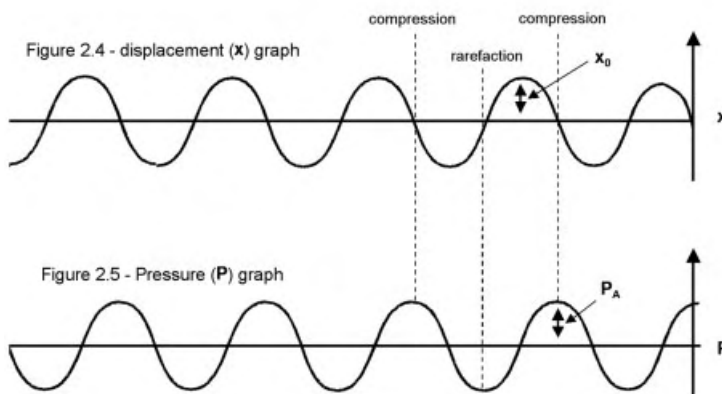


Fig. 2.4. Displacement (x) graph.

Fig. 2.5. Pressure (P) graph.

than normal at that instant, whereas at the region where the layers are furthest apart (i. e. the rarefaction region) the pressure is lower than normal.

As with displacement, the pressure (P_a) at any instant is time (t) and frequency (f) dependent (Eq. 2.3).

$$P_a = P_A \sin 2\pi ft \quad (2.3)$$

where P_A is the pressure amplitude.

From Figs. 2.4 and 2.5, the maximum particle displacement appears at the point of minimum pressure ($P = 0$) – i. e. the displacement and pressure are out of phase. Although this may at first cause some confusion it may be easily demonstrated by reference to Fig. 2.6.

On passage of the wave, the particles, originally at the rest positions A, B, C etc are displaced to their new positions A, B', C' etc. Displacements such as BB' (or CC') which are to the right and in the direction of the wave are represented by lines such as Bb and Cc above the x-axis. Displacements such as EE', to the left and in the opposite direction to the wave's movement are drawn as Ee below the x-axis – i. e. negative displacements. In the region P the particles (C', P, E') are crowded to-

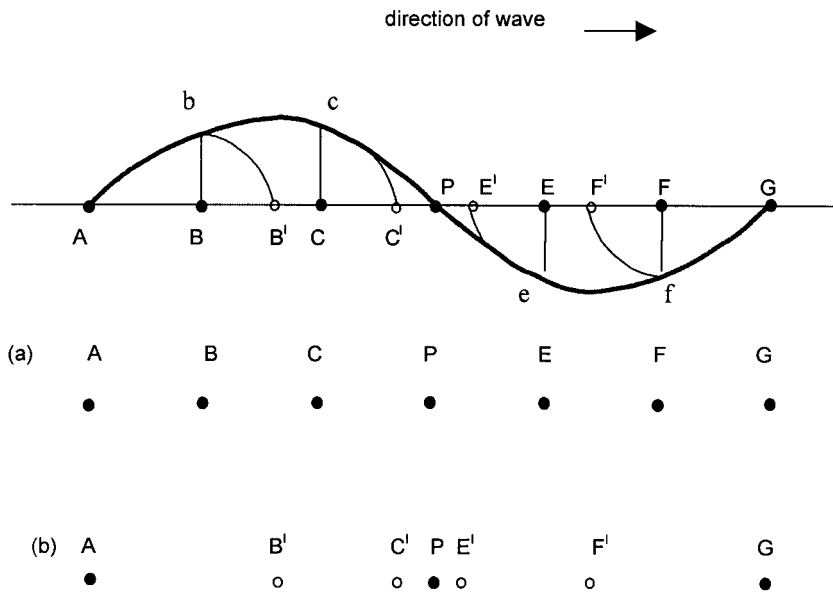


Fig. 2.6. Displacement of a longitudinal wave:
 • original position; o displaced position.

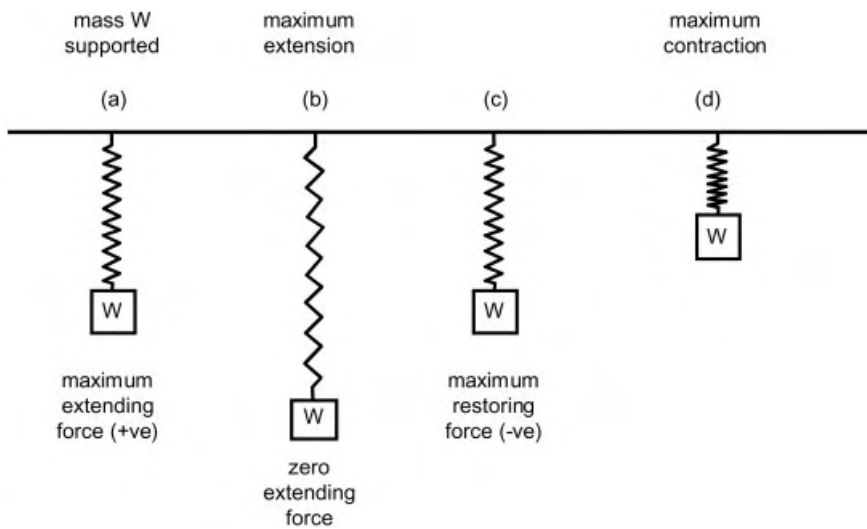


Fig. 2.7. Out of phase displacement; weights on spring.

gether and there is compression – i. e. high pressure values. At A the particles are more separated than normal and there is rarefaction i. e. decreased pressure. The displacement and pressure are out of phase.

Perhaps the most easily visualised demonstration of the out of phase nature of displacement and pressure is obtained by attaching a supported weight on a spring (Fig. 2.7a).

On removing the support the spring will immediately elongate due to the force (equivalent to pressure) of the weight acting on it. At maximum extension the overall force (or pressure) acting on the spring is zero (Fig. 2.7b). On recoil the spring contracts lifting the weight upwards and the force increases in magnitude but in the negative sense. At the instant of maximum contraction (i. e. negative displacement) the overall force on the spring is again zero (Fig. 2.7d).

One of the most important characteristics necessary to completely identify a wave is its intensity, where the intensity is a measure of the sound energy the wave produces. For a sound wave in air, the mass (m) of air moving with an average velocity (v) will have associated with it a kinetic energy of $(mv^2)/2$ (joules). In the strictest sense the intensity is the amount of energy carried per second per unit area by the wave. Since the units of energy are joules (J) and a joule per second is a watt (W), then the usual unit of sound intensity (especially in sonochemistry) will be W cm^{-2} . As we will see later (Eq. 2.13), the maximum intensity (I) of the sound wave is proportional to the square of the amplitude of vibration of the wave (P_A^2). This will have important repercussions in our study of chemical systems.

Let us now turn our attention to the application of the sound wave to a liquid since this is the medium of importance to the practising chemist. The sound wave is usually introduced to the medium by either an ultrasonic bath or an ultrasonic horn (see Chapter 7). In either case, an alternating electrical field (generally in the range 20–50 kHz) produces a mechanical vibration in a transducer, which in turn causes vibration of the probe (or bottom of the bath) at the applied electric field frequency. The horn (or bath bottom) then acts in a similar manner to one prong of a tuning fork. As in the case of air, the molecules of the liquid, under the action of the applied acoustic field, will vibrate about their mean position and an acoustic pressure ($P_a = P_A \sin 2\pi ft$) will be superimposed upon the already ambient pressure (usually hydrostatic, P_h) present in the liquid. The total pressure, P , in the liquid at any time, t , is given by Eq. 2.4.

$$P = P_h + P_a \quad (2.4)$$

where P_a is the applied acoustic pressure (Eq. 2.3). The displacement (x) and the velocity (v) of the particles are given, as before, by Eqs. 2.1 and 2.2.

It is worth noting here, that for the ultrasound, as for any sound wave, the wavelength of sound in the medium is given by the relationship in Eq. 2.5.

$$c = \lambda f \quad (2.5)$$

For the frequencies usually employed to influence chemical processes (20–50 kHz), the wavelengths produced in the liquid medium are in the range 7.5 to 3.0 cm. For diagnostic or relaxation investigations (see below), with greater frequencies (1–100 MHz), the wavelength range will be 0.15 to 0.0015 cm. These wavelengths are considerably longer than bond length values and sonochemical effects are not therefore the result of direct interactions between the reagent and the wave as is the case in photochemistry.

2.2

Intensity and Pressure Amplitude

In our previous discussions (tuning fork in air) we pointed out that sound was a form of energy. The particles of the medium were set into vibratory motion and thereby possessed kinetic energy. This energy was derived from the wave itself. Using this principle we can deduce the energy (and hence intensity) associated with our applied ultrasonic field.

Consider the movement of a layer of the medium of area A and thickness dx , (i. e. volume $A dx$) under the action of the ultrasonic wave (Fig. 2.8).

Then the kinetic energy ($mv^2/2$) of the layer is given by Eq. 2.6.

$$KE = \frac{1}{2} (\rho A dx) v^2 \quad (2.6)$$

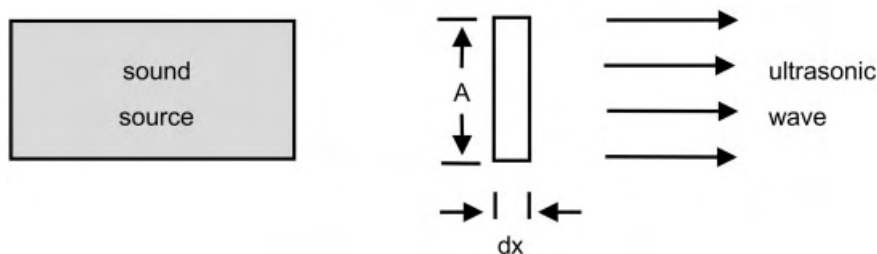


Fig. 2.8. Relationship between sound source and wave.

The energy for the whole wave E_t may be obtained by summing all such elements (i. e. integrating Eq. 2.6) to give Eq. 2.7.

$$E_t = \frac{1}{2} (\rho A x) v^2 \quad (2.7)$$

and the energy per unit volume (Ax) or energy density, E , given by Eq. 2.8.

$$E = \frac{1}{2} \rho v^2 \quad (2.8)$$

If the sound energy passes through unit cross-sectional area ($A = 1$) with a velocity of c , then the volume swept out in unit time is c (since $A = 1$), and the energy flowing in unit time is given by $E c$. Since intensity (I) has been defined as the amount of energy flowing per unit area ($A = 1$) per unit time (Eq. 2.9)

$$I = E c \quad (2.9)$$

and from Eq. 2.8

$$I = \frac{1}{2} \rho c v^2 \quad (2.10)$$

For a plane progressive wave, the particle velocity, v , can be shown [7] to be related to the acoustic pressure, P_a , by Eq. 2.11

$$\frac{P_a}{v} = \rho c \quad (2.11)$$

where ρ is the density of the medium and c the velocity of sound in the medium. (The derivation of Eq. 2.11 is given in Appendix 1). For maximum particle velocity, v_0 , the amplitude of the oscillating acoustic pressure, P_A , is given by Eq. 2.12.

$$\frac{P_A}{v_0} = \rho c \quad (2.12)$$

i. e.

$$v_0 = \frac{P_A}{\rho c} \quad (2.12a)$$

Thus the intensity of the sound wave (from Eqs. 2.10 and 2.12a), may be expressed as Eq. 2.13

$$I = \frac{P_A^2}{2\rho c} \quad (2.13)$$

i. e. the sound intensity is proportional to the square of the acoustic amplitude.

Clearly, to measure the sound intensity at a particular point in a medium, either the maximum particle velocity, v_0 (Eq. 2.2) or the maximum pressure amplitude, P_A (Eq. 2.13) must be determined. In practice, this is extremely difficult and for most sonochemical applications a calorimetric determination of the total ultrasonic energy delivered to the medium is considered to be sufficient (see below). As an example of the use of Eq. 2.13 let us consider the passage of a wave, of frequency 20 kHz and intensity 1 W cm^{-2} , through water at room temperature. If we take the density of water (ρ) to be 1000 kg m^{-3} and the velocity of sound (c) to be 1500 m s^{-1} , then the maximum pressure amplitude, P_A (which is calculated as $(2\rho c I)^{1/2}$) will be $+(1.73 \times 10^5) \text{ N m}^{-2}$. This means the acoustic pressure varies from approx. $+1.7 \text{ atm}$ to -1.7 atm twenty thousand times per second. The maximum particle velocity v_0 (given by Eq. 2.12) and displacement amplitude, x_0 , (from the relationship $v_0 = 2\pi f x_0$) can be calculated to be $11.55 \times 10^{-2} \text{ m s}^{-1}$ and $9.18 \times 10^{-5} \text{ cm}$ respectively. Also it can easily be shown that the particle acceleration, a (given by dv/dt) has an acceleration amplitude (a_0) is given by $a_0 = 4\pi^2 f^2 x_0$. For the above values of f , ρ and c , this yields a value of $1.45 \times 10^4 \text{ m s}^{-2}$, an acceleration which is approx. 1600 times greater than under the action of gravity.

2.3

Sound Absorption

During the propagation of a plane sound wave through a medium the intensity of the wave decreases as the distance from the radiation source increases. The intensity, I , at some distance, d , from the source is given by Eq. 2.14.

$$I = I_0 \exp(-2\alpha d) \quad (2.14)$$

where α is the absorption (attenuation) coefficient. This attenuation may arise as a result of reflection, refraction, diffraction or scattering of the wave or it may be the result of converting some of the mechanical (kinetic) energy of the wave into heat. For chemical applications, which usually take place in the gaseous or liquid phase, it is the latter process which is the most important. As the molecules of the medium vibrate under the action of the sound wave, they experience viscous interactions which degrade the acoustic energy into heat, and it is the absorption of this degraded acoustic energy by the medium which gives rise to the small observed bulk heating effect during the applications of high power ultrasound. In practice the experimental temperature often rises very quickly (approx. 5 °C) during the first few minutes of applying ultrasound. After this initial period the temperature remains effectively constant, provided the reaction vessel is effectively thermostatted. According to Stokes [8], the absorption coefficient in a liquid due to frictional losses, (α_s) is given by Eq. 2.15a

$$\alpha_s = (8 \eta_s \pi^2 f^2) / (3 \rho c^3) \quad (2.15a)$$

where η_s is the ordinary (or shear) viscosity of the liquid.

Kirchoff [9] has suggested that energy losses due to heat (thermal) conduction in the medium (α_{th}) must also be considered. At any instant the high pressure region will have a temperature above the average while the temperature of the low pressure regions will be below average. Heat will therefore be conducted from the high to low temperature regions and a compressed region will return less work on expansion than was required to compress it. This leads to a sound absorption coefficient (Eq. 2.15b).

$$\alpha_{th} = 2 \pi^2 K (\gamma - 1) f^2 / (\rho \gamma C_v c^3) \quad (2.15b)$$

The total loss, or absorption, caused by both viscosity and thermal conductivity is called the classical absorption coefficient α_{cl} , and is given by Eq. 2.15c.

$$\alpha_{cl} = \alpha_s + \alpha_{th} = \frac{2\pi^2}{\rho c^3} \left\{ \frac{4}{3} \eta_s + \frac{(\gamma - 1)K}{\gamma C_v} \right\} f^2 \quad (2.15c)$$

Since $C_p/C_v = \gamma$, i.e. $\gamma C_v = C_p$ then the above may be written as Eq. 2.16.

$$\alpha_{cl} = \frac{2 \pi^2 f^2}{\rho c^3} \left\{ \frac{4}{3} \eta_s + \frac{(\gamma - 1)K}{C_p} \right\} \quad (2.16)$$

However when values of the calculated absorption coefficient are compared with those obtained experimentally, the agreement is often poor. For example if we take water at 20 °C for which $\eta_s = 1c_p$, $\rho = 1 \text{ g cm}^{-3}$ and $c = 1500 \text{ m s}^{-1}$, and we pass a sound wave of 20 kHz, then α can be calculated to be approx. $3.5 \times 10^{-8} \text{ cm}^{-1}$. Experimentally α is found to be $8.6 \times 10^{-8} \text{ cm}^{-1}$ i.e. approx. two and a half times larger. In fact only in the case of monatomic gases is the observed absorption, α_{obs} , equal to the classical absorption. In all other cases the observed absorption is greater than the classical absorption by an amount called the excess absorption, α_{ex} (given by the expression $2\pi^2 f^2 \eta_B / \rho c^3$). For complete accuracy, Eq. 2.16 should be further modified to take account of the compressional viscous forces which act during rarefaction and compression given in Eq. 2.17.

$$\alpha_{cl} = \frac{2\pi^2 f^2}{\rho c^3} \left\{ \frac{4}{3} \eta_s + \eta_B + \frac{(\gamma - 1)K}{C_p} \right\} \quad (2.17)$$

where η_B is termed the bulk viscosity.

The bulk viscosity referred to here (η_B) should not be confused with the so-called bulk viscosity of polymers which refers to the steady flow shear viscosity of the bulk undiluted polymer. Here it represents all the causes of sound absorption other than those produced by shear viscosity or thermal conductivity. Typically these may be:

- Energy losses associated with the flow of liquid molecules between positions of different density.
- Relaxation processes e.g. rotational isomerisation or vibrational energy transfer.

According to the above expressions the value of α/f^2 is a constant for a given liquid at a given temperature. Any increase in sound frequency, f , must result in a compensatory increase in α and thus a more rapid attenuation of the sound intensity with distance (Eq. 2.14). This has important consequences. Consider for example the passage of sound through water at room temperature. According to Fox and Rock [10] the value of α/f^2 for a wide variety of frequencies in water is $21.5 \times 10^{-17} \text{ cm}^{-1}$. Using this value the absorption coefficients at 21.5 kHz and 127.0 kHz can be deduced to be $9.9 \times 10^{-8} \text{ cm}^{-1}$ and $3.47 \times 10^{-6} \text{ cm}^{-1}$ respectively, and the penetration depths (Eq. 2.14) at which the sound intensities are reduced to half of their original values to be 35 km and 1 km respectively. Calculations such as these demonstrate clearly

that in order to achieve identical intensities at a given depth (distance) in a liquid, it will be necessary to use a higher initial power for the source with the higher sound frequency. For example, to achieve an intensity of 20 W cm^{-2} at a liquid depth of 10 cm (typical sonochemical reaction vessel) using sound sources of 10 kHz and 10 MHz, will require initial intensities of 20 and 30.7 W cm^{-2} respectively. Moving to higher frequencies still (e. g. 20 MHz) requires even higher initial intensities (e. g. approx. 112 W cm^{-2}). However, although the constancy of a/f^2 is satisfied for many liquids, some highly structured liquids absorb more energy at one particular frequency than another and the value of a/f^2 is found to vary with the applied frequency, f . This variation in a/f^2 with f has been used to investigate the structure of the liquids through the measurement of relaxation phenomena.

2.4

Bubble Formation and the Factors Affecting Cavitation Threshold

2.4.1

Effect of Gas and Particulate Matter

It was suggested previously that the progression of a sound wave through a liquid medium caused the molecules to oscillate about their mean position. During the compression cycle, the average distance between the molecules decreased, whilst during rarefaction the distances increased. If a sufficiently large negative pressure, P_c , is applied to the liquid (here it will be the acoustic pressure on rarefaction, $P_c = P_h - P_a$), such that the average distance between the molecules exceeds the critical molecular distance (R) necessary to hold the liquid intact, the liquid will break down and voids or cavities will be created – i. e. cavitation bubbles will be formed. The production of such bubbles has been known for many years and a good example is provided by either a ship's propeller or a paddle stirrer where the cavities are produced by the rapid rotation of the blade through the liquid. Once produced these cavities, voids, or bubbles, may grow in size until the maximum of the negative pressure has been reached. In the succeeding compression cycle of the wave however, they will be forced to contract i. e. decrease in volume and some of them may even disappear totally. (In other cases bubble oscillations may result – see later.) The shock waves produced on total collapse of the bubbles as a result of the enormous energies generated are thought to be the cause of the considerable erosion observed for components in the vicinity of the bubble. An example of this is shown in Fig. 2.9 which shows the damage produced on the surface of a 1 cm diameter titanium alloy probe tip used in our laboratories after running at 20 W cm^{-2} for 2 h in benzene).

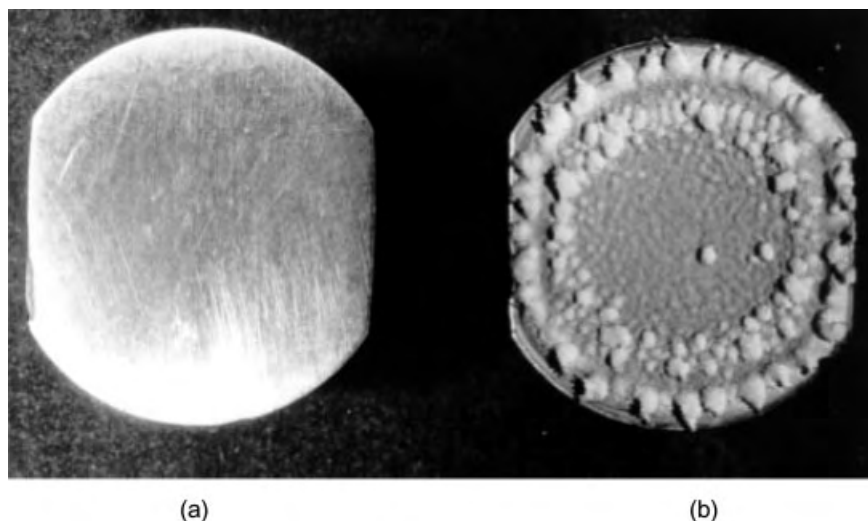


Fig. 2.9. Erosion of 1 cm diameter tip; (a) initial surface; (b) eroded surface (20 h at 20 W cm^{-2} in benzene).

Estimates of the acoustic pressure necessary to cause cavitation in water (see Appendix 2) has led to a value of approximately 1500 atm. In practice, cavitation occurs at considerably lower values ($< 20 \text{ atm}$) and this is undoubtedly due to the presence of weak-spots in the liquid which lower the liquid's tensile strength. There is now sufficient experimental evidence to suggest that one cause of weak-spots is the presence of gas molecules in the liquid. For example, it has been observed that the degassing of liquids has led to increases in the cavitation threshold – i. e. to increases in the values of the applied acoustic pressure necessary before cavitation bubbles were observed. Further, the application of external pressures which would cause any suspended gas molecules to dissolve, thereby effectively removing the gas nuclei, has also been found to lead to increases in the cavitation threshold. It can be argued for the pressure experiments that since cavitation can only be produced when the (negative) acoustic pressure exceeds the 'liquid' pressure holding the liquid intact, the application of an external pressure (i. e. pressurising the system) will necessitate the application of a higher negative acoustic pressure (P_a). This in turn will require the use of higher intensity sound waves ($P_a = P_A \sin 2\pi ft : P_A^2 = 2 I \rho c$), to overcome the liquids' cohesive forces – i. e. the threshold is seen to be raised.

It has also been found that the presence of particulate matter, and more especially the occurrence of trapped vapour-gas nuclei in the crevices and recesses of these particles, also lowers the cavitation threshold. The way in which nucleation occurs at these sites (and from similar sites on the vessel walls) is shown in Fig. 2.10.

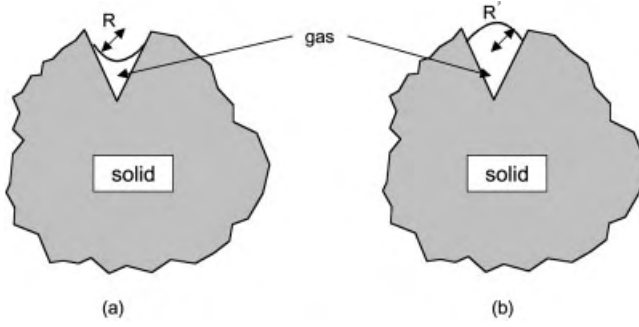


Fig. 2.10. Crevice model for stabilising cavitation nuclei; (a) for external positive pressure; (b) for external negative pressure.

During the rarefaction cycle of the acoustic wave, as the pressure in the liquid decreases the liquid gas interface becomes increasingly more convex, its angle of contact decreases, until, at sufficiently low pressure it breaks away from the surface to produce a bubble of radius, R_i .

Attempts to totally remove all particulate matter (i. e. ultrafiltration) have not been completely successful in that the theoretical limit for water's tensile strength (~ 1500 atm) has not been achieved. One of the largest experimental threshold values (~ 200 atm) is that found by Greenspan [11].

In the absence of all moieties (i. e. gas or particulate matter) it is possible to deduce an equation relating the critical pressure (P_K) which must be exceeded to create a bubble (or void) of radius R_e in an ultrapure liquid (Eq. 2.18). Provided vapour pressure is neglected then:

$$P_K = -\frac{2}{3} \left\{ \frac{(2\sigma/R_e)^3}{3(P_h + 2\sigma/R_e)} \right\}^{1/2} \quad (2.18)$$

The fact that the pressure is negative implies that a negative pressure must be applied to overcome the cohesive forces of a liquid. Those readers interested in the derivation of this equation should turn to Appendix 2.

To create a bubble in water ($\sigma = 0.076 \text{ N m}^{-1}$), of radius 10^{-4} cm will require a rarefaction pressure (i. e. negative pressure) in excess of 1.78 atm. Provided the maximum rarefaction pressure (P_A) is larger than 1.6 atm, the bubble created will expand during the rarefaction cycle. During this expansion cycle liquid vapour may evaporate into the partial void. Thus there will probably be several different types of cavity in the liquid:

- the empty cavity (true cavitation),
- the vapour filled cavity,
- the gas filled cavity, unless the liquid is totally degassed, and
- a combination of vapour and gas filled cavities.

It is the subsequent fate of some of these bubbles, as they oscillate in the applied sinusoidal acoustic field, which is the origin of sonochemistry. However, before embarking upon a discussion of bubble dynamics let us consider what other factors apart from degassing, pressurising and filtration affect the onset of cavitation.

2.4.2

Effect of Viscosity

Since it is necessary for the negative pressure in the rarefaction cycle to overcome the natural cohesive forces acting in the liquid, any increase in these forces will increase the threshold of cavitation. One method of increasing these forces is to increase the viscosity of the liquid. Tab. 2.1 shows the influence of viscosity on the pressure amplitude (P_A) at which cavitation begins in several liquids at 25 °C, at a hydrostatic pressure of 1 atm.

The effect, though not insignificant, is hardly dramatic. Taking corn and castor oils as examples, a ten-fold increase in viscosity has only led to a 30% increase in the acoustic pressure needed to bring about cavitation.

2.4.3

Effect of Applied Frequency

To completely rupture a liquid and hence provide a void, which may subsequently become filled with gas or vapour, requires a finite time. For sound waves with high frequencies, the time required to create the bubble may be longer than that available during the rarefaction cycle. At 20 kHz, for example, the rarefaction cycle lasts 25 μ s, attaining its maximum negative pressure in 12.5 μ s, whereas at 20 MHz the rarefaction cycle lasts only 0.025 μ s. Thus it might be anticipated that as the frequency increases the production of cavitation bubbles becomes more difficult to achieve in the available time and that greater sound intensities (i. e. greater amplitudes) will need to be employed, over these shorter periods, to ensure that the cohesive forces of the liquid are overcome. This effect is demonstrated quite clearly in Fig. 2.11, where the variation in threshold intensity with frequency is shown for both aerated and gas free water.

As expected the threshold for aerated water is lower than that for gas free water (see earlier) and the threshold intensity increases with increase in frequency. In fact ten

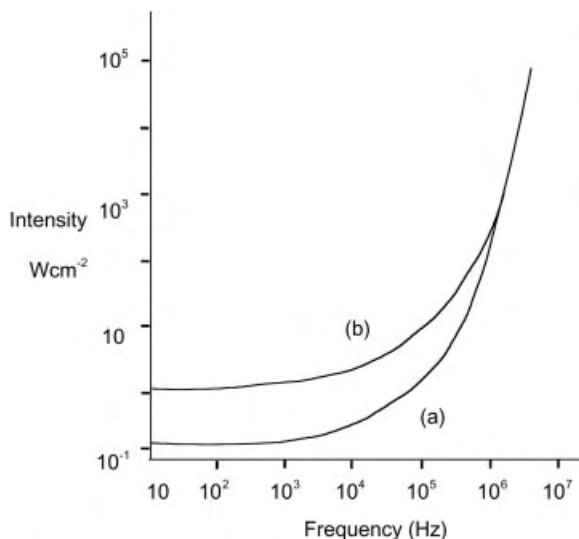


Fig. 2.11. Variation in threshold intensity with frequency; (a) aerated water; (b) air free water.

times more power is required to make water cavitate at 400 kHz than at 10 kHz. It is for this reason that 20–50 kHz frequencies were generally chosen for cleaning purposes and have subsequently been found of value in sonochemistry. As can be seen (Fig. 2.11) there is little extra energy needed to cause water to cavitate at 50 kHz than that required at 10 kHz. However, below 16 kHz there may be some noise discomfort to the user since it is within the audible range. It is for this reason that frequencies of 20 kHz or above are generally employed in sonochemical applications.

Most chemists working on sonochemistry in the laboratory will either use some form of ultrasonic bath or a commercial probe system. The latter instruments are often equipped with a pulse facility which was originally designed for biological cell disruption where temperature control is important. This pulse facility enables the power ultrasound to be delivered intermittently and thereby allow periods of cool-

Tab. 2.1. Sound pressure (P) producing cavitation in various liquids under a hydrostatic pressure of 1 atmosphere.

Liquid	η [poise]	ρ [g cm ⁻³]	c [km s ⁻¹]	P_A [atm]
Castor oil	6.30	0.969	1.477	3.90
Olive oil	0.84	0.912	1.431	3.61
Corn oil	0.63	0.914	1.463	3.05
Linseed oil	0.38	0.921	1.468	2.36
CCl ₄	0.01	1.60	0.926	1.75

ing. The time (i. e. pulse length) for which the sound energy is delivered to the system is controlled by an instrument setting and may be varied from 0 %, where no energy is supplied, to 100 %, which is continuous application of the energy. For sonochemical applications, however, there is a minimum time period (pulse) which must be exceeded if any cavitation effects are to be observed. This is due to the time delay between the application of the acoustic excitation (i. e. the sound wave) and the onset of cavitation, and the pulse of acoustic energy may not be present long enough to create the cavitation bubble. This is best visualised by considering Fig. 2.12 which illustrates the growth of a bubble of radius 8×10^{-5} cm in water at an ambient pressure of 1 atm and subject to an applied acoustic field of frequency 5 MHz and a pressure amplitude (P_A) of 4 atm.

For the first 1/8th of the acoustic cycle (i. e. 25 ns) there is only a small increase in the size of the bubble ($\sim 5\%$). Even after 1/4 of a cycle (i. e. 50 ns) it has only grown by $\sim 30\%$. During the next 1/4 of a cycle it grows to a size sufficiently large, approximately twice its initial radius, that under the action of the applied acoustic field it collapses totally – i. e. cavitation takes place. Thus, if the pulse is present for less than 1/4 a cycle (50 ns) at this frequency, the bubble will not have sufficient time to grow to a size capable of collapse. In general the threshold intensity is found to decrease as the pulse length is increased and an upper limit for pulse length is usually attained after which the threshold remains independent of the length of the pulse. For 20 kHz, the upper limit is approx. 20 ms.

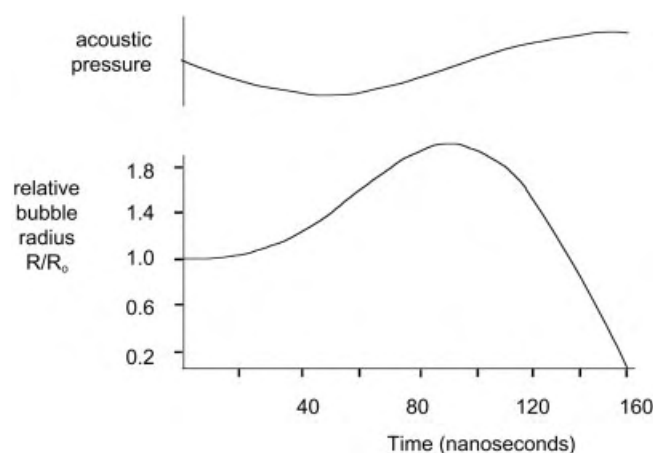


Fig. 2.12. Radius-time curve for an air bubble ($R_e = 8 \times 10^{-5}$ cm) sonicated in water at 5 MHz and 5.5 W cm^{-2} ; $P_A = 4 \text{ atm}$; $f = 5 \text{ MHz}$; $R_e = 8 \times 10^{-5} \text{ cm}$.

2.4.4

Effect of Temperature

The final factor to be considered here, and known to affect the cavitation threshold, is the temperature. In general, the threshold limit has been found to increase with decrease in temperature. This may in part be due to increases in either the surface tension (σ) or viscosity (η) of the liquid as the temperature decreases, or it may be due to the decreases in the liquid vapour pressure (P_v). To best understand how these parameters (σ , η , P_v) affect the cavitation threshold, let us consider an isolated bubble, of radius R_0 , in water at a hydrostatic pressure (P_h) of 1 atm.

Any bubble within a liquid is subject to both the crushing force of the hydrostatic pressure (P_h) and those due to surface tension effects ($2\sigma/R_0$). In order that the bubble should remain in equilibrium, the supporting forces due to the pressure of gas (P_g) and vapour (P_v) in the bubble must equal the crushing forces (Eq. 2.19).

$$P_v + P_g = P_h + 2\sigma/R_0 \quad (2.19)$$

Obviously, if the pressure within the bubble ($P_v + P_g$) exceeds those trying to collapse the bubble ($P_h + 2\sigma/R_0$), the bubble will expand (and vice-versa). In other words a bubble will grow (expand) when ($P_v + P_g$) is greater than ($P_h + 2\sigma/R_0$) (Eqs. 2.20 and 2.21).

$$P_v + P_g > P_h + 2\sigma/R_0 \quad (2.20)$$

or

$$P_v > P_h + 2\sigma/R_0 - P_g \quad (2.21)$$

If we neglect, momentarily, any surface tension effects (i. e. $2\sigma/R_0 \sim 0$) and assume that the liquid contains only a small amount of gas ($P_g \sim 0$), then we may deduce that ‘expanding’ bubbles are created in a liquid when the vapour pressure exceeds the atmospheric pressure ($P_v > P_h$). For water the vapour pressure at 100 °C is 1 atm and hence water, at a hydrostatic pressure of 1 atm, boils as soon as the temperature exceeds 100 °C. At 25 °C the vapour pressure of water is 0.023 atm and thus water will only boil, at 25 °C, if the atmospheric pressure is less than this value. This can readily be achieved by evacuating the system.

Let us now consider the effect of applying an ultrasonic wave to the liquid. The pressure within the liquid will now become ($P_h + P_a$), where P_a ($= P_A \sin 2\pi ft$) is

time dependent. During the compression cycle of the wave P_a is positive, rising from zero to P_A in quarter of a cycle before falling to zero after half of a cycle. During this time the pressure in the liquid will have risen from P_h to $P_h + P_A$ before returning again to P_h . In the rarefaction cycle P_a will become negative, the pressure in the liquid at any time being given by $P_h - P_a$. Thus, for example, after 3/4 of a cycle the wave will be at the maximum of its rarefaction cycle and the liquid pressure will be $(P_h - P_A)$. Hence in the presence of an acoustic field Eq. 2.21 becomes Eq. 2.22.

$$P_v > (P_h - P_a) + 2\sigma/R_0 - P_g \quad (2.22)$$

or neglecting surface tension effects and gas pressure this becomes Eq. 2.23

$$P_v > (P_h - P_g) \quad (2.23)$$

i. e. the liquid boils, (produces cavitation bubbles), when the vapour pressure exceeds that of $(P_h - P_a)$. For the examples of water at 100 °C ($P_v = 1$ atm) and 25 °C ($P_v = 0.023$ atm), the magnitudes of the applied acoustic pressure (P_a) will be approximately zero and 1 atm respectively. In other words, a greater intensity, I , ($= P_a^2/2\rho c$) will be necessary to cause water to cavitate at the lower temperature. If surface tension is not neglected Eq. 2.22 may be represented as Eq. 2.24.

$$P_v - 2\sigma/R_0 = P'_v > (P_h - P_a) \quad (2.24)$$

Thus if we employ different liquids with decreasing surface tensions (σ), the value of P'_v (assuming constant P_v) will increase and lower P_a values, at a given temperature, will need to be applied before P'_v exceeds $(P_h - P_a)$.

For water the surface tension varies with temperature as shown in Fig. 2.13 – i. e. a lowering of surface tension with increase in temperature. If it can be assumed that P_v remains constant with increase in temperature then there will be a small increase in P'_v and a lowering of the intensity (P_a) necessary to cause cavitation. Obviously P_v does not remain constant with increase in temperature but increases quite rapidly. Consequently there is a rapid rise in P'_v with increase in temperature and the threshold decreases accordingly. The corollary is that liquids with high vapour pressures or low surface tensions cavitate at a lower intensity.

Let us now consider the effect of solvent viscosity on the cavitation threshold. According to Tab. 2.1, an increase in the solvent viscosity required the application of a

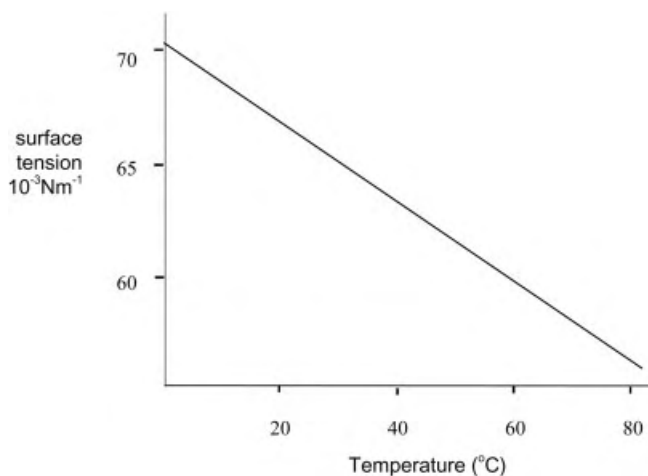


Fig. 2.13. Variation of the surface tension of water with temperature.

greater sound intensity (i. e. P_a) before cavitation bubbles were observed. For example, castor oil ($\eta = 0.63 \text{ N m}^{-1}$) and corn oil ($\eta = 0.063 \text{ N m}^{-1}$) require acoustic pressures of 3.9 and 3.05 atm respectively. For water, viscosity decreases with increased temperature, and hence lower P_a values (i. e. lower intensities) will be needed to cause cavitation as the temperature is increased. Overall then, the general conclusion is that cavitation bubbles are more easily produced as the temperature is raised. However the sonochemical effects of such bubbles may be reduced (see Section 2.6.3).

Before leaving this section let us consider the effect of increasing the atmospheric pressure – i. e. pressurising the system. In the previous discussions it was suggested that pressurising the system raised the cavitation threshold. A consideration of Eq. 2.23 shows why this is so. If a liquid will only create cavitation bubbles when $P_v > P_h - P_a$, then any increase in P_h (i. e. pressurising) will by necessity require larger P_a values and hence larger intensities.

Having identified the factors affecting the production of these microbubbles or voids, we must now turn our attention to their fate in the presence of the oscillating sinusoidally applied acoustic field. For any bubble created early in the rarefaction cycle, or initially present in the liquid, a growth in size will occur during the remainder of the cycle. During the compression cycle all bubbles will be made to contract or collapse. However if during growth, some gas, or vapour has diffused into the void or bubble, complete collapse may not occur and the bubble may in fact oscillate in the applied field. We must therefore consider two types of bubble, those which collapse completely (*transient*) and those which oscillate and exist for some considerable period of time (*stable*). Whether they collapse or oscillate depends upon many factors, e. g. temperature, acoustic ampli-

tude, frequency, external pressure, bubble size, gas type and content. There is a further complication in that transient bubbles may grow into stable bubbles and vice versa. What is certain however, is that compression of a bubble, containing gas or vapour, occurs very rapidly and leads to enormous temperatures (~ 5000 K) and pressures (~ 2000 atm) within the bubble itself, and that on complete collapse, should it occur, these pressures must be released as shock waves into the liquid.

2.5

Motion of the Bubble in the Applied Acoustic Field

The important break through in the understanding of cavitation came in 1917 when Lord Rayleigh [12] published his paper “On the pressure developed in a liquid during the collapse of a spherical cavity”. By considering the total collapse of an empty void under the action of a constant ambient pressure P_0 , Rayleigh deduced both the cavity collapse time τ , and the pressure P in the liquid at some distance R from the cavity to be respectively (Eqs. 2.25 and 2.26).

$$\tau = 0.915 R_m (\rho/P_0)^{1/2} \quad (2.25)$$

$$P/P_0 = 1 + (R/3r)(Z - 4) - (R^4/3r^4)(Z - 1) \quad (2.26)$$

where R_m is the radius of the cavity at the start of collapse (see Appendix 3), $Z = (R_m/R)^3$ and $r = R/R_m$

Schematically, Eq. 2.26 may be represented by Fig. 2.14 with the maximum in pressure, p_{\max} , occurring at a distance $4^{1/3}R$ from the cavity.

Eq. 2.25 is useful in that it allows an estimate of the point in the compression cycle where total collapse is likely to occur. For example, the collapse time of a bubble of radius 10^{-3} cm (R_m), in water at an ambient pressure (P_0) of 1 atm, is approximately $1 \mu\text{s}$. Since an applied acoustic field of 20 kHz has a compression cycle of $25 \mu\text{s}$, it is expected that total collapse will occur in the first 4 % of the cycle.

However, this can only be an estimate since it is unlikely that a bubble in a sound field will feel a constant pressure, P_0 , exerted during its collapse (acoustic pressure is time dependent, i. e. $P_a = P_A \sin 2\pi ft$) nor will it be an empty void, being filled with either gas or vapour. As such, Eq. 2.25 must be modified (Eq. 2.27).

$$\tau = 0.915 R_m (\rho/P_m)^{1/2} (1 + P_{vg}/P_m) \quad (2.27)$$

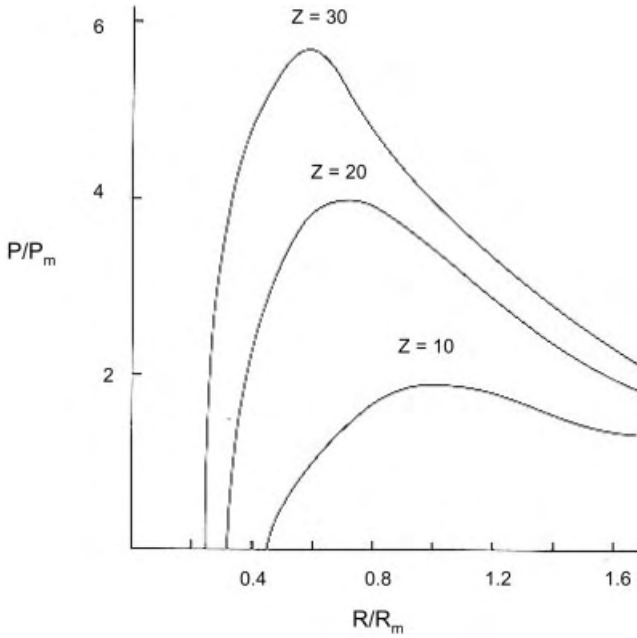


Fig. 2.14. Pressure developed in a liquid surrounding a collapse Rayleigh cavity; Z = volume compression ratio.

where P_m is the pressure in the liquid and P_{vg} the pressure in the bubble at the start of bubble collapse (see Appendix 3). If it can be assumed that the bubble collapse time is small in comparison with the time period of the compression cycle then P_m can be assumed to be constant and may be approximated to $(P_a + P_h)$. For an empty void (i. e. $P_{vg} = 0$) in the absence of an applied acoustic field (i. e. $P_a = 0$) then P_m may be replaced by $P_h (= P_0)$ and Eq. 2.27 reverts to the Rayleigh equation.

In any cavitation field most of the visible bubbles will be oscillating in a stable manner and it is perhaps pertinent that we concentrate our discussions first on the fate of such bubbles in the acoustic field. If we assume that we have a bubble with an equilibrium radius, R_e , existing in a liquid at atmospheric pressure P_h , then the oscillation of the bubble and in particular the motion of the bubble wall, under the influence of the applied sinusoidal acoustic pressure (P_a) is a simple dynamical problem, akin to simple harmonic motion for a spring.

Although there exist many sophisticated mathematical treatise which derive the motion of the bubble wall, all yield equations similar in form to Eq. 2.28.

$$R\ddot{R} + (3/2)\dot{R}^2 = 1/\rho \left[(P_h + \frac{2\sigma}{R_e} - P_v) \left(\frac{R_e}{R} \right)^{3K} - \frac{2\sigma}{R} - 4\eta \frac{\dot{R}}{R} - (P_h - P_a) \right] \quad (2.28)$$

where $\dot{R} = \frac{dR}{dt}$ = velocity of the cavity wall, \ddot{R} = acceleration of the cavity wall, R_e = radius of the bubble at its rest (equilibrium) position, σ = surface tension of the liquid, η = viscosity of the liquid, P_v = vapour pressure of the liquid, ρ = density of the liquid, P_h = atmospheric (hydrostatic) pressure, P_a = applied acoustic pressure and K is the polytropic index of the gas. (K varies between γ , the specific heat ratio, and unity, the limit for adiabatic and isothermal conditions). [For the reader interested in the derivation of this equation, see Appendix 4.]

Neglecting the vapour pressure and viscosity contributions and replacing P_a by $P_A \sin w_a t$ gives Eq. 2.29.

$$R\ddot{R} + (3/2)\dot{R}^2 = 1/\rho \left[(P_h + \frac{2\sigma}{R_e}) \left(\frac{R_e}{R} \right)^{3K} - \frac{2\sigma}{R} - P_h + P_A \sin w_a t \right] \quad (2.29)$$

where $w_a (= 2\pi f_a)$ is the applied circular frequency.

Provided we neglect damping effects (viscous and thermal), Eq. 2.29 adequately describes the motion of stable bubbles over several cycles. Before proceeding to discuss the effect that P_h , σ , ρ , P_A , f and R_e , have on the solutions of Eq. 2.29 (i. e. radius time variation), it may be instructive to consider here a simple modification of the equation such that with the aid of a computer one might deduce how the variation in some of the above parameters affects the radius-time of the bubble.

Let us assume that the bubble on expansion (or contraction) increases (or decreases) its radius by an amount r , such that R , the bubble radius at any time is given by $R = R_e + r$. Then provided $r \ll R_e$, substitution into Eq. 2.29, followed by expanding in powers of $1/R_e$ (and retaining only the first order terms) gives Eq. 2.30.

$$\frac{d^2 r}{dt^2} + w_r^2 r = \frac{P_A}{\rho R_e} \sin w_a t \quad (2.30)$$

where w_a is the equal applied circular frequency ($= 2\pi f_a$) and w_r is the resonant frequency of the bubble. For small amplitude vibrations the resonance frequency is given by Eq. 2.31.

$$w_r^2 = \left(\frac{1}{\rho R_e^2} \right) \left[3K \left(P_h + \frac{2\sigma}{R_e} - P_v \right) - \frac{2\sigma}{R_e} - \frac{4\eta^2}{\rho R_e^2} \right] \quad (2.31)$$

Neglecting the effects of viscosity (η) and solvent vapour pressure (P_v) Eq. 2.31 reduces to Eq. 2.32.

$$w_r^2 = \left(\frac{1}{\rho R_e^2} \right) \left[3K \left(P_h + \frac{2\sigma}{R_e} \right) - \frac{2\sigma}{R_e} \right] = (2\pi f_r)^2 \quad (2.32)$$

a form similar to that derived by Minneart (Eq. 2.33) for the natural resonance frequency (f_r) of a bubble of resonance radius, R_r , in a liquid medium of density ρ .

$$f_r = \frac{1}{2\pi R_r} \left[\frac{3\gamma}{\rho} \left(P_h + \frac{2\sigma}{R_r} \right) \right]^{1/2} \quad (2.33)$$

(NB for large bubbles, in which the surface tension effects are negligible ($P_h \gg 2\sigma/R_r$), Eq. 2.33 reduces to

$$f_r = \frac{1}{2\pi R_r} \left[\frac{3\gamma P_h}{\rho} \right]^{1/2}$$

which for a bubble in water ($\rho = 1000 \text{ kg m}^{-3}$) at 1 atm ($1.013 \times 10^5 \text{ N m}^{-2}$) and with $\gamma = 1$ may be approximated to $f_r R_r \sim 3$ (with R_r in metres). It is important to recognise that not all bubbles are capable of producing significant cavitation effects. The greatest coupling of the ultrasonic energy will occur when the natural resonance frequency (f_r) of the bubble is equal to the applied ultrasonic frequency (f_a). This may be demonstrated by considering the general solution of Eq. 2.34.

$$r = \frac{P_A}{\rho R_e (w_r^2 - w_a^2)} \left[\sin w_a t - \frac{w_a}{w_r} \sin w_r t \right] \quad (2.34)$$

which reduces to an indeterminate form at resonance – i.e. when $w_a = w_r$.

Appendix 6 contains a basic program which Eq. 2.34, to generate bubble radius-time curves for various values of P_A and R_e . If this programme, or one similar to it, is used

then in order to keep the computational times in bounds it will be necessary to limit the values of P_A, f , etc. For instance, a bubble whose initial radius (R_e) is 8×10^{-5} cm oscillates in a stable though complex manner for several cycles under an applied acoustic frequency of 15 MHz (Fig. 2.15a), yet collapses in less than one cycle if the acoustic frequency is 5 MHz (Fig. 2.15b).

In other words, the tendency of a bubble to collapse is frequency dependent and is more likely to occur at the lower frequencies where the time available in the compression cycle is longer. We will return to this frequency dependence later.

According to Eq. 2.33, the resonance size of a bubble in water insonated at 20 kHz (a typical sonochemical frequency) is approximately 1.5×10^{-2} cm. If an acoustic pressure amplitude of 1 atm is assumed, then a bubble of radius 10^{-2} cm will collapse (Fig. 2.16), whereas one of radius 2×10^{-2} cm will not (Fig. 2.17).

Further, if an insonation frequency of 50 kHz is employed neither of these two bubbles undergo collapse (Figs. 2.18 and 2.19). Only a bubble close to the resonance size (0.6×10^{-2} cm) will undergo collapse at the higher frequency (Fig. 2.20).

In general for small P_A/P_h ratios, with $R_e \sim R_r$ (the resonant bubble radius), oscillations take place at approximately the excitation frequency (Fig. 2.21). For $R_e > R_r$ bubble oscillation has a strong component of its own natural resonant frequency (Fig. 2.22). However for very small bubbles, $R_e \ll R_r$, transient conditions are attained as P_A increases beyond P_h (Fig. 2.23, $P_A = 4$ and 10 atm). It may be that as

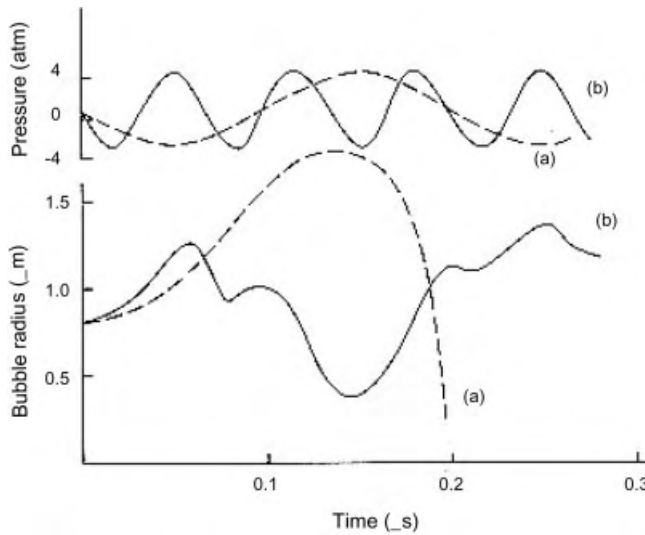


Fig. 2.15. Radius time curve for an air bubble in sonicated water at (a) 5 MHz; (b) 15 MHz; $R_e = 8 \times 10^{-5}$ cm; $P_A = 4$ atm; $P_h = 1$ atm.

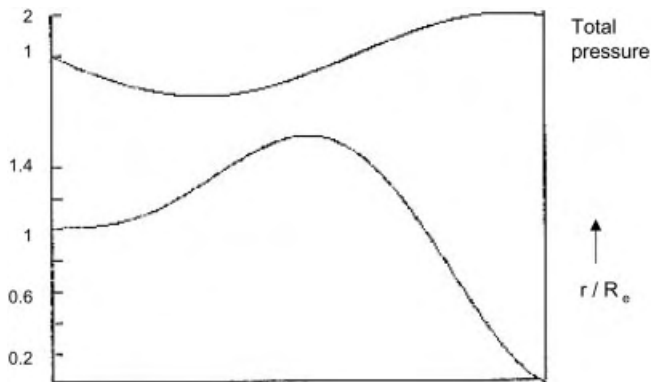


Fig. 2.16. Radius time curve for an air bubble in sonicated water at 20 kHz; $R_e = 10^{-2}$ cm; $P_A = 1$ atm; $P_h = 1$ atm.

P_A is further increased the bubble grows so large in the tension phase that it has insufficient time to collapse before the end of the pressure cycle and collapse occurs at the end of the second positive peak (Fig. 2.23, $P_A = 25, 100, 200$ atm). Eventually if $P_A/P_h \gg 1$ the bubble may never undergo transient collapse.

(NB. It is not possible to faithfully reproduce Fig. 2.23 using the basic program outlined in Appendix 6. The program is based upon Eq. 2.34 where the damping effects of viscosity and temperature upon the bubble wall have been neglected and r has been assumed to be less than R_e .)

What is apparent from Fig. 2.23 is that the fate of the bubble, i. e. whether it remains as a stable bubble or is transformed into a transient, depends upon many factors such as temperature, vapour pressure, hydrostatic pressure, acoustic pressure amplitude

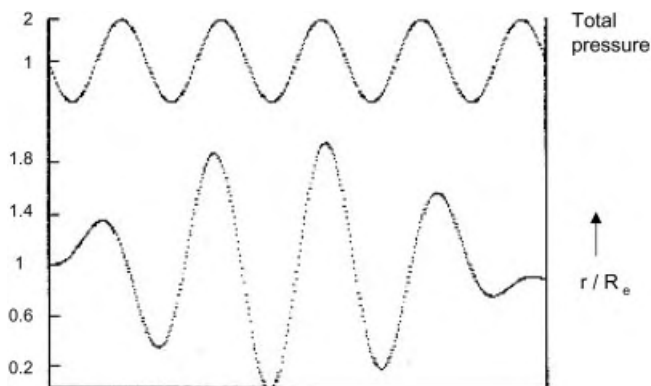


Fig. 2.17. Radius time curve for an air bubble in sonicated water at 20 kHz; $R_e = 2 \times 10^{-2}$ cm; $P_A = 1$ atm; $P_h = 1$ atm.

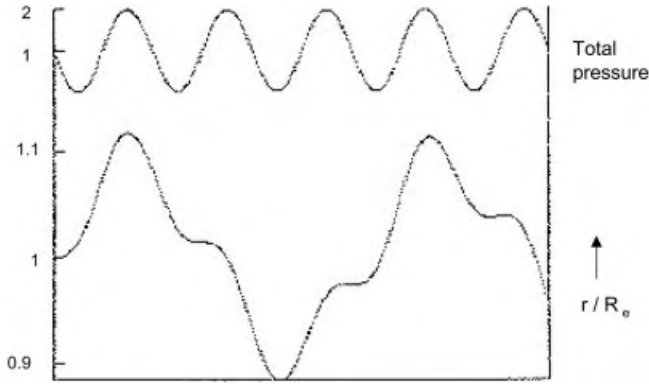


Fig. 2.18. Radius time curve for an air bubble in sonicated water at 50 kHz; $R_e = 2 \times 10^{-2}$ cm; $P_A = 1$ atm; $P_h = 1$ atm.

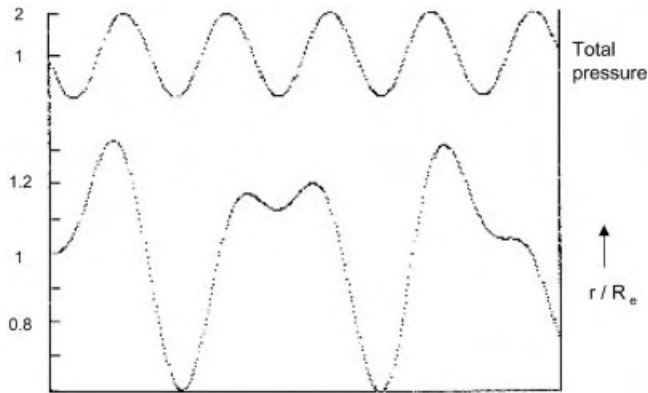


Fig. 2.19. Radius time curve for an air bubble in sonicated water at 50 kHz; $R_e = 10^{-2}$ cm; $P_A = 1$ atm; $P_h = 1$ atm.

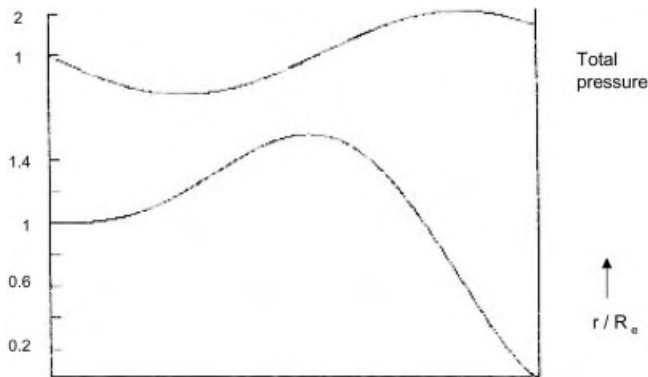


Fig. 2.20. Radius time curve for an air bubble in sonicated water at 50 kHz; $R_e = 0.5 \times 10^{-2}$ cm; $P_A = 1$ atm; $P_h = 1$ atm.

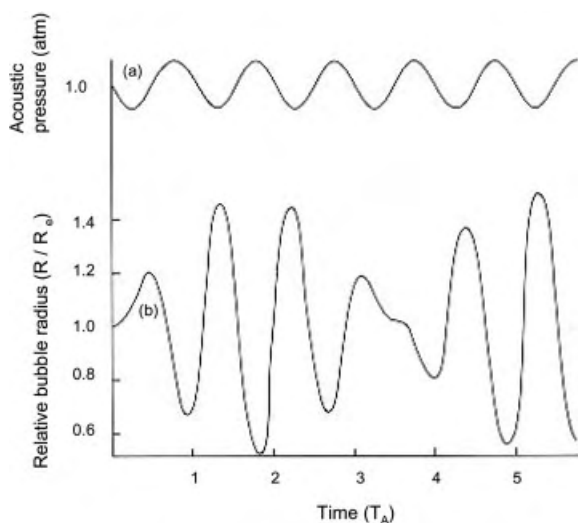


Fig. 2.21. Radius-time curve for a cavity insonated below resonance frequency; $R_e = 2.6 \times 10^{-3}$ cm; $P_A = 0.333$ atm; $P_h = 1$ atm; (a) applied frequency, 83.4 kHz; (b) relative radius of bubble.

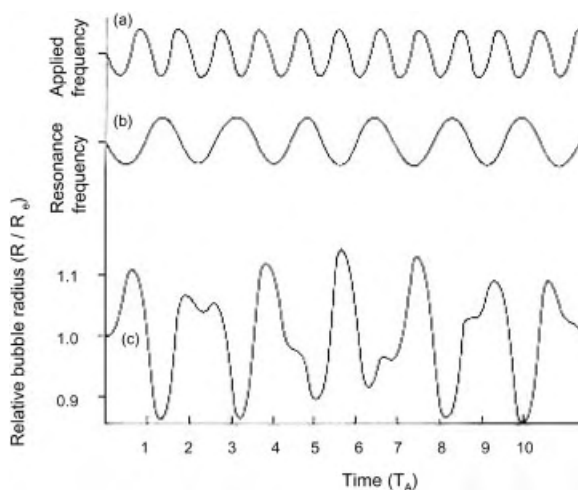


Fig. 2.22. Radius-time curve for a cavity insonated above resonance frequency; $R_e = 2.6 \times 10^{-3}$ cm; $P_A = 0.333$ atm; $P_h = 1$ atm; (a) applied frequency, 190 kHz; (b) resonance frequency; (c) relative radius of bubble.

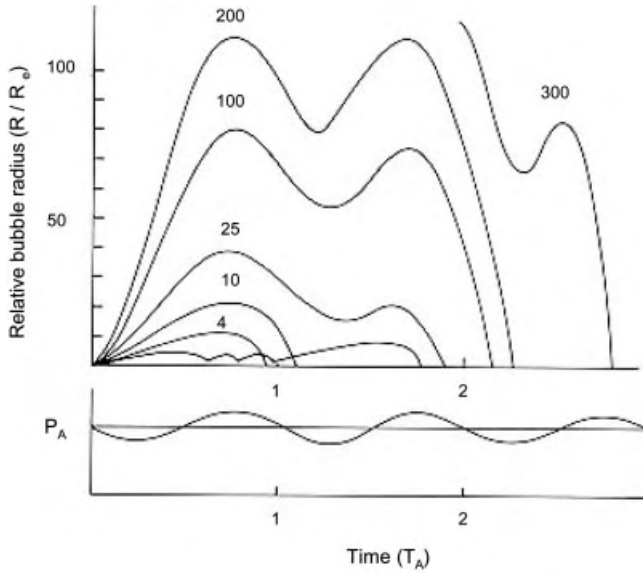


Fig. 2.23. Radius-time curve for an insonated air bubble in water; $R_e = 10^{-4}$ cm; $f = 500$ kHz. Numbers on the curves refer to the ratio of P_A/P_h . Time is measured in units of the period (T_A) of the applied acoustic field.

(intensity), initial bubble size, viscosity and surface tension. However before discussing the specific effects of some of these parameters let us consider transient and stable cavitation bubbles in more general terms.

2.5.1

Transient Cavitation

Transient cavitation bubbles are voids, or vapour filled bubbles, believed to be produced using sound intensities in excess of 10 W cm^{-2} . They exist for one, or at most a few acoustic cycles, expanding to a radius of at least twice their initial size, (Figs. 2.16 and 2.20), before collapsing violently on compression often disintegrating into smaller bubbles. (These smaller bubbles may act as nuclei for further bubbles, or if of sufficiently small radius (R) they can simply dissolve into the bulk of the solution under the action of the very large forces due to surface tension, $2\sigma/R$. During the lifetime of the transient bubble it is assumed that there is no time for any mass flow, by diffusion of gas, into or out of the bubble, whereas evaporation and condensation of liquid is assumed to take place freely. If there is no gas to cushion the implosion

a very violent collapse will result. Theoretical considerations by Noltingk and Neppiras [13] and later by Flynn [14], and separately by Neppiras [15], assuming adiabatic collapse of the bubbles, allows for a calculation of the temperatures (T_{\max}) (Eq. 2.35) and pressures (P_{\max}) (Eq. 2.36) within the bubble at the moment of total collapse as being

$$T_{\max} = T_0 \left\{ \frac{P_m(K-1)}{P} \right\} \quad (2.35)$$

$$P_{\max} = P \left\{ \frac{P_m(K-1)}{P} \right\}^{K/(K-1)} \quad (2.36)$$

where T_0 is the ambient (experimental) temperature, K is the polytropic index of the gas (or gas vapour) mixture, P is the pressure in the bubble at its maximum size (usually assumed to be equal to the vapour pressure (P_v) of the liquid), and P_m is the pressure in the liquid at the moment of transient collapse. Those readers who are interested will find a derivation of Eqs. 2.35 and 2.36 in Appendix 5. Since the collapse time, τ , for an empty bubble is normally not longer than one fifth of the period of vibration, P_m can be regarded as constant during the collapse and may be represented as $(P_h + P_A)$. The assumption that the pressure in the bubble may be replaced by the vapour pressure is a direct consequence of the initial assumption that transient bubbles grow without the influx of gas into the cavity. If gas does enter the cavity, the value of $P(= P_g + P_v)$ will depend upon the value of P_g when the bubble is at its maximum size, R_{\max} . Using Eqs. 2.35 and 2.36, estimates of the temperatures and pressures involved in the final phase of the implosion can be obtained. For example, for a bubble containing nitrogen ($K = 1.33$) in water at an ambient temperature of 20°C (T_0) and an ambient pressure of 1 atm (P_m), Eqs. 2.35 and 2.36 provide values of 4200 K and 975 atm respectively. It is the existence of these very high temperatures within the bubble that have formed the basis for the explanation of radical production and sonoluminescence, whilst the release of the pressure, as a shock wave, is a factor which has been used to account for both increased chemical reactivity (due to increase molecular collision) and polymer degradation.

2.5.2

Stable Cavitation

We now turn our attention to stable cavitation, a phenomenon which at one time was not thought to be of much significance in terms of chemical effects. Stable bubbles are thought to contain mainly gas and some vapour and are believed to be produced at fairly low intensities ($1 - 3 \text{ W cm}^{-2}$), oscillating, often non linearly, about some equilibrium size for many acoustic cycles – Fig. 2.20. The time scale over which they exist is sufficiently long that mass diffusion of gas, as well as thermal diffusion, with consequent evaporation and condensation of the vapour can occur, resulting in significant long term effects. If the rates of mass transfer across the gas-liquid interface are not equal, it may result in bubble growth. The mechanism by which small microbubbles in the liquid (which normally dissolve instantly due to surface tension) grow is termed rectified diffusion. In the expansion phase of the acoustic cycle gas diffuses from the liquid into the bubble, whilst in the compression phase gas diffuses out of the bubble into the liquid. Since the interfacial area is greater in the expanded phase, the inward diffusion is greater and leads to an overall growth of the bubble. As the bubble grows the acoustic and environmental conditions of the medium will change and the bubble may be transformed into a transient bubble and undergo collapse (Fig. 2.23). The violence of collapse however, will be less than that for a vapour filled transient since the gas will cushion the implosion. On the other hand the bubbles may continue to grow during subsequent cycles until they are sufficiently buoyant to float to the surface and be expelled – this is the process of ultrasonic degassing. As with transient cavitation, estimates have been made of the temperatures and pressures produced in stable bubbles as they oscillate in resonance with the applied acoustic field. Griffing has derived an expression (Eq. 2.37) for the ratio T_0/T_{\max} :

$$\frac{T_0}{T_{\max}} = \left\{ 1 + Q \left[\left(\frac{P_h}{P_m} \right)^{1/3\gamma} - 1 \right] \right\}^{3(\gamma-1)} \quad (2.37)$$

where Q is the ratio of the resonance amplitude to the static amplitude of vibration of the bubble and $P_m = P_h + P_A$ is the peak pressure of the bubble. For a bubble at ambient temperature ($T_0 = 300 \text{ K}$) containing a monatomic gas ($\gamma = 1.666$) and with $P_m/P_h = 3.7$ (corresponding to an intensity of 2.3 W cm^{-2}) and assuming a value of $Q = 2.5$, the maximum temperature developed in the bubble (T_{\max}) is deduced to be $1,665 \text{ K}$. Calculations of the local pressures due to these resonance vibrations has resulted in values which exceed the hydrostatic pressure by a factor of $150\,000$. There is no doubt that the intense local strains in the vicinity of the resonating bubble are the cause of the many disruptive mechanical effects of sound. Given the

differences in irradiation conditions (i. e. frequency, solvents, vapour pressure, intensity of irradiation, hydrostatic pressure etc) it is pertinent to conclude our discussions with a summary of how these various parameters effect the distinct stages of acoustic cavitation: namely nucleation, bubble growth and collapse.

2.6

Summary

2.6.1

Frequency

It is found that as the ultrasonic frequency is increased the production and intensity of cavitation in liquids decreases. Although various proposals have been offered to explain this observation, in qualitative terms at least it may be argued that at very high frequency, where the rarefaction (and compression) cycles are very short, the finite time required for the rarefaction cycle is too small to permit a bubble to grow to a size sufficient to cause disruption of the liquid. Even if a bubble was to be produced during rarefaction, the time required to collapse that bubble may be longer than is available in the compression half cycle. The resultant cavitation effects, e.g. shock wave pressure, will therefore be less at the higher frequencies. (Fig. 2.24 shows the variation of maximum fluid-pressure against frequency for constant pressure amplitude (P_A), and bubble radius).

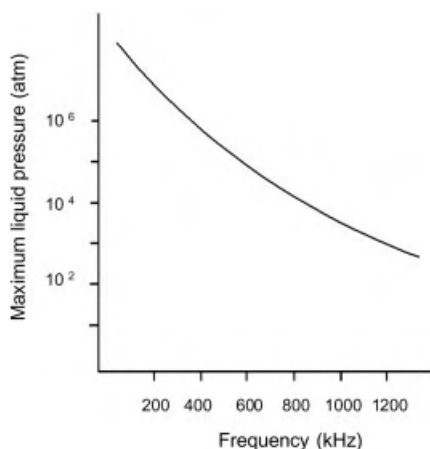


Fig. 2.24. Variation with frequency of maximum fluid pressure during collapse; $R_e = 3.2 \times 10^{-4}$ cm; $P_A = 4$ atm.

2.6.2

Solvent

The formation of voids or vapour filled microbubbles (cavities) in a liquid requires that the negative pressure in the rarefaction region must overcome the natural cohesive forces acting within the liquid. It follows therefore that cavitation should be more difficult to produce in viscous liquids, or liquids with high surface tensions, where the forces are stronger and waves with greater amplitude (P_A) and hence greater intensity will be necessary. Once a liquid produces cavitation bubbles however, the temperature (T_{\max}) and pressure (P_{\max}) effects resulting from the bubbles collapse will be greater, since the pressure at the start of collapse (P_m) will be larger (see Eqs. 2.35 and 2.36).

Another solvent factor affecting cavitation is that of vapour pressure. Since vapour pressure (P_v) and temperature are directly related this is dealt with below in Section 2.6.3.

2.6.3

Temperature

Increasing the reaction temperature allows cavitation to be achieved at lower acoustic intensity. This is a direct consequence of the rise in vapour pressure associated with heating the liquid. The higher the vapour pressure the lower the applied acoustic amplitude (P_A) necessary to ensure that the “apparent” hydrostatic pressure, $P_h - P_a$, is exceeded – see Section 2.4.4. Unfortunately the effects resulting from cavitation collapse are also reduced. A consideration of Eqs. 2.35 and 2.36 show that T_{\max} and P_{\max} fall due to the increase in P_v and decrease in $P_m (= P_h + P_A)$. In other words to get maximum sonochemical benefit any experiment should be conducted at as low a temperature as is feasible or with a solvent of low vapour pressure.

Tab. 2.2. Rate of formation of free chlorine by irradiation of water containing CCl_4 in relation to the nature of the saturating gas.

Gas	Reaction rate [mM min ⁻¹]	γ	Thermal conductivity [10 ⁻² W m ⁻¹ K ⁻¹]
Argon	0.074	1.66	1.73
Neon	0.058	1.66	4.72
Helium	0.049	1.66	14.30
Oxygen	0.047	1.39	1.64
Nitrogen	0.045	1.40	2.52
Carbon monoxide	0.028	1.43	2.72

2.6.4

Gas Type and Content

According to Eqs. 2.35, 2.36 and 2.37, employing gases with large γ values will provide for larger sonochemical effects from gas filled bubbles. For this reason monatomic gases (He, Ar, Ne) are used in preference to diatomics (N_2 , air, O_2). It must be remembered that this dependence on γ is a simplistic view since the extent of the sonochemical effects will also depend upon the thermal conductivity of the gas, i.e. the greater the thermal conductivity of the gas, the more heat (formed in the bubble during collapse) will be dissipated to the surrounding liquid, effectively decreasing T_{\max} . Unfortunately a strict correlation between thermal conductivity and sonochemical effect has not been observed (Tab. 2.2).

Increasing the gas content of a liquid leads to a lowering of both the cavitation threshold (Fig. 2.25) and the intensity of the shock wave released on the collapse of the bubble. The threshold is lowered as a consequence of the increased number of gas nuclei (or weak spots) present in the liquid, whilst the cavitation collapse intensity is decreased as a result of the greater “cushioning” effect in the microbubble. The latter point may be deduced semiquantitatively from a consideration of Eqs. 2.35 and 2.36, where P should be replaced by $P_{vg}(= P_v + P_g)$. Increasing the gas content of the liquid, P_g , leads to an increase in P_{vg} and a decrease in both P_{\max} and T_{\max} . It might be anticipated that employing gases with increased solubility will also reduce both the threshold intensity (by virtue of providing a large number of nuclei in the solvent) and the intensity of cavitation. Indeed there is a definite correlation between gas solubility and cavitation intensity. The greater the solubility of the gas the greater the

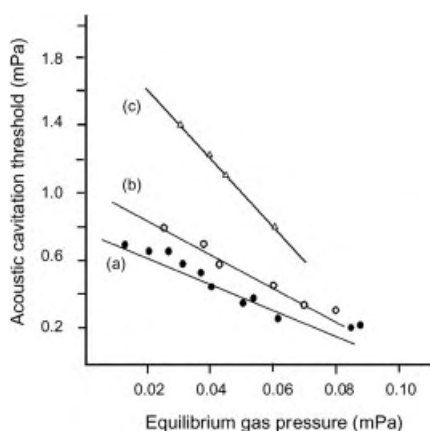


Fig. 2.25. Variation of acoustic threshold of water with dissolved gas content; (a) distilled water, $\sigma = 7.2 \times 10^{-2} \text{ N m}^{-1}$; (b) aqueous guar gum (100 ppm), $\sigma = 6.2 \times 10^{-2} \text{ N m}^{-1}$; (c) aqueous photo-flow (80 ppm), $\sigma = 4.0 \times 10^{-2} \text{ N m}^{-1}$.

amount which penetrates into the cavitation bubble and the smaller the intensity of the shock wave created on bubble collapse. A further factor effecting the intensity of collapse may be that the more soluble the gas the more likely it is to re-dissolve in the medium during the compression phase of the acoustic cycle.

2.6.5

External Applied Pressure

Increasing the external pressure (P_h) leads to an increase in both the cavitation threshold and the intensity of bubble collapse. Qualitatively it can be assumed that there will no longer be a resultant negative pressure phase of the sound wave (since $P_h - P_A > 0$) and so cavitation bubbles cannot be created. Clearly, a sufficiently large increase in the intensity, I , of the applied ultrasonic field could produce cavitation, even at high overpressures, since it will generate larger values of $P_a(I\alpha P_A^2$; $P_a = P_A \sin 2\pi ft$) making $P_h - P_A < 0$. In that P_m (the pressure in the bubble at the moment of collapse) is approximately $P_h + P_A$, increasing the value of P_h will lead to a more rapid (Eq. 2.27) and violent (Eq. 2.36) collapse.

2.6.6

Intensity

In general an increase in intensity (I) will provide for an increase in the sonochemical effects. Cavitation bubbles, initially difficult to create at the higher frequencies (due to the shorter time periods involved in the rarefaction cycles) will now be possible, and since both the collapse time (Eq. 2.27), the temperature (Eq. 2.35) and the pressure (Eq. 2.36) on collapse are dependent on $P_m (= P_h + P_A)$, bubble collapse will be more violent. However it must be realised that intensity cannot be increased indefinitely, since R_{max} (the maximum bubble size) is also dependent upon the pressure amplitude (Eq. 2.38). With increase in the pressure amplitude (P_A) the bubble may grow so large on rarefaction (R_{max}) that the time available for collapse is insufficient.

$$R_{max} = \frac{4}{3w_a} (P_A - P_h) \left(\frac{2}{\rho P_A} \right)^{1/2} \left[1 + \frac{2(P_A - P_h)}{3P_h} \right]^{1/3} \quad (2.38)$$

As an example to illustrate this point consider the effect of applying an acoustic wave of 20 kHz and pressure amplitude 2 atm (P_A) to a reaction in water. According to Eq. 2.38, this amplitude will produce a bubble of maximum radius, R_{max} , 1.27×10^{-2} cm, which if it can be assumed that $P_m = P_A + P_h$, collapses in approx. 6.8 μ s, (Eq. 2.27). This is less than 1/5th of a cycle (10 μ s), the assumption often

made for the time interval during which a bubble can undergo transient collapse, and so the bubble could undergo complete collapse. If the 20 kHz wave's amplitude is increased to 3 atm, the maximum size of the bubble can be calculated to be 2.31×10^{-2} cm and the collapse time to be $10.7 \mu\text{s}$ i.e. a value $> 1/5$ th of a cycle. In other words, this latter bubble does not have sufficient time to undergo transient collapse. Obviously the above is a simplified example and only serves to illustrate the fact that there is a P_A value above which a bubble will have grown so large it will not collapse. This has already been shown graphically in Fig. 2.23.

References

1. F.R. Young, *Cavitation*, McGraw Hill, Maidenhead, England, 1989, ISBN 0-07-707094-1.
2. T.G. Leighton, *The Acoustic Bubble*, Academic Press, London, England, 1994, ISBN 0-12-441920-8.
3. J.R. Blake, J.M. Boulton-Stone, and N.H. Thomas (eds.), *Bubble Dynamics and Interface Phenomena*, Kluwer Academic, Dordrecht, The Netherlands, 1994, ISBN 0-7923-3008-0.
4. M.A. Margulis, *Sonochemistry and Cavitation*, Gordon and Breach Science Publishers, Luxembourg, 1995, ISBN 2-88124-849-7.
5. L.A. Crum, T.J. Mason, J.L. Reisse, and K.S. Suslick (eds.), *Sonochemistry and Sonoluminescence*, NATO ASI Series, Kluwer Academic Publishers, 1999, ISBN 0-7923-5549-0.
6. J.R. Blake (ed.), Acoustic cavitation and sonoluminescence, *Theme issue of Philosophical Transactions of the Royal Society London A*, 1999, **357**, 199–369.
7. A.B. Wood, *A Textbook of Sound*, G. Bell & Son, 1930.
8. G.G. Stokes, *Trans. Camb. Phil. Soc.*, 1849, **8**, 287.
9. G. Kirchoff, *Ann. Phys. (Leipzig)*, 1868, **134**, 177.
10. F.E. Fox and G.D. Rock, *J. Acoust. Soc. Am.*, 1951, **12**, 505.
11. M. Greenspan and C.E. Tschiegg, *J. Res. Natl. Bur. Stand. Sect. C*, 1967, **71**, 229.
12. Lord Rayleigh, *Philos. Mag.*, 1917, **34**, 94.
13. B.E. Noltingk and E.A. Neppiras, *Proc. Phys. Soc. B (London)*, 1950, **63B**, 674; 1951, **64B**, 1032.
14. H.G. Flynn, *Physical Acoustics*, W.P. Mason (ed.), Academic Press, New York, 1964, Vol. 1B.
15. E.A. Neppiras, *Phys. Rep.*, 1980, **61**, 160.

Appendices to Chapter 2

Appendix 1: Relationship Between Particle Velocity (v) and Acoustic Pressure (P_a)

Consider an element (DEFG) of a liquid (Fig.A1.1) at a normal pressure of P and density of ρ subject to an applied acoustic wave of pressure P_a .

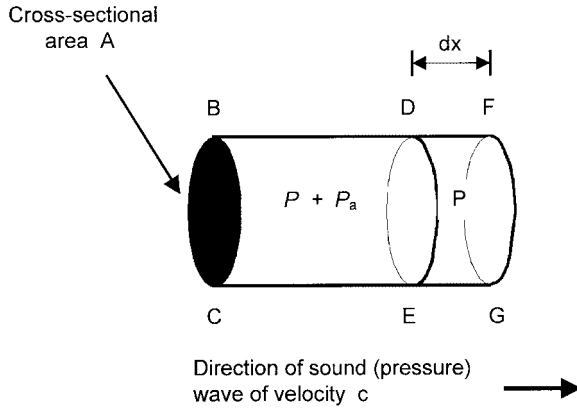


Fig. A1.1. Element of liquid subjected to acoustic pressure.

Under the action of the excess pressure, P_a , the molecules in the element BC will be displaced in the direction of the wave, the particles' velocity increasing from zero at B to v at DE . The sound wave itself, of velocity c , will pass from DE to FG (i. e. through the distance dx) in $\frac{dx}{c}$ seconds and hence the acceleration (velocity/time) of the particles in this volume element will, on average, be $\frac{vc}{dx}$, since for such a small element v can be assumed to remain constant.

Obviously the force attained by these accelerating particles (= mass \times acceleration) derives from the excess pressure (= pressure \times area), such that:

$$(\rho A dx) \times (vc/dx) = (P_a) \times (A)$$

$$\text{i. e. } \rho v c = P_a$$

$$\text{or } P_a/v = \rho c \quad (2.11)$$

Appendix 2: Critical Pressure (P_k) and Bubble Radius Relationship

If a bubble of radius R_e , present in a liquid is to remain in equilibrium (i. e. neither contracting nor expanding), then the forces (or pressure) acting on the bubble walls attempting to collapse the bubble must equal those forces responsible for attempting to expand the bubble. In the case of expansion this pressure, P_{bub} , will be due to the trapped gas and vapour in the bubble, so that

$$P_{bub} = P_v + P_g \quad (A.1)$$

whilst for contraction the pressure, P_L , is the combined effect of the hydrostatic pressure (P_h) within the liquid and the surface tension effect ($2\sigma/R_e$)

$$\text{i.e. } P_L = P_h + (2\sigma/R_e) \quad (A.2)$$

At equilibrium, when neither expansion nor contraction occurs then $P_L = P_{bub}$. Substitution from Eq. A.1 and A.2 gives

$$P_h + (2\sigma/R_e) = P_v + P_g \quad (A.3)$$

Suppose the bubble now changes size to some new radius, R , as a result of a change in the hydrostatic pressure to a new value P'_h . Then, assuming ideal gas behaviour, the new gas pressure (P'_g) inside the bubble will become $P_g (R_e/R)^3$ and the new pressure in the bubble (P'_{bub}) will be given by:

$$P'_{bub} = P_v + P'_g = P_v + P_g (R_e/R)^3 \quad (A.4)$$

Since expansion of the bubble to R will decrease the surface tension effects, the new liquid pressure P'_L will be given by:

$$P'_L = P'_h + 2\sigma/R \quad (A.5)$$

and if the bubble is still to be in equilibrium (i. e. $P'_L = P'_{bub}$) then

$$P'_h + 2\sigma/R = P_v + P_g (R_e/R)^3 \quad (\text{A.6})$$

or

$$P'_h = P_g (R_e/R)^3 + P_v - 2\sigma/R \quad (\text{A.7})$$

In other words the dependence of the radius, R , on the hydrostatic pressure of the liquid, P'_h , is not linear but has an inverse cubic dependence, such that for small but constant reductions in P'_h the radius increases quite rapidly. This is especially so when the hydrostatic pressure is quite small. In fact there is a minimum critical hydrostatic pressure, a very small reduction of which causes a dramatic increase in R , i.e. the bubble becomes unstable and grows explosively. The radius at which this occurs may be termed the critical radius, R_K , and occurs when dP'_h/dR is effectively zero. (i.e. small change in P'_h , large change in R).

An estimate may be made of this critical bubble radius, R_K , by differentiating the RHS of Eq. A.7, with respect to R , and equating to zero.

$$\text{i.e. } 0 = -3P_g \frac{R_e^3}{R^4} - 0 + \frac{2\sigma}{R^2}$$

Replacement of R by R_K yields

$$R_K^2 = \frac{3}{2\sigma} P_g R_e^3 \quad (\text{A.8})$$

If the critical pressure at which the bubble attains its critical radius, R_K , is denoted as P_K , then from Eq. A.7

$$P_K = P_g \left(\frac{R_e}{R_K} \right)^3 + P_v - \frac{2\sigma}{R_K} \quad (\text{A.9})$$

and replacement of R_K (from Eq. A.8) yields

$$P_K = P_v - \frac{2}{3} \left\{ \frac{(2\sigma/R_e)^3}{3P_g} \right\}^{1/2} \quad (\text{A.10})$$

Substitution of $P_g (= P_h - P_v + 2\sigma/R_e)$ from Eq. A.3 gives

$$P_K = P_v - \frac{2}{3} \left\{ \frac{(2\sigma/R_e)^3}{3(P_h - P_v + 2\sigma/R_e)} \right\}^{1/2} \quad (\text{A.11})$$

Finally, if the presence of vapour in the bubble is neglected (i.e. $P_v \sim 0$) then the critical pressure may be given by

$$P_K = -\frac{2}{3} \left\{ \frac{(2\sigma/R_e)^3}{3(P_h + 2\sigma/R_e)} \right\}^{1/2} \quad (2.18)$$

The fact that the pressure is negative implies that a negative pressure must be applied to overcome the cohesive forces of a liquid and produce a bubble of radius R_e . Writing $P_K = P_h - P_B$ allows the estimation of P_B , (known as *Blake threshold pressure*), which is the negative (or rarefaction) pressure which must be applied in excess of the hydrostatic pressure (P_h) to create a bubble of radius R_e . e.g. for large bubbles (i.e. $2\sigma/R_e \ll P_h$)

$$P_B \sim P_h + \frac{8\sigma}{9} \left\{ \frac{3\sigma}{2P_h R_e^3} \right\}^{1/2}$$

and for small bubbles ($2\sigma/R_e \gg P_h$)

$$P_B \sim P_h + 0.77\sigma/R_e$$

This latter equation is helpful when attempting to deduce an estimate of the theoretical strength of water.

For example if we assume a void would be created in water when the molecules are separated by more than the Van der Waals distance ($R_e = 4 \times 10^{-10}$ m say), then taking σ as 76×10^{-3} Nm, P_B can be estimated to be approximately 1500 atm.

$$P_B(0.77 \times 76 \times 10^{-3})/(4 \times 10^{-10})\text{Nm}^{-2}$$

Appendix 3: Time of Bubble Collapse

Consider an empty bubble collapsing under the influence of a constant external pressure P_h from an initial radius R_m to a final radius R (Fig. A3.1a).

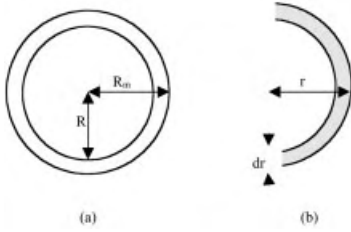


Fig. A3.1. (a) Change in radius of bubble during collapse; (b) volume of liquid moving on bubble collapse.

The work done by the (hydrostatic) pressure, P_h , neglecting surface tension effects, is the product of the pressure and the change in volume and is given by

$$\int_R^{R_m} P_h 4\pi R^2 dR = P_h \frac{4\pi}{3} [R_m^3 - R^3] \quad (\text{A.12})$$

This work will be equal to the kinetic energy ($mv^2/2$) of the liquid as it moves to fill the space vacated by the collapse of the bubble and is given by $\frac{1}{2} \rho 4\pi r^2 dr (dr/dt)^2$ (Fig. A3.1b) where ρ is the density of the liquid, $4\pi r^2 dr$ = the volume of liquid moving and (dr/dt) is the velocity. Thus

$$P_h \frac{4\pi}{3} [R_m^3 - R^3] = 2\pi\rho \int_R^\infty r^2 dr (dr/dt)^2 \quad (\text{A.13})$$

At first sight this integration appears somewhat difficult to perform since it contains both dr and (dr/dt) . However, if it is assumed that the liquid is incompressible then the volume lost by the cavity ($4\pi R^2 dR$) is equal to that filled by the liquid ($4\pi r^2 dr$) – i. e. $4\pi R^2 dR = 4\pi r^2 dr$, or

$$R^2 dR = r^2 dr \quad (\text{A.14})$$

Dividing both sides of Eq. A.14 by dt and rearranging gives

$$\frac{dt}{dt} = \frac{R^2}{r^2} \times \frac{dR}{dt} \quad (\text{A.15})$$

Substitution into Eq. A.13 yields

$$\frac{4\pi}{3} P_h (R_m^3 - R^3) = 2\pi\rho \int_R^\infty r^2 dr \frac{R^4}{r^4} (dR/dt)^2 = 2\pi\rho R^4 \left(\frac{dR}{dt} \right)^2 \int_R^\infty (dr/r^2) \quad (\text{A.16})$$

which on integration gives

$$\frac{4\pi}{3} P_h (R_m^3 - R^3) = 2\pi\rho R^4 \left(\frac{dR}{dt} \right)^2 \left[-\frac{1}{r} \right]_R^\infty$$

or more precisely

$$\frac{4\pi}{3} P_h (R_m^3 - R^3) = 2\pi\rho R^3 \left(\frac{dR}{dt} \right)^2 \quad (\text{A.17})$$

where the right hand side is equivalent to the kinetic energy of the liquid. Rearranging gives

$$\left(\frac{dR}{dt} \right) = \left(\frac{2P_h}{3\rho} \right)^{1/2} \left(\frac{R_m^3}{R^3} - 1 \right)^{1/2} \quad (\text{A.18})$$

such that

$$dt = \frac{dR}{\left[\left(\frac{2P_h}{3\rho} \right) \left(\frac{R_m^3}{R^3} - 1 \right) \right]} \quad (\text{A.19})$$

The time to collapse the bubble can now be obtained by integrating the right hand side of Eq. A.19 from R_m to zero to give

$$\tau \approx 0.915R_m(\rho/P_h)^{1/2} \quad (\text{A.20})$$

In the presence of an acoustic field the pressure in the liquid (P_m) will be greater than the atmospheric pressure by an amount P_a , i.e. $P_m = (P_h + P_a)$ where $P_a = P_A \sin 2\pi ft$, and Eq. A.20 may be modified to yield

$$\tau \approx 0.915R_m(\rho/P_m)^{1/2} \quad (\text{A.21})$$

where P_m is the pressure in the fluid at the start of collapse of a bubble of radius R_m .

The above deduction of τ although neglecting the effect of both surface tension and the pressure (P_{vg}) of liquid vapour (or gas) most certainly present in the bubble, does allow an estimate of the time involved for collapse.

For example, in the absence of an applied acoustic field ($P_a = 0$), a bubble of radius 10^{-3} cm, (R_m), present in water ($\rho = 10^3 \text{ kgm}^{-3}$) at 1 atm, will collapse in approx. 1 μs . If this collapse were to occur in the presence of an applied acoustic field, of say 20 kHz (period, $T = 50 \mu\text{s}$), then the collapse will occur in a much shorter time than the compression cycle acts (i.e. 25 μs). In other words, $P_m (= P_h + P_a)$, the pressure at the start of bubble collapse may be assumed to remain effectively constant over the collapse period since $P_a (= P_A \sin 2\pi ft)$ remains effectively constant. Obviously, the greater the intensity (I) of the applied field, the larger is $P_A (= (2\rho cI)^{1/2})$, P_a and hence P_m , and the faster is the collapse of the bubble. On the other hand, the larger the bubble at the start of collapse (R_m), the longer collapse will take and the less certain is the assumption that P_m remains constant. In fact, if R_m is very large, there may be insufficient time for collapse. Interestingly, a bubble of radius 10^{-3} cm ($\tau \approx 1 \mu\text{s}$) will be unable to collapse in an applied acoustic field of 1 MHz (period = 1 μs) or greater.

Subsequent modifications by Zhoroshev, for the collapse of vapour filled transients from their maximum radius, R_m , under a liquid pressure of P_m gives

$$\tau = 0.915R_m \left(\frac{\rho}{P_m} \right)^{1/2} (1 + P_v/P_m) \quad (2.27)$$

where P_v = vapour pressure in bubble.

In the absence of an ultrasonic field ($P_m = P_h$), Zhoroshev's expression reduces to the Rayleigh (Eq. A.20), provided the pressure in the bubble (P_v) is less than that in the liquid (P_h).

Appendix 4: Motion of Cavity Wall

In Appendix 3, it was shown (Eq. A.12) that the work done by an external pressure, P_h , in collapsing a cavity from a radius of R_m to R , was given by

$$\int_R^{R_m} P_h 4\pi R^2 dR \quad (\text{A.12})$$

and that this work was equivalent to the kinetic energy of the liquid moved:

$$KE = 2\pi \rho R^3 \dot{R}^2 \quad (\text{A.17})$$

where $\dot{R} = dR/dt$.

The arguments used, however, referred to an empty cavity and neglected the effects of surface tension (σ).

Consider now the movement of a cavity containing gas and vapour, originally at a radius, R_e , due to an increase in the ambient hydrostatic pressure (P_h) by the application of an acoustic pressure wave (P_a).

At any instant in the compression cycle the new hydrostatic pressure, $P'_h (= P_h + P_a)$ will cause the cavity radius to decrease from R_e to R (Fig. A4.1).

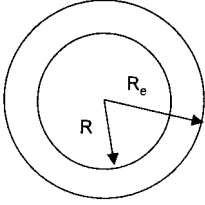


Fig. A4.1. Radius change during bubble collapse

This collapse will be augmented by an increase in the surface tension effect ($2\sigma/R$) as the cavity becomes smaller i. e. the total 'collapse' pressure is $(P'_h + 2\sigma/R)$, but will be opposed by the increase in the pressure within the bubble due to the compression of gas i. e. expanding pressure, P'_{bub} . By analogy with the empty cavity, the work done by the new hydrostatic pressure (P'_h), minus that of the layer adjacent to the bubble, is equal to the kinetic energy of the liquid.

$$-\int_{R_e}^R \left[\left(P'_h + \frac{2\sigma}{R} - P'_{bub} \right) 4\pi R^2 dR \right] = 2\pi \rho R^3 \dot{R}^2 \quad (\text{A.22})$$

Differentiation of Eq. A.22 yields

$$\left(P'_{bub} - P'_h - \frac{2\sigma}{R} \right) 4\pi R^2 dR = 2\pi \rho (3R^2 \dot{R}^2 dR + R^3 2\ddot{R} dR) \quad (\text{A.23})$$

which on dividing by $2\pi R^2 dR$ and rearranging gives

$$R\ddot{R} + \frac{3}{2}\dot{R}^2 = \frac{1}{\rho} \left[P'_{bub} - P'_h - \frac{2\sigma}{R} \right] \quad (A.24)$$

In Appendix 2, it was shown that

$$P'_{bub} = P_v + P'_g = P_v + P_g (R_e/R)^3$$

and

$$P_g = P_h + (2\sigma/R_e) - P_v$$

Substitution into Eq. A.24, and replacement of P'_h by $(P_h + P_a)$, gives, on neglecting vapour pressure ($P_v = 0$), Eq. A.25.

$$R\ddot{R} + \frac{3}{2}\dot{R}^2 = \frac{1}{\rho} \left[(P'_h + \frac{2\sigma}{R_e}) \left(\frac{R_e}{R} \right)^3 - \frac{2\sigma}{R} - P_h - P_a \right] \quad (A.25)$$

If the acoustic pressure, P_a , is replaced with $-P_A \sin w_A t$ (the form appropriate for a sinusoidal wave of pressure amplitude P_A and circular frequency $w_A (= 2\pi f)$), Eq. A.25 reduces to that first derived by Noltingk and Neppiras.

$$R\ddot{R} + \frac{3}{2}\dot{R}^2 = \frac{1}{\rho} \left[(P'_h + \frac{2\sigma}{R_e}) \left(\frac{R_e}{R} \right)^3 - \frac{2\sigma}{R} - P_h + P_A \sin w_A t \right]$$

More strictly the equation is

$$R\ddot{R} + \frac{3}{2}\dot{R}^2 = \frac{1}{\rho} \left[(P'_h + \frac{2\sigma}{R_e}) \left(\frac{R_e}{R} \right)^{3K} - \frac{2\sigma}{R} - P_h + P_A \sin w_A t \right] \quad (2.29)$$

where K is the polytropic index of the gas and varies between γ , the specific heat ratio, and unity, the limits for adiabatic and isothermal conditions.

Appendix 5: Maximum Bubble Temperature (T_{max}) and Pressure (P_{max})

In Appendix 4 we derived the equation for the motion of a cavity wall, as it collapsed due to an external pressure P'_h , to be

$$R\ddot{R} + \frac{3}{2}\dot{R}^2 = \frac{1}{\rho} \left[P'_{bub} - P'_h - \frac{2\sigma}{R} \right] \quad (A.24)$$

and where P'_{bub} , the pressure inside the bubble at a radius of R , was given by

$$P'_{\text{bub}} = P_v + P'_g = P_v + P_g (R_e/R)^3$$

(P_g = gas pressure in a bubble of initial radius R_e).

It has been argued (Appendix 3, Eq. A.21) that the collapse time for a bubble, initially of radius R_e , is considerably shorter than the time period of the compression cycle. Thus the external pressure $P'_h (= P_a + P_h)$, in the presence of an acoustic field, may be assumed to remain effectively constant (P_m) during the collapse period. Neglecting surface tension, assuming adiabatic compression (i.e. very short compression time), and replacing R_e by R_m , the size of the bubble at the start of collapse, the motion of the bubble wall becomes

$$R\ddot{R} + \frac{3}{2}\dot{R}^2 = \frac{1}{\rho} \left[P_g \left(\frac{R_m}{R} \right)^{3\gamma} - P_m \right] \quad (\text{A.24a})$$

Unlike Rayleigh's original example of a collapsing empty cavity, this bubble will reduce to a minimum size, R_{min} , on compression, after which it will expand to R_m and subsequently it will oscillate between the two extremes R_m and R_{min} . Obviously at the two extremes of radii, motion of the bubble wall is zero – i.e. $\dot{R} = 0$. To determine these radii it is necessary to integrate Eq. A.25. With $Z = (R_m/R)^3$, the integration yields:

$$\frac{\rho \dot{R}}{2} = P_m (Z - 1) - \left[\frac{P_g (Z - Z^\gamma)}{(1 - \gamma)} \right] \quad (\text{A.26})$$

which on setting $\dot{R} = 0$ and rearranging gives

$$P_m (Z - 1) (\gamma - 1) = P_g (Z^\gamma - Z) \quad (\text{A.27})$$

For very small values of R , (i.e. R_{min}), Z will be extremely large and $(Z - 1)$ approximates to Z , such that Eq. A.27 may be written as

$$P_m (\gamma - 1) \sim P_g Z^{\gamma-1} \quad (\text{A.28})$$

which on rearrangement yields

$$Z = \left(\frac{P_m (\gamma - 1)}{P_g} \right)^{1/(\gamma-1)} \quad (\text{A.29})$$

Now at minimum cavity volume (V_{min}) the gas will have its maximum pressure value, P_{max} , such that

$$P_{\text{max}} V_{\text{min}}^\gamma = P_g V_{\text{max}}^\gamma$$

And, since the volume of the cavity (V) is related to its radius (R) by

$$V = \frac{4}{3} \pi R^3$$

$$\text{then } \frac{V_{max}}{V_{min}} = \left\{ \frac{R_m}{R_{min}} \right\}^3 = Z \quad (\text{A.31})$$

$$\text{and } \left\{ \frac{V_{max}}{V_{min}} \right\}^\gamma = \frac{P_{max}}{P_g} = Z^\gamma \quad (\text{A.32})$$

Replacement of Z from Eq. A.29 and rearrangement gives

$$P_{max} = P_g \left\{ \frac{P_m (\gamma - 1)}{P_g} \right\}^{\gamma/(\gamma-1)} \quad (2.36)$$

At the instant of bubble collapse, this pressure will be released into the liquid. It is these very high liquid pressures which give rise to certain of the well-known effects of ultrasonic irradiation, such as erosion, dispersion and molecular degradation.

To find the maximum gas temperature attained at V_{min} , we apply

$$T_{max} V_{min}^{\gamma-1} = T_{min} V_{max}^{\gamma-1}$$

i. e.

$$T_{max} = T_{min} \left\{ \frac{P_m (\gamma - 1)}{P_g} \right\} \quad (2.35)$$

In most sonochemical applications T_{min} is taken to be the ambient (experimental) temperatures, and P_g as the vapour pressure of the liquid at that temperature.

Thus, even if a bubble does not undergo transient collapse, extremely high temperatures and pressures are developed within the bubbles as they oscillate from R_m to R_{min} . It is these large temperatures and pressures within the bubble which are thought to contribute to the significant increases in chemical reactivity observed in the presence of ultrasound. This does suppose however, that the reactant species is sufficiently volatile to enter the bubble. If it is not, increased chemical reactivity can only be assumed to have occurred due to increased molecular interaction within the liquid due to the large build up of pressure at the bubble wall. If the bubble is not to completely collapse then this will be equal to the liquid pressure at the liquid-bubble wall interface.

Appendix 6 Bubble Dynamics

Some years ago we designed this basic programme to help in the teaching of our undergraduate courses in sonochemistry. At that time the computer system used was a BBC microcomputer (built in the UK) with limited speed and memory. Some of the programming terminology is specific to the BBC but can be recognized and adapted for other systems. We found it to be of considerable benefit at this introductory level of bubble dynamics for chemists. Nowadays far more sophisticated approaches are available but, in writing this book, it was not our intention to become overly embroiled in mathematics. We have therefore reproduced our programme below so that it can either be used directly or adapted in order to demonstrate some simple manipulations.

Operation of the Programme

1) Lines 20 to 310

In order that the programme can be used to calculate both the resonance frequency (RF) and angular resonance frequency (WR) for a chosen bubble (radius, br) it will be necessary to input the solvent density (d), the surface tension of the solvent (σ), the solvent viscosity (η) and the solvent vapour pressure (pv). The programme can correct the data to the appropriate SI unit. For example, if a bubble radius of 10^{-2} cm was entered the correct response to the question "Type in the initial (equilibrium) bubble radius in cm" - line 280 – would be either 0.01 or 1E-2 followed by return. The programme will convert the value to metres - (i.e. $BR=.01*br$).

2) Lines 320 to 410

This section of the programme allows an estimation of the acoustic amplitude (P_A) of the wave from knowledge of the intensity (Int) of the wave and the velocity (vel) of sound in the medium. The value for velocity must be either entered in full (i.e. 1500) or by using the mathematical notation 1.5E3.

3) Lines 410 to 640

This section of the programme determines the maximum and minimum acoustic pressure and bubble radius and ensures optimum use of the screen.

4) Lines 650 to 1250

This section of the programme calculates and displays the variation in the applied acoustic pressure, the resonance pressure (or frequency) and the bubble dimensions with time. The GCOL statements in lines 1200 and 1220 refer to colour (e.g. GCOL0,1 is red and GCOL0,3 is white).

This programme is called "BUBBLE" (line 1270).

```

10 GOSUB1290:PRINTTAB(12,5);"BUBBLE
  DYNAMICS""TAB(B,B)"Copyright J P Lorimer and
  T.J.Mason""TAB(14,10)" Jan 1988":FOR
  Q=1TO15000:NEXT
20 GOSUB1290:N=O:GCOLO,3:CLS:PRINT"":INPUT" Is
  the solvent water. Y/N";ANS$
30 IF ANS$="Y" THEN 40 ELSE 50
40 D=1000: S=076: V=.001: PV=(.023*1.013E5) :
  GOTO250
50 GOSUB1300:INPUT" Input solvent density";
  d:GOSUB1300:PRINT "Are the density units"" (1)
  g/cc "" (2) Kg/m3":GOSUB1310
60 IF ANS=1 THEN 70 ELSE 80
70 D=1000*d: GOTO 90
80 D=d
90 GOSUB1310: INPUT"Input solvent surface tension";
  s:GOSUB1300:PRINT " Are the units "" (1) dyne/cm
  "" (2) N/m":GOSUB1310
100 IF ANS=1 THEN 110ELSE 120
110 S=.001*s:GOTO 130
120 S=s
130 GOSUB1300: INPUT" Input solvent viscosity";
  v:GOSUB1300:PRINT " Are the units (1) centipoise
  "" (2) poise "" (3) Kg/m/s":GOSUB1310
140 IF ANS=1 THEN 150ELSE 160
150 V= .001*v:GOTO 190
160 IF ANS=2 THEN 170 ELSE 160
170 V=.1*v:GOTO 190
180 V=v
190 GOSUB1300:INPUT" Input solvent vapour pres-
  sure":pv:GOSUB1300:PRINT " Are the units "" (1)
  Torr "" (2) bar "" (3) N/sq m":GOSUB1310
200 IF ANS=1 THEN 210 ELSE 220
210 PV=(pv/760)*1.013E5:GOTO 250
220 IF ANS=2 THEN 230 ELSE 240
230 PV= (pv*1.013E5) :GOTO 250
240 PV=pv
250 REM ATMOS PRESSURE TAKEN TO BE 1 BAR
260 PO=1.013E5
270 GOSUB1300: INPUT" Type in the exptl freq in
  KHz":f:W=1E3*f^2*3.142
280 GOSUB1300:INPUT" Type in the initial (equil) bubble
  "" radius in cm":br:BR=.01*br:IF br<1.01E-2 THEN
  G=1 ELSE G=1.333
290 REM - CALCULATION OF RESONANCE FREQ
300 a=(PO+(2*S/BR)-PV):b=(2*S/BR):c=((4*V*V)/
  (D*BR*BR)):e=(3*G*a)-b-c:WR((1/( D*BR*BR))*e)^.5:
  RF=WR/ (2*3.142)
310 REM to calculate r value for various PA and t

320 GOSUB1300: INPUT" Do you know intensity of sound
  wave";ANS$
330 IF ANS$="Y" THEN 340 ELSE 360
340 INPUT "Input Intensity in W/sq cm";Int
350 GOSUB1610:INPUT" Input velocity of sound (m/s)
  in your medium";vel:PA=(2*Int*D*vel*1E4)^.5:GOTO
  420
360 GOSUB1300: INPUT" Input pressure amplitude (PA)
  value";pa:GOSUB1300:PRINT" Are the units"" (1)
  Torr"" (2) bar"" (3) N/m2":GOSUB1310
370 IF ANS=1 THEN 380 ELSE 390
380 PA=(pa/760)*1.013E5:GOTO 420
390 IF ANS=2 THEN 400 ELSE 410
400 PA=pa*1.013E5:GOTO 420
410 PA=pa
420 ff=((WR^2)-(W^2))
430 CONST= (PA/ (D*BR*ff))
440 GOSUB1300: INPUT" How many cycles (MAX 10)";N
450 IF N>10 THEN N=10 ELSE N=N
460 FC=500/N: INC=1/(FC*f*1E3) :T=0:T=T+INC
470 GOSUB1300: INPUT" Do you want res freq on
  graph";ANS$
480 RMAX=1:RMIN=1:PMAX=1:PMIN=1:GOSUB1300
490 VDU5:MOVE150,500:PRINT"LOOKING FOR MAX
  AND MIN PRESSURES":VDU 4
500 FOR I= 1 TO 500
510 GOSUB1320
520 IF RR<0.01*BR THEN 530 ELSE 630
530 C=C+1
540 IF RR>RMAX THEN 550 ELSE 560
550 RMAX=RR
560 IF RR<RMIN THEN 570 ELSE 580
570 RMIN=RR
580 IF P= PMAX THEN 590 ELSE 600
590 PMAX=P
600 IF P<PMIN THEN 610 ELSE 640
610 PMIN=P
620 GOTO 640
630 I=500
640 NEXT
650 NEWN= (N*C) /500: NNEWN: GOSUB 1290:
  IF PMIN=0 THEN 660 ELSE 670
660 AA=800:GOTO680
670 AA=900
680 XS=(1000-AA)/
  PMAX:NN=(INT((ABS(PMAX)+ABS(PMIN)))/
  (2*PO/1.013E5)))+1
690 IF ANS$="Y" THEN 700 ELSE 710
700 BB=600:GOTO 720

```

```

710 BB=800
720 YS=1000/N:FC=500/N:RS=(BB-200) / (RMAX-RMIN):
    INC=1/ (FC*f*1E3) :T=INC
730 TO=1/ (f*1E3)
740 FOR I = 1 TO (FC*N)
750 GOSUB 1320
760 t=T/TO:TT=t*YS:PP=(P*XS) +AA:RRR=((RR-RMIN)
    *RS) :RRP= (XS*RP) +BB:@%=&50405
770 VDU 5: GCOL0 ,3: MOVE 100, 100: DRAW100, 1000
780 IF ANS$="Y" THEN 790 ELSE 800
790 GCOL 0,2:PLOT69, (TT+100) ,RRP
800 GCOL 0,3:PLOT69, (TT+100) ,PP
810 GCOL 0, 1:PLOT69, (TT+100) ,RRR+100:VDU4
820 NEXT I
830 GCOL0,3:VDU5:MOVE TT+100, 100:DRAW TT+100,
    1000:MOVE 100, 100:DRAW TT+100,100:VDU 4
840 IF NN<3 THEN 850 ELSE 860
850 PAP=1:GOTO 910
860 IF NN<3 AND NN<5 THEN 870 ELSE 880
870 PAP=0.5:GOTO 910
880 IF NN<5 AND NN<10 THEN 890 ELSE 900
890 PAP=0.25:GOTO 910
900 IFNN<10 AND NN<20 THEN PAP=0.1 ELSE PAP=0.05
910 IP=-NN+1
920 FOR I = 1 TO (2*PAP*NN)
930 IP=IP+(1/PAP):IPP=(IP*XS)+AA:GCOL
    0,3:VDU5:MOVE 100,IPP:DRAW 120, IPP:VDU 4
940 IF ANS$="Y" THEN 950 ELSE 960
950 VDU5: MOVE 100, (IPP+BB-AA) : DRAW 60,
    (IPP+BB-AA) : VDU4
960 VDU5:MOVE 20,IPP+10:PRINT" ";IP:VDU4
970 IF ANS$="Y" THEN980 ELSE 990
980 GCOL0,2: VDU5:MOVE -20, IPP+10+BB-AA:
    PRINT" "; IP: VDU4
990 NEXT
1000 IF RMAX-RMIN<0 AND RMAX-RMIN<0.8 THEN
    1010 ELSE 1020
1010 AB=0.1:GOTO 1130
1020 IF RMAX-RMIN>0.8 AND RMAX-RMIN<1.6 THEN
    1030 ELSE 1040
1030 AB=0.2 :GOTO 1130
1040 IF RMAX-RMIN<1 .6 AND RMAX-RMIN<3.3 THEN
    1050 ELSE 1060
1050 AB=0.4:GOTO 1130
1060 IF RMAX-RMIN>3.3 AND RMAX-RMIN<6.5 THEN
    1070 ELSE 1060
1070 AB=0.8:GOTO 1130
1080 IF RMAX-RMIN<6.5 AND RMAX-RMIN<9 THEN
    1090 ELSE 1100
1090 AB=1:GOTO 1130
1100 IF RMAX-RMIN>9 AND RMAX-RMIN<20 THEN
    1110 ELSE 1120
1110 AB=2:GOTO 1130
1120 IF RMAX-RMIN<20 AND RMAX-RMIN<40 THEN
    AB=4 ELSE AB=8
1130 D=INT((RMAX-RMIN)/AB)+1:DD=-(D*AB):NR=DD
1140 FOR I= 1 TO (2*D)
1150 DD=DD+AB:NR=NR+AB:Sr=DD*BR:R=
    BR+Sr:RR=R/BR: IIR((RR-RMIN)*RS) :
    IIRMAX=((RMAX-RMIN) *RS): IIRMIN=
    ((RMIN-RMIN) *RS)
1160 IF IIR<IIRMAX THEN 1190 ELSE 1170
1170 IF IIR<IIRMIN THEN 1190 ELSE 1180
1180 GCOL0,1:VDU5:MOVE100,IIR+100:
    DRAW120,IIR+100:MOVE0,IIR+120:PRINT" ";
    NR+1:VDU4
1190 NEXT
1200 GCOL0, 1: VDU5: MOVE 250,70: PRINT"Radius-time
    curve": VDU4
1210 GCOL0,3:VDU5:MOVE 30,30:PRINT"PA=";
    PA/ 1.013E5; " atmos";" f=";f;" kHz"; "R0=";br;"
    cm":VDU4
1220 GCOL0, 1:VDU5:MOVE
    TT+150,300:PRINT"r":MOVE TT+150, 270: PRINT"-":
    MOVE TT+150,240:PRINT"Re":MOVE
    TT+150,400:PRINT """:MOVE
    TT+150,370:PRINT":":GCOL0,3:VDU4
1230 IF ANS$="Y" THEN 1240 ELSE 1250
1240 GCOL0,2:VDU5:MOVE
    TT+120,BB+100:PRINT"reson":MOVE
    TT+120,BB+50:PRINT"press" : VDU4
1250 GCOL0 ,3: VDU5 :MOVE TT+120,AA+100:
    :PRINT"appl":MOVE TT+120,AA+50:
    PRINT"press":VDU4
1260 GCOL0 ,3: VDU5: MOVE300,800: INPUT" RUN
    AGAIN. Y/N ";ANS$
1270 IF ANS$="Y" THEN CHAIN "BUBBLE"
1260 END
1290 MODE 1:GCOL 0,129:VDU 19,0,4;0:CLG:GCOL
    0,3:RETURN
1300 CLS:PRINT"" :RETURN
1310 PRINT:INPUT" Insert the appropriate
    number";ANS:RETURN
1320 T=T+INC:P=(PO-(PA*SIN(W*T)))/1.013E5:RP=
    (PO -(PA*SIN(WR*T)))/1.013E5:r=
    CONST*(SIN(W*T)-((W/WR)*SIN(WR*T)):
    R=BR+r:RR=R/BR:RETURN

```

3

Synthesis

3.1

Introduction

The term *sonochemistry* is used to describe a subject which uses sound energy to affect chemical processes and the terminology is in keeping with that of the longer established methods such as *electrochemistry* (the use of electricity to achieve chemical activation). These “older” technologies require some special attribute of the system being activated in order to produce an effect e. g. the use of microwaves (dipolar species), electrochemistry (conducting medium) and photochemistry (the presence of a chromophore) whereas sonochemistry requires only the presence of a liquid to produce its effects.

At the beginning of laboratory research into sonochemistry, the use of ultrasonic waves in chemistry was viewed as merely a convenient technique for starting the more recalcitrant types. Its development in the past 15 years however has revealed both its broad applicability and the scientific challenge involved in understanding its underlying physical phenomenon – acoustic cavitation [1–3]. Fortunately an absolute understanding of the physical principles has not stopped an ever expanding number of applications in synthesis which has made sonochemistry attractive to many experimentalists. Its usage has spread beyond academic laboratories into industry and chemical engineering and there are now a number of texts available for study [4–12]. In recent years a major collaborative effort aimed at understanding the principles of sonochemistry has brought together chemists, physicists, engineers and mathematicians in an alliance which bodes well for the future of international co-operation in this domain.

The potential of sonochemistry was identified over sixty years ago in a wide ranging paper entitled “The Physical and Biological Effects of High Frequency Sound-Waves of Great Intensity” [13]. Over the few years which followed this paper a great deal of pioneering work in sonochemistry was carried out and, as a result of this, two reviews on the applications of ultrasound in polymer and chemical processes were published

in the 1940's [14, 15]. There are very few references to ultrasound in chemistry from about 1955 to when a major renaissance in the subject began to occur which has accelerated dramatically over the last few years. This revival of interest is undoubtedly due to the more general availability of commercial ultrasonic equipment particularly the simple laboratory ultrasonic cleaning bath. It was in 1986 that the first ever International Symposium on Sonochemistry was held at Warwick University U.K. as part of the Autumn Meeting of the Royal Society of Chemistry [16]. This meeting was significant in that it was the beginning of serious interest in the uses of ultrasound in chemistry as a study in itself. Following the conference a Royal Society of Chemistry Sonochemistry Group was founded in the UK in 1987 followed by a series of other national groups (Germany, Romania and Japan). The European Society of Sonochemistry was established in 1990. Historical background to the development of sonochemistry can be found in three review articles [17–19].

For the majority of synthetic chemists interest in sonochemistry will be in power ultrasound – the type of sound which provides sufficient energy to affect chemical reactivity (see Chapter 1). When one wishes to change the reactivity of a system the method of choice would normally be an alteration in one of the external physical variables such as heat, light or pressure. The choice will be made based upon one's experience of the type of effect induced by such alterations. Ultrasound provides energy in a form which is different from the above. The effects of ultrasound however are not as quantifiable as those produced by the more conventional physical variables although the underlying reason for its mode of action is recognised as being due to cavitation.

We have already seen how cavitation can be induced in any liquid provided the appropriate ultrasonic energy is applied and that cavitation is the source of the dramatic effect of power ultrasound on chemical reactivity. A number of external parameters influence the efficacy of ultrasonic irradiation in promoting cavitation and thus chemical reactivity and these have been discussed in detail in Chapter 2. Here we will re-examine briefly the experimental parameters which are more commonly varied. As the frequency is increased cavitation bubble lifetime and collapse energy are reduced. At high frequency (> 3 MHz) there is not enough time during the rarefaction cycle for bubble growth to achieve sufficient size to disrupt the liquid. For cavitation at high frequency more power is needed since more energy is lost to molecular motion of the liquid. It is for this reason that most commercially available pieces of ultrasonic equipment used in sonochemistry operates at the lower end of the ultrasonic range (20–50 kHz). However, as we will see later, higher frequencies are advantageous when radical production is important.

The first requirement for the level of ultrasonic power required to cause chemical effects in a reaction is that sufficient acoustic energy must be supplied to overcome the cavitation threshold of the medium. Once this has been exceeded then the region of

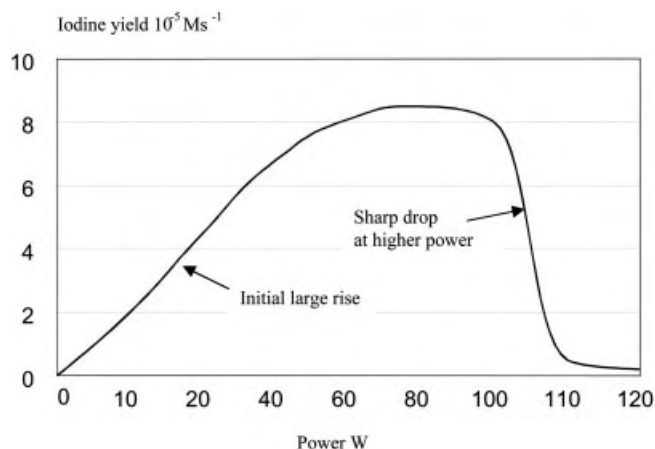


Fig. 3.1. Effect of increasing power on a sonochemical reaction.

cavitation around the radiating source, the “cavitation zone”, will increase with intensity and one might expect that the sonochemical rate would also increase in parallel with this. Thus the observed increase in the rate of hydrolysis of methyl ethanoate in the presence of ultrasound has been found to be directly proportional to intensity. A limiting value is reached however and beyond this limit the sonochemical rate is found to decrease with power [20, 21]. A further example can be found in the effect of power on the liberation of iodine from the sonolysis of aqueous KI (Fig. 3.1) [19]. The initial response of iodine yield appears to be proportional to power but this effect is reduced beyond 40 W and drops dramatically above 100 W. The explanation for these power effects lies in the production of a large number of cavitation bubbles on and near the acoustic source which act as a “cushion” to dampen the efficiency of energy transmission into the reaction medium. As more and more such bubbles are produced they act as a barrier to energy transmission into the system and the sonochemical effects are substantially reduced.

When considering the reaction conditions for a sonochemical process the choice of solvent and the bulk working temperature are significant factors and are often inter-related. Any increase in solvent vapour pressure would decrease the maximum bubble collapse temperature and pressure. Hence for a reaction where cavitation collapse is the primary cause of sonochemical activation then a low bulk temperature would be preferred, particularly if a low boiling solvent is used. Conversely for a reaction requiring elevated temperatures a high boiling solvent would be appropriate. For heterogeneous reactions where the effect of sonication is action on the surface of either a catalyst or an inorganic solid a balance must be struck between ensuring enough cavitation to ensure reagent activation without overly disturbing the thermodynamics of the

reaction. It must also be remembered that in some cases where extended reaction periods are required the solvent itself may not be totally inert, discoloration and charring may occur. In most synthetic reactions however solvent reaction can be ignored because reaction times are short.

Application of an external pressure to a reaction system, which increases the hydrostatic pressure of the liquid, leads to an increase in the energy required to initiate cavitation. In practical terms if this threshold energy can be exceeded with the available irradiation source then an increase in hydrostatic pressure would lead to an increase in sonochemical effect. This is because the maximum temperatures and pressures experienced during bubble collapse will be higher under these conditions. Conversely, bubbling a gas through a liquid during ultrasonic irradiation should decrease both the cavitation threshold and intensity. This is a direct consequence of the increase in the number of gas nuclei available to initiate cavitation and the “cushioning” effect on the collapse of the bubbles caused by the gas present in them.

3.2

The Various Sites for Sonochemical Reactions

In order to understand the way in which cavitation collapse can effect chemical processes one must consider the possible effects of this collapse in different types of liquid system.

In the case of a *homogeneous liquid phase*, as with any other liquid system, the cavity will almost certainly contain vapour from the liquid medium or dissolved volatile reagents (Fig. 3.2). On collapse, these vapours will be subjected to extremely large increases in temperature and pressure resulting in molecular fragmentation with generation of highly reactive radical species. In order for a chemical to experience the extreme conditions generated inside the cavitation bubble during collapse it must enter the bubble and so should be volatile. The “concentration” of cavitation bubbles produced by sonication using conventional laboratory equipment is very small and so overall yields in this type of reaction are low. Thus in the sonication of water small quantities of HO^\bullet and H^\bullet radicals are generated in the bubble and these undergo a range of subsequent reactions including the generation of H_2O_2 . The highly oxidising HO^\bullet species can react with other moieties in the bubble or migrate to the bulk solution where they have only transient existence. Such radicals can have a significant effect on both biological and chemical species in aqueous solution and can be detected chemically [22]. Organic solvents will also slowly decompose on sonication but solvent decomposition is normally only a minor contribution to any sonochemical reaction taking place in the medium.

The sudden collapse of the bubble also results in an inrush of liquid to fill the void. So powerful is this inrush that it will produce shear forces in the surrounding bulk

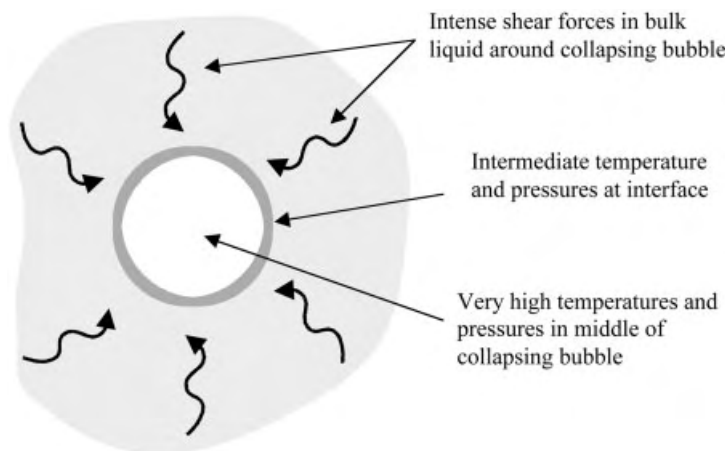


Fig. 3.2. Effect of sonication in a homogeneous liquid phase.

liquid capable of breaking the chemical bonding in any polymeric materials which are dissolved in the fluid (see subsequent chapter).

It is cavitation in a *heterogeneous* medium which is the most studied by sonochemists. When produced next to a phase interface, cavitation bubbles are strongly deformed. A liquid jet propagates across the bubble towards the interface at a velocity estimated to hundreds of metres per second. At a *liquid-liquid* interface, the intense movement produces a mutual injection of droplets of one liquid into the other one, i. e. an emulsion (Fig. 3.3). Such emulsions, generated through sonication, are smaller in size and more stable than those obtained conventionally and often require little or no surfactant to maintain stability. It can be anticipated therefore that Phase Transfer Catalysed (PTC) reactions will be improved by sonication. Examples are provided later in this chapter.

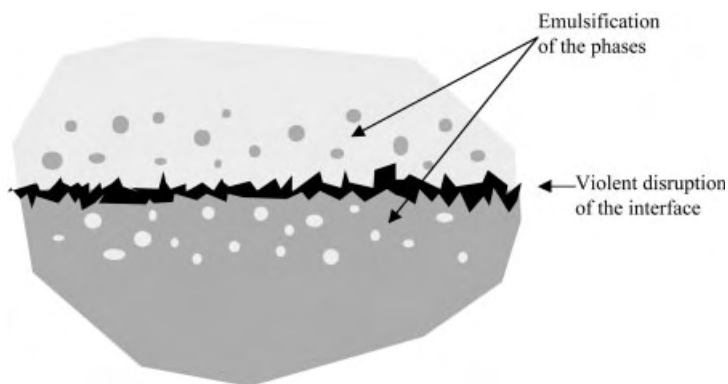


Fig. 3.3. Effect of sonication in a biphasic liquid system.

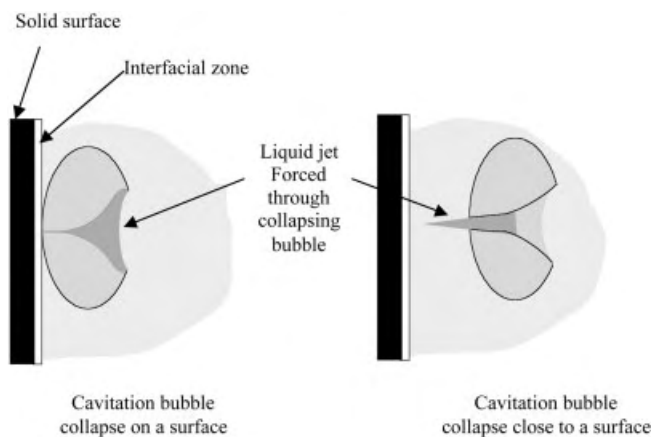


Fig. 3.4. Effect of sonication in a liquid near a solid surface.

At a *solid-liquid interface*, the evolution of the cavitation bubbles has been observed with high speed cameras and the generation of a “jet” impinging upon the surface has been recorded (Fig. 3.4) [23]. In this case, the shock on the surface produces erosion at and around the point of jet impact. Particles which may be ejected from the surface by this action react more efficiently than the bulk solid surface due to an increased surface area. When a passivating coating is present on the solid surface the jetting will remove it leaving “clean” surface and activation results [24]. At the same time, the surface is disorganised, local defects, dislocations, vacancies are produced and this generates a positive effect on reactivity. Associated with the collapse, and of particular importance in both catalysis and electrochemistry, is the increase in mass transfer to the surface by disruption of the interfacial boundary layers.

In the case of solid interfaces which are in the form of coarse powders, cavitation collapse can produce enough energy to cause fragmentation and activation through surface area increase. For very fine powders the particles are accelerated to high velocity by cavitation collapse and may collide to cause surface abrasion (Fig. 3.5). For some metal powders these collisions generate sufficient heat to cause particle fusion.

The qualitative description above shows the complexity of the effects of cavitation on solids. The superficial modifications can be described by a mathematical parameter, the *fractal number*. A value of 2 corresponds to a quasi planar geometry, 3 represents a three dimensional space. For silica, commonly used in solid supported reactions, the fractal number, originally 1.8–2.3, increases to 2.8 by sonication [25]. The higher reactivity of sonicated solids can then be explained by the transformation of a surface reaction to a process occurring in a volume. A more complex aspect is the tribochemical effect, according to which mechanical shocks are capable of ejecting high energy

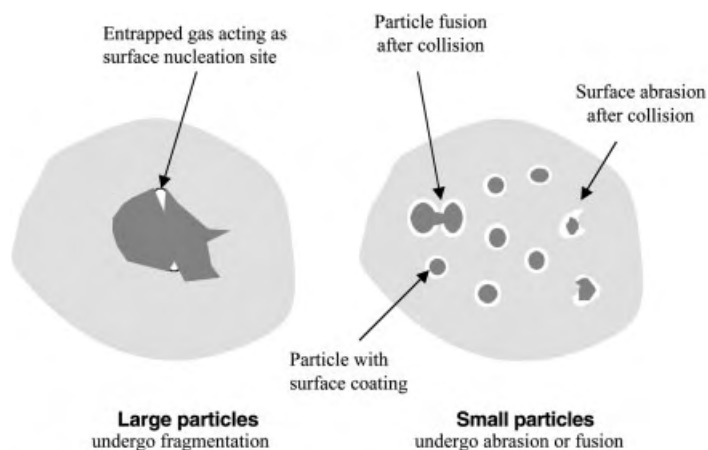


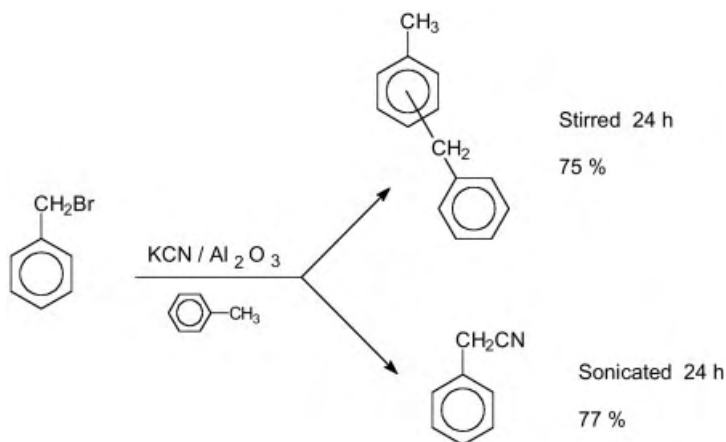
Fig. 3.5. Effect of sonication in a liquid containing suspended particles.

electrons from solids. As a result of such processes chemical reactions, e. g. polymer formation or cleavage and radical generation from small molecules, can result [26]. It seems possible therefore that the tribochemical effect might well contribute to the higher reactivity of sonicated solids [27, 28].

3.3

An Attempt to Define the Laws of Sonochemistry

From a survey of past literature in sonochemistry it can be seen that ultrasonic irradiation in synthesis seems to have been developed on a practical rather than theoretical basis. Justification for enhanced reactivity was generally rationalised using the intuitively straightforward (at least in a qualitative sense) “hot spot” approach. Many advances were made by experimentalists, who proceeded essentially by “trial and error”. Critics of the technique regarded sonochemistry merely as a kind of super-agitation. The first paper which evidenced the specific nature of sonochemistry was published by Ando et al. who described the first case of “sonochemical switching” [29]. The original system which led to this discovery (Scheme 3.1) consisted of a suspension of benzyl bromide and alumina-supported potassium cyanide in toluene. The *stirred* reaction provided regio-isomeric diphenylmethane products *via* a Friedel-Crafts reaction between the bromo compound and the solvent, catalysed by the solid phase reagent. In contrast, *sonication* of the same constituents furnished only the substitution product, benzyl cyanide. According to the authors, a structural change on the catalytic sites of the solid support could be responsible for this effect.



Scheme 3.1

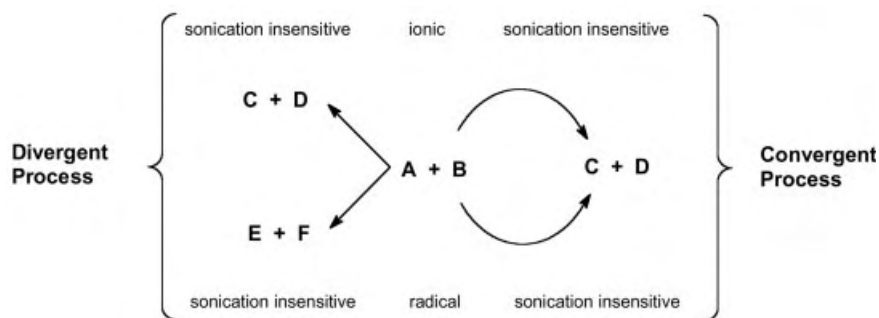
Since this type of result shows that sonication is definitely not just another method of providing agitation of a medium, but exhibits its own peculiarities, it stands to reason that it should obey some rules of its own. An examination and classification of published material led to an empirical systemisation of sonochemistry [28, 30]. This classification concentrates on the chemical effects in sonochemistry but it should also be recognised that in some cases ultrasound does act in a mechanical sense achieving remarkable results through super agitation. Sometimes the mechanical and chemical effects occur together.

Rule 1 applies to homogeneous processes and states that those reactions which are sensitive to the sonochemical effect are those which proceed via radical or radical-ion intermediates. This statement means that sonication is able to effect reactions proceeding through radicals and that ionic reactions are not likely to be modified by such irradiation.

Rule 2 applies to heterogeneous systems where a more complex situation occurs and here reactions proceeding *via* ionic intermediates can be stimulated by the mechanical effects of cavitation agitation. This has been termed “false sonochemistry” although many industrialists would argue that the term false may not be correct because if the result of ultrasonic irradiation assists a reaction it should still be considered to be assisted by sonication and thus “sonochemical”. In fact the true test for “false sonochemistry” is that similar results should, in principle, be obtained using an efficient mixing system in place of sonication. Such a comparison is not always possible.

Rule 3 applies to heterogeneous reactions with mixed mechanisms *i. e.* radical and ionic. These will have their radical component enhanced by sonication although the general mechanical effect from Rule 2 may still apply. Two situations which may occur in heterogeneous systems involving two mechan-

istic paths are shown below (Scheme 3.2) [31]. When the two mechanisms lead to the same product(s), which we will term a “convergent” process, only an overall rate increase results. If the radical and ionic mechanisms lead to different products, then sonochemical switching can take place, by enhancing the radical pathway only. In such “divergent” processes, the nature of the reaction products is actually changed by sonication. Examples will be discussed later in this chapter.



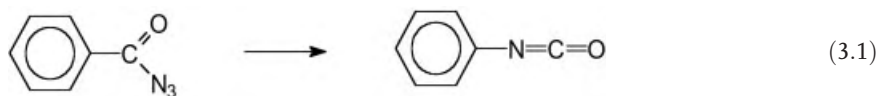
Scheme 3.2

It is worth noting that the use of a very high-speed stirrer e.g. an Ultra-Turax can produce similar effects to sonication in heterogeneous systems. This may well be a case of chemistry induced by hydrodynamic rather than acoustic cavitation [32, 33].

3.4 Homogeneous Reactions

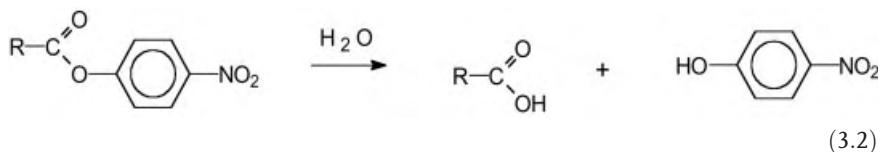
Any system involving a homogeneous liquid in which bubbles are produced is not strictly homogeneous however in sonochemistry it is normal to consider the state of the system to which the ultrasound is applied. Sonochemical effects generally occur either inside the collapsing bubble where extreme conditions are produced, at the interface between the cavity and the bulk liquid where the conditions are far less extreme or in the bulk liquid immediately surrounding the bubble where the predominant effects will be mechanical (Fig. 3.2).

The origins of sonochemistry lie in the study of homogeneous systems and among the examples of early synthesis is the Curtius rearrangement which appeared in 1938 [34]. In this example benzazide gives nitrogen and phenyl isocyanate when sonicated in benzene (Eq. 3.1), and the rate is increased in comparison to the normal thermal reaction. This reaction was not fully investigated at the time and the observation that the reaction stopped after rapid initial steps was not explained.

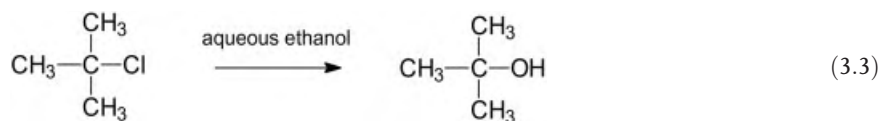


There have been very few detailed investigations of the kinetics of ultrasonic acceleration in homogeneous systems. An exception to this has been the study of a range of homogeneous hydrolysis reactions. Fogler and Barnes conducted one of the first of these in 1968 [21]. They reported that ultrasonic irradiation increased the rates of hydrolysis of methyl ethanoate and attributed the increase in reaction rate to the high temperatures reached within the cavitation bubbles. Subsequent studies of the same system by other groups suggested that the increase in reaction rate might also be due to an increase in frequency of collisions between molecules caused by cavitation pressure gradient and temperature rise [22, 35]. Studies on the effect of temperature on the increased rate induced by irradiating the system at 540 kHz revealed a 28 % enhancement at 20 °C and yet only a 20 % enhancement at 30 °C. This inverse relationship between ultrasonically induced rate acceleration and reaction temperature is now recognised as normal behaviour for systems under irradiation. It is the direct result of the lowering in solvent vapour pressure with a fall in temperature of the system.

In 1981 Kristol reported ultrasonically induced rate enhancements for the hydrolysis of the 4-nitrophenyl esters of a number of aliphatic carboxylic acids (1, R = Me, Et, *i*-Pr, *t*-Bu) (Eq. 3.2) [36]. The rate enhancements at 35 °C were all in the range of 14–15 % and were independent of the alkyl substituent (R) on the carboxylic acid. It was concluded that the rate enhancements could not be due simply to any increase in the macro reaction temperature (due to the bulk heating effect of the ultrasonic irradiation) since there are marked differences in the energy of activation (E_a) for the hydrolyses of each of these substrates. Given such differences in activation energy, any bulk heating effect (which would be similar in magnitude for each system studied) must result in widely different rate enhancements and not the uniform value of around 15 % observed throughout.



Another example of the effects of ultrasound on a solvolysis reaction can be found in the homogeneous hydrolysis of 2-chloro-2-methylpropane in aqueous alcoholic media (Eq. 3.3). This system has been the subject of numerous kinetic studies since it is one of the classic examples of a unimolecular nucleophilic displacement reaction (termed S_N1).



The homogeneous solvolysis of this substrate in aqueous ethanolic solvents can be monitored by the change in conductance as HCl is produced. Initial studies of the reaction in aqueous ethanol as solvent at 25 °C using a cleaning bath (45 kHz) revealed modest rate enhancements (up to about 2-fold) with the larger values being obtained in the more alcoholic media [37]. Similar results were found for the solvolyses in aqueous propan-2-ol and 2-methylpropan-2-ol. More substantial rate enhancements were obtained in the more ethanolic media and at lower temperature [38, 39]. Detailed studies of the aqueous ethanol system led to the following main conclusions:

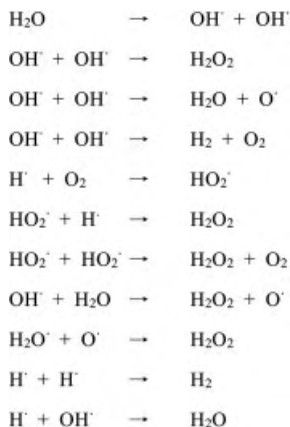
- The effect of ultrasound increased with increased ethanol content and decreased temperature giving rate enhancements up to 20-fold at 10 °C in 60 % w/w.
- At ethanol concentrations of 50 and 60 % the actual rates of reaction under ultrasonic irradiation increased as the temperature was reduced from 20 °C to 10 °C (by factors of 1.4 and 2.1 respectively).
- A maximum effect of ultrasound appeared to occur at a solvent composition of around 50 % w/w at 25 °C.

The explanation for the above is twofold. Firstly there is the effect of increasing cavitation collapse energy *via* a lowering in vapour pressure as the temperature is reduced (see above). This does not adequately explain the effect of the change in solvent. The primary process is unlikely to occur inside the cavitation bubbles and a radical pathway should be discarded. The most likely explanation is that the disruption induced by cavitation bubble collapse in the aqueous ethanolic media is able to break the weak intermolecular forces in the solvents. This will alter the solvation of the reactive species present. Significantly the maximum effect is found in 50 % w/w solvent composition – the solvent composition very close to the maximum hydrogen bonded structure.

The above studies were carried out at relatively low powers – typically a few W cm^{-2} produced by a cup-horn. When greater acoustic power is applied through a probe system (of the order of 20 – 30 W cm^{-2}) it is possible to induce some quite specta-

cular chemical reactions involving direct bond cleavage from reaction inside the bubble.

Water itself can be decomposed with the formation of radical species and the production of oxygen gas and hydrogen peroxide (Scheme 3.3).



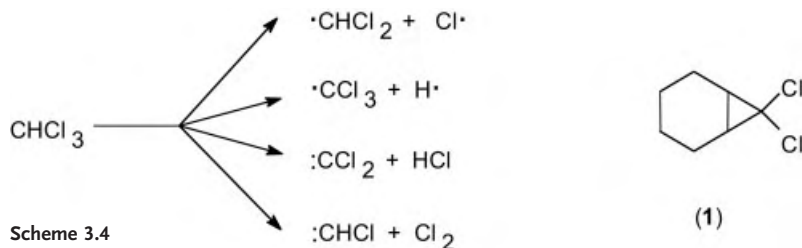
Scheme 3.3

Any species dissolved in the water is clearly going to be subject to chemical reaction with these ultrasonically produced radicals and/or hydrogen peroxide. Thus if iodide ion is present in solution iodine will be liberated. Spin trapping ESR techniques afforded positive identification of the radical species sonically generated in water [40].

Although the first example of sonolysis in a non-aqueous solvent, the decolourisation of diphenylpicrylhydrazyl (DPPH) radical in methanol, was reported in 1953 [41], it took some 20 years to realise that cavitation could successfully be supported in organic solvents. The lack of progress in this area was the result of a number of factors including the generalised observation that the addition of organic solutes suppressed sonochemically induced aqueous reactions. Another problem encountered was that in a large proportion of non-aqueous homogeneous sonochemistry solvents with high vapour pressures (e. g. ethers) were often used. At room temperature volatile solvents easily enter the bubble and cushion bubble collapse. To achieve effective cavitation in such solvents lower temperatures are normally required. The synthetic applications of non-aqueous sonochemistry will be discussed in this chapter but two areas relating to homogeneous polymer chemistry (synthesis and degradation) will be treated in a separate chapter.

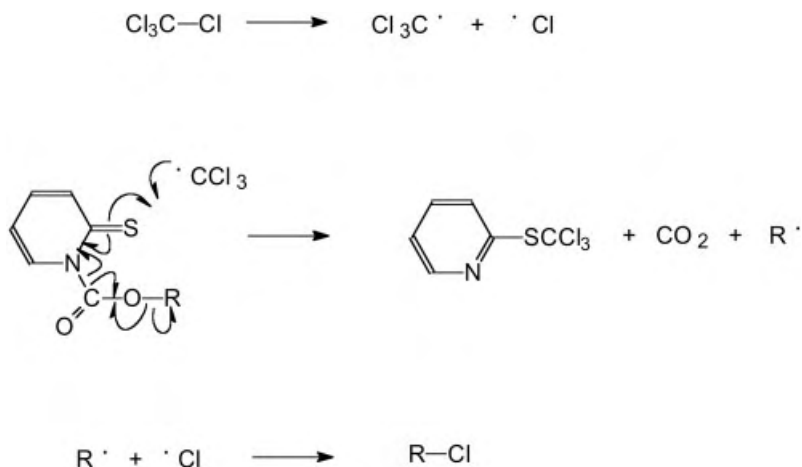
Homogeneous non-aqueous sonochemistry is typified by the sonolysis of chloroform which has been studied using ultrasonic irradiation of frequency 300 kHz ($I = 3.5 \text{ W cm}^{-2}$) to yield a large number of products amongst which are HCl, CCl_4 and C_2Cl_2 [42]. Decomposition was found to only occur in the presence of

mono or diatomic gases e.g. argon or nitrogen but not with larger gas molecules like CO_2 . The underlying reasons for this, i. e. the dependence of the energy of cavitation bubble collapse on the ratio of specific heats of the gas, has already been covered in Chapter 2. The precise mechanisms involved in the decomposition are complex but almost certainly involve the homolytic fission of chloroform to radicals and the formation of carbenoid intermediates as shown in Scheme 3.4.



Evidence for the generation of these reactive intermediates was obtained from a study of the effect of added cyclohexene on the sonication of chloroform. The presence of free radicals in the system was confirmed by the appearance of chlorocyclohexane as a product and by the increased rate of decomposition of CHCl_3 in the presence of cyclohexene. The increased decomposition rate is a consequence of the presence, in the cavitation bubble, of the alkene which “mops up” the $\text{Cl}\cdot$ radical as it is formed and prevents the regeneration of chloroform – i. e. the kinetic steps in Scheme 3.4 are “driven” from left to right. Carbene intermediates are implicated by the formation of tricyclic compounds such as (1) *via* dichlorocarbene addition to cyclohexene.

Dauben et al. found that the CCl_3 radical produced by sonolysis of carbon tetrachloride can be used in a decarboxylation-halogenation sequence (Scheme 3.5) [43]. Sonication of a thiohydroxamic ester at 33°C for 10–50 min in carbon tetrachloride leads to the corresponding chloride in high yield. In the presence of bromotrichloromethane or iodoform, bromides and iodides are formed in yields $> 80\%$. This reaction can be successfully applied to primary, secondary, or tertiary esters and offers an interesting variant to the usual Hunsdiecker procedure.



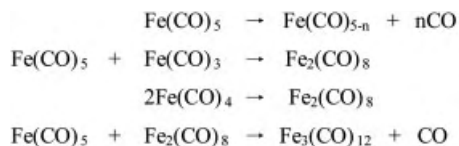
Scheme 3.5

Aromatic compounds undergo carbonisation during sonication [44]. The reaction can occur either at the bubble interface or inside the cavity, according to the hydrophilicity of the substrate. Generally it would appear that apolar, hydrophobic compounds, e. g. benzene and halocarbons are pyrolysed inside the bubble [45, 46].

In 1983 Suslick reported the effects of high intensity (ca. 100 W cm^{-2} , 20 kHz) irradiation of alkanes at 25°C under argon [47]. These conditions are of course, well beyond those which would be produced in a reaction vessel immersed in an ultrasonic bath and indeed those normally used for sonochemistry with a probe. Under these extreme conditions the primary products were H_2 , CH_4 , C_2H_2 and shorter chain alk-1-enes. These results are not dissimilar from those produced by high temperature ($> 1200^\circ\text{C}$) alkane pyrolyses. The principal degradation process under ultrasonic irradiation was considered to be C-C bond fission with the production of radicals. By monitoring the decomposition of $\text{Fe}(\text{CO})_5$ in different alkanes it was possible to demonstrate the inverse relationship between sonochemical effect (i. e. the energy of cavitation collapse) and solvent vapour pressure [48].

The use of $\text{Fe}(\text{CO})_5$ as a dosimeter in the above reaction was the result of previous studies on the decomposition of metal carbonyls in long chain alkanes as solvents. Suslick studied the sonolysis of volatile $\text{Fe}(\text{CO})_5$ which produced $\text{Fe}_3(\text{CO})_{12}$ together with finely divided iron (the proportion of each depending on the solvent vapour pressure). This is a significant result since it differs from both thermolysis (which yields finely divided iron) and uv photolysis (which yields $\text{Fe}_3(\text{CO})_9$). The iron metal produced in this reaction in the sonolysis of $\text{Fe}(\text{CO})_5$ (0.4 M) in decane under argon is amorphous [49]. The fact that an amorphous (rather than crystalline) material is produced confirms that very high temperatures are generated in the bubble and that extreme cooling rates are involved. Conventional production of amorphous

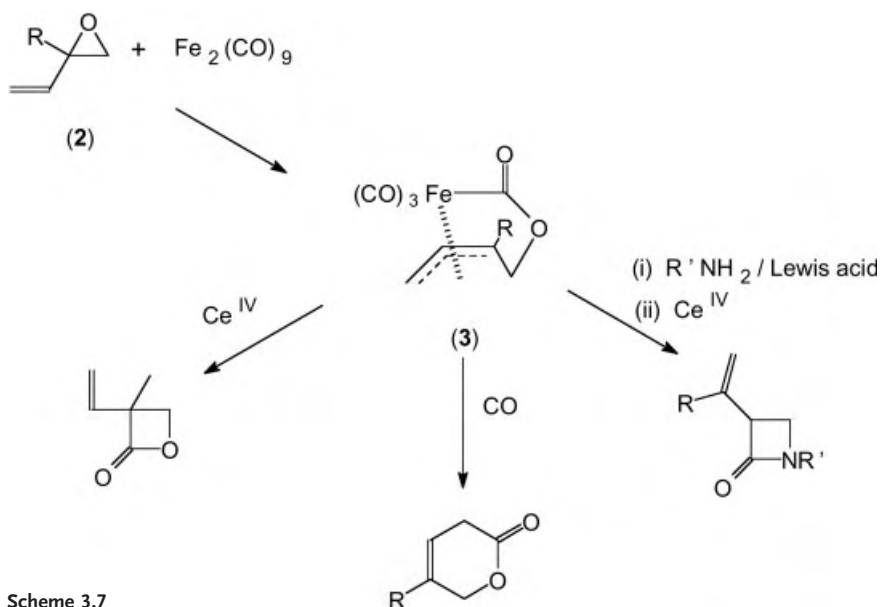
iron requires rapid cooling from the vapour to solid state of the order of 10^6 K s^{-1} . Sonolytic decomposition of iron pentacarbonyl in pentane (a more volatile solvent) yields $\text{Fe}_3(\text{CO})_{12}$ rather than the metal indicating that the cavitation collapse is not so extreme in this solvent. The reaction is thought to proceed *via* the following mechanism (Scheme 3.6). It is interesting to note that this type of reaction cannot be performed in a cleaning bath [50] but this is almost certainly due to the fact that in an ultrasonic bath there is a greatly reduced intensity of sonication compared with that achievable with a probe.



Scheme 3.6

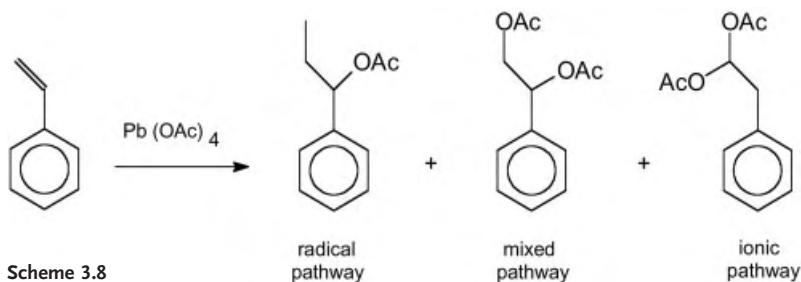
This mechanism was supported by evidence obtained from the sonolysis of any one of the three individual iron carbonyls $\text{Fe}(\text{CO})_5$, $\text{Fe}_2(\text{CO})_9$ and $\text{Fe}_3(\text{CO})_{12}$ in the presence of pent-1-ene [51]. In each case the pent-1-ene isomerised to give the same *cis*- to *trans*- isomer ratio of pent-2-ene indicating that the same catalytic species is generated from each carbonyl. For the same system, ligand substitution by phosphines or phosphites (L) occurred readily to give $\text{Fe}(\text{CO})_{5-n}\text{L}_n$ ($n = 1, 2, 3$). The rates of these reactions were independent of ligand concentration that lends further support to a mechanism involving the ultrasonic generation of a highly reactive co-ordinatively unsaturated intermediate. Similar ligand exchange reactions have been observed with $\text{Mn}_2(\text{CO})_{10}$ and $\text{Re}_2(\text{CO})_{10}$ [52].

A synthetic application of the sonolysis of iron carbonyls is the preparation of useful ferrilactones. The alkenyl epoxides (**2**, $\text{R} = \text{H, Ph, 1-hexanyl}$) are smoothly converted to the corresponding ferrilactone complexes (**3**) on reaction with $\text{Fe}_2(\text{CO})_9$ suspended in THF and sonicated at room temperature [53]. Such complexes undergo several synthetically useful transformations (Scheme 3.7) including oxidation with Ce(IV) as a route to β -lactone natural products or β -lactam antibiotics and reaction with CO to afford δ -lactones [54]. Somewhat surprisingly this reaction is efficient even in diethyl ether, a volatile solvent which delivers low cavitation energy.



Scheme 3.7

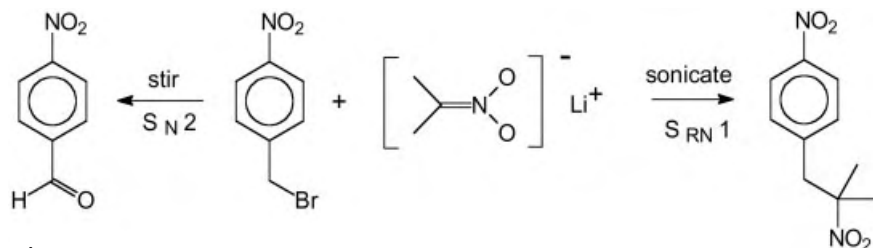
There have been examples of sonochemical switching in homogeneous reactions. The decomposition of lead tetraacetate in acetic acid in the presence of styrene at 50°C generates a small quantity of diacetate *via* an ionic mechanism. Under otherwise identical conditions sonication of the mixture gives 1-phenylpropyl acetate predominantly through an intermediate methyl radical which adds to the double bond (Scheme 3.8) [55, 56]. These results are in accord with the proposition that radical processes are favoured by sonication.



Scheme 3.8

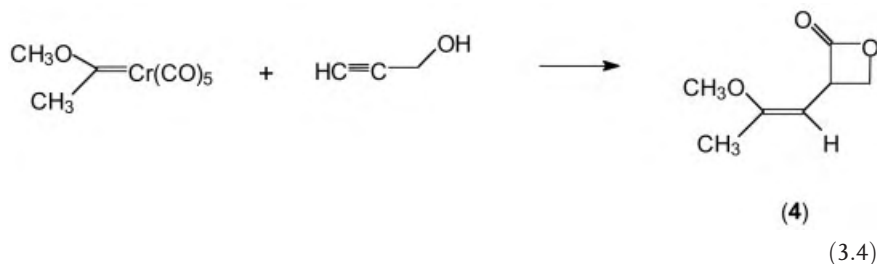
Another example of sonochemical switching is found in the Kornblum-Russell reaction (Scheme 3.9). 4-Nitrobenzyl bromide reacts with 2-lithio-2-nitro-propane *via* a predominantly polar mechanism to give, as a final product, 4-nitrobenzaldehyde [57]. An alternative SET pathway exists in this reaction leading to the formation of a dinitro compound. Sonication changes the normal course of the reaction and gives

preferentially the latter compound, in amounts depending on the irradiation conditions and the acoustic intensity.

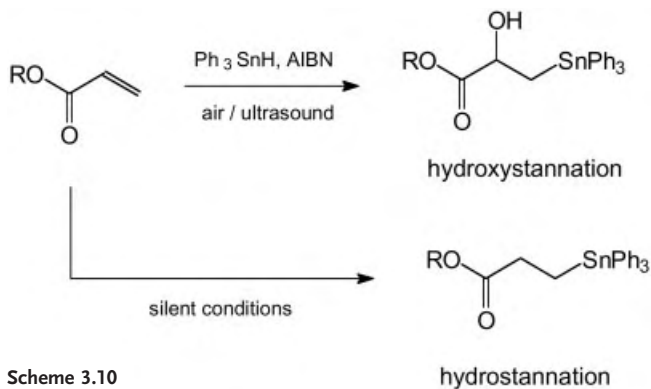


Scheme 3.9

Condensation of chromium alkyl(alkoxy)carbene complexes with propargylic alcohols gives rise to functionalised β -lactones [58]. In the example given only 2 % of (4) is obtained after refluxing the reagents for 5 h (in Ac_2O , Et_3N and THF) whereas sonication (in benzene and Et_3N) for 3 h affords a 34 % yield. Sonication proved to be a more effective procedure, particularly in terms of accessing the less heavily substituted β -lactones, for which the silent reaction gives very poor yields (Eq. 3.4). This can be attributed to the rapid reaction with the less stable alkyl carbene complexes, thereby avoiding the possibilities of decomposition.

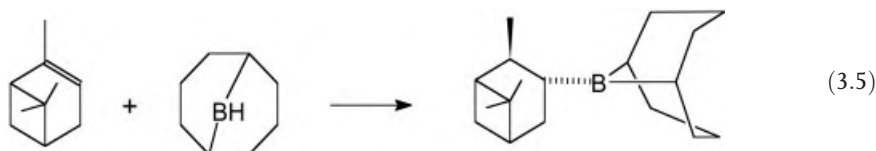


Results of a chemical activation induced by ultrasound have been reported by Nakamura et al. in the initiation of radical chain reactions with tin radicals [59]. When an aerated solution of R_3SnH and an olefin is sonicated at low temperatures (0 to 10 °C), *hydroxystannation* of the double bond occurs and not the conventional hydrostannation achieved under silent conditions (Scheme 3.10). This point evidences the differences between radical sonochemistry and the classical free radical chemistry. The result was interpreted on the basis of the generation of tin and peroxy radicals in the region of hot cavities, which then undergo synthetic reactions in the bulk liquid phase. These findings also enable the sonochemical synthesis of alkyl hydroperoxides by aerobic reductive oxygenation of alkyl halides [60], and the aerobic catalytic conversion of alkyl halides into alcohols by trialkyltin halides [61].



Scheme 3.10

Another example of great synthetic interest, involves the hydroboration reaction of alkenes [62]. In general, the addition of borane to alkenes proceeds stepwise, the final product being the trialkylborane. However, hindered alkenes react slowly, especially when the dialkylborane precipitates from the medium. It was found that trialkyl boranes could be obtained rapidly under sonication, even with highly hindered substrates (Eq. 3.5). Applications of this useful modification were published, among which were the reduction-hydroxylation of vinyl groups by 9-BBN [63, 64].



There are few references to homogeneous sonochemical processes involving C_{60} (fullerene) solutions although there has been a claim that very small quantities can be prepared from the sonolysis of benzene [65]. The ultrasonic irradiation at 20 kHz of a solution of C_{60} in decahydronaphthalene results in the formation of $C_{60}H_2$ [66]. Owing to its low vapour pressure at room temperature, no C_{60} will be inside the cavitation bubbles, although it will experience secondary reactions in the liquid phase. The dihydrofullerene results from the reaction with atomic hydrogen generated by sonolysis of the solvent. Although there are already many studies on hydrogenated fullerenes, it is remarkable that sonication does not produce more highly hydrogenated derivatives. Moreover, continued sonication results in the disappearance of both C_{60} and $C_{60}H_2$ from the solution, presumably by fragmentation into smaller hydrocarbons or by formation of polymeric structures, although the latter points have not yet been confirmed.

3.5

Heterogeneous Sonochemistry

The majority of reactions which have been reported to be enhanced by ultrasound are of the heterogeneous type (either liquid/liquid or liquid/solid). Within these it is the applications in organometallic chemistry which have received the most attention.

3.5.1

Heterogeneous Reactions Involving a Metal as a Reagent

Ultrasound is widely used for the preparation of organometallic compounds from reactive metals [67]. Here the mode of action of ultrasound is twofold:

1. As a direct result of transient bubble collapse on or near the metal surface a jet of liquid is directed towards it (Fig. 3.4). This phenomena has been recorded using high-speed microphotography [23]. Along with the shock wave associated with cavitation collapse the jet causes localised deformation and surface erosion involving intensive cleaning and also the removal of oxide layers and impurities together with pitting of the metal surface (which increases the possible reaction area). Surfaces thus treated contain an increased number of dislocations that are widely considered to be the active sites in catalysis.
2. Acoustic streaming (which aids mass transport) is the movement of the liquid induced by the sonic wave which can be considered to be simply the conversion of sound to kinetic energy and is not a cavitation effect.

The erosion effects of cavitation on solid surfaces have been extensively investigated both in terms of surface erosion [68] and corrosion [69]. The consequences of these effects on metal reactivity are important since passivating coatings are frequently present on a metal surface (e. g. oxides, carbonates and hydroxides) and can be removed by the impacts caused by collapsing cavitation bubbles. An illustration can be found with the activation of nickel powder and the determination of the change in its surface composition under the influence of cavitation by Auger spectroscopy (Fig. 3.6) [70].

3.5.1.1 Preparation of Active Metals from Metals their Salts and Complexes

The preparation of an activated metal for use in an organometallic synthesis can be effected in a separate sonication step. An early example of this was the preparation of finely dispersed mercury for the reduction of *a,a'*-dibromoketone to a mixture of *a*-acetoxyketones which favours the tertiary product (Eq. 3.6) [71]. The procedure is simple in that the dibromocompound, dissolved in acetic acid is subjected to sonication in a bath in the presence of a small amount of mercury. In this particular case

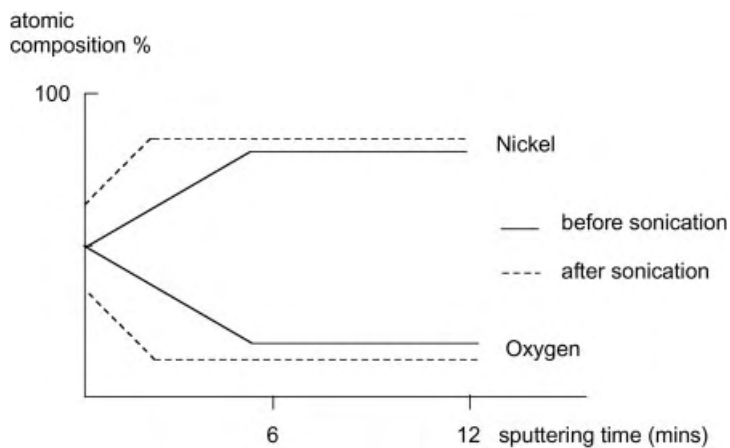
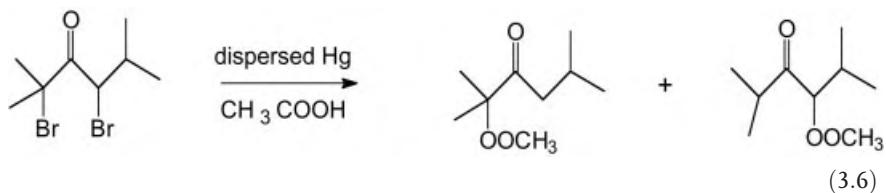
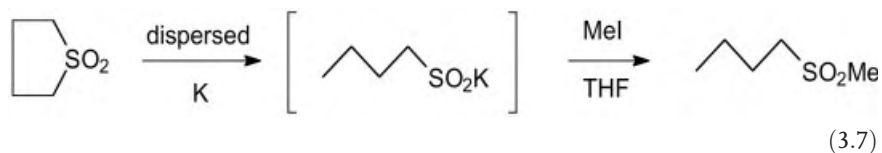


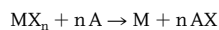
Fig. 3.6. Effect of sonication on the surface composition of nickel by Auger spectroscopy.

similar results can be obtained by generating the mercury emulsion through high speed stirring.



Sodium or potassium metals in aromatic solvents rapidly transform to a silvery blue “colloidal” suspension when sonicated using a bath [72]. While it is possible to disperse metallic sodium in xylene (bp 138 °C) it cannot be accomplished in toluene (bp 110 °C). This is another example of the more powerful cavitation in the higher boiling solvents being an important factor. These colloidal systems have been used in a range of reactions including Dieckmann condensations, the generation of ylide intermediates for Wittig reactions and in the desulphurisation of sulphones. An example of the latter is given in (Eq. 3.7) [73].



Tab. 3.1. The generation of Rieke metal powders (M).

X = Cl, Br, I

A = Li, Na, K

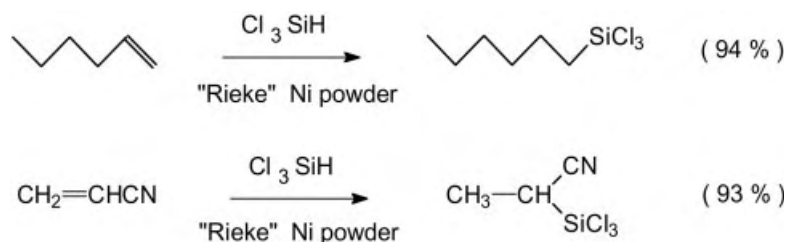
Method	Time
$\text{CuI}_2 + \text{K}$ reflux in THF	8 h
$\text{CuBr}_2 + \text{Li}$ ultrasonic bath at 25 °C in THF	less than 40 min
$\text{NiCl}_2 + \text{Li}$ (powder) stir at 25 °C	14 h
$\text{NiCl}_2 + \text{Li}$ (powder) stir in ultrasonic bath at 25 °C	less than 40 min

Active powder can be produced from molten zinc, less than 100 μm in size, at a rate of 1 kg/h under sonication [74]. Dispersed palladium, platinum and rhodium prepared by sonochemical reduction of aqueous salts also exhibit a higher reactivity, assigned to a surface area increase [75].

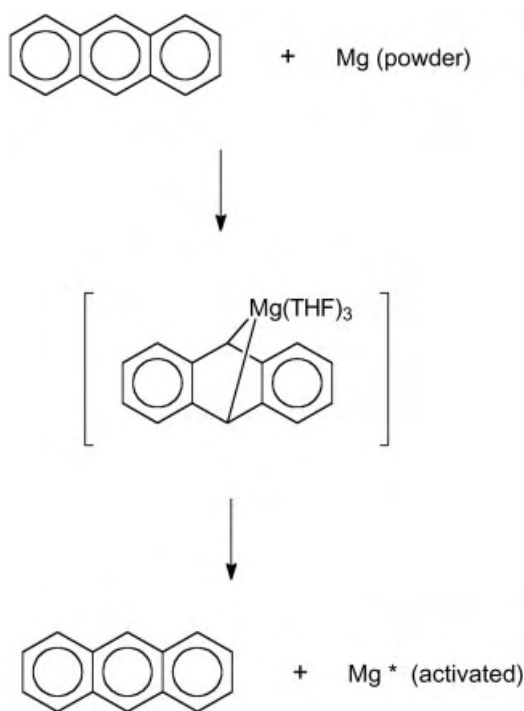
The metallic couples of zinc with copper, nickel or cobalt form readily by sonication of zinc dust with salts, mainly halides, of the second metal in aqueous organic solvents. This method avoids the usual tedious preparative methods [76–78].

A very reactive form of a finely divided metal is a so-called Rieke powder [79]. These materials are produced as fine powders by chemical precipitation during the reduction of various metal halides with potassium metal in refluxing tetrahydrofuran. Obviously this is a potentially hazardous laboratory procedure and ultrasound has provided an alternative method of preparation of these extremely valuable reagents [80]. The sonochemical technique involves the reduction of metal halides with lithium in THF at room temperature in a cleaning bath and gives rise to metal powders that have reactivities comparable to those of Rieke powders. Thus powders of Zn, Mg, Cr, Cu, Ni, Pd, Co and Pb were obtained in less than 40 min by this ultrasonic method compared with reaction times of 8 h using the experimentally more difficult Rieke method (Tab. 3.1).

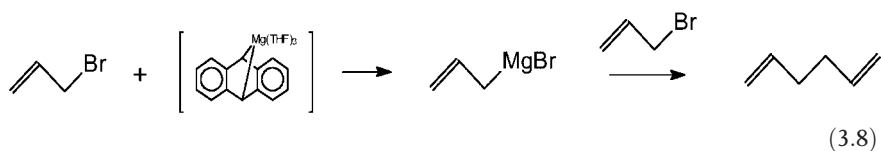
These sonically prepared Rieke powders show enhanced reactivity in organic synthesis involving metals e.g. in the preparation of organosilicon compounds (Scheme 3.11) [81].

**Scheme 3.11**

A highly active form of metallic magnesium is formed when commercial magnesium powder in THF is subjected to low intensity ultrasound in the presence of anthracene [82]. The anthracene forms an electron transfer complex with magnesium and this effectively acts as a phase transfer agent (Scheme 3.12). The magnesium produced in this way is an excellent reducing agent for metal salts and when the reduction is carried out in the presence of Lewis base ligands it is a useful route to organo-transition metal complexes for example (5-cyclopentadienyl complexes Cp_2M ($\text{M} = \text{V}, \text{Fe}, \text{Co}$), (3-allyl complexes ($\text{M} = \text{Co}, \text{Ni}$), alkene complexes ($\text{M} = \text{Ni}, \text{Pd}, \text{Pt}, \text{Mo}$) and phosphine complexes ($\text{M} = \text{Pd}, \text{Pt}$). The magnesium anthracene complex is also a convenient route to allyl Grignard reagents at temperatures as low as -35°C . This eliminates the coupling of allyl magnesium halides with the starting alkyl halide which is a common side reaction with conventional methods (Eq. 3.8) [83].

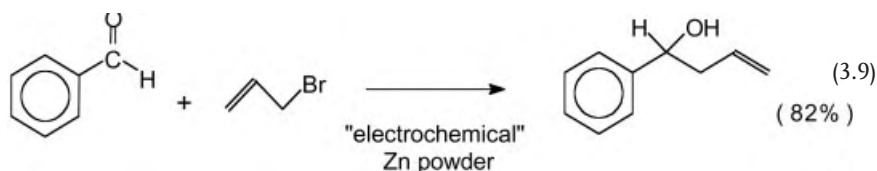


Scheme 3.12



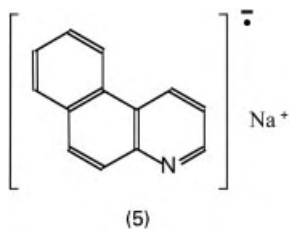
Sonication of titanium trichloride and lithium at 30 °C provides the so-called “low valent” titanium, whereas the silent reaction requires reflux conditions [84].

A novel method of generating finely divided zinc metal is by the use of pulsed sonoelectrochemistry using an ultrasonic horn as the cathode [85]. Normal electrolysis of ZnCl_2 in aqueous NH_4Cl affords a zinc deposit on the cathode. When the electrolysis is pulsed at 300 ms on/off and the cathode is pulsed ultrasonically at a 100 ms:200 ms on:off ratio the zinc is produced as a fine powder. This powder is considerably more active than commercial zinc powder e.g. in the addition of allyl bromide to benzaldehyde (Eq. 3.9).



3.5.1.2 *In situ* Sonochemical Activation of Metals

In many syntheses activation is not effected by sonochemical preparation of the metal alone but rather by sonication of a mixture of the metal and an organic reagent(s). The first example was published many years ago by Renaud, who reported the beneficial role of sonication in the preparation of organo-lithium, magnesium, and mercury compounds [86]. For many years, these important findings were not followed up but nowadays this approach is very common in sonochemistry. In another early example an ultrasonic probe (25 kHz) was used to accelerate the preparation of radical anions [87]. Unusually for this synthesis of benzoquinoline sodium species (5) the metal was used in the form of a cube attached to the horn and preparation times in diethyl ether were reduced from 48 h (reflux using sodium wire) to 45 min using ultrasound.



Alkali metals and magnesium

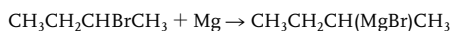
A particularly important group of synthetic reactions involve the formation of organo-metallic reagents from organic halides including the widely used syntheses of Grignard and organolithium reagents. Frequently there is an induction period which can make these reactions somewhat hazardous when performed on an industrial scale. Sonication usually reduces the induction period or even completely suppresses it.

Today one of the most common chemical applications of ultrasound is the initiation of a reluctant Grignard reaction. The quantitative effects of ultrasound on the induction times for the formation of a Grignard reagent in various grades of ether is given in Tab. 3.2 [88].

The term “crushed” in the table refers to the methodology commonly employed to activate magnesium – mechanical crushing of the metal to expose fresh surface to the reactants. In each of the three solvents there was no significant difference in yield of the alkylmagnesium bromide with or without sonication the figures being 65, 55 and 55 %. Significantly prior sonication of the metal in ether had no effect on the induction time when the subsequent preparation was performed under non-ultrasonic conditions. This clearly eliminates simple surface cleaning as the source of the effect and it was suggested that during sonication adsorbed water was removed from the metal surface, kept clear while irradiation continued, but was re-adsorbed on switching off the bath. When all the water dislodged from the surface has reacted with the newly formed Grignard reagent the system was essentially “dry” and reaction continued normally.

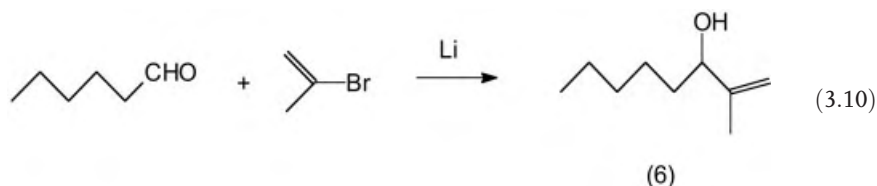
In 1980 Luche published the first of a series of papers dealing with ultrasound promoted reactions of organometallics of use in organic synthesis [89]. He reported the direct, *in situ*, formation of alkyl and aryl lithiums by the reaction of an organic halide with lithium wire (or lithium with 2 % sodium sand) in ether immersed in an ultrasonic bath. The technique avoided the use of activating reagents (e. g. I_2 or iodo-methane) and afforded a significant amelioration of the reaction both by increasing reactivity and removing the induction period which is often involved. This methodol-

Tab. 3.2. The preparation of butan-2-yl magnesium bromide in ether in an ultrasonic bath.

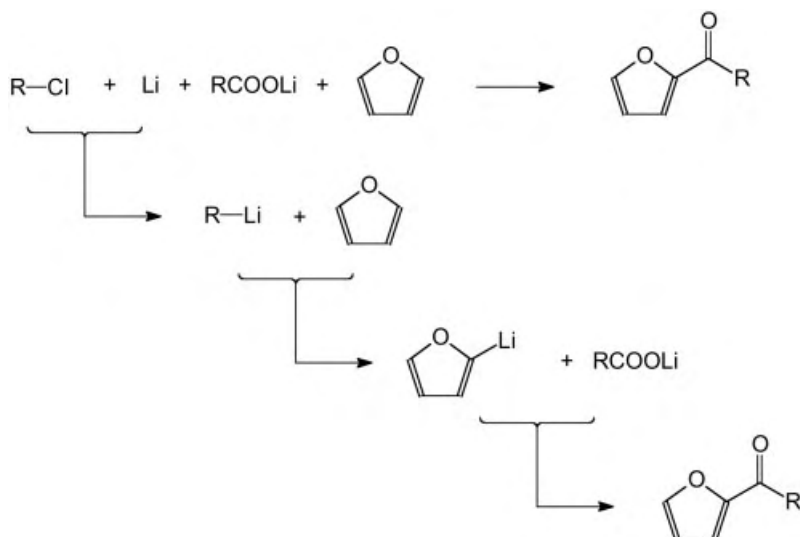


Type of diethyl ether used	Method	Induction time
Pure, dried	stirred	6–7 min
(0.01 % water, 0.01 % ethanol)	sonicated	less 10 s
Reagent grade	stirred	2–3 h (“crushed”)
(0.5 % water, 2.0 % ethanol)	sonicated	3–4 min
50 % Saturated	stirred	1–3 h (“crushed”)
(0.01 % ethanol)	sonicated	6–8 min

ogy finds a particularly notable application in the Barbier reaction – the one step coupling of an organic halide with a carbonyl compound in the presence of magnesium or lithium metal. Significant improvements both in yields and simplification of experimental techniques over conventional methods were obtained. A significant advantage of this method is that the syntheses are largely free from side reactions such as reduction and enolisation which are common in conventional methodology. Thus allylic alcohol (**6**) has been isolated in 96 % yield from the reaction between hexanal and 2-bromopropene (Eq. 3.10). Even benzyl halides gave yields in excess of 95 % and very little Wurtz coupling was observed, which often predominates with non ultrasonic methods. A further advantage is that such reactions can be performed in damp, technical grade tetrahydrofuran, a potential boon for large scale industrial operations.

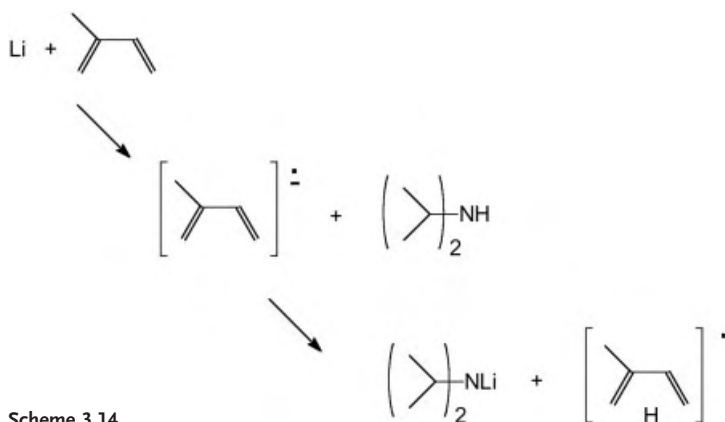


An extension of the Barbier reaction to carboxylates salts [90] affords a simple access to furanyl ketones [91]. By sonication of a mixture of a lithium carboxylate, an alkyl chloride and lithium in THF at room temperature, the intermediate organolithium reagent forms rapidly, then generates the 2-furanyl lithium which adds to the carboxylate group in high yields. The method constitutes an example of a reaction “cascade”, in which several intermediates are generated sequentially (Scheme 3.13).



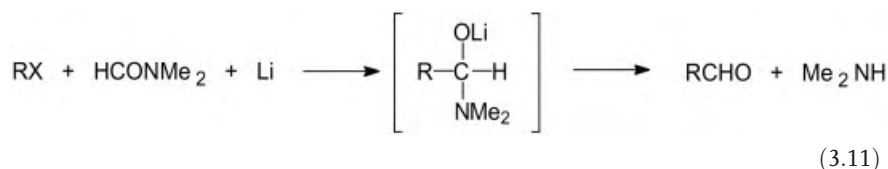
Scheme 3.13

The synthetic importance of non-nucleophilic strong bases such as lithium diisopropylamide (LDA) is well known but its synthesis involves the use of a transient butyl lithium species. In order to shorten the preparation and make it economically valuable for larger scale experiments an alternate method of synthesis has been developed which also involves a reaction “cascade” (Scheme 3.14) [92]. The direct reaction of lithium with diisopropylamine does not occur, even with sonication. An electron transfer agent is necessary, and one of the best in this case is isoprene. Styrene is used in the commercial preparation of LDA, but it is inconvenient in that it is transformed to ethylbenzene which is not easily removed. It can also lead to undesired reactions in the presence of some substrates. The advantages of isoprene are essentially that it is a lighter compound (R.M.M. = 68 instead of 104 for styrene) and it is transformed to the less reactive 2-methylbutene, an easily eliminated volatile compound. In the absence of ultrasound, attempts to use this electron carrier proved to be unsatisfactory. In this preparation lithium containing 2 % sodium is necessary, as pure lithium reacts much more slowly.



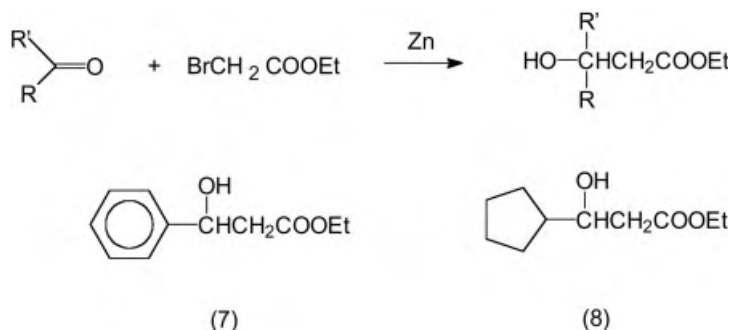
Scheme 3.14

The Bouveault reaction is the preparation of an aldehyde by a one pot reaction between an organic halide and lithium metal in dimethylformamide. Ultrasound has been found to markedly enhance this reaction when it is performed in tetrahydrofuran [93]. Use of an ultrasonic bath at 10–20 °C affords short reaction times of between 5 and 15 min and generates yields in the range 70–88 %. Using this methodology the conversion of 1-bromobutane to pentanal (88 %) can be achieved in only 5 minutes. This must be contrasted with the yield of less than 10 % which is obtained under the normal stirred conditions in the same time period. This result confirms that the effect of irradiation goes beyond mere agitation (Eq. 3.11).



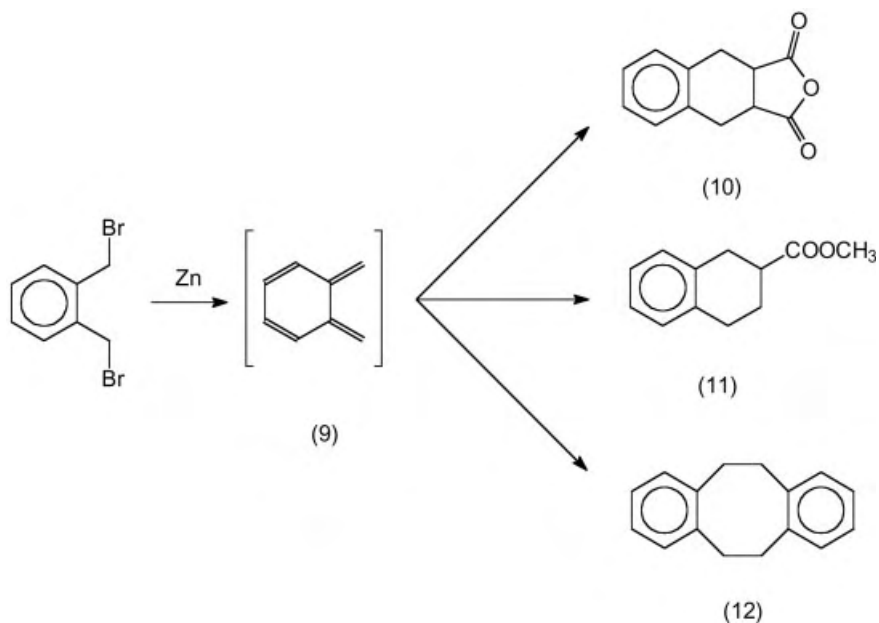
Zinc

Low intensity ultrasound also facilitates the Reformatsky reaction of α -haloesters with aldehydes and ketones (Scheme 3.15) [94]. The ultrasonic method gave ethyl 2-hydroxyphenylacetate (**7**, 98 %) in 5 min for $\text{R} = \text{C}_6\text{H}_5$ and $\text{R}' = \text{H}$ compared with 98 % obtained in 1 h using activated zinc powders, 95 % in 5 h using the $(\text{MeO})_3\text{B}/\text{THF}$ solvent system and only 61 % after 12 h using the conventional methodology. Similarly the reaction between ethyl bromoacetate and cyclopentanone generated (**8**, 98 %) in 30 min at 25 °C compared with 80 % in 12 h at 80 °C by conventional methods. It is interesting to note that these improved yields were obtained using dioxane as solvent. With the more conventional, but lower boiling, Reformatsky solvents – benzene or ether – there was no improvement using ultrasound. This lends strong support to the importance of the choice of solvent when embarking upon sonochemistry research.



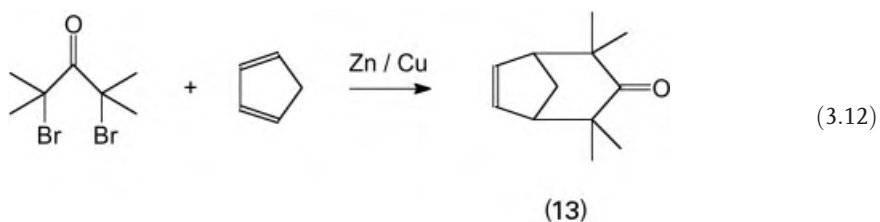
Scheme 3.15

Ultrasonic irradiation of a mixture of zinc and α,α' -dibromo-orthoxylyene in dioxane results in dehalogenation and the generation of a xylylene intermediate (**9**) which readily adds to any dienophiles present in the reaction mixture e. g. with maleic anhydride or methyl propenoate to afford high yields of (**10**) and (**11**) respectively [95]. In the absence of dienophile the product is mainly polymer with a trace of (**12**) (Scheme 3.16). The work was performed in a cleaning bath at 25 °C on 10 mmol scale using 23 mmol zinc under N_2 . There was no reaction in the absence of ultrasound.



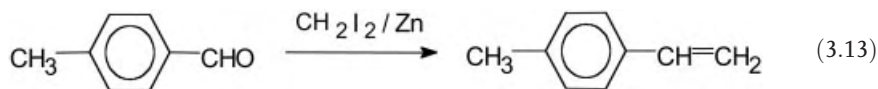
Scheme 3.16

The zinc promoted cycloaddition of α,α' -dibromoketones to 1,3-dienes is enhanced by ultrasound to such an extent that compounds such as the highly hindered bicyclo[3.2.1]oct-6-en-3-ones (**13**) become easily accessible (Eq. 3.12) [96]. Reactions of this type, in the absence of ultrasound, give only low to moderate yields and require much longer reaction times of the order of 24 h.

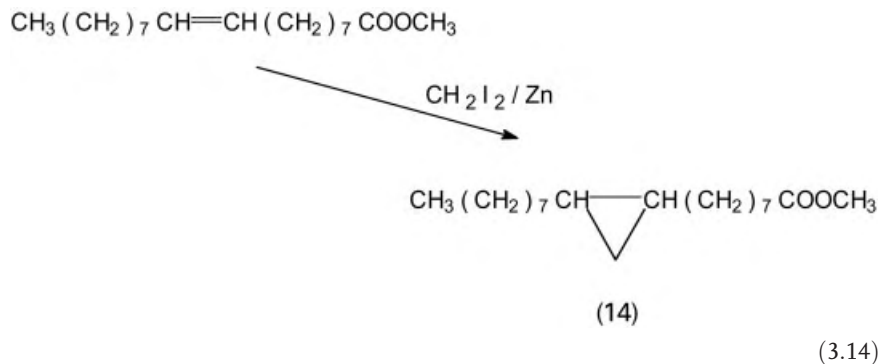


A convenient method for the conversion of aldehydes (RCHO) to alkenes (RCH = CH₂), known as methylenation, involves the reaction of a zinc/copper couple with diiodomethane in the presence of the carbonyl compound dissolved in tetrahydrofuran. The reaction first generates an organometallic intermediate (ICH₂ZnI) which then reacts with the carbonyl compound. The conversion of benzaldehyde to styrene using this conventional methodology required a reaction time of 6 h at 40 °C. When the reaction was sonicated however comparable yields of around 70 %

were obtained in the production of the corresponding styrenes from benzaldehyde, 4-chlorobenzaldehyde and 4-methylbenzaldehyde after irradiation times of 20, 15 and 120 min respectively at room temperature (Eq. 3.13) [97]. Somewhat poorer yields are obtained from the methylenation reactions of ketones.



When the $\text{Zn}/\text{CH}_2\text{I}_2$ reaction is applied to an alkene the result is the formation of a cyclopropane and this is generally known as the Simmons Smith reaction. Unfortunately, while the reaction itself is quite useful, on a preparative scale it suffers from several drawbacks one of the major ones being the sudden exotherm which occurs after an unpredictable induction period. In 1982 Repic described a modification of the Simmons-Smith reaction using sonochemically activated zinc which eliminated the sudden exotherm normally associated with the reaction. Using ultrasound it was found that (14) could be produced in 91 % yield compared with 51 % by the normal route (Eq. 3.14) [98]. The normal method for enhancing this reaction relied upon activation of the zinc metal by using it in the form of a zinc-silver or zinc-copper couple and/or using iodine or lithium in conjunction with the metal. In the sonochemical procedure no special activation of the zinc was required and in fact equally good and reproducible yields were obtained using zinc dust or even the metal in the form of mossy rods or foil. This methodology has now been successfully scaled up to run in a 22 dm³ vessel immersed in a 50 gallon bath (Fig. 3.7). In the scale-up rig the zinc was cast in two 800 g lumps (using 125 cm³ conical flasks as molds). The reagents were methyl oleate (0.6 kg), diiodomethane (1.3 dm³), dimethoxyethane (2.7 dm³). Under nitrogen at 100 °C the reaction yielded (14) 0.5 kg (82 %) after 2.25 h [99].



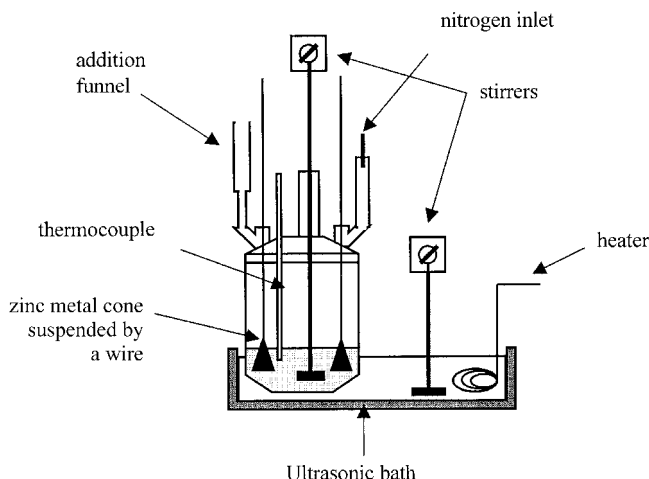
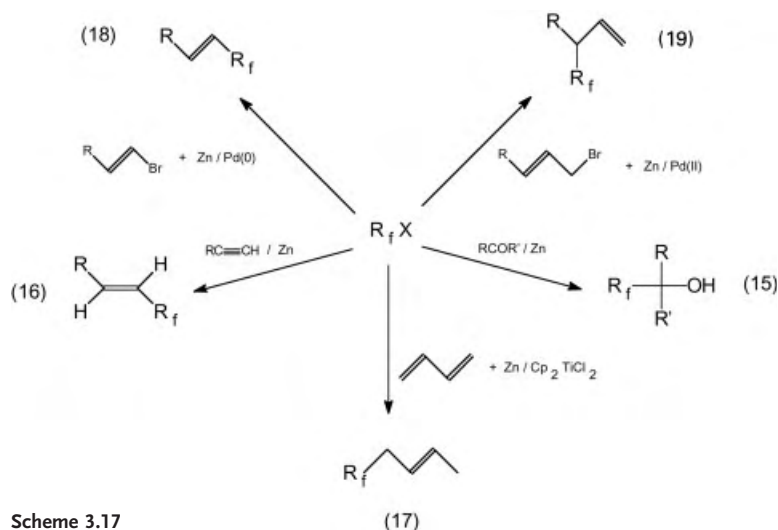


Fig. 3.7. Schematic diagram of large scale cyclopropanation apparatus.

The method has several advantages over the normal method of cyclopropanation which involves several experimental problems:

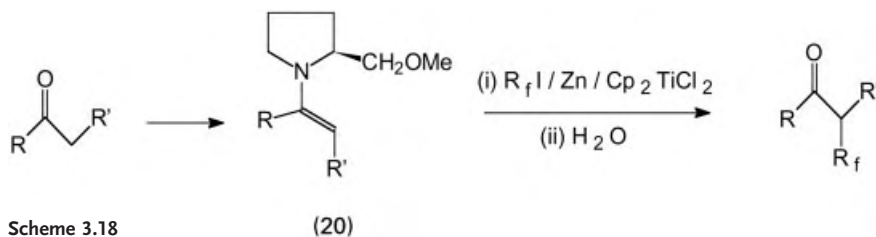
- There is a reduction in foaming (normally associated with ethene and cyclopropane formation);
- the exotherm is more evenly distributed (only a small clean area of metal is available throughout the reaction);
- the reaction can be controlled by removing the lump of metal from the reaction (this is not unlike the use of fuel rods in a nuclear reactor);
- the residual metal can be removed from the reaction as a lump.

Methods for the introduction of the perfluoroalkyl group R_f into organic compounds are not as plentiful as those for the introduction of simple alkyl groups. The standard organometallic routes for perfluoroalkyl substitution are not generally available due to the low stability or low reactivity of the perfluoroalkylmetal intermediates, thus both R_fMgX and R_fLi readily decompose into perfluoroalkenes. Ultrasound has now provided a solution to this problem and a range of synthetic routes have been developed each starting from a perfluoroalkane and employing powdered zinc (Scheme 3.17) [100].



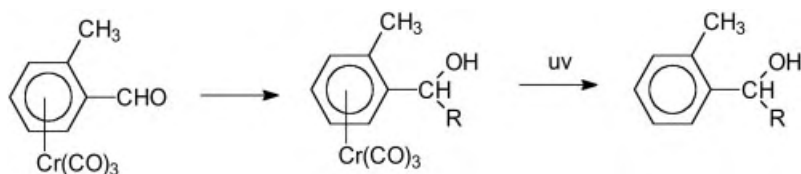
Scheme 3.17

The synthesis of alcohol (15) can be achieved by a form of Barbier reaction in which a carbonyl compound, in DMF as solvent, reacts with perfluoroalkylzinc which is sonochemically generated *in situ*. Hydroperfluoroalkylation can be achieved by the direct reaction of alkynes with perfluoroalkylcuprates, again generated *in situ* from the reaction of perfluoroalkyl halides with zinc and copper(I) iodide in THF. Good yields of fluoroalkyl substituted alkenes (16) are obtained with terminal alkynes and the reaction is regiospecific (but not stereospecific). Similar results are obtained in the preparation of (17) by the perfluoroalkylation of dienes catalysed by Cp_2TiCl_2 (Cp = cyclopentadienyl). High yield cross coupling reactions of vinyl halides with perfluoroalkylzinc reagents to (18) are catalysed by $Pd(0)$ [$Pd(PPh_3)_4$] while similar reactions of allyl halides to (19) require $Pd(II)$ [$Pd(OAc)_2$]. The same group have also reported a synthesis of chiral ketones (Scheme 3.18) *via* the optically active enamine (20). Sonication of zinc powder and Cp_2TiCl_2 in THF produces bis- $[\eta^5\text{-cyclopentadienyl}]titanium(II)$ which is believed to be the catalytic species involved in the degradation of (20) to the target ketone in optical purities of between 60 and 70%.



Scheme 3.18

Asymmetric induction of between 30 and 66 % has been reported for the addition of perfluoroalkyl iodides to chiral arene/chromiumtricarbonyl complexes using ultrasonically dispersed zinc at room temperature (Scheme 3.19) [101]. Photochemical decomposition of the organometallic intermediate affords a chiral alcohol product. The reaction is carried out in DMF as solvent and high overall yields are reported e. g. 80 % ($R = \text{Et}$). Only a small excess of the perfluoroalkyl iodide is required and the conversion is complete in under 1 h.



Scheme 3.19

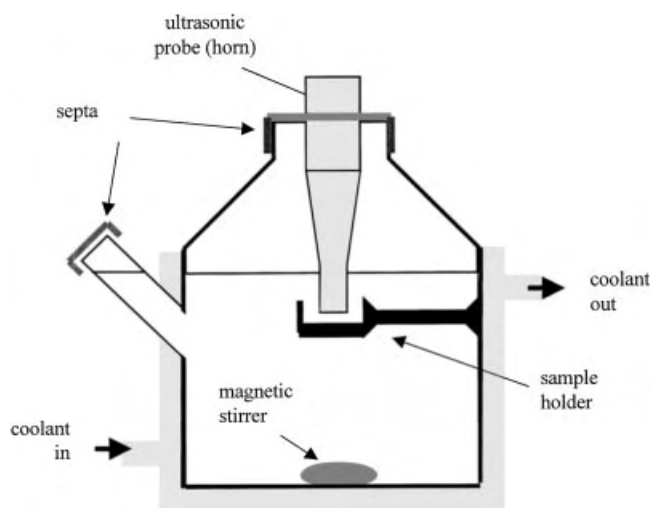
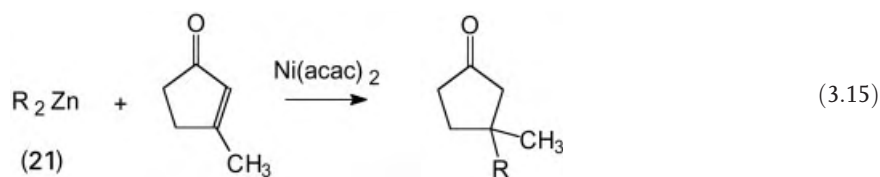
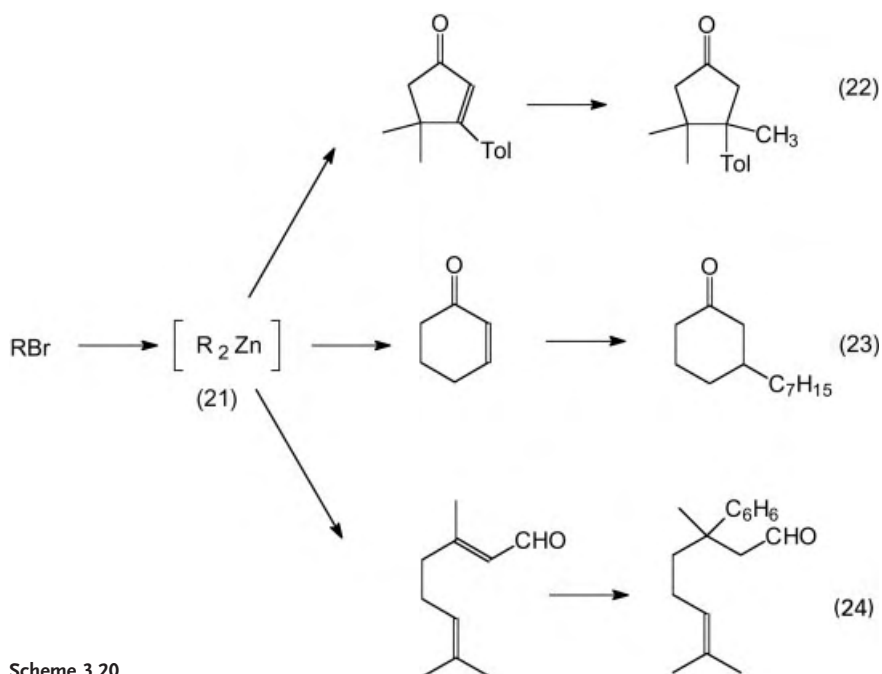


Fig. 3.8. Apparatus for the production of organo-zinc reagents.

The increased ultrasonic energy available through the use of a probe rather than a bath can provide more effective reactions involving metals. Two reactions can be used to illustrate this, the preparation of organozinc reagents and the use of copper bronze in an Ullmann coupling reaction both of which were originally explored in baths. Diaryl zincs (**21**) can be prepared by sonication of a mixture of aryl bromide, zinc bromide and lithium metal in dry ether or tetrahydrofuran in a cleaning bath [102]. Generation of the diaryl zinc takes 30–45 min after which the cleaning bath can be turned off and the substrate added to the mechanically stirred solution together with nickel acetylacetonate ($\text{Ni}(\text{acac})_2$) which acts as a catalyst. In this way conjugate addition can be achieved in relatively high yield. For example (**21**, $\text{R} = 2\text{-CH}_3\text{C}_6\text{H}_4$) adds to 3-methylcyclopentenone (72 %) compared with only a 20 % yield under normal conditions (Eq. 3.15). This procedure proved to be less effective for dialkyl zinc reagents but a modification has led to a more generalised method in which an ultrasonic probe has replaced the cleaning bath [103]. Using toluene:tetrahydrofuran (85:15) as solvent, dialkyl or diaryl zincs can be generated in 10–15 min at 0 °C. The specially designed apparatus used for this preparation is shown (Fig. 3.8). The organolithium is first formed by direct sonication of the metal and this is transformed immediately into the organozinc. Subsequent addition of an enone, in the absence of irradiation, gives rapid reaction at room temperature in the presence of $\text{Ni}(\text{acac})_2$ (Scheme 3.20). This approach has proved to be a particularly useful alternative to methods involving either lithium dialkyl copper reagents (LiCuR_2) or copper catalysed Grignard additions for conjugate addition. Thus while (+)-cuparenone (**22**) cannot be prepared by these conventional techniques from 4,4-dimethyl-3-*para*-tolylcyclopentenone the conversion can be achieved smoothly and in 84 % yield via sonochemically prepared dimethyl zinc. Similar conjugate additions have also been achieved with cyclohexenone (**23**, 88 %) and unsaturated aldehydes (e.g. **24**, 69 %).

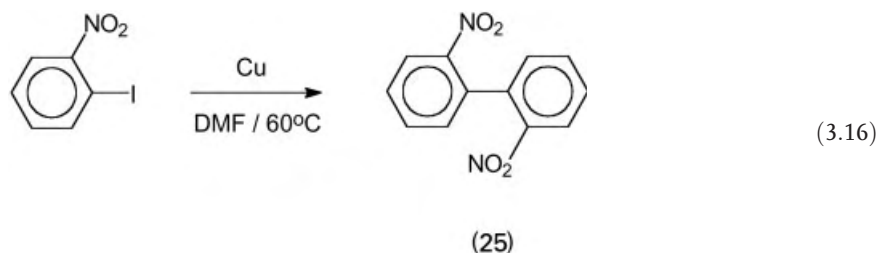




Scheme 3.20

Copper

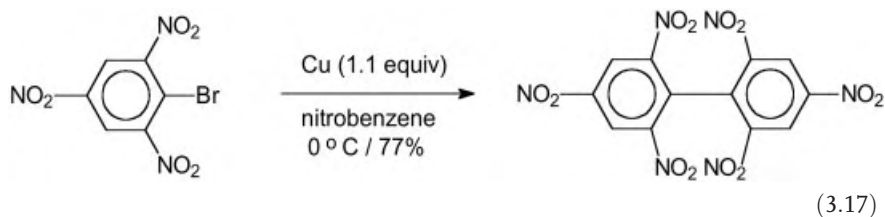
An Ullmann coupling reaction is the linking of two aryl rings by reaction of the corresponding haloarenes with an excess of copper metal in a high boiling solvent. When the arene is activated by the presence of an 2-nitro group the reaction can be performed under milder conditions. For example 2-iodonitrobenzene can be converted to the corresponding biphenyl (25) in 48 h at 60 °C using a 10-fold excess of copper bronze (Eq. 3.16) [104]. For such activated aryl halides dimethylformamide (DMF) is a recommended solvent for the coupling reaction and commercial copper bronze or freshly precipitated copper obtained by reduction of a copper salt have been claimed to give satisfactory results. Pretreatment of the copper with EDTA or iodine to remove surface impurities is claimed to give more consistent results. It was the importance of clean copper surfaces in these reactions together with the well known cleansing action of ultrasound which led us to investigate the effect of ultrasonic irradiation on this Ullmann coupling reaction. Initial studies were carried out using an ultrasonic laboratory cleaning bath operating at 45 kHz.



Although the results showed a rate enhancement of 60 % over the control experiment the total conversion was only 21 % over 2 h. Further investigations revealed that using a 1:1 mole ratio of copper (15 mmol) to 2-iodonitrobenzene (15 mmol) in DMF (40 cm³) at 65 °C gave 48 % (25) in 2 h. Investigations into the effect of copper to halide ratio revealed that a 4:1 ratio is optimum yielding 80 % product in 1.5 h. During these studies it was observed that the average particle size of the copper, as determined by laser light scattering, fell from 87 μ to 25 μ over 1 h of sonication in DMF. This factor alone however was shown to be insufficient to explain the large (50-fold) enhancement in reactivity produced by ultrasonic irradiation. These studies suggested several advantages in using ultrasound:

- It cleaned the metal surface.
- It reduced the particle size of the metal.
- It increased the rate, suggesting that sonication assisted in breaking down intermediates and/or assisted in the desorption of products.
- It prevented the adsorption of copper on the walls of reaction vessels which is a common problem with conventional methodology.

Picryl bromide can be coupled at or below room temperatures by copper powder used in only 10 % excess, to give coupling or reduction products depending on the solvent and stoichiometric conditions (Eq. 3.17) [105]. Sonications were performed with a pulsed wave, a technique not frequently used.



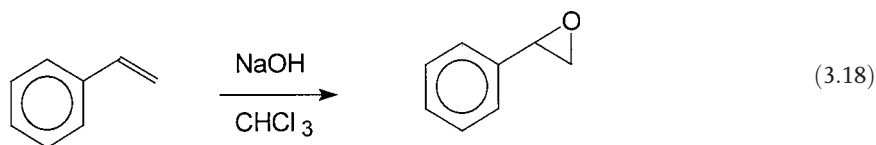
3.5.2

Heterogeneous Reactions Involving Non-Metallic Reagents

There are many examples in the literature of synthetic applications of sonochemistry involving either solid non-metallic reagents in suspension or the use of simple ultrasonically induced emulsions [106]. The process by which a reagent is transferred from a solid to a solution is multistep involving disturbance or destruction of the surface. One classic way of achieving this is with the help of a Phase Transfer Catalyst (PTC). This type of activation can also be produced by sonication under appropriate conditions, depending on the properties of the solid. Mass transfer phenomena are enhanced by ultrasonic microstreaming and the overall accelerations are then a composite effect. In some situations the presence of a PTC may not be necessary, and some authors consider sonication as “a substitute to PTC” [107]. Some examples of the variety of such are given below.

3.5.2.1 Addition Reactions

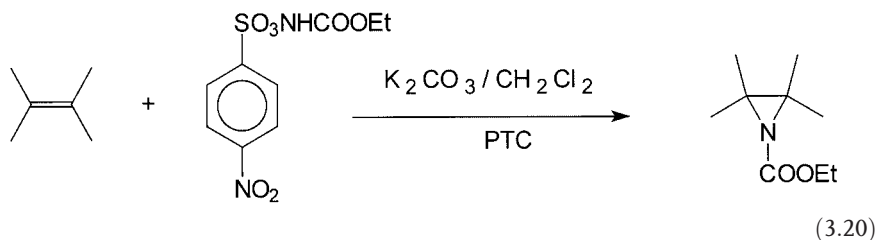
An early example of ultrasound being used in place of a phase transfer catalyst is in the generation of dichlorocarbene by the direct reaction between powdered sodium hydroxide and chloroform [108]. The reported procedure is both simple and efficient in that irradiation of a stirred mixture of powdered NaOH in chloroform containing an alkene generates high yields of the corresponding dichlorocyclopropanes in 4 h at 40 °C. With styrene the cyclopropanation occurs in 96 % yield in 1 h when a combination of both sonication (using a bath) and stirring is used, the yield is much reduced to 38 % in 20 h with sonication alone and to 31 % in 16 h with only simple mechanical stirring (Eq. 3.18). These results make it clear that both mechanical stirring and ultrasonic irradiation are necessary using this type of low power apparatus with a solid suspension. Additions to alkenes occur in yields higher or at least equivalent to that of conventional methods, with the advantage of shorter reaction times [109].



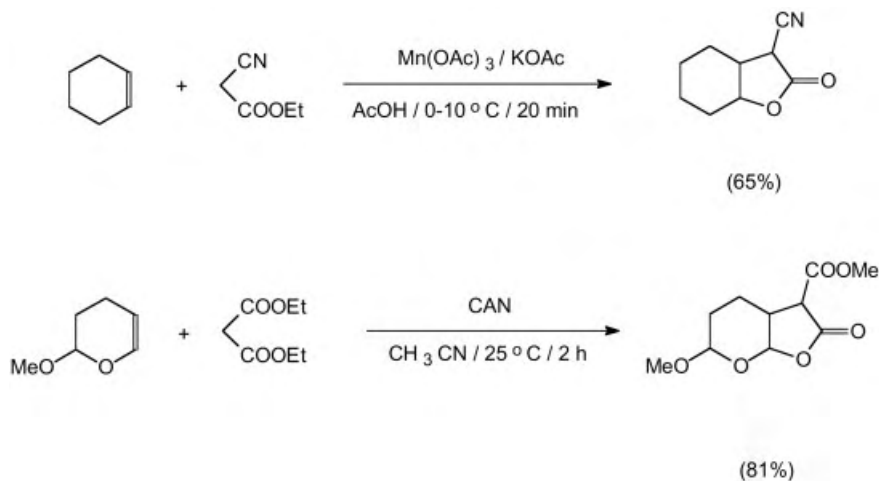
An alternative cyclopropane synthesis via an active methylene compound can also be enhanced by sonication [110]. The number of examples quoted in the literature is low but in the case of ethyl cyanoacetate and dibromoethane sonicated with potassium carbonate and polyethylene glycol in ethylene dichloride the expected cyclopropane is generated in 85 % yield (Eq. 3.19).


$$\text{CH}_2=\text{CH}(\text{CH}_2)_7\text{CH}=\text{CHCOOMe} \xrightarrow[25^\circ\text{C} / 15\text{ min}]{\text{MCPBA} / \text{H}_2\text{O}} \text{CH}_2=\text{CH}(\text{CH}_2)_7\text{CH}(\text{CH}_2)_2\text{COOMe} + \text{epoxide} \quad 47\%$$


Aziridine synthesis can be achieved *via* nitrene addition to alkenes making use of a sulfonylcarbamate [112]. Treatment of this reagent with potassium carbonate in the presence of an alkene together with a PTC leads to the aziridine (Eq. 3.20). The reaction time is reduced from 2–3 h to 15 min when sonication is applied.



The addition of radicals to olefins at the α -position of carbonyl groups in the presence of manganese triacetate is a straightforward method for the synthesis of γ -lactones [113]. The reaction generally occurs under heating and implies a sequence of enolisation of the carbonyl group, oxidation of the enolate by the manganic salt to the radical, and addition of the latter to the $C = C$ bond. With monomethyl malonate in acetic acid solution under silent conditions, no reaction occurs at $0-10^\circ\text{C}$. In contrast, the conversion is rapid under sonication [114, 115]. Excellent yields were obtained, even in the difficult cases of enol ethers, stilbene, or cyclohexene (Scheme 3.22). In the latter case, only the *cis* ring junction in the bicyclic lactone is observed. With cyanoacetic acid, good results are also obtained but the stereoselectivity is lower. An improvement to the method is obtained using ceric ammonium nitrate (CAN) in place of the manganese salt.



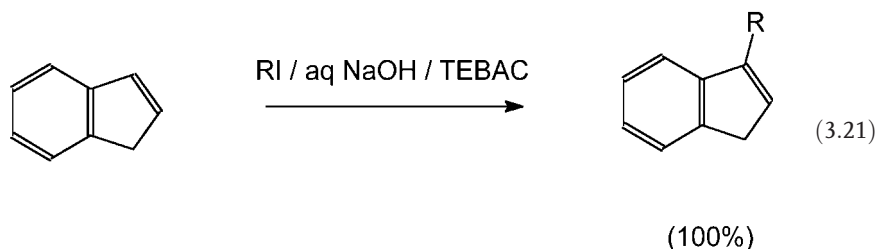
Scheme 3.22

Addition of cyanide ion to a carbonyl compound leads to a cyanohydrin, a process with many applications including the synthesis of amino acids *via* an aminonitrile. The direct reaction between an aldehyde, KCN and NH_4Cl in acetonitrile leads to a mixture

Tab. 3.3. Strecker synthesis of aminonitriles.

Method	PhCHO	PhCH(OH)CN	PhCH(NH ₂)CN	PhCH(OH)COPh
Stirred	35	38	6	21
Stirred + Al ₂ O ₃	8	19	64	9
Sonicated	11	45	23	22
Sonicated + Al ₂ O ₃	0	3	90	7

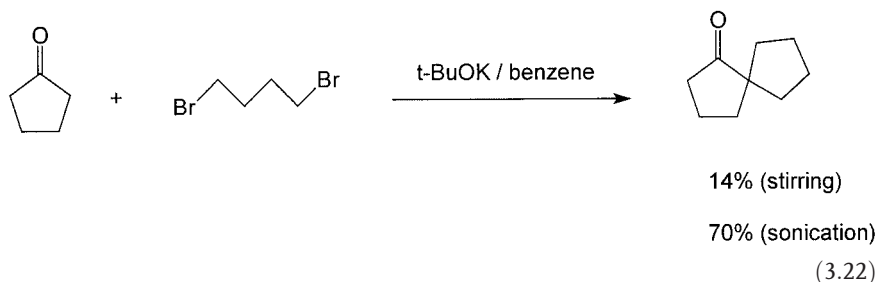
of products but in the presence of alumina and sonication the reaction can be made more specific [116]. In the case of benzaldehyde the yield of the target aminonitrile PhCH(NH₂)CN is poor under normal stirred conditions with benzoin PhCH(OH)COPh and hydroxynitrile PhCH(OH)CN predominating (Tab. 3.3). The presence of alumina suspended in acetonitrile increases the proportion of aminonitrile but the overall results make it clear that the optimum reaction conditions require the presence of suspended alumina together with sonication and then the yield of target aminonitrile reaches 90 %.



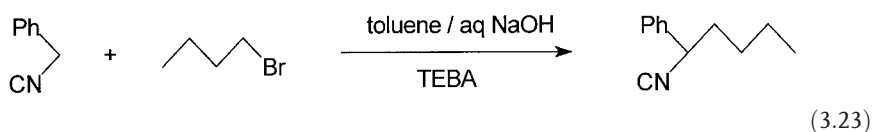
3.5.2.2 C Alkylation Reactions

The general feature of alkylation reactions at a carbon atom is that they can be achieved under sonication using solid bases even in apolar solvents. The advantage is that side reactions are generally minimised. Deprotonation occurs readily on a benzylic position in the presence of aqueous sodium hydroxide, as shown with indene (Eq. 3.21) [117]. A quantitative yield of the alkylated product can be obtained using sonication in the presence of a PTC. It was suggested that alkylation of cyclopentadiene or indene by secondary or tertiary alkyl halides in the presence of potassium hydroxide and Aliquat occurred *via* a SET process [118].

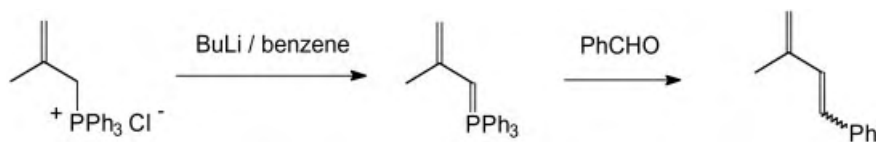
Alkylation at carbon positions activated by electron-withdrawing groups is illustrated by the spiroannellation of cyclopentanone and cyclohexanone by sonication of the parent compound with potassium *t*-butoxide and 1,4-dibromobutane (Eq. 3.22). The sonochemical improvement is especially large with cyclopentanone which is normally particularly prone to self-condensation [119].



The alkylation of phenylacetonitrile with butyl bromide using a PT catalyst supported on insoluble polystyrene cross-linked with divinylbenzene has been studied with respect to large-scale implementation (Eq. 3.23) [120]. Using the supported PTC means that catalyst disruption and subsequent separation from the product mixture could be minimised. The efficiencies of several types of reactors were compared using either a suspension of the catalyst in the medium (slurry reactor) or the catalyst supported on a fixed bed of polymer. Using either sonication or a turbine mixer (700 rpm) results showed that ultrasonic mixing was more efficient and similar rate constants were obtained with either a slurry or a fixed bed catalyst. Since the latter has the advantage of avoiding pulverisation of the catalyst it was proposed that this method should be employed in any reaction using a solid catalyst and an ultrasonic source to increase the reactivity with respect to silent conditions [121].

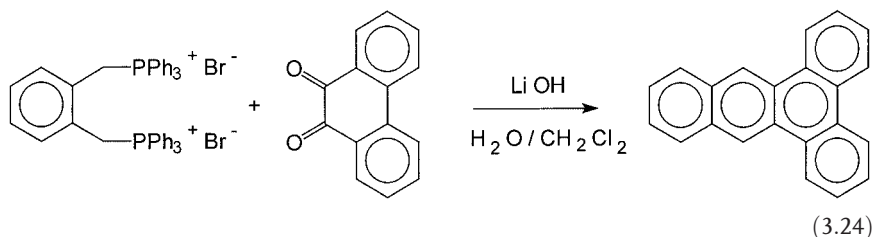


Wittig reactions have been studied and extended by sonochemists. Starting from allylic phosphoranes, it was shown that the initial deprotonation step could be effected with an increased efficiency using butyl lithium in THF or even in benzene (Scheme 3.23) [122]. The insoluble phosphorane disappears after 5–15 min sonication. This superposition of the two essential roles of sonication is reflected by the change in the stereoselectivity, larger proportions of the trans-diene being formed under irradiation.



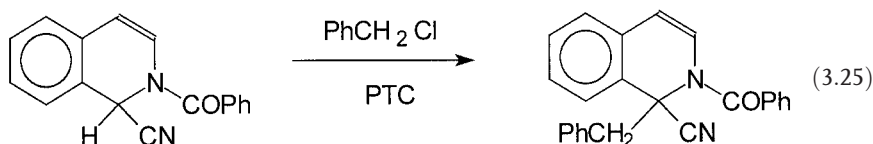
Scheme 3.23

A rather difficult double Wittig reaction (Eq. 3.24) has been effected with enhanced efficiency under sonication [123]. The process constitutes a novel type of annelation of an aromatic ring when applied to *o*-quinones.



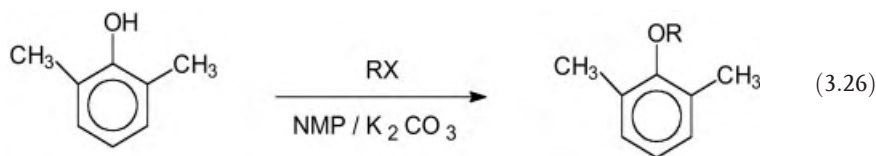
It is liquid-liquid reactions involving phase transfer catalysts which generally benefit from the use of ultrasound. Sonication produces homogenisation – i. e. very fine emulsions – which greatly increase the reactive interfacial area and allows faster reaction at lower temperatures. Davidson has reported an example of this with the ultrasonically enhanced saponification of wool waxes by aqueous sodium hydroxide using tetra *n*-heptyl ammonium bromide as a PTC [124].

In another example increased yields of products are obtained under ultrasonic irradiation in the PTC alkylation of the isoquinoline derivatives using 50% aqueous NaOH as base [125]. Efficient mixing is not easy to achieve for this system under normal reaction conditions due to the viscosity of the aqueous base. In the specific case of alkylation with benzyl chloride ultrasound plus [Et₃NCH₂Ph]⁺Cl[−] achieved 60% yield in 20 min compared with only 50% in 2 h with stirring (Eq. 3.25).



3.5.2.3 O and N Alkylation Reactions

The O-alkylation reactions of hindered phenols are normally sluggish reactions and attempts to improve reactivity have received considerable attention from synthetic organic chemists. Ultrasonic irradiation has been used to greatly enhance the rate of alkylation of 2,6-dimethylphenol with several different primary halides under heterogeneous conditions using K₂CO₃ in *N*-methylpyrrolidinone (NMP) (Eq. 3.26) [126].

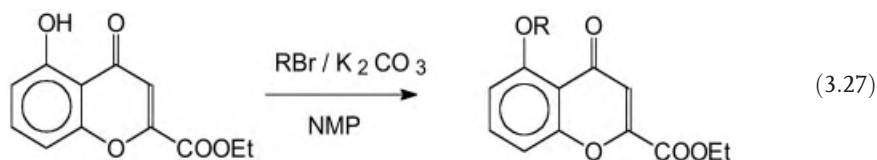


The results in Tab. 3.4 show that the most obvious benefit of ultrasonic irradiation on these *O*-alkylation reactions is the substantial acceleration in rate giving almost complete alkylation in about 1.5 h for all three systems. The Table also reveals a characteristic of such alkylations namely that under normal, stirred, conditions there is a distinct fall-off in reactivity as the reaction proceeds. Since it is known that sonication is capable of reducing particle size in reactions involving powders, the possibility that simple particle size reduction (i. e. increase in surface area) of the potassium carbonate might explain the sonochemical enhancement was investigated. This was accomplished by first suspending K_2CO_3 in NMP and subjecting it to sonication for one hour. During this period the initial agglomerates of powder, some 100–300 μm in diameter, were broken down to particles with a fairly even size distribution of around 3–5 μm . When this material was used to perform the alkylation of 2,6-dimethylphenol with iodopropane under normal stirred conditions the reaction was found to proceed very rapidly initially but the rate tailed off at about 85 % completion. By applying ultrasound to the system at this point the reaction could be rapidly forced to completion. Such results support the hypothesis that sonication has a two-fold effect on heterogeneous reactions namely (a) a reduction in particle size affording a far larger surface area for reactivity and (b) much more efficient reagent mixing and mass transfer than can be achieved by normal stirring.

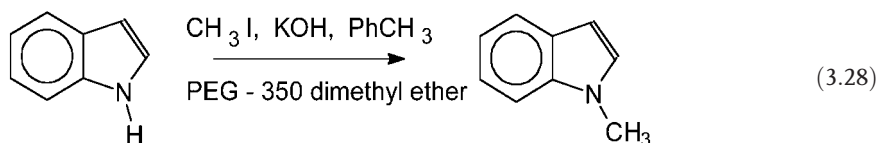
This methodology was found to be highly successful when applied to the *O*-alkylation of 5-hydroxychromones, reactions that are normally very difficult to perform due to electronic hindrance to the OH group caused by hydrogen bonding between it and the carbonyl group [127]. For example the alkylation of 5-hydroxy-2-carboxyethyl-4H-1-benzopyran-4-one with 1-iodopropane at 65 °C in NMP is only 28 % complete after 1.5 h (Eq. 3.27) whereas under ultrasonic irradiation complete reaction was obtained in this time period.

Tab. 3.4. Yield of ether from the alkylation of 2,6-dimethylphenol.

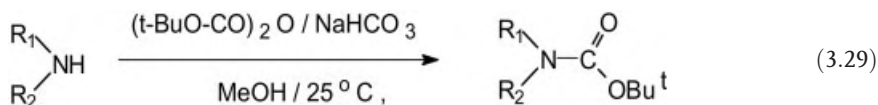
Halocompound	Yield [%] (glc) after 1.5 h	
	Sonicated	Silent
Iodomethane	90	45 (60 after 4 h)
1-Iodopropane	95	33 (45 after 4 h)
3-Bromoprop-1-ene	100	38



Nitrogen alkylation occurs easily under sonochemical conditions [128]. Indole and carbazole undergo *N*-alkylation with increased rates and yields under sonication in the presence of polyethylene glycol methyl ether as PTC. No reaction occurs in the absence of the PTC (Eq. 3.28).

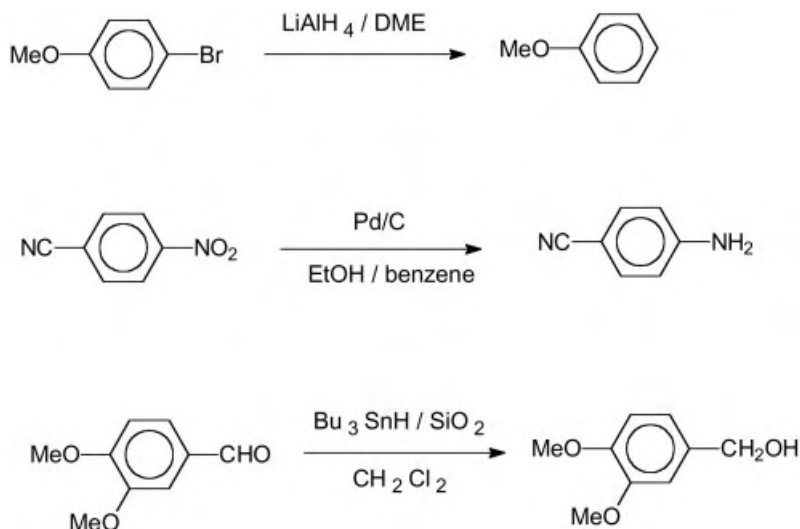


A synthetically important *N*-acylation reaction is the formation of Boc protected amines [129]. A rapid and simple method has been reported using sonication which allows this reaction to be effected in the absence of water using solid sodium hydrogen carbonate as the base in a methanol suspension (Eq. 3.29).



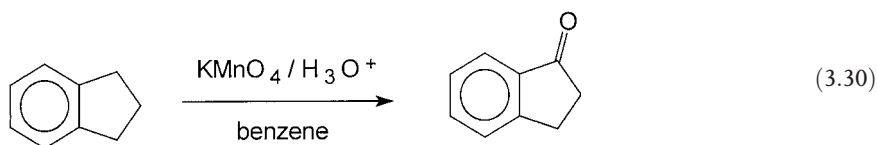
3.5.2.4 Reduction and oxidation Reactions

A few examples of sonochemical reductions have been investigated (Scheme 3.24). Thus the cleavage of aromatic carbon-halogen bond by lithium aluminium hydride can be achieved under sonication even in difficult cases such as that of bromoanisole [130]. The yield under sonication in DME is 70 % (35 °C, 7 h) compared with only 35 % (reflux, diglyme, 24 h). Reduction of the aromatic nitro group to amine occurs in good yields using a catalytic procedure with palladium and hydrogen [131]. The reduction of aldehydes with tributyltin hydride in biphasic systems at room temperature also affords good yields [132].

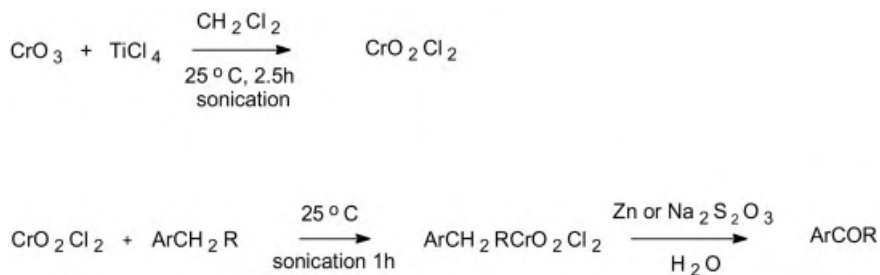


Scheme 3.24

Oxidation at the benzylic position of indane with potassium permanganate (Eq. 3.30) gives indanone in good yields and no PTC is necessary [133]. In a two-phase system consisting of an aqueous solution of KMnO_4 and indane in benzene an 80 % yield can be obtained under a reduced pressure of ca. 450 Torr. The authors explain this effect by the size of the cavitation bubbles, which is dictated to some extent by the over pressure. An optimal energy transformation, from acoustic to chemical, can thus take place.

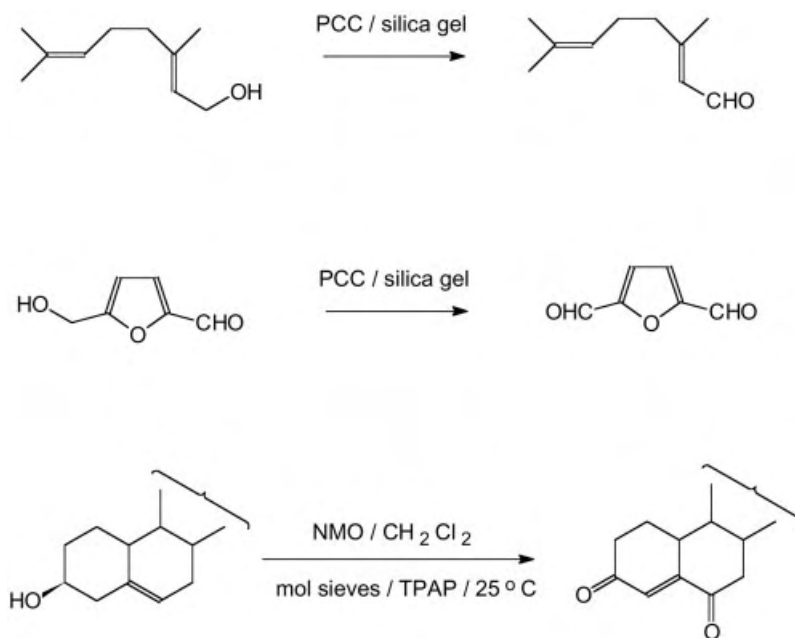


Etard reagents (chromyl chloride and some derivatives) suffer from the problem that occasionally they can exhibit a lack of selectivity and low yields. They are useful in the selective oxidation of aromatic side-chains to a carbonyl group, aldehyde or ketone but in many instances, the formation of the initial complex is slow and yields are low because of difficulties in the work-up which lead to undesired over-reaction. Attempts have been made to solve the problems by the use of sonication [134]. A simple preparation of the liquid reagent was proposed and the Etard reaction itself together with the hydrolytic step were conducted under sonication, with some success (Scheme 3.25).



Scheme 3.25

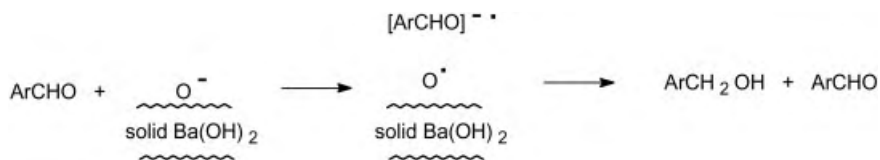
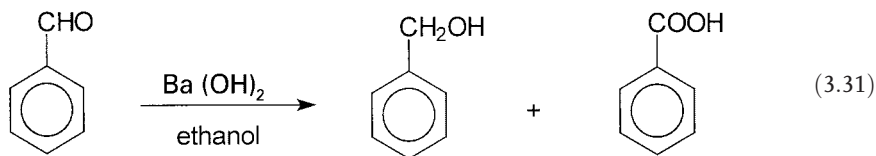
The oxidation of alcohols to carbonyl compounds has been studied by several authors and a variety of methods have been used. Papers concerned with such oxidations are illustrated (Scheme 3.26). Good results have been obtained using pyridinium chlorochromate (PCC) adsorbed onto silica gel for the selective oxidation of unsaturated substrates e.g. terpene [135] and furanyl derivatives [136]. Steroidal homoallylic alcohols can be converted to the corresponding 4-ene-3,6-diones using tetrapropylammonium per-ruthenate (TPAP) in catalytic amounts [137]. In this case, the oxidising agent is *N*-methyl morpholine *N*-oxide (NMO).



Scheme 3.26

The Cannizzaro reaction under heterogeneous conditions (solid-liquid) using calcined barium hydroxide as base is greatly accelerated by low intensity ultrasound (cleaning

bath). Yields of 100 % of the disproportionation products are obtained after 10 min sonication of benzaldehyde whereas no reaction is observed during this period in the absence of ultrasound (Eq. 3.31) [138].



The catalyst surface contains both reducing and basic sites and experiments involving selective poisoning of the former by *m*-dinitrobenzene demonstrated the high probability of a SET mechanism. The same group also concluded that an SET mechanism was probably involved for Michael, Wittig-Horner, and Claisen-Schmidt condensations in the presence of the same catalyst [139, 140].

3.6

Sonochemical Preparation of Ultrafine Powders and Nanostructured Materials

Ultrafine powders are usually considered to be particles with diameters between 1–100 nm [141]. A focus for recent work in material chemistry has been the preparation of such particles [142] because of their special properties: optical, photocatalytic, electrochemical, magnetic, thermal resistance, high melting point and sintering abilities [143, 144]. A variety of chemical and physical methods have been used for the synthesis of such materials including the decomposition of organometallics [145] and the controlled reduction of salts [146–148].

Metastable amorphous materials can be produced by the rapid quenching of melts in the form of metallic alloys with glassy structures [149]. These materials have attracted the attention of metallurgists, physicists, and, recently, chemists because of their exceptional properties (easy magnetisation, superior corrosion resistance, high mechanical toughness, interesting electronic properties) [150]. The use of these materials in catalysis was reported some years ago [151].

Sonochemistry affords a technology which can be used to generate ultrafine powders and nanostructured materials of significant commercial interest which encompass both amorphous and crystalline properties [152].

3.6.1

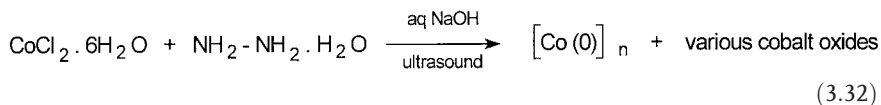
Metal Powders

One of the earliest sonochemical methods for the preparation of amorphous nanopowders was the sonochemical decomposition of organometallic compounds. The first example was the synthesis of amorphous iron. Ultrasonic irradiation of iron pentacarbonyl, either pure or as a 1 M solution in decane with a high-intensity 20-kHz probe at 100 W cm^{-2} , yields a dull black powder [49, 153]. Elemental analysis of the product revealed a $> 96\%$ iron composition by weight, with small amounts of carbon (3 %) and oxygen (1 %), presumably from the decomposition of the alkane solvent or carbon monoxide during sonication [154]. It is the high temperatures and pressures created during cavitation bubble collapse (on a microsecond time scale) coupled with the rapid cooling rate associated with the disappearance of the bubble ($> 10^9 \text{ K/s}$) which provide the conditions for such preparations. The cooling rate is much greater than that obtained by conventional melt quenching techniques ($10^5\text{--}10^6 \text{ K/s}$) [155]. The amorphous nature of this powder was confirmed by several techniques, including X-ray powder diffraction and electron-beam micro-diffraction, differential scanning calorimetry, and transmission electron microscopy, which reveal the microstructure of the powder. Moreover, the material has a surface area as high as $120 \text{ m}^2 \text{ g}^{-1}$ (by the BET gas adsorption isotherm method), i. e., 150 times larger than a commercially available $5 \text{ }\mu\text{m}$ -diameter iron powder. Sonochemically produced amorphous iron powder sinters at unusually low temperatures. At 350°C , the amorphous powder acquires a metallic luster, associated with the growth of ca 50 nm crystallites and the loss of porosity: the surface area decreases roughly one hundredfold and becomes comparable to that of the commercial crystalline powder.

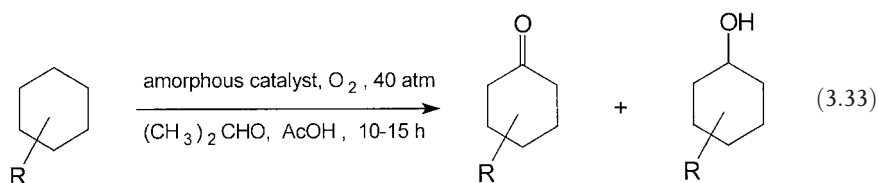
From a catalytic viewpoint, the material was tested for two commercially important reactions: the Fischer-Tropsch process of CO hydrogenation and the hydrogenolysis and dehydrogenation of saturated hydrocarbons [156]. The Fischer-Tropsch conversion of carbon monoxide and hydrogen to low molecular-weight alkanes occurs at very low temperatures (200°C). The amorphous powder is roughly ten times more reactive per gram than common commercial samples. At 250°C , the overall activity for the dehydrogenation of cyclohexane to benzene, and its hydrogenolysis predominantly to methane, is > 30 times greater for the sonochemically produced amorphous iron relative to the crystalline one. As expected, sintering and crystallisation of the metallic glass powder above 300°C decreased its catalytic activity. Amorphous nickel

powder has been prepared in a similar manner by the sonochemical decomposition of $\text{Ni}(\text{CO})_4$ as a neat liquid or in decalin solution [157].

The preparation of cobalt nanoclusters has been performed by sonicating basic solutions of $\text{Co}(\text{II})$ and hydrazine [158] (Eq. 3.32). The colloidal cobalt nanoclusters consist primarily of cobalt, although a small amount of oxygen, possibly as a very thin oxide coating, is also present. The cobalt nanoclusters are ferromagnetic and, as such, may prove useful in the construction of high-density recording media or permanent magnets.



Recently, the amorphous magnetic metals (Fe, Ni, and Co), and some amorphous magnetic alloys have been used as catalysts in the aerobic oxidation of hydrocarbons such as cyclohexane, methyl cyclohexane, and adamantane [159]. Thus, the oxidation of cyclohexane is carried out up to 40 % conversion with 80 % selectivity for cyclohexanone and cyclohexanol using nanostructured amorphous metals like Fe and Co, and amorphous alloy like $\text{Fe}_{20}\text{Ni}_{80}$ with oxygen (40 atm) at 25–28 °C in the absence of any solvent. In the aerobic oxidation isobutyraldehyde as co-reductant and a catalytic amount of acetic acid are used (Eq. 3.33). Such oxidations can be accomplished at room temperature under 1 atm of oxygen, albeit oxygen at 40 atm gives better conversion (Tab. 3.5).



Palladium metallic clusters have been prepared at room temperature by sonochemical reduction of $\text{Pd}(\text{OAc})_2$ and a surfactant, myristyltrimethylammonium bromide, in THF or MeOH [160]. It is noteworthy that nanosized amorphous Pd is obtained in THF, but in a crystalline form in MeOH. In this solvent, and in higher homologous alcohols, sonolysis of tetrachloropalladate(II) leads to Pd nanoclusters in which carbon atoms, formed by complete decomposition of the solvent, can diffuse. This results in an interstitial solid having the formula PdC_x ($0 < x < 0.15$) [161]. Noble metal nanoparticles of Au, Pd, and Ag are obtained by sonicating aqueous solutions of the corresponding salts in the presence of a surfactant, which largely stabilise the naked col-

Tab. 3.5. Performance of sonochemically prepared amorphous catalysts in the aerobic oxidation of cyclohexanes (Equation 3.33).

Hydrocarbon	Catalyst size	Temp.	Conversion	Ratio
	[nm]	[°C]	[%]	Ketone:Alcohol
R = H (cyclohexane)	Fe (20)	28	40	1:4.5
	Co (20)	28	41	1:5
	Fe ₂₀ Ni ₈₀ (25)	28	38	1:3.6
	Fe (20)	70	62	1:5
	Fe ₂₀ Ni ₈₀	70	56	1:2
R = CH ₃ (methylcyclohexane)	Fe (20)	28	32	1:1
	Co (20)	28	38	1:3
	Fe ₂₀ Ni ₈₀ (25)	28	36	1:2

loid [162]. Amorphous silver particles (ca. 20 nm size) can be prepared by the sonolysis of aqueous silver nitrate in an argon/hydrogen atmosphere [163].

An interesting sonochemical synthesis of elongated copper nanoparticles (approx. 50×500 nm) has been described [164]. The principle of the method is the use of an organised medium of aqueous cetyltrimethylammonium *p*-toluenesulphonate as the supporting fluid for sonication. The resulting nanoparticles are produced from the sonication of copper hydrazine carboxylate in the interconnected threadlike micelles which act as a template. The nanoparticles are coated with a layer of the surfactant. In the absence of the detergent the particles were spherical (ca. 50 nm).

3.6.2

Metal Oxide and Other Powders

Ultrafine powders of Cr₂O₃ and Mn₂O₃ have been prepared by sonochemical reduction of aqueous solutions of ammonium dichromate and potassium permanganate, respectively [165]. The powders are nanosized (50–200 nm) and crystallisation may be induced by heating. Nanosized amorphous oxides, such as NiFe₂O₄ powder, can be prepared by sonochemical decomposition of Fe(CO)₅ and Ni(CO)₄ in decalin solutions under an oxygen pressure of 100–150 kPa [166]. Microscopic characterisation gives no evidence of crystalline formation and the material is an agglomerate of nanoparticles with diameters < 10 nm. Magnetic measurements also indicate that NiFe₂O₄ particles are superparamagnetic.

A recent investigation has demonstrated the usefulness of ultrasonic irradiation in the preparation of delaminated zeolites, which are a particular type of modified oxides – microporous crystalline aluminosilicates with three-dimensional structures – having a greater catalytic activity than the layered structures (clays) and mesoporous catalysts. In an attempt to increase the pore size of zeolites, a layered zeolite precursor was

delaminated in an ultrasonic bath operating at 40 kHz for 1 h [167]. This layered aluminosilicate and a typical zeolite have similar activities for *n*-decane cracking. In addition, delamination provides a greater site accessibility for larger molecules, catalysing the formation of more liquid (gasoline) and less gaseous products and coke.

Irradiation of a slurry of Mo(CO)_6 and sulfur in 1,2,3,5-tetramethylbenzene gives rise to amorphous MoS_2 [168]. It was converted to the crystalline state, hexagonal MoS_2 , by heating. The particles were examined for their catalytic activity for hydrodesulfurisation, a key process in petrochemistry and were found to be superior to commercially available ReS_2 , RuS_2 , and MoS_2 .

Although the topic of sonoelectrochemistry will be treated in the subsequent section, it should also be mentioned that pulsed sonoelectroreduction of metallic salts gives rise to finely divided reactive metals which can be employed in organometallic synthesis see above [85]. The synthesis of nanocompounds of semiconductors such as cadmium and lead selenides can also be achieved using similar methodology [169].

A continuous process based on *hydrodynamic cavitation* can be employed to prepare a wide variety of metal oxides in grain sizes of 1–10 nm, such as iron oxide, bismuth molybdate, perovskites, platinum-loaded zeolite, and other ceramics and superconductors [170]. The method uses a microfluidiser for mechanically generating hydrodynamic cavitation and the internal pressure of the liquid media is elevated from ambient pressure to between 1000 to 25 000 psi.

The shape of a magnetic particle generated using sonochemistry can be modified by the use of an external magnetic field [171]. In the absence of a magnetic field sonication of Fe(CO)_5 dissolved in decalin yielded sponge-like particles with a mean size of 25 nm. Remarkably the same sonication conditions but in a 7 kG magnetic field produced highly acicular particles (5×50 nm).

3.6.3

Supported Nanopowders

From the above it is clear that a great advantage of the sonochemical synthesis of nanostructured materials is that different forms can be generated simply by changing the reaction medium. One such variation is sonolysis in the presence of inorganic supports (e.g. silica, alumina) to yield nanostructured materials distributed on solid supports. These are very useful as catalysts since they have a large proportion of active metal atoms exposed at the surface interface between solid and liquid. A simple example of this is the ultrasonic irradiation of iron pentacarbonyl in decane solution in the presence of silica gel to produce a silica-supported amorphous nanostructured iron. The iron particles range in size from 3 to 8 μm . This catalyst is a very active material for Fischer-Tropsch hydrogenation of CO [156].

Tab. 3.6. Dispersion data of Pd catalysts on alumina prepared with and without ultrasound.

Sample	Pd [%]	Precursor	D _M [%]
us	0.5	PdCl ₂	62.6
silent	0.5	PdCl ₂	31.2
us	1	PdCl ₂	45.7
silent	1	PdCl ₂	27.8
us	0.5	Pd(NO ₃) ₂ , 2 H ₂ O	64.2
silent	0.5	Pd(NO ₃) ₂ , 2 H ₂ O	44.1
us	1	Pd(NO ₃) ₂ , 2 H ₂ O	48.3
silent	1	Pd(NO ₃) ₂ , 2 H ₂ O	17.7

Ruthenium catalysts, supported on a commercial alumina (surface area 155 m² g⁻¹), have been prepared using two different precursors: RuCl₃ and Ru(acac)₃ [172, 173]. Ultrasound is used during the reduction step performed with hydrazine or formaldehyde at 70 °C. The ultrasonic power (30 W cm⁻²) was chosen to minimise the destructive effects on the support (loss of morphological structure, change of phase). Palladium catalysts have been supported both on alumina and on active carbon [174, 175]. Tab. 3.6 lists the dispersion data D_M provided by hydrogen chemisorption measurements of a series of Pd catalysts supported on alumina. D_M is the ratio between the surface atoms accessible to the chemisorbed probe gas (H₂) and the total number of catalytic atoms on the support. An increase in the dispersion value is observed in all the sonicated samples but the effect is more pronounced for low metal loading.

Nanosized nickel can be produced as coatings on submicrospheres of amorphous alumina by simply sonicating Ni(CO)₄ with the amorphous alumina in decalin [176]. When crystallised alumina is used as substrate the nickel particles are distributed in the freespace among the submicrospheres. This technology can also be used in the preparation of phosphors, comparable or better than existing commercial samples, from the sonochemical doping of alumina with Eu₂O₃ and Tb₂O₃ [177].

References

1. F.R. Young, *Cavitation*, McGraw Hill, UK, 1989.
2. T.G. Leighton, *The Acoustic Bubble*, Academic Press, London, 1994.
3. L.A. Crum, T.J. Mason, J.L. Reisse, and K.S. Suslick (ed.), *Sonochemistry and Sonoluminescence*, NATO ASI Series, Kluwer Academic Publishers, 1999.
4. K.S. Suslick (ed.), *Ultrasound, its Chemical, Physical and Biological Effects*, VCH, Weinheim, 1988.
5. T.J. Mason and J.P. Lorimer, *Sonochemistry, Theory, Applications and Uses of Ultrasound in Chemistry*, Ellis Horwood Publishers, 1989.
6. S.V. Ley and C.M.R. Low, *Ultrasound in Synthesis*, Springer Verlag, 1989.
7. T.J. Mason (ed.), *Sonochemistry the Uses of Ultrasound in Chemistry*, Royal Society of Chemistry, London, 1990.
8. T.J. Mason, *Practical Sonochemistry, A Users Guide to Applications in Chemistry and Chemical Engineering*, Ellis Horwood Publishers, 1991.
9. G.J. Price, *Current Trends in Sonochemistry*, Royal Society of Chemistry, Oxford, 1993.
10. M.A. Margulis, *Sonochemistry and Cavitation*, OPA, Amsterdam, 1995.
11. T.J. Mason, *Sonochemistry*, Oxford University Primer Series, No 70, Oxford Science Publications, 1999.
12. M. Povey and T.J. Mason (eds.), *Ultrasound in Food Processing*, Blackie Academic and Professional, London, 1998.
13. R.W. Wood and A.L. Loomis, *Phil. Mag.*, 1927, 4, 414.
14. H. Mark, *J. Acoust. Soc. Amer.*, 1945, E16, 183.
15. A. Weissler, *J. Chem. Ed.*, 1948, 28.
16. Special edition of the journal "Ultrasonics" covering the R.S.C. Sonochemistry Symposium, Warwick, 1986, *Ultrasonics*, 1987, 25, January Issue.
17. D. Bremner, Historical introduction to sonochemistry, *Advances in Sonochemistry*, T.J. Mason (ed.), JAI Press, London, 1990, 1, 1–38.
18. D.W. Gillings, Ultrasound and colloid science – the early years, *Advances in Sonochemistry*, T.J. Mason (ed.), JAI Press, London, 1993, 3, 1–16.
19. A. Henglein, Contributions to various aspects of cavitation chemistry, *Advances in Sonochemistry*, T.J. Mason (ed.), JAI Press, London, 1993, 3, 17–84.
20. E.C. Couppis and G.E. Klinzing, *A. I. Ch. E. J.*, 1974, 20, 485.
21. S. Folger and D. Barnes, *Ind. Eng. Chem. Fundam.*, 1968, 7, 222.
22. P. Riesz, Free radical generation by ultrasound in aqueous solutions of volatile and non-volatile solutes, *Advances in Sonochemistry*, T.J. Mason (ed.), JAI Press, London, 1991, 2, 23.
23. See for example: W. Lauterborn and W. Hentschell, *Ultrasonics*, 1985, 23, 260.
24. See for example: (a) B. Pugin and A.T. Turner, Influence of ultrasound on reactions with metals, *Advances in Sonochemistry*, T.J. Mason (ed.), JAI Press, London, 1990, 1, 81–118; (b) K.S. Suslick and D. Docketycz, Effects of ultrasound on surfaces and solids, *ibid* 187–230.
25. K. Starchev and S. Stoilov, *Phys. Rev. B, Condens. Matter.*, 1993, 47 11 725.
26. H. Kashiwagi, S. Enomoto, and M. Inoue, *Chem. Pharm. Bull.*, 1989, 37, 3181.
27. V.V. Boldyrev, *J. Chim. Phys.*, 1986, 83, 821.
28. J.-L. Luche, Sonochemistry: from experiment to theoretical considerations, *Advances in Sonochemistry*, T.J. Mason (ed.), JAI Press, London, 1993, 3, 85–124.
29. (a) T. Ando, S. Sumi, T. Kawate, J. Ichihara, and T. Hanafusa, *J. Chem. Soc. Chem. Commun.*, 1984, 439.
30. J.-L. Luche, C. Einhorn, J. Einhorn, and J.V. Sinisterra-Gago, *Tetrahedron Lett.*, 1990, 31, 4125.
31. T.J. Mason and J.-L. Luche, Ultrasound as a new tool for synthetic chemists, *Chemistry Under Extreme or Non-Classical Conditions*,

- Rudi van Eldik (ed.), John Wiley, 1996, 317–381.
32. V.S. Moholkar, P.S. Kumar, and A.B. Pandit, *Ultrasonics Sonochemistry*, 1999, **6**, 53.
33. J. Reisse, C. Caulier, Y. Dekerckheer Kegelaers, N. Segebarth, and K. Bartik, *Sonochemistry and Sonoluminescence*, L.A. Crum, T.J. Mason, J.L. Reisse, and K.S. Suslick (eds.), NATO ASI Series, Kluwer Academic Publishers, 1999, 205.
34. C.W. Porter and L. Young, *J. Am. Chem. Soc.*, 1938, **60**, 1497.
35. J.W. Chen and W.M. Kalback, *Ind. Eng. Chem. Fundam.*, 1967, **6**, 175.
36. D.S. Kristol, H. Klotz, and R.C. Parker, *Tetrahedron Lett.*, 1981, **22**, 907.
37. T.J. Mason and J.P. Lorimer, *J. Chem. Soc., Chem. Commun.*, 1980, 1135.
38. T.J. Mason, J.P. Lorimer, and B.P. Mistry, *Tetrahedron Lett.*, 1982, **23**, 5563.
39. T.J. Mason, J.P. Lorimer, and B.P. Mistry, *Tetrahedron*, 1985, **26**, 5201.
40. K. Makino, M.M. Mossoba, and P. Riesz, *J. Phys. Chem.*, 1983, **87**, 1369.
41. R. Schultz and A. Henglein, *Z. Naturforsch.*, 1953, **8**, 160.
42. A. Henglein and C.H. Fischer, *Ber. Bunsenges Phys. Chem.*, 1984, **88**, 1196.
43. W.G. Dauben, D.P. Bridon, and B.A. Kowalczyk, *J. Org. Chem.*, 1989, **54**, 6101.
44. A. Kotronarou, G. Mills, and M.R. Hoffmann, *J. Phys. Chem.*, 1991, **95**, 3630.
45. J. Reisse, Yang Danhui, M. Maeck, J. Vandercammen, and E. Vander Donckt, *Ultrasonics*, 1992, **30**, 397.
46. H.M. Cheung and S. Kurup, *Environ. Sci. Technol.*, 1994, **28**, 1619.
47. K.S. Suslick, J.J. Gawlenowski, P.F. Schubert, and H.H. Wang, *J. Phys. Chem.*, 1983, **87**, 2299.
48. K.S. Suslick, D.A. Hammerton, and R.F. Cline Jr., *J. Am. Chem. Soc.*, 1986, **108**, 5641.
49. K.S. Suslick, S.-B. Choe, A.A. Chichowlas, and M.W. Grimstaff, *Nature*, 1991, **353**, 414.
50. A.M. Horton, D.M. Hollinshead, and S.V. Ley, *Tetrahedron*, 1984, **40**, 1737.
51. K.S. Suslick, J.W. Goodale, P.F. Schubert, and H.H. Wang, *J. Am. Chem. Soc.*, 1983, **105**, 5781.
52. K.S. Suslick and P.F. Schubert, *J. Am. Chem. Soc.*, 1983, **105**, 6042.
53. A.M. Horton, D.M. Hollinshead, and S.V. Ley, *Tetrahedron*, 1984, **40**, 1737.
54. C.M.R. Low, *Ultrasonics Sonochemistry*, 1995, **2**, 153.
55. T. Ando, P. Bauchat, A. Foucaud, M. Fujita, T. Kimura, and H. Sohmiya, *Tetrahedron Lett.*, 1991, **32**, 6379.
56. T. Ando, J.-M. Leveque, J.P. Lorimer, J.-L. Luche, and T.J. Mason, *J. Org. Chem.*, 1998, **63**, 9561–9564.
57. M.J. Dickens and J.-L. Luche, *Tetrahedron Lett.*, 1991, **32**, 4709.
58. J.J. Caldwell, W.J. Kerr, and S. McKendry, *Tetrahedron Lett.*, 1999, **40**, 3485.
59. E. Nakamura, Y. Imanishi, D. Machii, *J. Org. Chem.*, 1994, **59**, 8178.
60. E. Nakamura, K. Sato, and Y. Imanishi, *Synlett*, 1995, 525.
61. M. Sawamura, Y. Kawaguchi, K. Sato, and E. Nakamura, *Chem. Lett.*, 1997, 705.
62. H.C. Brown and U.S. Racherla, *Tetrahedron Lett.*, 1985, **26**, 2187.
63. M.T. Crimmins and R. O'Mahony, *Tetrahedron Lett.*, 1989, **30**, 5993.
64. G.E. Keck, A. Palani, S.F. McHardy, *J. Org. Chem.*, 1994, **59**, 3113.
65. R. Katoh, E. Yanase, H. Yokoi, S. Usuba, Y. Kakudate, and S. Fujiwara, *Ultrasonics Sonochemistry*, **5**, 37, 1998.
66. D. Mandrus, M. Kele, R.L. Hettich, G. Guiochon, B.C. Sales, and L.A. Boatner, *J. Phys. Chem. B*, 1997, **101**, 123.
67. J.-L. Luche and P. Cintas, *Active Metals, Preparation, Characterization, Applications*, A. Fürstner (ed.), VCH, Weinheim, 1996, 133–190.
68. B. Pugin and A.T. Turner, Influence of ultrasound on reactions with metals, *Advances in Sonochemistry*, T.J. Mason (ed.), JAI Press, London, 1990, **1**, 81–118.
69. W.J. Tomlinson, Effect of ultrasonically induced cavitation on corrosion, *Advances in*

- Sonochemistry*, T.J. Mason (ed.), JAI Press, London, 1990, **1**, 173–186.
70. K.S. Suslick and S.J. Doktycz, Effects of ultrasound on surfaces and solids, *Advances in Sonochemistry*, T.J. Mason (ed.), JAI Press, London, 1990, **1**, 187–230.
 71. A.J. Fry and S.S. Hong, *J. Org. Chem.*, 1981, **42**, 1962.
 72. J.-L. Luche, C. Petrier, and Dupuy, C. *Tetrahedron Lett.*, 1984, **25**, 753.
 73. T.S. Chou and M.L. You, *Tetrahedron Lett.*, 1985, **26**, 4495.
 74. P. Kruus, *Ultrasonics*, 1988, **26**, 216.
 75. A.N. Maltsev, *Russ. J. Phys. Chem.*, 1976, **50**, 995.
 76. C. Petrier, C. Dupuy, and J.-L. Luche, *Tetrahedron Lett.*, 1986, **27**, 3149.
 77. C. Petrier and J.-L. Luche, *Tetrahedron Lett.*, 1987, **28**, 2347.
 78. P. Kruus, D.A. Robertson, and L.A. McMillen, *Ultrasonics*, 1991, **29**, 370.
 79. R.D. Rieke, *Acc. Chem. Res.*, 1987, **10**, 301.
 80. P. Boudjouk, D.P. Thompson, W.H. Ohrbom, and B.H. Han, *Organometallics*, 1986, **5**, 1257.
 81. W.L. Parker, P. Boudjouk, and A.B. Rajkumar, *J. Am. Chem. Soc.*, 1991, **113**, 2785.
 82. H. Bonnermann, B. Bogdanovic, R. Brinkman, D.W. He, and B. Spliethoff, *Angew. Chem., Int. Ed. Engl.*, 1983, **22**, 728.
 83. W. Oppolzer and P. Schneider, *Tetrahedron Lett.*, 1984, **25**, 3305.
 84. S.K. Nayak and A. Banerji, *J. Org. Chem.*, 1991, **56**, 1940.
 85. A. Durant, J.-L. Delplancke, R. Winand, and J. Reisse, *Tetrahedron Lett.*, 1995, **36**, 4257.
 86. P. Renaud, *Bull. Soc. Chim. Fr.*, 1950, 1044.
 87. W. Slough and A.R. Ubbelohde, *J. Chem. Soc.*, 1957, 918.
 88. J.D. Sprich and G.S. Lewandos, *Inorg. Chim. Acta.*, 1982, **76**, 1241.
 89. J.-L. Luche and J.C. Damania, *J. Am. Chem. Soc.*, 1980, **102**, 7926.
 90. D.H. Yang, J. Einhorn, C. Einhorn, M.J. Aurell, and J.-L. Luche, *J. Chem. Soc., Chem. Commun.*, 1994, 1815.
 91. M.J. Aurell Piquer, C. Einhorn, J. Einhorn, and J.-L. Luche, *J. Org. Chem.*, 1995, **60**, 8.
 92. A. De Nicola, J. Einhorn, and J.-L. Luche, *J. Chem. Res., (S)*, 1991, 278.
 93. C. Petrier, A.L. Gemal, and J.-L. Luche, *Tetrahedron Lett.*, 1982, **23**, 3361.
 94. B.H. Han and P. Boudjouk, *J. Org. Chem.*, 1982, **47**, 5030.
 95. B.H. Han and P. Boudjouk, *J. Org. Chem.*, 1982, **47**, 751.
 96. N. Joshi and H.M.R. Hoffmann, *Tetrahedron Lett.*, 1986, **27**, 687.
 97. J. Yamashita, Y. Inoue, T. Kondo, and H. Hashimoto, *Bull. Chem. Soc. Jpn.*, 1984, **57**, 2335.
 98. O. Repic and S. Vogt, *Tetrahedron Lett.*, 1982, **23**, 2729.
 99. O. Repic, P.G. Lee, and N. Giger, *Org. Prep. Proc. Int.*, 1984, **16**, 25.
 100. T. Kitazume and N. Ishikawa, *J. Am. Chem. Soc.*, 1985, **107**, 5186.
 101. A. Solladie-Cavallo, D. Farkharic, S. Fritz, T. Lazrak, and J. Suffert, *Tetrahedron Lett.*, 1984, **25**, 4117.
 102. J.-L. Luche, C. Petrier, J.P. Lansard, and A.E. Greene, *J. Org. Chem.*, 1983, **48**, 3837.
 103. C. Petrier, J.-L. Luche, and C. Dupuy, *Tetrahedron Lett.*, 1984, **25**, 3463.
 104. J. Lindley, P.J. Lorimer, and T.J. Mason, *Ultrasonics*, 1986, **24**, 292.
 105. K.A. Nelson and H.G. Adolph, *Synth. Commun.*, 1991, 21.
 106. A. Loupy and J.-L. Luche, Sonochemistry in biphasic systems, *Synthetic Organic Sonochemistry*, J.-L. Luche (ed.), Plenum Press, 1998, 107–166.
 107. T. Ando and T. Kimura, Ultrasonic organic synthesis involving non-metal solids, *Advances in Sonochemistry*, T.J. Mason (ed.), JAI Press, London, 1991, **2**, 211–252.
 108. S.L. Regen and A. Singh, *J. Org. Chem.*, 1982, **47**, 1587.
 109. L. Xu, W.B. Smith, and U.H. Brinker, *J. Am. Chem. Soc.*, 1992, **114**, 783.

110. Lin, Q., Zhang, Y., Zhang, C., Song, W., and Qiu, Q. *Chin. Chem. Lett.*, 1991, **2**, 517; *Chem. Abstr.*, 1992, **116**, 193 753t.
111. M.S.F. Lie Ken Jie, and C.K. Lam, *Ultrasonics Sonochemistry*, 1995, **2**, 11–14.
112. V.V. Dirnens, Yu. Goldberg, and E. Lukevics, *Dokl. Akad. Nauk SSSR*, 1988, **298**, 116–118; *Chem. Abstr.* 1989, **110**, 8270y.
113. E.I. Heiba and R.M. Dessau, *J. Am. Chem. Soc.*, 1970, **93**, 995–999.
114. M. Allegretti, A.D'Annibale, and C. Trogolo, *Tetrahedron*, 1993, **49**, 10 705.
115. A. D'Annibale and C. Trogolo *Tetrahedron Lett.*, 1994, **35**, 2083.
116. T. Hanafusa, J. Ichihara, and T. Ashida, *Chem. Lett.*, 1987, 687.
117. F.Z. Galin, U.K. Ignatyuk, S.N. Lareev, and G.A.I. Tostikov, *Org. Chem. USSR*, 1987, **23**, 1214-1215.
118. E.V. Dehmlow and C. Bollmann, *Tetrahedron Lett.* 1991, **32**, 5773–5776.
119. T. Fujita, S. Watanabe, M. Sakamoto, and H. Hashimoto, *Chem. Ind. (London)*, 1986, 427.
120. V. Ragaini, C. Colombo, P. Barzaghi, E. Chiellini, and D. Antona, *S. md. Eng. Chem. Res.*, 1988, **27**, 1382–1387.
121. V. Ragaini, US Patent 5,108,654 (1992).
122. C.M.R. Low, *Syn. Lett.*, 1991, 123.
123. C. Yang, D.T.C. Yang, and R.G. Harvey, *Syn. Lett.*, 1992, 799.
124. R.S. Davidson, A. Safdar, J.D. Spencer, and D.W. Lewis, *Ultrasonics*, 1987, **25**, 35.
125. J. Ezquerria and J. Alvarez-Builla, *J. Chem. Soc., Chem. Commun.*, 1984, 54.
126. T.J. Mason, J.P. Lorimer, A. Moore, A.T. Turner, and A.R. Harris, *Ultrasonics Int. 87, Conf. Proc.*, 1988, 767.
127. T.J. Mason, J.P. Lorimer, A.T. Turner, and A.R. Harris, *J. Chem. Res. (S)*, 1988, 80.
128. R.S. Davidson, A. Patel, A. Safdar, J.D. Spencer, and B. Robinson, *Tetrahedron Lett.*, 1983, **24**, 5907.
129. J. Einhorn, C. Einhorn, and J.-L. Luche, *Synlett*, 1991, 37.
130. B.H. Han and P. Boudjouk, *Tetrahedron Lett.*, 1982, **23**, 1643.
131. B.H. Han, D.H. Shin, H.R. Lee, and D.G. Jang, *J. Korean Chem. Soc.*, 1989, **33**, 436.
132. B. Figadere, C. Chaboche, X. Franck, J.F. Peyrat, and A. Cavé, *J. Org. Chem.*, 1994, **59**, 7138.
133. G. Cum, G. Galli, R. Gallo, and A. Spadaro, *J. Chem. Soc. Perkin Trans. II*, 1988, 375.
134. F.A. Luzzio and W.J. Moore, *J. Org. Chem.*, 1993, **58**, 512.
135. L.L. Adams and F.A. Luzzio, *J. Org. Chem.*, 1989, **54**, 5387.
136. L. Cottier, G. Descotes, J. Lewkowski, and R. Skowronski, *Pol. J. Chem.*, 1994, **68** 693.
137. M.J.S. Miranda Moreno, M.L. Sa e Melo, and A.S. Campos Neves, *Tetrahedron Lett.*, 1991, **32**, 3201.
138. A. Fuentes and J.V. Sinisterra, *Tetrahedron Lett.*, 1986, **27**, 2967.
139. A. Fuentes, J.M. Marinas, and J.V. Sinisterra, *Tetrahedron Lett.* 1987, **28**, 2947.
140. O. Farooq, S.M.F. Farnia, M. Stephenson, and G.A.I. Olah, *Org. Chem.*, 1988, **53**, 2840.
141. A. Henglein, *Topics in Current Chemistry*, Springer-Verlag, Berlin Heidelberg, 1988, **143**, 115–180.
142. H. Weller, *Adv. Mater.*, 1993, **5**, 88-95; G.A. Ozin, *Adv. Mater.*, 1992, **4**, 612–649.
143. A. Henglein, Small-particle research: Physico-chemical properties of extremely small colloidal metal and semiconductor particles, *Chem. Rev.*, 1989, **89**, 1861.
144. M.L. Steigerwarld and L.E. Brus, *Ann. Rev. Mater. Sci.*, 1989, **19**, 471.
145. A.S. Lisitsyn, A.V. Colovin, A.L. Chuvilin, V.L. Kuznetsov, A.V. Romanenko, A.F. Danilyuk, and Y.I. Yermakov, *Appl. Catal.*, 1989, **55**, 235–258.
146. H. Bönemann, W. Brijoux, W. Brinkmann, E. Dinjus, and T. Jousen, *Angew. Chem.* 1991, **103**, 324–326.
147. K.L. Tsai and J.L. Dye, *J. Am. Chem. Soc.*, 1991, **113**, 1650–1652.

148. R.D. Rieke, M.S. Sell, W.R. Klein, T. Chen, J.D. Brown, and M.V. Hanson, *Active Metals*, A. Furstner (ed.), VCH, Weinheim, 1996, 1–59.
149. (a) K. Klement Jr., R.H. Willens, and P. Duwez, *Nature*, 1960, **187**, 869–870; (b) K.J. Klabunde and C. Cardenas-Trivino, *Active Metals*, A. Furstner (ed.), VCH, Weinheim, 1996, 237–278.
150. A. Molnar, G.V. Smith, and M. Bartok, *Adv. Catal.*, 1989, **36**, 329.
151. A. Yokoyama, H. Komiyama, H. Inoue, T. Masumoto, and H. Kimura, *J. Catal.*, 1981, **68**, 355–361.
152. V. Ragaini and C.L. Bianchi, Catalytic reactions, *Synthetic Organic Sonochemistry*, J.-L. Luche (ed.), Plenum Press, NY, 1998, 235–261.
153. M.W. Grinstaff, A.A. Cichowslav, S.B. Choe, and K.S. Suslick, *Ultrasonics*, 1992, **30**, 168–172.
154. E.B. Flint and K.S. Suslick, *J. Am. Chem. Soc.*, 1989, **111**, 6987–6992.
155. A.L. Greer, *Science*, 1995, **267**, 1947.
156. M. Fang, T. Hyeon, A.A. Cichowslav, and K.S. Suslick, *Division of Petroleum Chemistry: Symp. Advanced Techniques in Catalyst Preparations*, ACS Proc. National Meeting, 1995.
157. Yu. Koltypin, G. Katabi, X. Cao, R. Prozorov, and A. Gedanken, *J. Non-Cryst. Sol.*, 1996, **201**, 159.
158. C.P. Gibson and K.J. Putzer, *Science*, 1995, **267**, 1338.
159. V. Kesavan, P.S. Sivanand, S. Chandrasekaran, Yu. Koltypin, and A. Gedanken, *Angew. Chem., Int. Ed.*, 1999, **38**, 3521.
160. N.A. Dhas and A. Gedanken, *J. Mater. Chem.*, 1998, **8**, 445.
161. K. Okitsu, Y. Mizukoshi, H. Bandow, T.A. Yamamoto, Y. Nagata, and Y. Maeda, *J. Phys. Chem. B*, 1997, **101**, 5470.
162. Y. Mizukoshi, K. Okitsu, Y. Maeda, T.A. Yamamoto, R. Oshima, and Y. Nagata, *J. Phys. Chem. B*, 1997, **101**, 7033.
163. R.A. Salkar, P. Jeevanandam, S.T. Aruna, Yu. Koltypin, and A. Gedanken, *J. Mater. Chem.*, 1999, **9**, 1333.
164. R.A. Salkar, P. Jeevanandam, G. Kataby, S.T. Aruna, Yu. Koltypin, O. Palchik, and A. Gedanken, *J. Phys. Chem. B*, 2000, **104**, 893.
165. N.A. Dhas, Yu. Koltypin, A. Gedanken, *Chem. Mater.*, **9**, 3159, 1997.
166. K.V.P.M. Shafi, Yu. Koltypin, A. Gedanken, R. Prozorov, J. Balogh, J. Lendvai, and I. Felner, *J. Phys. Chem. B*, 1997, **101**, 6409.
167. A. Corma, V. Fornes, S.B. Pergher, Th.L.M. Maesen, and J.G. Buglass, *Nature*, 1998, **396**, 353.
168. M.M. Mdeleleni, T. Hyeon, and K.S. Suslick, *J. Am. Chem. Soc.*, 1998, **120**, 6189.
169. Y. Mastai, G. Hodes, R. Polsky, Yu. Koltypin, and A. Gedanken, *J. Am. Chem. Soc.*, 1999, **121**, 10 047.
170. W.R. Moser, B.J. Marshik, J. Kingsley, M. Lemberger, R. Willette, A. Chan, J.E. Sunstrom IV, and A. Boye, *J. Mater. Res.*, 1995, **10**, 2322.
171. T. Prozorov, R. Prozorov, Yu. Koltypin, I. Felner, and A. Gedanken, *J. Phys. Chem., B*, 1998, **102**, 10 165.
172. C.L. Bianchi, R. Carli, S. Lanzani, D. Lorenzetti, C. Vergani, and V. Ragaini, *Ultrasonics Sonochemistry*, 1994, **1**, S47–49.
173. C.L. Bianchi, R. Carli, C. Fontaneto and V. Ragaini, *Preparation of Catalysts VI*, C. Poncelet (ed.), Elsevier Science, Amsterdam, 1995, 1095.
174. R. Giannantonio, V. Ragaini, and P. Magni, *J. Catal.*, 1994, **146**, 103–115.
175. V. Ragaini, R. Ciannantonio, P. Magni, L. Lucarelli, and C. Leofanti, *J. Catal.*, 1994, **146**, 116–125.
176. Z. Zhong, Y. Mastai, Y. Zhao, Yu. Koltypin, and A. Gedanken, *J. Mater. Chem.*, 1999, **11**, 2350.
177. A. Patra, E. Sominska, S. Ramesh, Yu. Koltypin, Z. Zhong, H. Minti, R. Reisfeld, and A. Gedanken, *J. Phys. Chem., B*, 1999, **103**, 3361.

4

Sonochemistry in Environmental Protection and Remediation

4.1

Introduction

Research into the use of ultrasound in environmental protection has received a considerable amount of attention with the majority of investigations focusing on the harnessing of cavitation effects for the destruction of biological and chemical pollutants in water. The field is not restricted to these two topics however, it is much broader (Tab. 4.1), and in this chapter we will review several aspects in addition to the decontamination of water

Tab. 4.1. General uses of ultrasound in environmental protection.

Water treatment	Biocidal action
	<ul style="list-style-type: none">• direct mechanical action e.g. cell rupture and the break-up of bacterial clumps• indirect mechanical action e.g. increased cell permeability to bactericide
	Removal of chemical contamination
	<ul style="list-style-type: none">• direct oxidation of chemical and pesticide residues• in combination with other techniques e.g. ozonation, uv light
Efficient surface cleaning	Removal of surface contamination and biofilms
Washing of soils	Removal of organic and inorganic contamination
Control of air-borne contamination	Agglomeration of smokes and aerosols
	Defoaming of liquids
Sewage treatment	Stabilisation and dewatering of sludge

4.2

Water Purification

4.2.1

Biological Decontamination

Water treatment can be broadly divided into two types, wastewater and potable (drinking) water. Sewage treatment plants deal with the treatment of wastewater which consists of sewage, road and agricultural surface run-offs as well as industrial effluent. Potable water treatment produces the final product for human consumption. Primary treatment processes are able to reduce the number of microorganisms in water but they can never ensure complete removal and so final disinfection (polishing) is perhaps the most important stage of water treatment. In Europe and U.S.A. chlorination is widely used but there are problems associated with using this method, these include:

- Microorganisms (especially bacteria) are capable of producing strains which are tolerant to normal chlorine treatment levels. This can be overcome by employing higher chlorine levels; however, this can lead to the formation of unpleasant flavours and odours due to the formation of chlorophenols and other halocarbons.
- Certain species of microorganisms produce colonies and spores which agglomerate in spherical or large clusters. Chlorination of such clusters may destroy microorganisms on the surface leaving the innermost organisms intact.
- Fine particles such as clays are normally removed by flocculation using chemicals such as aluminium sulphate. The flocs can entrap bacteria and their spores protecting them from chlorination. The vast majority of floc particles are removed during processing but if one or two pass through the system the entrapped bacteria will be unaffected by the final disinfection stage.

4.2.1.1 The Mechanisms of Ultrasonic Action on Cellular Material

In the 1960's research was targeted at understanding the mechanism of ultrasound interaction with microbial cells [1]. Cavitation phenomena and associated shear disruption, localised heating and free radical formation were found to be primary causes. By 1975, it was shown that brief exposure to ultrasound caused a thinning of cell walls attributed to the freeing of the cytoplasm membrane from the cell wall [2]. The types of apparatus used for this purpose were acoustic horn (probe) systems operating at 20 kHz. These were the forerunners of the modern acoustic horns routinely used for the sonication of cell suspensions in order to release their contents without at the same time destroying or denaturing them. Several theories have been proposed

to describe the mechanism of cell damage through exposure to ultrasound, some physical or mechanical and others more chemical in nature. All of them have their origin in cavitation.

The mechanical effects of power ultrasound on chemical systems in a liquid medium are mainly attributed to cavitation and these same forces have a dramatic effect on biological systems [3]. The imploding bubble produces high shear forces and liquid jets in the solvent that may also have sufficient energy to physically damage the cell wall/membrane. Mechanical effects of this type have been used on a small scale for the disinfection of water contaminated with microbial spores e.g. *cryptosporidium* although the acoustic energy required is high [4]. Such collapse will also produce free radical species which are also capable of killing microorganisms.

On the other hand stable cavitation (bubbles that oscillate in a regular fashion for many acoustic cycles) induce microstreaming in the surrounding liquid which can also induce stress in any microbiological species present [5]. This type of cavitation may well be important in a range of applications of ultrasound to biotechnology [6]. An important consequence of the fluid micro-convection induced by bubble collapse is a sharp increase in the mass transfer at liquid-solid interfaces. In microbiology there are two zones where this ultrasonic enhancement of mass transfer will be important. The first is at the membrane and/or cellular wall and the second is in the cytosol i.e. the liquid present inside the cell.

Most ultrasonic experiments are carried out in temperature controlled systems to ensure that isothermal conditions are maintained. Even a small general increase in microbial temperature can influence both the active and passive transport systems of the cell membrane/wall and this in turn may lead to an increased uptake of compounds. If the temperature is not controlled then sonication could result in a large temperature increase which will lead to the denaturation (deactivation) of enzymes, proteins and other cellular components present within the microorganism [7].

The effects of ultrasound upon the permeability of the cell walls of the gram-negative bacteria *Pseudomonas aeruginosa* toward hydrophobic compounds particularly antibiotics have been examined [8]. The penetration and distribution of 16-dosylstearic acid (16-DS) in the cell membranes of the bacteria was quantified by a spin-labeling electron spin resonance (ESR) method. The results indicated that the intracellular concentration of 16-DS was higher in insonated cells and increased linearly with the sonication power. ESR spectra indicated that ultrasound enhanced the penetration of 16-DS into the structurally stronger sites of the inner and outer cell membranes. The effect of ultrasound on the cell membranes was transient in that the initial membrane permeability was restored upon termination of the ultrasound treatment. These results suggested that the resistance of gram-negative bacteria to the action of hydrophobic antibiotics was caused by a low permeability of the outer cell membranes and that this resistance may be reduced by the simultaneous application of antibiotic and ultrasound.

At an appropriate intensity level of ultrasound, intracellular microstreaming has been observed inside animal and plant cells with rotation of organelles and eddying motions in vacuoles of plant cells [9]. These effects can produce an increase in the metabolic functions of the cell that could be of use in both biotechnology and microbiology, especially in the areas of biodegradation and fermentation.

Cavitation induced in any liquid system will result in the formation of radicals (see Section 4.2.2). In the case of water sonication one chemical product is hydrogen peroxide which, together with the radical species provides a powerful bactericide and oxidant.

4.2.1.2 Ultrasonic Destruction of Biological Contaminants in Water

In order to achieve complete destruction of biological contaminants in water through sonication very high ultrasonic intensities are necessary. Unfortunately this makes the technique expensive to use for general microbiological decontamination. However over the last two decades some conventional disinfection techniques involving chemicals, ultraviolet light and heat treatment have become less effective as some bacteria become more resistant. Such processes have become a focus for the use of sonication as an adjunct to other techniques.

Low power ultrasound offers the possibility of enhancing the effects of chlorine. The results of a study of the combined effect of low power ultrasound and chlorination on the bacterial population of raw stream water are shown (Tab. 4.2). Neither chlorination alone nor sonication alone was able to completely destroy the bacteria present. When sonication is combined with chlorination however the biocidal action is significantly improved [10]. The effect can be ascribed partly to the break-up and dispersion of bacterial clumps and flocs which render the individual bacteria more susceptible to chemical attack. In addition cavitation induced damage to bacterial cell walls will allow easier penetration of the biocide.

A continuing problem in water treatment is the occurrence of algal blooms. Algae may be killed relatively easily on exposure to ultrasound and a lightly “polluted” system

Tab. 4.2. The effect of ultrasound and chlorination on bacterial growth.

Treatment	% Bacteria kill	
	after 5 min	after 20 min
No treatment	0	0
Chlorine, 1 ppm	43	86
Ultrasound alone	19	49
Ultrasound in the presence of 1 ppm chlorine	86	100

Conditions: 1:10 dilution of raw stream water, using ultrasonic bath (power input to system = 0.6 W cm^{-2}), $T = 20^\circ\text{C}$.

provides very little attenuation to sound transmission. In such cases it is possible to use high frequency ultrasound which can be operated at low power. High frequency ultrasound has been shown to give high radical activity at the interface between liquids and gases (as shown through sonoluminescence measurement). Logically then if a large number of small bubbles were introduced into a field of high frequency ultrasound there would be a very large gas/liquid surface area for cavitation activity and the bubbles themselves should also provide “seeds” for cavitation events. This is the basis of an approach to algae removal and control proposed by the Belgian company Undatim [11]. In a trial involving the monocellular algae species *Scenedesmus Capricornutum* some spectacular results were obtained. A cell was constructed to treat water at a rate of $2 \text{ m}^3 \text{ h}^{-1}$ using an acoustic power of 450 W. At a temperature of 25°C a single pass through the cell of a deep green, highly concentrated, solution of the algae containing some 4×10^6 algal cells per cm^3 reduced the recovery threshold of the microorganism by some 60%. This indicates that the treatment even operating at algal concentrations that are far higher than might be encountered in normal treatments offers the potential not only to kill the microorganism but also to severely restrict its reproductive ability.

This ultrasonic anti-algae methodology has been combined with an electromagnetic anti-scaling treatment to provide a new global water remediation technology for half-closed circuits, e. g. cooling towers, known as Sonoxide [12]. This process tackles two major problems of cooling circuits, namely the build up of scale and algae. These are solved with a minimal energy requirement, without the need to use soft water and without the addition of chemicals.

Many microorganisms have the ability to form resistant and dormant structures when subjected to a stress which are known as either spores or cysts. Spore production is a phenomenon amongst some species of microorganisms. Spores have two functions (a) as an agent for dispersal of the organism and (b) as a method for its survival during adverse conditions. Fungal spores are abundant in the foam of rivers and streams through which they are dispersed. To ensure spore survival they must be more resistant to adverse conditions than their parent cell to ensure dormancy occurs after its formation. Some spores have a very long life e. g. *anthrax* spores in the soil can live for over 50 years. The bacterial endospore literally represents suspended animation, and can germinate when conditions for growth are ideal. The endospores of *Bacillus* and *Clostridium* species are of extreme importance to man; for example *Bacillus thermophilus* spores are only destroyed by heating at 100°C for 4 h. Spores possess a great resistance to desiccation (removal of water from cell), ultraviolet light, chemical and enzymatic attack. It is obvious therefore that any water treatment techniques should not only be able to destroy microorganisms but also be able to destroy or remove any of the much more difficult to kill spores which might be present.

The protozoa, *Cryptosporidium parvum*, is the cause of a water-borne disease called cryptosporidiosis which causes severe upset of the digestive system in humans and which can be particularly serious in young children and the elderly. Many cases have been reported in the last decade. Outbreaks have occurred throughout Europe as well as the USA and are not only associated with the developing countries. The main concern of water suppliers is that conventional treatment methods are inadequate and are not a sufficient barrier in preventing the water-borne transmission of cryptosporidiosis. *Cryptosporidium parvum* forms spores known as oocysts which have a very thick outer wall. This prevents or makes it very difficult for normal disinfectants to penetrate into the oocyst. The most commonly used disinfectant techniques in water treatment i.e. chlorination and ultraviolet light are ineffective but ozone seems to be able to destroy some of these oocysts. The use of ultrasound as an aid for the disinfection of water contaminated with *cryptosporidium* oocysts has been evaluated at Coventry University [13]. It was found that sonication reduced the number of oocysts by 25 % in 2 min. And more importantly the proportion of oocysts rendered non-viable increases with duration of sonication. Similar work has been carried out by Leeds University in conjunction with Biwater and their findings have been released as part of a patent [4]. It is however clear that the power required for the complete removal of oocysts in mains water treatment will be extremely high.

Although the predominant efforts in biological decontamination has been aimed at water treatment, sonication has also been investigated in food sterilisation. Heat treatment is one of the most frequently used methods for stabilising foods because of its ability to inactivate enzymes and destroy microorganisms. However, since heat can also alter many organoleptic properties and diminish the content or availability of some nutrients, there is a growing interest in searching for methods that are able to stabilise foods with little or no heat added. The first report on the synergy between ultrasound and heat as a mechanism for killing the vegetative bacterium *Staphylococcus aureus* was published by a Spanish group [14]. They found that the use of power ultrasound allowed a reduction in the effective temperatures at which sterilisation could be achieved. Thermosonication is the term now given to the combined application of heat and ultrasound and it was found to reduce the concentration of *Bacillus subtilis* spores by up to 99.9 % in the 70 to 90 °C range in a small scale ultrasonic reactor using a 20 kHz, 150 W ultrasound source [15]. Work carried out at Coventry University has addressed the issues of the effect of the food substrate (orange juice, milk and rice pudding) on the thermosonication phenomenon using a range of organisms (*Zygoillus polymyxa*) [16]. The studies confirmed the synergistic effect of ultrasound and heat thus in milk, the heat resistance (*D* value) of *L monocytogenes* was approx. 6-fold lower at 60 °C when sonicated at 20 kHz and the *D* value of *Z. bailii* in orange juice was approx. 10-fold lower at 55 °C when sonicated at 38 kHz.

Similar results were obtained in a study of the combined effect of ultrasound (20 kHz) and heat treatment on the survival of two strains of *Bacillus subtilis* in distilled water, glycerol and milk [17]. When spores, suspended in water or milk, were subjected to ultrasonic waves before heat treatment little or no decrease of the heat resistance was observed. However when heat and ultrasound were applied simultaneously the heat treatment times in milk were reduced by 74 % for *B. subtilis* var, niger-40 and by 63 % for *B. subtilis* var, ATCC 6051 and similar results were obtained in glycerol. Thermosonication in water was more marked reducing the heat resistance of the spores by up to 99.9 % in the 70–95 °C range. The effect of thermosonication was slightly diminished to 75 % as the temperature reached the boiling point of water.

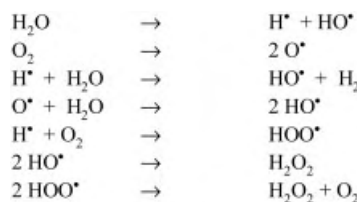
4.2.2

Chemical Decontamination

Ultrasonic irradiation has also been employed for chemical remediation of water but the mode of sonochemical degradation of organic compounds in aqueous solution depends upon their physical and chemical properties. This is because there are two ways in which the cavitation bubble can function. In the case of volatile chemicals which enter the bubble, destruction occurs through the extreme conditions generated on collapse. In the case of chemicals remaining in the aqueous phase the bubble acts as a source of radicals (H^\bullet , HO^\bullet and HOO^\bullet) which enter the bulk solution and react with pollutants.

4.2.2.1 The Sonication of Water

If an aqueous solution saturated with oxygen is sonicated hydrogen peroxide formation occurs. This is due to hydroxyl (OH^\bullet) and hydroperoxyl (HO_2^\bullet) radical recombination outside the cavitation bubble (Scheme 4.1). These radicals result from H_2O and O_2 homolytic cleavage inside the bubble and have been observed by spin trapping experiments (Scheme 4.1) [19].



Scheme 4.1. Mechanisms involved in the sonochemical decomposition of water.

When sonication is carried out in air saturated medium the formation of H_2O_2 is accompanied by the generation of nitrous and nitrate ions. These species originate from the oxidation of molecular nitrogen with HO^\bullet and O^\bullet inside the bubble [20, 21]. During the first stages of the treatment H_2O_2 and NO_2 build up simultaneously. As the reaction progresses, the rate of H_2O_2 production decreases and nitrite ions appear with a concentration that increases at the expense of that of nitrous ions. This suggests that H_2O_2 and NO_2^- are the primary products of sonication of air-equilibrated water and that the NO_3^- results from the oxidation of NO_2^- by hydrogen peroxide. The nitrogen containing species are however unlikely to be major participants in sonochemically induced organic oxidations.

4.2.2.2 The Effect of Ultrasound Alone

The majority of systems studied have been aqueous solutions of either aromatic compounds or halogenated hydrocarbons. Such materials represent models for the major classes of organic pollutants in waste and ground water. The primary products resulting from the sonochemical treatment of phenol at 541 kHz (27 °C with bubbled air) are hydroquinone and catechol [22]. These compounds are easy to monitor and are clearly seen to be intermediates which disappear as the reaction progresses (Fig. 4.1). Similarly the sonolysis of aqueous 4-chlorophenol leads to products mainly characteristic of oxidation by $^\bullet\text{OH}$ radical e.g. 4-chlorocatechol but in both cases the final organic products are CO , CO_2 and HCOOH (Scheme 4.2) [22–25].

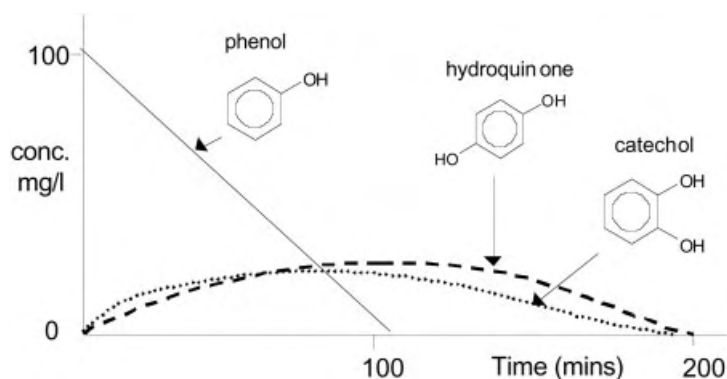
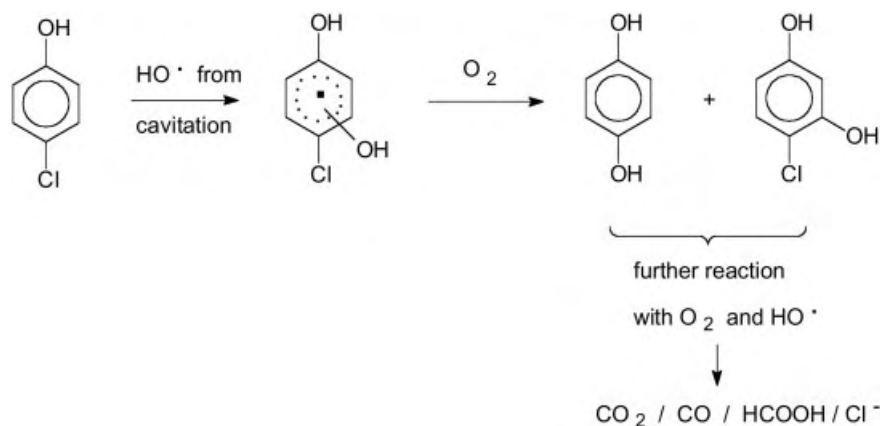


Fig. 4.1. Sonochemical decomposition of phenol in aerated water.



Scheme 4.2. Sonochemical decomposition of 4-chlorophenol in aerated water.

After an irradiation time of 300 min, (500 kHz, 30 W, 20 °C) the hydroxylated intermediates disappear and the chlorine atoms are completely mineralised to chloride ions. The concentrations of the final products (CO and CO_2) rise slowly and after 400 min they represent 21 % when starting with chlorophenol and 18 % when starting with phenol. These results are in agreement with previous studies in which it was demonstrated that “the sonochemical reactivity” of an organic compound is related to its vapor pressure and hydrophobicity. [26, 27]. These studies have been extended to the destruction of a number of chloroaromatics [25] (Tab. 4.3).

In general chloroaromatic hydrocarbons decompose faster than the more hydrophilic compounds such as phenols. The destruction of these two kinds of pollutants occurs at different sites in or around the cavitation bubble and follows different pathways. The difference becomes even more pronounced when more volatile contaminants are used.

Tab. 4.3. Initial concentration and chloride yield after 150 min irradiation for the degradation of chloroaromatics.

Chloroaromatic compound	Concentration [mM]	Yield of Cl^- [%]
1,2-Dichlorobenzene	0.4	90
1,3-Dichlorobenzene	0.05	89
1,4-Dichlorobenzene	0.2	95
1,3,5-Trichlorobenzene	0.02	95
1-Chloronaphthalene	0.04	98

Volume treated: 250 cm³, ultrasonic power: 30 W, electric power: 50 W, frequency 500 kHz.

Tab. 4.4. Comparison between H_2O_2 production and the rates of phenol and carbon tetrachloride disappearance at different frequencies ($\mu\text{M min}^{-1}$)

Frequency [kHz]	20	200	500	800
H_2O_2 formation	0.7	5.0	2.1	1.4
Phenol degradation	0.5	4.9	1.9	1.0
CCl_4 degradation	19	33	37	50

This is neatly illustrated in a comparative study of the decomposition of phenol (to carboxylic acids) and carbon tetrachloride (to CO_2 and Cl^-) in water saturated with oxygen at different frequencies (Tab. 4.4) [28]. The results clearly show a difference in the behaviour of the chemical contaminants (original concentration 10^{-3} M) with the phenol degradation mirroring the peroxide formation indicating this reaction proceeding at the bubble interface or outside of the bubble. The volatile CCl_4 however is decomposed within the bubble and increased frequency slightly accelerates the process. An intriguing calculation for these reactions shows that the efficiency for each of these processes over one ultrasonic cycle decreases as frequency increases.

The occurrence of an optimum frequency at 200 kHz was explained through a two step reaction pathway. In the first step water sonolysis produces radicals within the bubble. In step two the radicals must migrate to the bubble interface or into the bulk aqueous medium to form peroxide or react with the phenolic substrate. The authors suggest that the lower frequencies are the most efficient for the decomposition of molecules inside the bubble but a proportion of the radicals recombine inside the bubble at high temperature to form water thereby reducing the overall yield of H_2O_2 (Eqs. 4.1 and 4.2).



As the frequency increases the pulsation and collapse of the bubble occurs more rapidly and more radicals escape from the bubble. However as the frequency increases the cavitation intensity decreases and this reduces the yield of radicals and consequently the number which reach the interface and bulk solution.

A study of sonochemical treatment of chlorinated hydrocarbons in water demonstrated the homogeneous destruction of CH_2Cl_2 , CCl_4 , MeCCl_3 , and $\text{ClCH}=\text{CCl}_2$ in solution at concentrations of 100–1000 ppm by volume [29]. The method appears to be potentially quite powerful for the purification of contaminated water. In a separate study when saturated aqueous solutions of CH_2Cl_2 (110 ppm) and MeCCl_3 (1300 ppm) were sonicated for 20 min some 75 % of the contaminant was degraded [30].

4.2.2.3 Combined Application of Ultrasound with Ozone

Advanced oxidation processes (AOPs) are a range of water treatments which involve the *in situ* formation of radicals, particularly hydroxyl radicals, in sufficient quantity to affect chemical or biological contaminants. These include ultrasonic and ultraviolet irradiation but they are sometimes ineffective for the remediation of water which contains a mixture of organic and inorganic compounds. Chemical oxidants can be used to add additional oxidising power to such processes and ozone in conjunction with ultrasound is one such option [31].

Ozone (O_3) is a very strong oxidant which can oxidise organic compounds to carbon dioxide and water but the reaction rates for many pollutants are slow. Nevertheless ozone has been used at water and wastewater treatment plants in a variety of applications [32].

The combination of sonication and ozonation provides three sources of OH^\bullet [33]:

1. from sonochemical decomposition of water
2. from the normal chemical degradation of ozone
3. from the thermolytic decomposition of ozone in the acoustic cavitation bubble.

Studies of the combined process involving ultrasound and ozone have shown faster degradation rates for a range of chemical contaminants than either method applied alone. Sonolytic ozonation has also been found effective for the disinfection of water but in these cases sonication also has a number of direct effects on the bacteria and viruses (see above).

An environmental problem which has existed for a long time has been the removal of colour from the effluent streams of textile factories since the presence of residual dyes is rather obvious even at low dilutions. There are several conventional approaches to the solution of this problem including absorption onto activated charcoal, flocculation, chemical oxidation, ozonolysis and irradiation with UV light. Sonication can be added to any of these and the combination of ultrasound with ozonolysis seems particularly efficient. A sonic processor operating at 430 Hz (i. e. within the normal hearing range of frequencies) has been used to study the pilot scale decolourisation of dyes using ozone. The device operates at 20 kW with a 3.2 L flow reactor supplied with ozone from a laboratory scale generator. [34]. The study demonstrated that water soluble textile dyes can be destroyed and decolorised by low frequency sonication combined with ozonation. Basic, acid, direct and even some disperse dyes, which tend to have low solubility, were all rapidly decolorised. For most of the dyes the toxicity of the decolorised dye to microorganisms was the same as, or less than, the dye solution. This would make them suitable for further treatment on site or for immediate discharge to a publicly operated treatment plant. The amount of ozone required ranged from 1.1 to 1.9 kg of ozone per kg of dye. The rate of dye destruction was about twenty times faster

than a simple mechanically stirred gas to liquid mixer. The rate is sufficiently large for short residence times of less than 60 s to be possible in a continuous flow process with industrial ozonisers and for dye concentrations within the range typical of wastewater from textile dyeing plants.

4.2.2.4 Combined Application of Ultrasound with Ultraviolet Light

There are a few reports on the combined application of ultrasound and ultraviolet light (UV) for the destruction of chemical pollutants. A study of the oxidation of humic acid and trihalomethane precursors with ozone revealed that the most effective destruction of the organic carbon compounds was achieved when both uv and ultrasound were used in combination with ozonation [35]. In other cases e. g. the removal of 1,1,1-trichloroethane from aqueous solutions, the combined application of ultrasound and UV proved to be more efficient than the use of either technique individually [36].

Photochemical decomposition can also be carried out in the presence of a suspension of photoactive material such as TiO_2 where substrate absorption onto the uv activated surface can initiate chemical reactions e. g. the oxidation of sulphides to sulphones and sulphoxides [37]. This technology has been adapted to the destruction of polychlorobiphenyls (PCB's) in wastewater and is of considerable interest in environmental protection. Using pentachlorophenol as a model substrate in the presence of 0.2% TiO_2 uv irradiation is relatively efficient in dechlorination (Tab. 4.5) [38]. When ultrasound is used in conjunction with photolysis, dechlorination is dramatically improved. This improvement is the result of three mechanical effects of sonochemistry namely surface cleaning, particle size reduction and increased mass transport to the powder surface.

A similar combination of ultrasound and photocatalysis has also been reported to destroy 2,4,6-trichlorophenol in aqueous solution [39]. An ultrasonic probe (22 kHz) with a uv light source (15 W) was used to examine the effect of changing such operating conditions as ultrasonic intensity, reaction temperature and uv transmission. The experiments involved using 2,4,6-trichlorophenol (100 ppm) and TiO_2 (0.1 g L^{-1}) and showed that the degradation rates increased with the temperature of the solution. The cumulative effect was more pronounced at lower ultrasonic intensities with little additional benefit derived at increased ultrasonic powers.

4.2.2.5 Combined Application of Ultrasound with Electrochemistry

The advantages of using ultrasound in the electrochemistry of organic compounds has been reviewed elsewhere [40]. The combination has been found to be particularly useful in the destruction of chemical pollutants. It has been applied to the destruction of phenols by electrochemical oxidation. Ultrasound (25 kHz , 10^4 W m^{-2}) when applied

Tab. 4.5. Photolysis of aqueous pentachlorophenol (2.4×10^{-4} M) containing 0.2 % TiO_2 .

Treatment	Yield of Cl^-	
	after 50 min	after 120 min
UV irradiation alone	40 %	no change
UV irradiation together with sonication	60 %	quantitative

to a solution containing phenol (100 g L^{-1}) and NaCl (2 g L^{-1}) achieves better than 80 % oxidation to maleic acid. In the absence of ultrasound only 50 % decomposition was obtained under the same conditions. An almost complete sonoelectrochemical destruction of phenol can be achieved in saline solution (0.5 g L^{-1} NaCl) at pH 6 [41]. The cell operated at 1 amp using a nickel mesh cathode (area $115 \times 10^{-4} \text{ m}^2$) and a platinum mesh anode (area $47 \times 10^{-4} \text{ m}^2$) and complete destruction of the phenol was achieved within 20 min at 25°C (Fig. 4.2). The reaction was shown to proceed *via* intermediate chlorinated phenols.

Sonoelectrochemical destruction of dyes has also been investigated. Solutions of the acidic dye Sandolan Yellow have been decolourised by a sonoelectrochemical process in aqueous saline solution using platinum electrodes [42]. The process entails the electrolysis of aqueous NaCl solution which involves the liberation of chlorine at the anode and hydroxide ion at the cathode. The overall cell reaction is:



The rate of electrochemical decolourisation in the absence of ultrasound was dependent on the electrolyte concentration, reaction temperature and the current density.

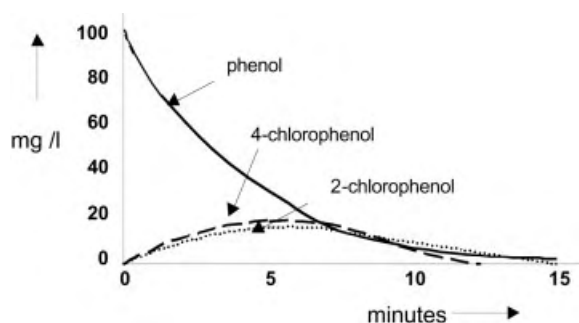


Fig. 4.2. Sonoelectrochemical destruction of phenol in saline solution (500 kHz, 1 A, 7 V).

The rate was enhanced using ultrasound when carried out in a semi-sealed cell, which minimised the effects of ultrasonic degassing. An optimum acoustic power was found when using a source at a frequency of 20 kHz.

4.3

Surface Decontamination

The use of power ultrasound for surface cleaning, is a long-established and efficient technology. Ultrasound is particularly effective in this type of decontamination because the cleaning action is induced by cavitation collapse on and near surfaces which will dislodge bacteria adhering to them. The particular advantage of ultrasonic cleaning in this context is that it can reach crevices which are not easily reached by conventional cleaning methods. Objects for cleaning can range from large crates used for food packaging and transportation to delicate surgical implements such as endoscopes. This was recognised some years ago, see for example a general patent that relates to the use of ultrasound as a method of pasteurisation, sterilisation and decontamination of instruments and surfaces used within the medical, surgical, dental and food processing industries [43].

The removal of bacteria from various surfaces is of particular importance to the food industry and can be efficiently accomplished with the combined use of sonicated hot water containing biocidal detergents [44]. The core of most ultrasonic cleaning systems is a heated stainless steel tank which contains a number of ultrasonic transducers and a dilute detergent/sterilising solution. The items to be cleaned are passed through the tank and subjected to the ultrasound as they pass in front of the transducers. In the case of a poultry processing factory the cleaning is expected to remove fat, blood, skin, meat and lime scale and sterilise the surface of the item. There has to be a balance struck between the tank temperature in terms of solubilising the contaminants (a detergent is invariably used) and the dependence of ultrasonically induced cavitation on temperature. In general a higher temperature will result in a lower gas solubility in the medium. As a consequence there will be a reduction in the number of cavitation bubbles. In fact every solvent has its own cavitation behaviour with respect to the temperature and for water the maximum efficiency for cavitation is obtained at 35 °C [45]. For cleaning the optimum temperature range is generally considered to be about 65–70 °C.

Chemicals such as chlorine are often used to clean and decontaminate food products and food processing surfaces. The increased effectiveness of ultrasound in combination with chlorine in decontaminating broiler breast skin inoculated with *Salmonella* has been investigated [46]. The mechanism suggested involved the release of *Salmonella* cells from the skin by sonication together with the improved penetration of chlorine into the cells through the action of ultrasound (see above).

A synergistic effect has been reported in biocidal action between ultrasound and various antibiotics at levels and concentrations which individually did not themselves reduce bacteria viability [47]. This synergy reduced the viability by several orders of magnitude for cultures of *Pseudomonas aeruginosa*, *Escherichia coli*, *Staphylococcus epidermidis* and *Staphylococcus aureus*. Measurements of the bactericidal activity of gentamicin against *P. aeruginosa* and *E. coli* demonstrated that simultaneous application of 67 kHz ultrasound enhanced the effectiveness of the antibiotic. As the age of these cultures increased, the bacteria became more resistant to the effect of the antibiotic alone and the application of ultrasound appeared to reverse this resistance. The ultrasonic treatment-enhanced activity was not observed with cultures of gram-positive *S. epidermidis* and *S. aureus*. These results may have application in the treatment of bacterial biofilm infections on implant devices, where sequestered bacteria are usually more resistant to antibiotic therapy. Synergistic killing was observed to be a function of ultrasonic intensity [48]. Greatest killing (approx. 5 log reduction in viable population) was realised at full intensity (4.5 W cm^{-2}), and decreased with reductions in power density. At the lowest intensity used (10 mW cm^{-2}) there was no significant evidence of acoustically enhanced killing.

An *in vitro* investigation into the bactericidal effects of a dental ultrasonic scaler on bacterial biofilms using *Actinobacillus actinomycetemcomitans* and *Porphyromonas gingivalis* has been reported [49]. Suspensions of the bacteria were subjected to the vibrations of a Cavitron P1 insert for 2.5 and 5.0 min in an acoustically-simulated model substrate. A 60 % kill rate was achieved at a temperature of around 50°C which constituted an alternative treatment for bacterial biofilms. This study suggested that a similar approach could be used in the clean-up of a range of biofilms considered to be the cause of a range of environmental hazards.

4.4

Decontamination of Soil

Power ultrasound can be used for the rehabilitation of industrial sites or the reclamation of polluted land by the removal of chemical and biological contamination from soil. There are two basic mechanisms through which this can occur either via the removal of contaminated material from the surface of soil particles or the leaching out of more deeply entrenched materials.

4.4.1

Surface Cleaning of Particles

Many conventional soil washing processes are based on the principle that pollutants adsorb onto very small particles “fine fractions” of the soil such as silt, clay and humic matter which tend to be attached to coarser sand and gravel particles. These larger particles make up the majority of the soil content. A primary aim in soil washing is therefore to dislodge and separate these fine components from the bulk soil. If the pollutant materials can be detached from the bulk, possibly together with some other surface contamination, a “concentrated” volume of polluted soil can be produced. This can then be treated or disposed of, and a large volume of residual soil which requires relatively little treatment and can be returned to the site as back fill.

A comparison has been made of the efficiencies of conventional and ultrasonically assisted pollutant extraction procedures using model soil samples (granular pieces of brick) which had been deliberately contaminated with copper oxide at 51 ppm [50]. Analysis of the brick particles after 30 min sonication on a Vibrating Tray™ [51] revealed an average reduction in copper content to 31 ppm, a reduction of about 40 %. Using a conventional mechanically shaken tray for the same time period the residual contamination was 48 ppm representing a reduction of only 6 % (Tab. 4.6).

The Vibrating Tray has been used to enhance the clean-up of soil contaminated with PCB's (Fig. 4.3).

Tab. 4.6. Ultrasonic washing of brick particles.

Washing with conventional mechanical shaker			
Brick remaining after washing	Particulate material < 20 mesh	Fines	Aqueous wash
746.5 g	2.9 g	0.63 g	12.6 L
(48 ppm Cu)	(310 ppm Cu)	(3200 ppm Cu)	(0.22 ppm Cu)
Total reduction in copper contamination in treated brick = 6 %			
Washing with ultrasonic Vibrating Tray™			
Brick remaining after washing	Particulate material < 20 mesh	Fines	Aqueous wash
744.7 g	3.4 g	1.89 g	13.5 L
(31 ppm Cu)	(96 ppm Cu)	(4700 ppm Cu)	(0.49 ppm Cu)
Total reduction in copper contamination in treated brick = 40 %			
Initial mass of brick 750 g, copper contamination 51.4 ppm			

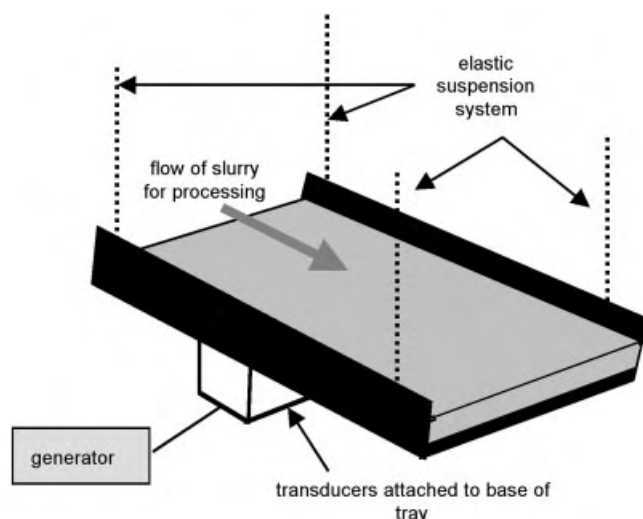


Fig. 4.3. Ultrasonic soil washing, pilot scale equipment giving a 15 % improvement in PCB extraction using a Vibrating Tray™.

4.4.2

Leaching of Pollutants from within Particles

Any improvement in the penetration of solvent into particulate matter will result in the enhanced removal of soluble material which may be trapped inside the solid particles. This process is referred to as ultrasonic leaching and has been investigated in hydrometallurgy for the removal of metals from ores [52]. Dramatic increases in leaching rates induced by ultrasonic irradiation have been reported for many ores [53]. For example, ultrasonic irradiation of galena, crocoite and arsenolite, resulted in 20, 30 and 50 times faster rates of dissolution respectively when compared to those in the absence of an ultrasonic field. This is particularly important in cases where high grade ores are no longer available and poorer mineral resources must be used for the extraction of metals.

These investigations into ultrasonic leaching can be extended to the decontamination of different types of soils e.g. landfills, mining spills and river sediments. Batch tests for accelerating leaching using ultrasound on five metal finishing residues of hazardous, radioactive and mixed wastes have been carried out [54] as has the removal of radio nucleotides and heavy metals from soils [55]. The application of ultrasound was found to aid precious metal recovery from waste products including industrial, municipal and mine wastes [56].

Ultrasonically assisted extraction is particularly useful for the environmental analytical chemist because it facilitates a more complete extraction of absorbed chemicals e.g. the extraction of pesticides [57, 58] and of heavy metals from soils [59].

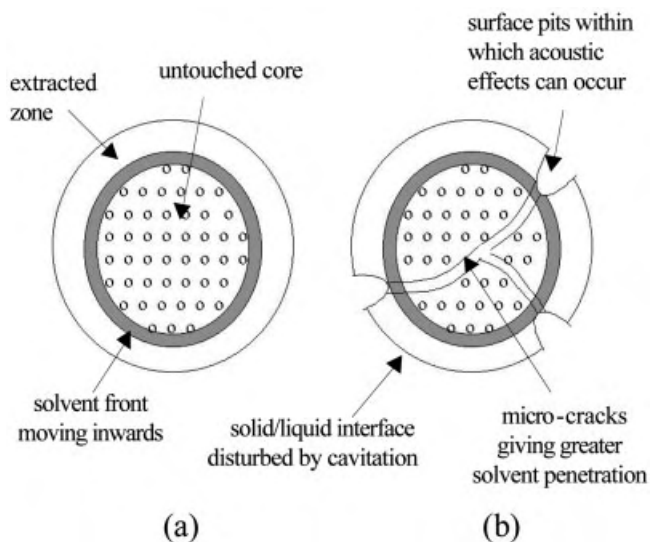


Fig. 4.4. Leaching of contaminants from soil particles; (a) normal leaching; (b) in the presence of ultrasound.

Although there is plenty of experimental evidence that ultrasound improves leaching the exact mechanism is not fully understood. Swamy and Narayana [60] have suggested models for leaching in the presence and absence of ultrasound (Fig. 4.4). Normal leaching takes place as the solvent front moves inwards and a steady state diffusion occurs through the depleted outer region and is equal to the rate of reaction within the reaction zone itself (Fig. 4.4a).

Under the influence of ultrasound, normal leaching occurs but several additional factors contribute towards improvements in the efficiency. These include:

1. Asymmetric cavitation bubble collapse in the vicinity of the solid surface leading to the formation of high speed microjets targeted at the solid surface. The microjets can enhance transport rates and also increase surface area through surface pitting.
2. Particle fragmentation through collisions will increase surface area.
3. Cavitation collapse will generate shock waves which can cause particle cracking through which the leaching agent can enter the interior of particle by capillary action
4. Acoustic streaming leading to the disturbance of the diffusion layer on the surface
5. Diffusion through pores to the reaction zone will be enhanced by the ultrasonic capillary effect.

Thus, ultrasound can improve the leaching rate over the conventional method and the effects of ultrasound are summarised in Fig. 4.4b.

4.5

The Control of Air-Borne Contamination

There are two major problems which arise from exposure to fine particles or small suspended droplets in air. Both have the ability to penetrate deeply through the throat and into the lungs and to initiate infection or block efficient respiratory function.

A simple method of keeping down industrial dust is to generate a fine water spray which agglomerates the fine powdery material and allows it to settle. The conventional method of producing an atomised spray of water is to force it at high velocity through a small aperture, a typical domestic example being a spray mist bottle for perfume. The disadvantage in this design for conventional industrial equipment is that the requirement for a high liquid velocity combined with a small orifice restricts its usage to low viscosity liquids and, as a result, these atomisers are often subject to blockage. To avoid this problem ultrasonic atomising nozzles based on the whistle principle have been developed (Fig. 4.5). Air or gas is used to generate an intense field of ultrasonic oscillation in a resonant chamber. Any liquid which is pumped into this chamber is vigorously sheared into droplets by the acoustic field. Air by-passing the resonator carries the atomised droplets downstream in a soft plume shaped spray. The droplets have low mass and a low forward velocity. Atomised water sprays, produced in this way are ideally suited to dust suppression in industry. They can also be employed as humidifiers for horticultural use under glass.

An alternative approach to dust and mist suppression is the use of acoustic standing waves. When a sonic standing wave is set up in air the particles suspended in the air will migrate to the nodes of the sound wave and this phenomenon has been used in a variety of applications. Smoke particles normally remain suspended in air for a considerable period because of they are extremely light. In an acoustic field they will become concen-

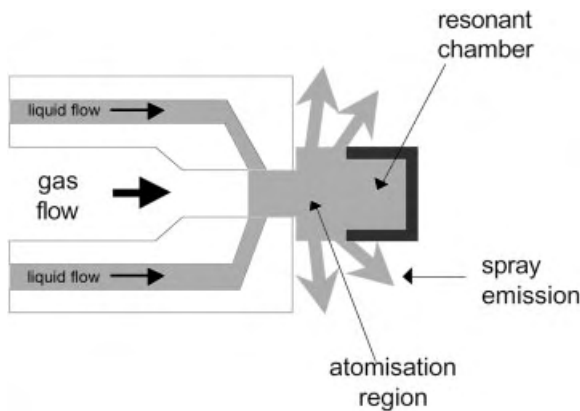


Fig. 4.5. Schematic diagram of a whistle for ultrasonic atomisation.

trated in the nodal zones which will lead to an increased possibility of collision resulting in the formation of larger fragments. As these fragments increase in size through further collisions they will eventually become large enough to fall to the floor of the chamber.

There is however a problem with generating power ultrasound in air because gases are of low density and present a very low specific acoustic impedance and a high acoustic absorption. Therefore, for an efficient generation and transmission of energy it is necessary to develop ultrasonic generators which have good impedance matching with the air, large amplitude of vibration, high directional or focused radiation, and high power capacity. Over the last few years, a new type of sonic and ultrasonic power generator for air-borne ultrasound has been developed [61]. The key to such a device is the design of the radiating plate. The plate is designed as a solid piece of titanium with concentric indentations. These indentations allow the surface to vibrate in a manner which generates planar sound waves into the surrounding air. A flat plate would not be capable of producing such a wave-form.

A semi-industrial pilot plant has been developed in which air-borne ultrasound has been applied to the reduction of particle emissions in coal combustion fumes [62]. The installation basically consists of an acoustic agglomeration chamber with a rectangular cross-section, driven by four high-power and highly directional acoustic transducers operating at 10 and/or 20 kHz, and an electrostatic precipitator (ESP). In the experiments, a fluidised bed coal combustor was used as fume generator with fume flow rates up to about 2000 m³/h, gas temperatures of about 150 °C. and mass concentrations in the range 1–5 g m⁻³. The acoustic filter reduced fine particle emissions by about 40 %.

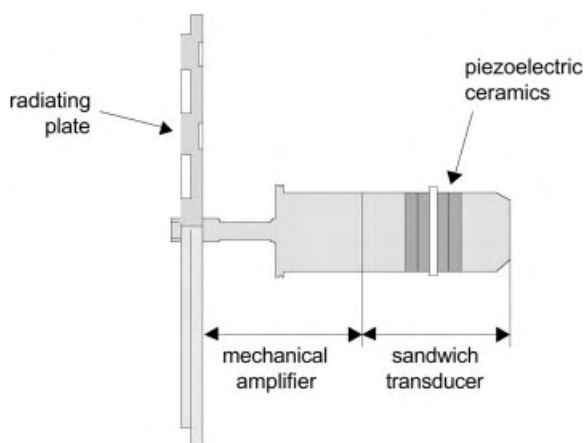


Fig. 4.6. Transducer assembly for the production of high power air-borne ultrasound.

The same airborne ultrasound which can be used to destroy smokes is also capable of defoaming liquids by placing the acoustic source above the liquid surface upon which the foam is being generated. Foam is a dispersion of gas in liquid in which the distances between the individual bubbles are very small. In a foam system the volume ratio of gas to liquid is very great and the bulk density approaches that of a gas. Foams cause, in general, difficulties in process control and in handling equipment. A typical example is in the fermentation industry where foam represents one of the bigger problems. The mechanism of acoustic defoaming which is insufficiently known, may be a combination of a number of factors [63] namely high acoustic pressure, radiation pressure, resonance of the foam bubbles and acoustic streaming. Other factors, such as atomisation from the film surface, may also have influence in this phenomenon.

The potential use of high-intensity sound for defoaming has been known for several decades but only a few acoustic defoamers have been reported in the technical literature. The majority of these defoaming devices were based on aerodynamic acoustic sources of various types such as whistles or rotary sirens. The main difficulties with these systems come from noise problems (they generally work at sonic rather than ultrasonic frequencies), the need for high air generation capacity, the control and sterilisation of the air flow and high energy consumption. An ultrasonic defoamer was developed using the stepped-plate transducer described above to generate airborne ultrasound. In this case there is no air flow required to produce the sound and it is readily sterilisable. It has been successfully applied to the control of excess foam produced on high-speed canning lines and in the dissipation of foams in reactors [64]. In canning lines, the air-borne ultrasonic radiation is focused on the working area where the foam excess is quickly destroyed to avoid liquid losses at a speed of more than 20 cans per second. Two focused transducers working at 20 kHz were used in parallel for an efficient and quick operation, in order to widely cover the can surface with high intensity sound pressure levels (about 165 dB). The power applied to each transducer was only of 150 W. These gives an energy consumption of only of about 5 mW h/can.

Ultrasound has also been successfully used in the suppression of chromic acid mist emission from chromium plating operations plating [65]. The mist arises because of the gases generated at the electrodes during the process. These gases rise to the surface as bubbles which burst and spray fine particles of the plating solution (predominantly chromic acid) into the atmosphere above the surface. The control of chromic acid mist within the electroplating industry is of great concern with respect to the health and safety of the plant operatives. The Health and Safety Executive in the UK suggest that the maximum emission of chrome mist from plating baths should not exceed levels of 0.05 mg m^{-3} . Currently levels are maintained within acceptable limits by the addition of fume suppressants and the removal of the gases and mist from above the surface of

the plating tank by lip extraction. A mist suppressant is a chemical which forms a layer of foam across the surface of the plating bath. This layer then restricts mist formation as the electrolytically generated gases reach the surface. Suppressants will alter the composition and can affect the efficiency of the plating bath whilst extraction must cope with the corrosive affects and disposal of chromic acid in air.

The potential advantage in the use of ultrasound for mist suppression is that it does not involve the addition of chemicals to the plating solution. Sonication is provided from within the bath itself and its efficacy is considered to be associated with ultrasonically induced changes in the type of gas emission (e. g. bubble size) evolved during plating (see 6.3.1). It is known that ultrasound can alter the character of gas emission from electrolytic processes e. g. the degassing of hydrogen from the cathode surface during chromium plating is considered to be an important factor in the properties of the plating [66]. It can also improve the discharge of gases in the electrolysis of hydrochloric acid (22 %) [67]. In this case ultrasound is able to drive almost all of the chlorine from the solution and the system operates with a 3 % increase in current efficiency. In general ultrasound has been shown to have many beneficial effects in electroplating when used within the plating solution [68].

4.6

Treatment of Sewage Sludge

In biological wastewater treatment large quantities of biomass (sludge) are produced. The sludge material will continue to degrade with the evolution of noxious gases under ambient conditions and must be stabilised before it can be used or disposed of. The stabilisation essentially consists of two stages (1) digestion to complete the break-down process [69] (2) dewatering to reduce its bulk [70].

4.6.1

Ultrasonically Assisted Digestion

Anaerobic digestion is the standard stabilisation technique for sludge and results in a reduced content of organic matter. In the European Union 50 % of the municipal sewage sludges are stabilised anaerobically [71]. The slow biological sludge hydrolysis is the rate-limiting step of the anaerobic degradation. Large fermenters are necessary and typical digestion times are 20 or more days. The degree of degradation of organic matter varies between 25 % and 60 %. Reduction of volatile solids (organic matter) is more pronounced in the digestion of primary sludge as compared to digestion of waste activated sludge.

Various methods for process improvement have been explored including thermal pre-treatment, chemical solubilisation by acid or base addition and mechanical sludge disintegration. Mechanical degradation [72] has some similarities to the effects of low frequency ultrasound in that it generates cavitation resulting in sludge disintegration. In the case of power ultrasound the microorganism cell walls are broken and intracellular material is released to the liquid phase. This makes the dissolved organic compounds more readily bioavailable in the anaerobic digestion process and the fermentation rate is greatly improved. Consequently the sludge retention time in the fermenter can be significantly reduced [73]. Using an ultrasonic treatment at a frequency of 31 kHz and high acoustic intensities at half technical scale, the residence time was reduced to eight days with a biogas production over twice as large as that of a control fermenter.

Recent developments in high power transducers now allow the treatment of large amounts of sewage sludge [74, 75]. The principal advantages of the sonochemical method are that it can be automated with no moving parts and involves no added chemicals.

4.6.2

Ultrasonically Assisted Dewatering

The requirement to remove suspensions of solids from liquids is common to many industries. This separation can be either for the production of solids-free liquid or to isolate the solid from its mother liquors. It is the latter process which is important in sewage treatment where the reduction in overall mass is a significant factor. The removal of water from sludge is a slow and difficult process since the water which must be removed is not only trapped between particulate material but is also held within the cellular material itself. A number of add-on techniques have been used to accelerate dewatering methods. One of these is acoustic filtration [76]. An improvement on this method can be achieved with the addition of an electrical potential across the slurry mixture while acoustic filtration is performed [77]. The filter itself is made the cathode while the anode, on the top of the slurry, functions as a source of attraction for the predominantly negatively charged particulate material. An example of its application can be found in the dewatering of coal slurry (50 % moisture content). While conventional filtration reduces the moisture to 40 %, the use of ultrasound improves it to 25 % and using electro-acoustic filtration gives further improvement to 15 %.

References

1. D.E. Hughes and W.L. Nyborg, *Science*, 1962, **138**, 108.
2. H. Alliger, *American Laboratory*, 1975, **10**, 75.
3. G. Scherba, R.M. Weigel, and J.R. O'Brien, *Applied and Environmental Microbiology*, 1991, **573**, 2079.
4. Biwater Treatment Ltd., European Patent 0 567 225 A1 (1993).
5. A.R. Williams, D.A. Stafford, A.G. Calley, and D.E. Hughes, *Journal of Applied Bacteriology*, 1970, **33**, 656.
6. C. Reynolds and C.D. Wills, *Int. J. Radiat. Biol.*, 1974, **25** 113.
7. E.D.P. DeRobertis and E.M.F. DeRobertis, *Cell and Molecular Biology*, Holt-Saunders, Tokyo, 1980.
8. N. Rapoport, A.I. Smirnov, A. Timoshin, A.M. Pratt, and W.G. Pitt, *Archives of Biochem. Biophys.*, 1997, **334**, 114.
9. W.L. Nyborg, *J. Cancer*, 1982, **45**, 156.
10. S.S. Phull, T.J. Mason, J.P. Lorimer, A.P. Newman, and B. Pollet, *Ultrasonics Sonochemistry*, 1997, **4**, 157.
11. Undatim Ultrasonics, Zoning Industriel, Rue de l'Industrie 3, B 1400 Nivelles, Belgium.
12. E. Cordemans and B. Hannecart, World Patent, WO 98/01394 (1998).
13. S.S. Phull, T.J. Mason, and B.C. Cope, CERC Report No. 162, Coventry University, 1996.
14. J.A. Ordóñez, *Journal of Dairy Research*, 1987, **54**, 61.
15. J.A. Ordóñez, B. Sanz, J. Burgos, and M.L. García, *J. Appl. Bacteriology*, 1989, **67**, 619.
16. T.J. Mason, S.S. Phull, G. Betts, and R.G. Earnshaw, Internal Report, Campden and Chorleywood Food Research Association, 1995.
17. R.G. Earnshaw, Ultrasound: a new opportunity for food preservation, *Ultrasound in Food Processing*, M. Povey and T.J. Mason (ed.), Blackie Academic and Professional, 1998, ISBN 0-7514-0429-2.
18. M.L. García, J. Burgos, B. Sanz, and J.A. Ordóñez, *J. Appl. Bacteriology*, 1989, **67**, 619.
19. P. Riesz and T. Kondo, *Free Rad. Biol. Med.*, 1992, **13**, 247.
20. E.J. Hart, C.H. Fischer, and A. Henglein, *J. Chem. Phys.*, 1986, **90**, 5989.
21. E.J. Hart and A. Henglein, *J. Phys. Chem.*, 1986, **90**, 5992.
22. J. Berlan, F. Trabelsi, H. Delmas, A.M. Wilhelm, and J.F. Petrigiani, *Sonochemistry*, 1994, **1**, S97.
23. N. Serpone, R. Terzian, H. Hidaka, and E. Pelizzetti, *J. Phys. Chem.*, 1994, **98**, 2634.
24. C. Pétrier, M.-F. Lamy, A. Francony, A. Benhcene, and B. David, *J. Phys. Chem.*, 1994, **98**, 10 514.
25. C. Petrier and D. Casadonte, The sonochemical degradation of aromatic and chloroaromatic contaminants, *Advances in Sonochemistry*, 6, Theme issue – *Ultrasound in Environmental Protection*, T.J. Mason and Andreas Tiehm (eds.), Elsevier, 2001.
26. A. Henglein and C. Kormann, *Int. J. Radiat. Biol.*, 1985, **48**, 251.
27. C. Von Sonntag, G. Mark, H.P. Schuchmann, J. Von Sonntag, and A. Tauber, *COST Meeting: Chemical Processes and Reactions Under Extreme or Non-Classical Conditions*, COST action D6, 1998, 11-18, ISBN 92-828-1986-8.
28. C. Petrier and A. Francony, *Ultrasonics Sonochemistry*, 1997, **4**, 295.
29. H.M. Cheung, A. Bhatnagar, and G. Jansen, *Environ. Sci. Technol.*, 1991, **25**, 1510.
30. Y. Nagata, Y. Kurosaki, M. Nakagawa, and Y. Maeda, *Chem. Express*, 1993, **8**, 657.

31. L.K. Weavers, Sonolytic ozonation for the remediation of hazardous pollutants, *Advances in Sonochemistry*, 6, Theme issue – *Ultrasound in Environmental Protection*, T.J. Mason and Andreas Tiehm (eds.), Elsevier, 2001.
32. B. Langlais, D.A. Reckhow, and D.R. Brink, *Ozone in Water Treatment Application and Engineering*; AWWA Research Foundation and Lewis Publishers, Chelsea, 1991.
33. L.K. Weavers and M.R. Hoffmann, *Environ. Sci. Technol.*, 1998, **32**, 3941–3947.
34. J.P. Russell and M. Smith, Sonic energy in processing: use of a large scale, low frequency sonic reactor, *Advances in Sonochemistry*, T.J. Mason (ed.), JAI Press, 1999, **5**, 175–208, ISBN 0-7623-0331-X.
35. R.A. Sierka and G.L. Amy, Catalytic effects of ultraviolet light and/or ultrasound on the ozone oxidation of humic acid and trihalomethane precursors, *Ozone Sci. & Eng.*, 1985, **6**, 275–290.
36. M.S. Toy, M.K. Carter, and T.O. Passell, *Environmental Technology*, 1990, **11**, 837.
37. R.S. Davidson and J.E. Pratt, *Tetrahedron Lett.*, 1983, **24**, 5903.
38. Information courtesy of SRI International, 333 Ravenswood Ave., Menlo Park, CA, USA, 1992.
39. I.Z. Shirgaonkar and A.B. Pandit, Sono-photochemical destruction of aqueous solution of 2,4,6-trichlorophenol, *Ultrasonics Sonochemistry*, 1998, **5**, 53–61.
40. D.J. Walton and T.J. Mason, Organic sonoelectrochemistry, *Synthetic Organic Sonochemistry*, J.-L. Luche (ed.), Plenum Press, 1998, 263–297, ISBN 0-306-45916-7.
41. F. Trabelsi *Les ultrason de haute frequence: Etude d'un reacteur, application a la degradation de composes organiques par sonochimie et sonoelectrochimie*, Ph.D. thesis, ENSIGC Toulouse, 1995.
42. J.P. Lorimer, T.J. Mason, M. Plattes, and S.S. Phull, *Ultrasonics Sonochemistry*, 2000, **7**, 237–242.
43. R.M.G. Boucher, US Patent 4 211 744 (1980).
44. T. Quartly-Watson, The importance of power ultrasound in cleaning and disinfection in the poultry industry – a case study, *Ultrasound in Food Processing*, M. Povey and T.J. Mason (eds.), Blackie Academic and Professional, 1998.
45. B. Niemczewski, *Ultrasonics*, 1980, **XXX**, 110.
46. H.S. Lillard, *Journal of Food Protection*, 1993, **56**, 716.
47. W.G. Pitt, Z. Qian, and R.D. Sagers, *Annals of Biomedical Engineering*, 1997, **25**, 69.
48. W.G. Pitt and R.G. Williams, *J. Biomaterial Applications*, 1997, **12**, 20.
49. R. O'Leary, A.M. Sved, E.H. Davies, T.G. Leighton, M. Wilson, and J.B. Kiesser, *Journal of Clinical Periodontology*, 1997, **24**.
50. A.P. Newman, J.P. Lorimer, T.J. Mason, and K.R. Hutt, *Ultrasonics Sonochemistry*, 1997, **4**, 153.
51. Vibrating Tray™ is a product of Lewis Corporation, 102 Willenbrock Road, Oxford, Connecticut 06478-1033, USA.
52. K.L. Narayana, K.M. Swamy, K. Sarveswara Rao, and J.S. Murty, *Min. Proc. Ext. Met. Rev.*, 1997, **16**, 239.
53. P.I. Polyukhin, *The use of ultrasonics in extractive metallurgy*, Techni copy: Stonehouse, UK, 1978, 157 pp (translated from Russian).
54. R.J. Caldwell, J.A. Stegemann, and C.C. Chao, *Stabilization and Solidification of Hazardous, Radio Active and Mixed Wastes*, ASTM Spec. Tech. Publ., STP 1240, 1996, 413–425.
55. M. Misra and R.K. Mehta, *J.O.M.*, vol 47, 1995, Issue 9, pp 45–53.
56. R.S. Steensma, *Application of ultrasonics in the extraction of noble metals. Process metallurgy 5, Precious and Rare Metal Technologies*, A.E. Torma and I.H. Gundiler (eds.), Elsevier, Oxford, 1989, 175–182.

57. S. Babic, M. Petrovic, and M. Kastelan-Macan, *J. Chromatogr.*, 1998, **A823** (1 + 2), 3.
58. J. Evans, R.H. Kaake, M. Orr, and M. Watwood, *J. Soil Contam.*, 1998, **7**, 589.
59. K. Ashley, *Trends Anal. Chem.*, 1998, **17**(6), 366.
60. K.M. Swamy and K.L. Narayana, Ultrasonically assisted leaching, *Advances in Sonochemistry*, 6, Theme issue – *Ultrasound in Environmental Protection*, T.J. Mason and Andreas Tiehm (eds.), Elsevier, 2001.
61. J.A. Gallego-Juárez, G. Rodriguez-Corral, J.L. San Emeterio, and F. Montoya-Vitini, *Electroacoustic unit for generating high sonic and ultrasonic intensities in gases and interphases*, 1989, Spanish Patent 8903371, European Patent nœ EP.450.030.A1 (1991), USA Patent nœ 5299175 (1994).
62. J.A. Gallego-Juarez, E.R.F. De Sarabia, G. Rodriguez-Corral, T.L. Hoffman, J.C. Galvez-Moraleda, J.J. Rodriguez-Maroto, F.J. Gomez-Moreno, A. Bahillo-Ruiz, M. Martin-Espigares and M. Acha, *Environmental Science and Technology*, 1999, **33**, 3843–3849.
63. R.M.G. Boucher and A.L. Weiner, *British Chemical Engineering*, 1963, **8**, 808–812.
64. J.A. Gallego-Juárez, Some applications of air-borne power ultrasound to food processing, *Ultrasound in Food Processing*, M. Povey and T.J. Mason (eds.), Blackie Academic and Professional, 1998, ISBN 0-7514-0429-2.
65. T.J. Mason, J.P. Lorimer, S. Saleem, and L. Paniwnyk, *Controlling emissions from electroplating by the application of ultrasound*, Research project sponsored by the UK Health and Safety Executive, 1996.
66. E. Namgoong and J.S. Chun, *Thin Solid Films*, 1984, **120**, 153–159.
67. F. Cataldo, *J. Electroanal. Chem.*, 1992, **332**, 325.
68. J.P. Lorimer and T.J. Mason, *Electrochemistry*, 1999, **67**, 924–930.
69. U. Neis, K. Nickel, and A. Tiehm, Ultrasonic disintegration of sewage sludge for enhanced anaerobic biodegradation, *Advances in Sonochemistry*, 6, Theme issue – *Ultrasound in Environmental Protection*, T.J. Mason and Andreas Tiehm (eds.), Elsevier, 2001.
70. P. Pirkonen, Ultrasound in filtration and sludge dewatering, *Advances in Sonochemistry*, 6, Theme issue – *Ultrasound in Environmental Protection*, T.J. Mason and Andreas Tiehm (eds.), Elsevier, 2001.
71. R.D. Davis and J.E. Hall, *Water Pollution Control*, 1997, **7**, 9–17.
72. J. Kopp, J. Müller, N. Dichtl, and J. Schwedes, *Wat. Sci. Tech.*, 1997, **36**(11), 129–136.
73. A. Tiehm, K. Nickel, and U. Neis, *Wat. Sci. Tech.*, 1997, **36**, 121.
74. A. Mues and A. Peiffer, Design of ultrasound systems for low and high frequencies, *Ultrasound in Environmental Engineering*, A. Tiehm and U. Neis (eds.), TU Hamburg-Harburg Reports on Sanitary Engineering, 1999, **25**, 91–99.
75. D. Schneider, Construction of a high performance reactor, *Ultrasound in Environmental Engineering*, A. Tiehm and U. Neis (eds.), TU Hamburg-Harburg Reports on Sanitary Engineering, 1999, **25**, 101–121.
76. E.S. Tarleton and R.J. Wakeman, Ultrasonically assisted separation processes, *Ultrasound in Food Processing*, M.J.W. Povey and T.J. Mason (eds.), Thomson Science, London, 1997, 193.
77. N. Senapati, Ultrasound in chemical processing, *Advances in Sonochemistry*, T.J. Mason (ed.), JAI Press, London, 1991, **2**, 187–210.

5

Polymers

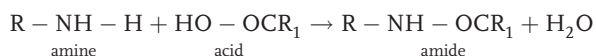
5.1

Introduction

A brief introduction to polymerisation mechanisms is given here for readers not familiar with the field. In this section some terms and concepts are introduced which will be used later in the chapter.

There are two main chemical mechanisms by which a synthetic polymer may be produced; namely by either a condensation (step growth) polymerisation or addition (chain) polymerisation.

Polymers produced by a condensation mechanism are simply extensions of the normal condensation reactions of organic chemistry where a small molecule e.g. H₂O or HCl is expelled as the link is built. For example:



Thus to provide a route to polymer chains, it is necessary for the starting materials to be *bifunctional*. Choosing the synthesis of terylene (Fig. 5.1) as an example:

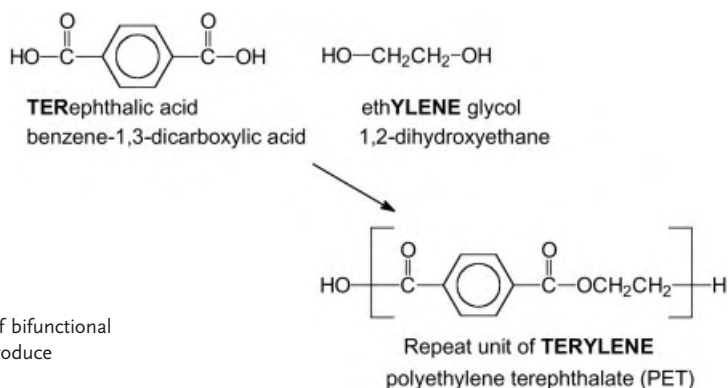


Fig. 5.1. Use of bifunctional monomers to produce linear chains.

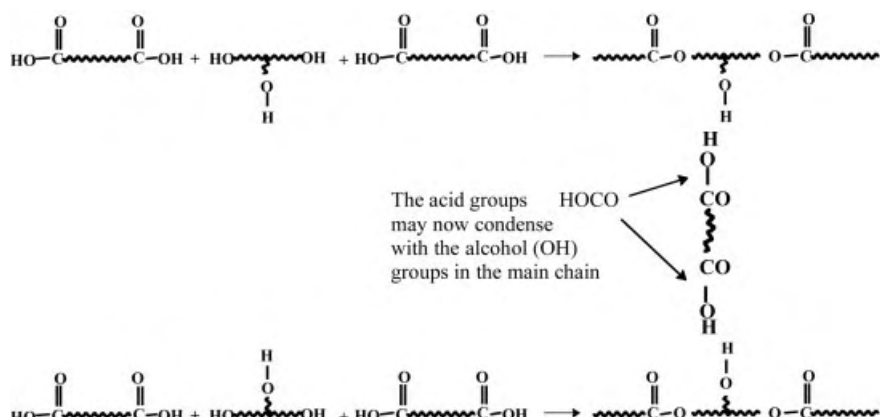


Fig. 5.2. Use of multifunctional monomers to produce network polymers.

However, using *multifunctional* monomers, network polymers can be produced. Fig. 5.2 gives an example of a polymer produced using a trifunctional alcohol monomer and a difunctional carboxylic acid.

Using *tetrafunctional* monomers will give network polymers (or ladder). These are highly condensed molecules which can have considerable heat stability. Often these do not melt but simply char or ablate.

The second common method of synthesising polymers (Fig. 5.3) is chain (addition) polymerisation. The most common type of addition polymer is based on ethene $\text{CH}_2 = \text{CH}_2$ in which the monomer contains at least one double (π) bond which on being activated, by free radical attack say, opens up to produce two single sigma bonds and the homopolymer poly(ethene). (Note in Fig. 5.3 the resultant polymer backbone is joined together by carbon-carbon bonds, unlike the condensation polymer systems (Fig. 5.1).)

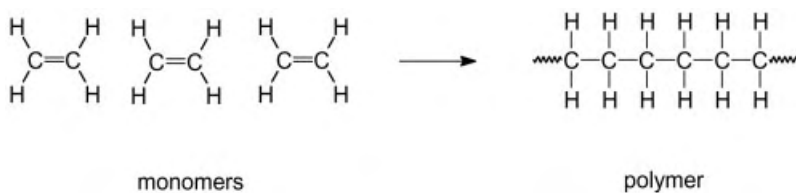


Fig. 5.3. Conversion of the monomer ethene into the polymer polyethene.

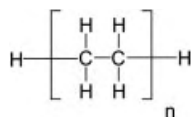


Fig. 5.4. Poly(ethene).

Poly(ethene) can be written as in Fig. 5.4.

The symbol n in Fig. 5.4 refers to the number of repeat units which are joined together in the polymer. This is termed the degree of polymerisation (X_n), and could easily be a number as high as 10 000. Thus for a repeat unit of mass 28 (ethene), this would give a polymer molar mass (R.M.M., M_n) of 280 000.

In other words the molar mass of the chain (M_n) = Molar mass of the repeat unit $\times X_n$

Chain polymerisation is characterised by three steps; namely initiation (Eq. 5.1), propagation (Eq. 5.2) and termination (Eq. 5.3) where I , R and M refer to the initiator molecule, free radical and monomer respectively and k_i , k_p and k_t are the respective rate constants for the processes.



In order to deduce the dependence of the polymerisation (propagation) rate and/or molar mass (M_n) upon the initiator and/or monomer concentrations, it is necessary to invoke a hypothesis called the "Steady State". Employing the "Steady State" allows one to set the rate of production of the radicals (i. e. $k_i [I]$) equal to the rate of loss of radicals (i. e. $k_t [R^\bullet]^2$), which enables one to write Eq. 5.4.

$$R_p = K[M][I]^{1/2} \quad (5.4)$$

$$\text{where } K = (k_p) \left(\frac{k_i}{k_t} \right)^{1/2}$$

Also since the propagation step (R_p) is the step which consumes monomer, and the termination step (R_t) the step which leads to the production of polymer chains, then the number of units in a chain (X_n) is given by $X_n = \frac{R_p}{R_t}$ which allows us to write

$$M_n = \frac{K[M]}{[I]^{1/2}} \quad (5.5)$$

The converse of propagation is depropagation. Most polymer molecules when subjected to a hostile environment (e. g. high temperature) will undergo C-C bond breakage of the backbone followed by a reduction in molecular weight (i. e. molar mass). Some polymers, such as polymethyl methacrylate, depolymerise (or degrade) by losing a monomer unit each time (Eq. 5.2a). (Ultrasonic degradation is dealt with in Section 5.2.)



If two monomers e. g. ethene, $\text{CH}_2 = \text{CH}_2$ and propene, $\text{CH}_2 = \text{CH}(\text{CH}_3)$ are reacted together, then there is the possibility of producing a copolymer. Fig. 5.5 is one particular example of a copolymer produced by the reaction of ethene and propene. The actual structure of the copolymer depends on the reaction conditions.

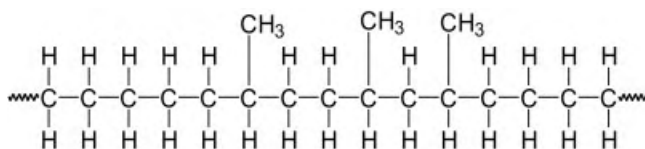


Fig. 5.5. Copolymer structure produced from ethene and propene.

Macromolecules are therefore simple extensions of micromolecules in which chains of atoms are held together by covalent bonds. The chemical bonds within the chain are very strong and directional along the chains. Bonding between chains is due to weak secondary van der Waal's bonding or slightly stronger hydrogen bonding. Although linear chains are normally produced, by changing the chemistry involved both branched and network structures can be produced.

For any given macromolecule (polymer), no matter whether it occurs naturally or is the result of some synthetic procedure, there is no unique molecular weight (relative molar mass, R.M.M.) as there is for small organic molecules such as the alkanes. Because of the randomness of the reactions which take place to produce the macromolecule, there will always be chains of differing length (R.M.M.) which give rise to the polymer sample having an R.M.M. distribution (Fig. 5.6).

Polymers are therefore mainly characterised in terms of two molar masses. These are the *Number Average Molar Mass*, \overline{M}_n (Eq. 5.6) and the *Mass Average Molar Mass*, \overline{M}_w (Eq. 5.7)

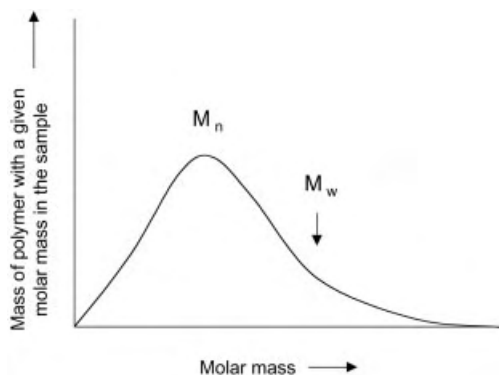


Fig. 5.6. Molar mass (R.M.M.) distribution.

$$\overline{M}_n = \frac{\sum N_i \times M_i}{\sum N_i} \quad (5.6)$$

where N_i is the number of chains (molecules) with R.M.M. of M_i .

$$\overline{M}_w = \frac{\sum W_i \times M_i}{\sum W_i} \quad (5.7)$$

where W_i is the mass (weight) of chains (molecules) with R.M.M. of M_i .

We are now in a position to discuss the effects of low frequency (< 400 kHz) high intensity (> 3 W cm⁻²) ultrasonic waves on macromolecules (polymers) and examine how the parameters such as frequency, intensity, hydrostatic pressure etc affect both the polymerisation and also the depolymerisation processes. We will also consider in this chapter the use of ultrasound in polymer processing.

5.2

Degradation of Polymers

Many investigators [1 – 3] have found a reversible reduction in viscosity after applying ultrasound to solutions of such naturally occurring high polymers as starch, gelatin and gum arabic. This reduction in viscosity has been explained in terms of the dispersion of aggregates or the breakage of weak Van der Waals bonds instrumental in holding the chains together. On the removal of the ultrasound source, the viscosity of the polymer solutions slowly returned to their original values over a time period of minutes, hours or even longer. However for most polymers in solution, a definite effect of depolymerisation (i. e. degradation) is observed especially on prolonged exposure to high intensity ultrasound. Typical examples of this irreversible reduction in viscosity

Tab. 5.1 Flow times of 1 % solution of polystyrene in toluene (air saturated) vs insonation flow time (960 kHz, 6.8 W cm⁻²).

Irradiation time [min]	0	30	60	90	120
Flow time [s]	23.6	19.7	19.0	18.4	18.3

have been observed for polystyrene (Tab. 5.1), polyvinylacetate, polyacrylates, DNA and dextran [1, 4] Even when the irradiated polymers are isolated and redissolved their viscosities still remain low in comparison to those of the non-irradiated solutions suggesting that the polymer has undergone some permanent damage.

If this viscosity reduction is the result of cavitation, then the extent of degradation for any system is expected to be zero if the process is carried out under conditions which eliminate cavitation – i. e. in either vacuo or at high overpressure. These conditions can be achieved by degassing the solution, to remove gas nuclei which subsequently could have led to a cavitation event, or increasing the external pressure (see Section 2.4.4). In contrast to this expectation early workers such as Schmid [5] and Mark [6] observed degradation both *in vacuo* and at a high overpressure. For example, Schmid studying the degradation of polystyrene in benzene at an acoustic pressure equivalent to 5 atm still observed degradation under 15 atm of applied pressure. Such an overpressure, in Schmid's view, ought to have been sufficient to inhibit the degradation. To explain these observations, Schmid and Mark suggested that the decreases in solution viscosity (i. e. degradation) on irradiation were as a result of increased frictional forces between the ultrasonically accelerated faster moving solvent molecules and the larger less mobile macromolecules. Although envisaging different modes of interaction between the solvent and polymer molecules, both investigators concluded that the increased forces were sufficient to break a C–C bond.

Schmid for his part considered two ideal cases for the degradation of the polymer in solution. The first considered the macromolecules to be immobile in solution and the solvent molecules were swept past them under the action of the applied acoustic field; the second involved an allowance for macromolecule movement, the macromolecule moving with the solvent under the action of the applied ultrasonic field.

In the case of an immobile macromolecule in solution it is possible to estimate a value of the frictional force (F) developed between the solvent and polymer molecules by assuming the macromolecule to consist of a number (n) of solid spherical entities and applying the Stokes formula in a modified form (Eq. 5.8).

$$F = 6\pi\eta rVn \quad (5.8)$$

In Eq. 5.8, η is the fluid viscosity, r is the radius of the sphere and V is the velocity of the solvent. Thus, for a polystyrene molecule (R.M.M. \sim 300 000; $n \sim$ 3000) in benzene as

Tab. 5.2 Degradation of polystyrene in CCl₄/toluene mixtures at 55 °C.

Time [min]	Solvent density [g cm ⁻³]				
	0.867	1.058	1.234	1.454	1.601
0	208 000	203 000	197 000	190 000	189 000
10	140 000	158 000	157 000	151 000	133 000
30	100 000	124 000	129 000	112 000	109 000
60	80 000	100 000	108 000	89 000	93 000
120	61 000	78 000	85 000	73 000	80 000

solvent (viscosity $\sim 6.2 \times 10^{-4}$ N s m⁻²), where the pendant benzene rings can be assumed to be acting as the spheres ($r = 3 \times 10^{-10}$ m), the total frictional force developed for the fluid flowing under the action of an ultrasonic field with a velocity of 0.5 m s^{-1} can be estimated to be 5.4×10^{-9} N [i. e. $F = (6\pi) \times (6.2 \times 10^{-4}) \times (3 \times 10^{-10}) \times (50 \times 10^{-2}) \times 3000$].

From spectroscopic data it has been deduced that the value needed to effect breakage of a C–C bond is 4.5×10^{-9} N. Since the value estimated from the frictional approach is some 20 % higher it could be inferred that Schmid's frictional approach to polymer degradation is in fact correct. If so, then there ought not to be any significant degradation in a system where the polymer and solvent molecules have similar densities. This is not the case as Tab. 5.2 shows, although there is a slight density dependence.

Further evidence that this model cannot be used to predict absolutely the course of degradation is afforded by the influence of changes in irradiation frequency on degradation. If, as Schmid suggested, degradation is the result of solvent movement past the macromolecule, then for a rigid macromolecular structure a decrease in frequency should allow the macromolecule more time to accommodate the impact of the solvent – i. e. degradation ought to decrease with decrease in frequency. In practise the opposite effect is observed – degradation increases with decrease in frequency (Fig. 5.7).

The second ideal case identified by Schmid assumed that the macromolecule moved with the solvent and in this case Eq. 5.9 must be employed:

$$F = \frac{nm\omega V}{N_A} \quad (5.9)$$

Here m is the molar mass (R.M.M.) of the monomer, N_A is the Avagadro number and ω is the angular frequency of the applied ultrasonic wave. For an applied frequency of 500 kHz, the frictional force developed in the above polymer system, according to Eq. 4.9, may be calculated to be approximately 7.8×10^{-16} N. This is obviously many orders of magnitude less than that required to rupture a C–C bond. The conclusion must be that the more dilute a polymer solution, the more likely it is that the

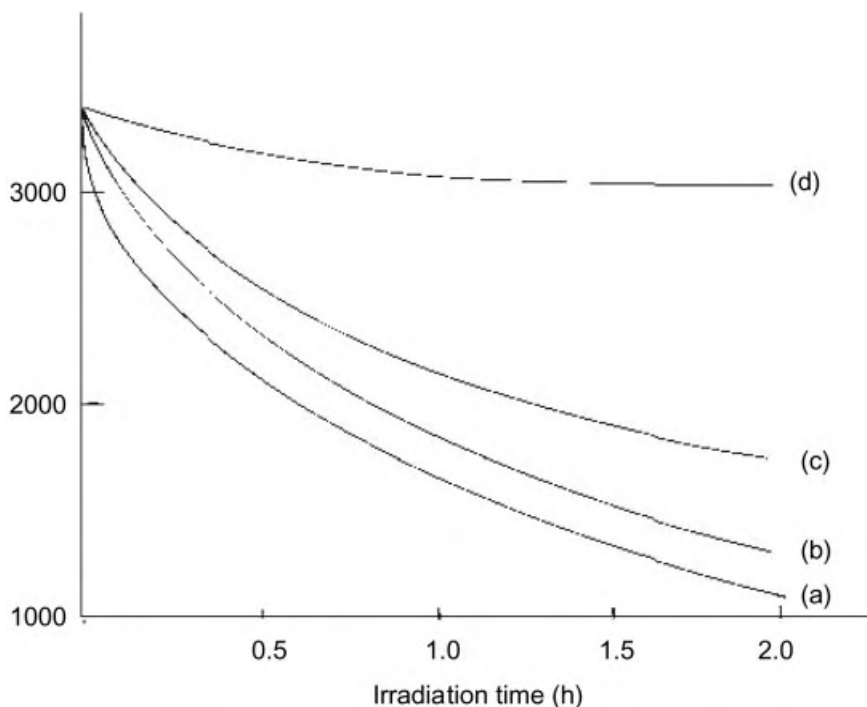


Fig. 5.7. Effect of frequency on the degradation of polystyrene (1 %) in benzene; (a) 1 MHz; (b) 1.25 MHz; (c) 1.5 MHz; (d) 2 MHz.

macromolecule will move with the solvent since there is less interaction, and the smaller will be the depolymerisation effect. This is certainly not observed in practice (see Section 5.3.7) and identifies a flaw in Schmid's argument. Further this second model, like the first implies that polymer degradation increases with increase in frequency. As already pointed out (Fig. 5.7) this is not observed experimentally (see Section 5.3.1).

Mark's hypothesis, on the other hand, although still suggesting that frictional forces were the origin of the degradation, took into account the molecular configuration of the polymer. It is well known that macromolecules in solution are neither completely stretched out in a straight line (Fig. 5.8a), nor are they completely coiled up in a ball (Fig. 5.8b), but exist in an intermediate shape of moderately undulated configurations (Fig. 5.8c).

Under the action of an applied acoustic field the suggestion was that there would be regions within the polymer where rotation (and vibration) of individual segments were able to take place freely, in phase with the rapid oscillatory movement of the solvent. This segmental movement (termed micro Brownian motion) was in addition to the movement of the macromolecule as a whole (macro Brownian motion). However, in that segmental motion is a cooperative effect and depends upon the interaction

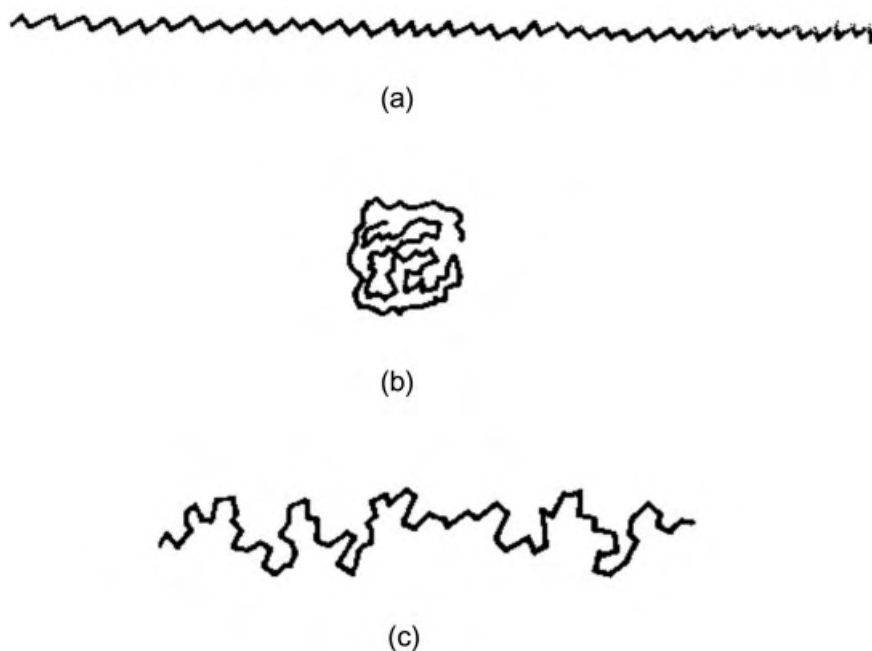


Fig. 5.8. The possible configurations of a macromolecule in solution; (a) stretched out; (b) coiled up; (c) intermediate.

between various units in the macromolecule, there will be regions where movement lags well behind the motion of the solvent molecules leading to a concentration of stress and consequent rupture of a C–C bond. Estimates by Mark of the frictional forces between the macromolecules and the solvent molecules provided values which were large enough to break not only C–C bonds, but also C = C and C = O bonds.

Despite the inability to account for several of the experimental observations the above theories predict that the frictional forces developed are dependent upon the size of the macromolecule and that the rate of degradation decreases with decrease in chain size (Figs. 5.9 and 5.10).

Based upon experimental data, Schmid was able to show this mathematically for dilute solutions ($< 0.02 \text{ mol dm}^{-3}$) as

$$\frac{dx}{dt} = k(P_t - P_L) \quad (5.10)$$

and for concentrated solutions as

$$\frac{dx}{dt} = k \log\left(\frac{P_t}{P_L}\right) \quad (5.11)$$

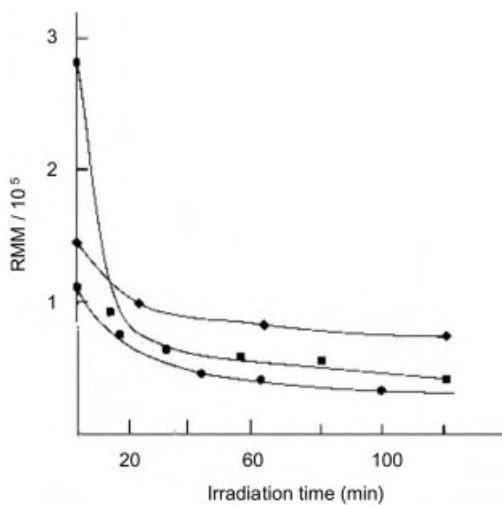


Fig. 5.9. Degradation rate vs initial R.M.M. (polystyrene in toluene, 70 °C).

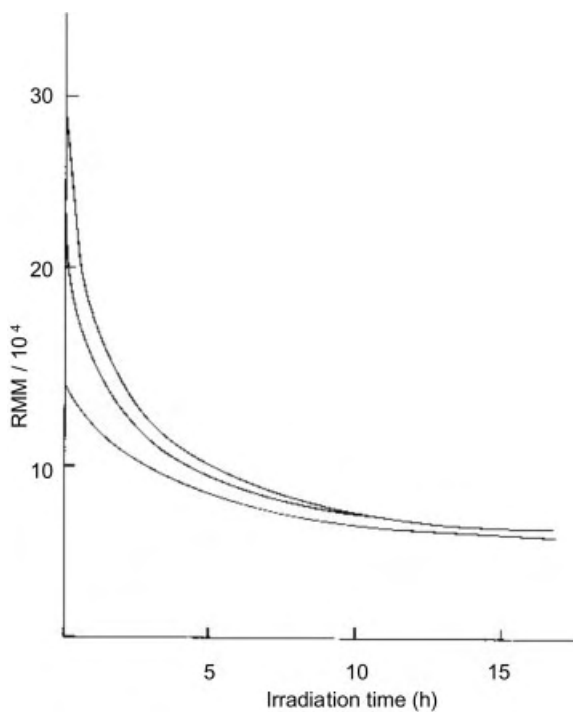


Fig. 5.10. Depolymerisation of polystyrene in benzene ($f = 750$ kHz; intensity = 12 W cm^{-2}).

where dx is the number of chemical bonds broken in unit volume in an irradiation time d_t , P_t is the degree of polymerisation at time t (i. e. number of monomer units in the chain) and P_L is the limiting degree of polymerisation – i. e. the lowest value chain length to which the polymer could be degraded. Eq. 5.10 was subsequently manipulated by Schmid so as to become dependent on the number average molar mass (M) as shown in Eq. 5.12.

$$\frac{M_t}{M_i} + \ln\left(1 - \frac{M_t}{M_i}\right) = -\frac{k}{c} \left(\frac{M_t}{M_0}\right)^2 t + \frac{M_t}{M_i} + \ln\left(1 - \frac{M_t}{M_i}\right) \quad (5.12)$$

In Eq. 5.12, M_t and M_i are the molar masses at time t and at $t = 0$ (i. e. initially) and M_0 is the molar mass of the monomer.

Both Eq. 5.10 and Eq. 5.12 have been modified by Malhotra [7] to give Eq. 5.13.

$$\frac{1}{M_t} - \frac{1}{M_i} = kt \quad (5.13)$$

The analysis of the kinetics of polymer degradation is complicated by the nature of the polymers. Degradation kinetics characterise the reaction in terms of the molar mass of the degrading species. Consequently, unless the polymer consists of chains which are all identical in terms of molar mass (e. g. number and/or mass average molar mass), there will be a series of degradation reactions occurring simultaneously. This was highlighted by Basedow and Ebert [8] who found that each molar mass degrades at a different rate. The authors found that high molar mass species degraded preferentially, while smaller molar mass species initially rose in concentration (due to the degradation of higher species) before themselves degrading.

Lorimer and Mason [4] have investigated the effect of ultrasound on aqueous solutions of “native” dextran. The initial dextran sample was prepared (industrially) by the fermentation of sucrose, a reaction which leads to a wide distribution of molar mass (Fig. 5.11). Using the GPC traces (mass % of polymer with a given molar mass), the authors identified, for each of several R.M.M. values, the masses of a particular molar mass as a function of irradiation time. Assuming the degradation process to be first order at each molar mass value, they plotted $\ln(\text{mass})$ as a function of the irradiation time and obtained the degradation rate constant for that particular R.M.M. On plotting the “deduced” rate constant against the corresponding molar mass, they obtained a linear response (Fig. 5.12). Where the plot met the x-axis was taken to be a measure of the limiting R.M.M. (Similar results were observed for plots at constant power variable temperature.)

Assuming that rate constant is dependent upon chain length, rate constants have been deduced by Jellinek from the initial rate of degradation for fractionated samples.

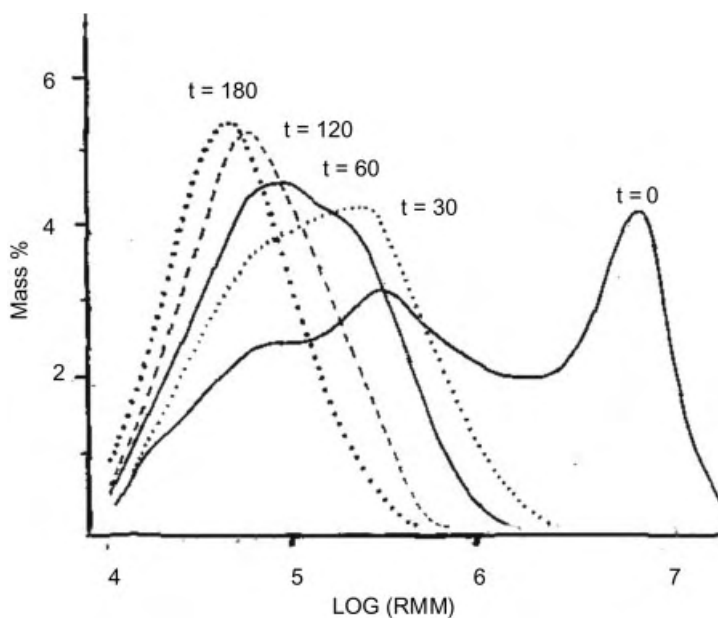


Fig. 5.11. Effect of irradiation time on the ultrasonic degradation of aqueous native dextran (2 % w/v; 60 W; 30 °C; 20 kHz).

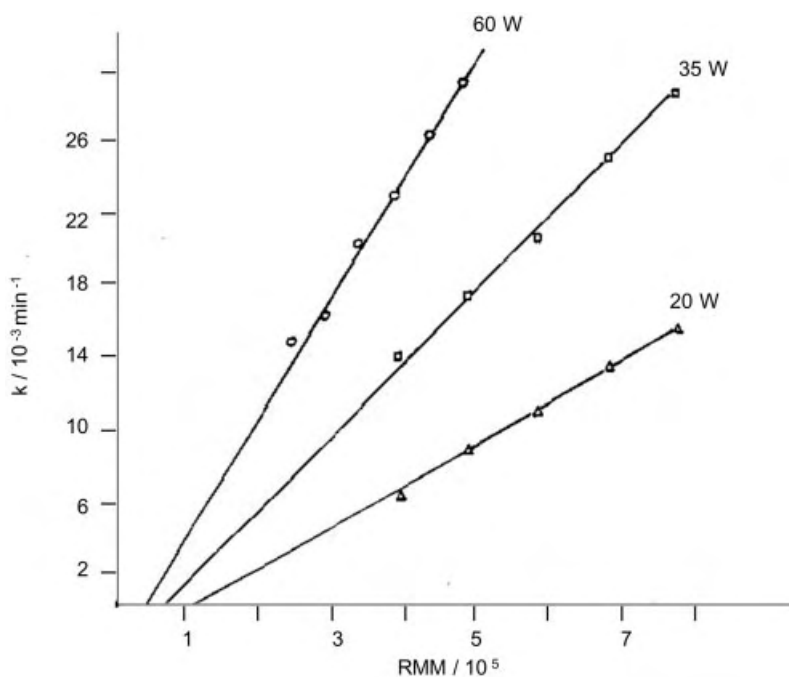


Fig. 5.12. Plot of \ln (mass) vs irradiation time.

Ovenall [9] assumed the rate constant was dependent upon the system and the experimental conditions and arrived at the first order rate equation given in (Eq. 5.14).

$$\ln\left(\frac{1}{M_L} - \frac{1}{M_t}\right) = \ln\left(\frac{1}{M_L} - \frac{1}{M_i}\right) - k\left(\frac{M_i}{cM_i}\right)t \quad (5.14)$$

Gooberman and Lamb [10] used molecular weight distributions to produce rate constants that were independent of any predetermined kinetics scheme. The effect due to degradation of higher species was also ignored to produce Eq. 5.15 where n_t is the number of molecules of length P_t .

$$n_t = n_0 e^{-kt} \quad (5.15)$$

El'tsefon and Berlin [11] derived the following equation:

$$M_t = M_i(1 + M_i^2 kt)^{-1/2} \quad (5.16)$$

Goto and Fujiwara [12] predicted an equation relating the degree of polymerisation to the rate constant (Eq. 5.17).

$$\frac{1}{(P_t - P_L)} = kt + \frac{1}{(P_i - P_L)} \quad (5.17)$$

Eq. 5.17 when written in terms of number average molar mass yields:

$$\frac{1}{(M_t - M_L)} = k't + \frac{1}{(M_i - M_L)} \quad (5.18)$$

where $k' = k/M_0$.

For a large degree of polymerisation, Sato and Nalepa [13] derived the following equation:

$$\frac{1}{M_t} = k't + \frac{1}{M_i} \quad (5.19)$$

where $k' = k/M_0$. This is identical to that proposed by Malhotra.

More recently, Chen et al. [14] have proposed Eq. 5.20.

$$\ln M_t = \ln M_i - kt \quad (5.20)$$

Other relationships which have been postulated are:

$$\frac{dx}{dt} = kP_t^2 n_t \quad (5.21)$$

where n_t is the number of molecules of length P_t [15], or linear relationships [16] between sonication time and $\frac{1}{(P-P_t)}$ (for poly(ethylene oxide)) or (for poly(acrylamide)).

Recently Madras et al. [17], studying the degradation of styrene and poly(vinyl acetate) in chlorobenzene have analysed their data using a continuous distribution kinetics model.

There is now a wealth of experimental information [5, 10, 18–28] to suggest that degradation is due to cavitation effects. For example:

- The ultrasonic degradation of polystyrene in benzene increases with a decrease in the applied ultrasonic frequency (see Section 2.6.1).
- The ultrasonic degradation of aqueous polyacrylic acid decreases with the addition of ether i. e. increased vapour pressure (see Section 2.6.2).
- The ultrasonic degradation of polystyrene in toluene decreases with an increase in the reaction temperature (see Section 2.6.3).
- The ultrasonic degradation of an air saturated toluene solution of polystyrene is greater than when the solution is degassed.
- The ultrasonic degradation of polystyrene in toluene increases with an increase in the externally applied pressure.

What is debatable however, is whether the degradation is caused by

1. The hydrodynamic forces of cavitation – i. e. the shock wave energies produced on bubble implosion.
2. The shear stresses at the interface of the pulsating bubbles.
3. The associated thermal and pressure increases within the bubbles themselves.

All the above are dependent upon the same factors i. e. intensity, frequency, gas content and gas type etc. The current view is that ultrasonic degradation is for the main part mechanical in its origin and due to the high pressures associated with the collapse of the bubble. There may be the possibility that part of the degradation is thermal but this would only be significant for those macromolecules with a sufficiently high vapour pressure to allow entry into the cavitation bubble.

5.3

Factors Affecting Polymer Degradation

5.3.1

Frequency

One of the earliest reports on the effect of frequency was by Schmid and Poppe [29]. Working at a constant ultrasonic intensity of 1 W cm^{-2} and irradiation frequencies of

300, 175 and 10 kHz, Schmid concluded that the frequency had practically no effect on the degradation of poly(methyl methacrylate) in benzene (0.3 % w/v) (Fig. 5.13). This was exactly as reported by Jellinek [30] who predicted that the degradation rate constant should be independent of the frequency for frequencies less than 500 kHz.

However a closer examination of Fig. 5.13 seems to indicate that the degradation rate, and to a lesser degree the extent of degradation, decreases with an increase in the irradiation frequency. The general conclusion that the higher the irradiation frequency the lower is the degradation rate, and the higher the limiting degree of polymerisation, P_L , is a view now shared by most workers in the field. Perhaps the only contentious point is the extent to which a polymer is degraded at a particular frequency. We have already seen (Section 2.3) that the higher the frequency of the ultrasonic wave the more rapidly it is attenuated. It is important, therefore, to recognise that when comparing the effects of frequency, intensity must be held constant. For example, Gaertner [18] observed depolymerisation at both 400 kHz and 2500 kHz, the lower frequency necessitating an intensity of only 0.5 W cm^{-2} whereas the higher frequency required approximately 2 kW cm^{-2} . Unfortunately until recently many workers in the field did not report the actual acoustic power entering the system but only the power delivered to the transducer.

However what is certain is that the higher the applied frequency the shorter is the period in which bubble growth and collapse can occur, and the more likely it is that there is insufficient time to produce cavitation. According to Neppiras and Noltingk [31] there is a frequency limit ($\sim 10 \text{ MHz}$) above which cavitation does not occur. This limit de-

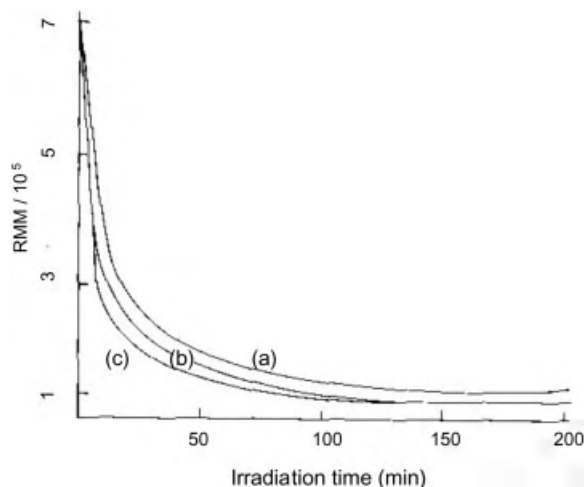


Fig. 5.13. Degradation of polymethyl methacrylate (PMMA) in benzene as a function of frequency. (Intensity = 1 W cm^{-2} ; concentration 0.3 % w/v; (a) $f = 300 \text{ kHz}$; (b) $f = 10 \text{ kHz}$; (c) $f = 175 \text{ kHz}$).

depends upon the initial size of the bubble, the external (hydrostatic) pressure (P_h) and the pressure amplitude (P_A) of the ultrasonic wave. Some workers have suggested that there is an optimum frequency at which the cavitation intensity attains a maximum value and at this frequency maximum degradation occurs. For example Mostafa [32] has observed (Fig. 5.7) maximum degradation at 1 MHz for polystyrene in benzene ($I = 12.5 \text{ W cm}^{-2}$). In Mostafa's view, the small observed degradation at the highest frequency (2 MHz), where presumably cavitation is negligible, is probably due to resonance effects of some kind. Whatever the form of resonance, it certainly cannot be between the frequency of the molecular vibrations and the frequency of the applied ultrasound since the former (estimated to be 10^8 MHz) is many orders of magnitude greater than the latter (max. 1 MHz). One possible explanation is that degradation is caused by the shear forces set up by the ultrasonic waves. As the frequency, and hence attenuation, of the wave decreases the shear forces will be complemented by the increased cavitational effects.

5.3.2

Solvent

Most of the experimental data indicates that there is a decrease in the extent of depolymerisation with increasing solvent vapour pressure. For example, Schmid and Rommel [33] observed slower degradation rates in benzene than in toluene for samples of polystyrene and various polyacrylates. Although at 20°C the viscosities of benzene and toluene are similar, 0.65 and 0.59 cp respectively, their vapour pressures differ appreciably being 9100 N m^{-2} and 3350 N m^{-2} respectively. Similar trends have been observed for the degradation of nitrocellulose in several solvents, the extent of degradation increasing in the order acetone, ethyl acetate, propyl acetate, isobutyl acetate, isoamylacetate and ethyl benzoate. Although the amount of degradation increases with decrease in the solvent vapour pressure, as predicted (see Section 2.6.2), the order is also that of increasing solvent viscosity (Tab. 5.3).

The effect of vapour pressure is most easily visualised when the rates of degradation are plotted as a function of the enthalpy of vaporisation (Fig. 5.14). Plainly the lower the enthalpy of vaporisation (ΔH_v), the more volatile the solvent and the more solvent vapour will enter the bubble. This effectively cushions the collapse of the bubble, so that the movement of solvent is slowed down, lessening the shock wave thereby leading to lower degradation rates.

Whilst vapour pressure may be the major solvent factor involved in the degradation process, there could also be a contribution from solvent viscosity or even, yet less likely, from surface tension. It has already been argued (see Section 2.6.2) that although an increase in viscosity raises the cavitation threshold, (i. e. makes cavitation more difficult), provided cavitation occurs, the pressure effects resulting from bubble collapse

Tab. 5.3 Values of vapour pressure, viscosity and surface tension of various solvents at 20 °C.

Solvent	Vapour pressure [mm Hg]	Viscosity [cp]	Surface tension [N m ⁻¹ /10 ⁻³]
Acetone	188.0	0.326	23.7
Ethylacetate	77.1	0.455	23.9
<i>n</i> -Propylacetate	28.4	0.590	24.3
<i>i</i> -Butylacetate	17.6	0.732	–
<i>i</i> -Amylacetate	5.0	0.872	–
Ethylbenzoate	0.3	2.24	35.5
Benzene	68.2	0.65	28.9
Toluene	25.1	0.59	28.5
CCl ₄	92.7	0.97	27.0

will be greater. In other words the cavitation effects of increasing vapour pressure and viscosity are partially compensatory – i.e. act in opposite directions.

An example of this effect may be seen by considering the data of Schmid and Beutenmuller [34] for the degradation of polystyrene in CCl₄/toluene mixtures of various

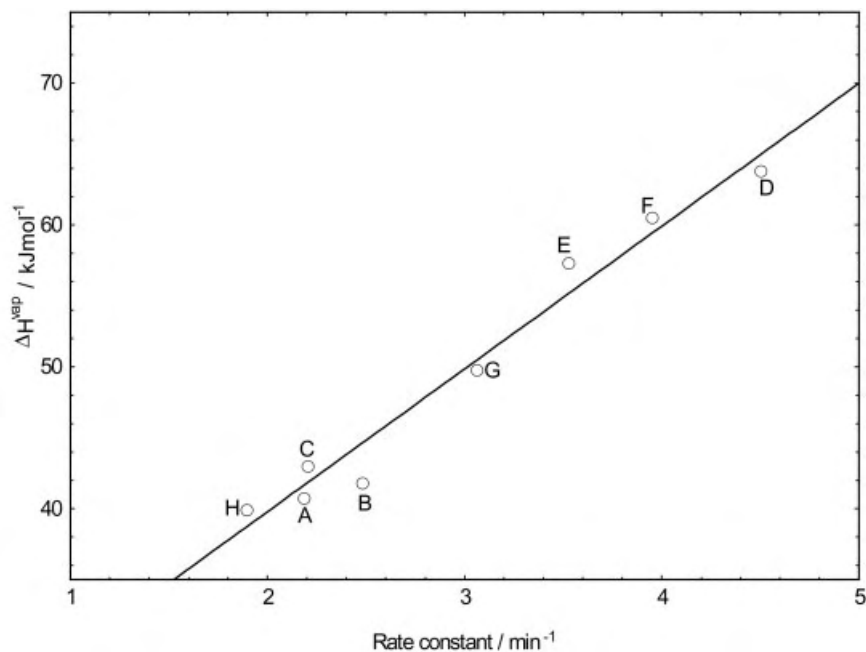


Fig. 5.14. The effect of the enthalpy of vaporisation on the degradation rate constant of dextran solutions. A – Water; B – Deuterium oxide; c – DMSO; D – Formamide; E – Ethylene glycol; F – Glycerol; G – Ethanolamine; H – 20% MeOH/H₂O

Tab. 5.4 Degradation of polystyrene in various CCl₄/toluene mixtures.

CCl ₄	[%]	0	25	50	80	100
Degradation rate	[% min ⁻¹]	5.5	3.1	2.7	2.6	4.8
* Vapour pressure at 55 °C	[mm Hg]	115	189	254	330	379
Viscosity at 55 °C	[cp]	0.4	–	–	–	0.6

* Calculated from $P = \chi_A P_A + \chi_B P_B$

composition (Tab. 5.4). On proceeding across the composition range from toluene to a 50/50 (v/v) mixture of CCl₄ and toluene, the increase in vapour pressure is accompanied by an almost proportional decrease in the degradation rate, measured as the percentage decrease in R.M.M. per minute.

It is surprising that further addition of CCl₄ (80 % and 100 %), which increase the vapour pressure, do not lead to a decrease in the degradation rate. On the contrary, the degradation for pure CCl₄ is almost identical to that of pure toluene even though the vapour pressure has increased more than threefold. The viscosity, however, has increased by approx. 50 % with change of solvent.

In contrast to the idea that vapour pressure is the major solvent parameter in determining the extent of degradation, Doulah has suggested it depends upon the solvent's solvating capacity. His proposal is that the energy released by the imploding cavitation bubbles, in the form of hydrodynamic shock waves, is more effective in 'good' solvents, where the chains are relatively extended (Fig. 5.8c), than in 'poor' solvents (Fig. 5.8b). This has also been demonstrated by Schmid and Beutenmuller who showed that the addition of the "non solvent" acetone to solutions of polystyrene in benzene decreased the degradation rate.

Several authors have attempted to corrolate the degradation rate with such solvent parameters as osmotic coefficient [35], viscosity [36–38] and the Flory Huggins interaction parameter, χ [39, 40] – a low χ value indicates a good solvent in which the polymer is expected to exhibit an open conformation (as opposed to coiled) and therefore is more susceptible to degradation (Fig. 5.15).

5.3.3

Temperature

An alternative method of raising the vapour pressure of a solvent is to increase the experimental temperature. The consequence should be both a decrease in the rate of degradation and an increase in the limiting degree of polymerisation (i. e. higher final R.M.M. value) as a result of the lower intensities of cavitation collapse at the higher temperatures (see Section 2.6.2). Tab. 5.5 and Fig. 5.16 [41] show these predictions are borne out in practice.

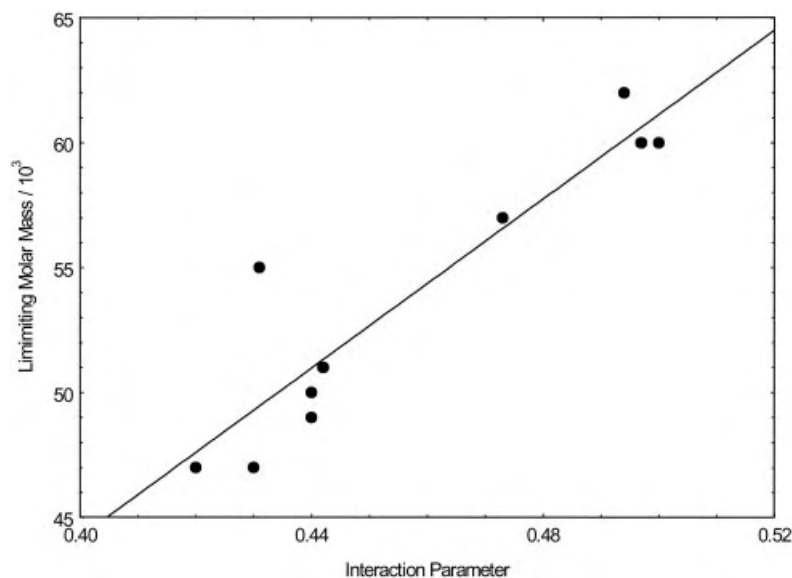


Fig. 5.15. Effect of interaction parameter on polystyrene limiting R.M.M. (25 °C).

5.3.4

Nature of the Gas

Whereas all workers agree that the extent of degradation is increased in the presence of gas, there is some dispute regarding the extent to which it takes place *in vacuo*. For example Weissler [22] (Fig. 5.17) and separately Prudhomme and Graber [19] (Tab. 5.6), investigating the degradation of polystyrene in toluene, failed to observe any appreciable degradation in the absence of gas.

Melville and Murray on the other hand, observed little if any degradation for polymethyl methacrylate samples of moderate R.M.M., but noted that a high R.M.M. sample was readily broken down. (Fig. 5.18).

If, according to the ideas presented earlier (Section 2.6.4), cavitation is the origin of degradation, then the extent of degradation should be greatest for gases with the highest specific heat ratio values (γ). This can in part be confirmed by considering Tab. 5.7 where the intrinsic viscosities (i. e. $[\eta]\alpha$ (R.M.M.) obtained at several irradiation time intervals are given for solutions of polystyrene in benzene (1 %) which have been saturated with a variety of different gases.

Although the degradation rates (Tab. 5.8) for the diatomic gases (N_2 , O_2 , H_2 , air) as measured by $\{[\eta]_{t=0} - [\eta]_{t=30}\} / [\eta]_{t=0}$ are higher than for the polyatomic gases (NH_3 , CO_2 , SO_2), the rate of degradation for argon, a monatomic gas, is surprisingly, lower than for the diatomics (Fig. 5.19).

Tab. 5.5 Percentage ultrasonic degradation and final R.M.M. of polystyrene in toluene at various temperatures.

Temperature	[°C]	40	60	80	100	120
Degradation	[% h ⁻¹]	79	78	71	57	32
R.M.M.	[10 ³]	80	65	128	270	—

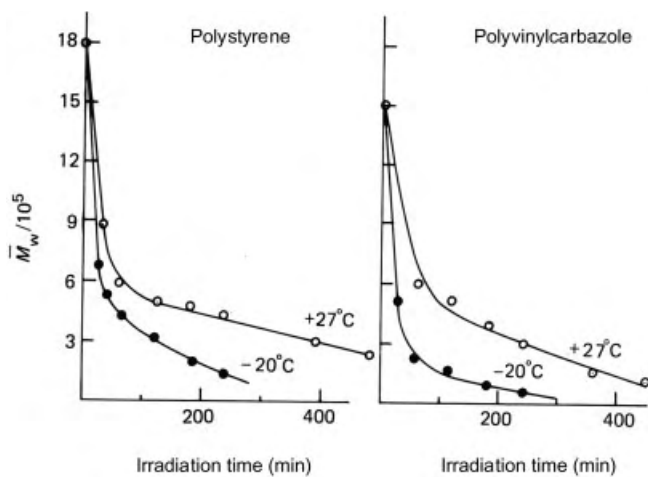


Fig. 5.16. Effect of temperature on degradation rate.

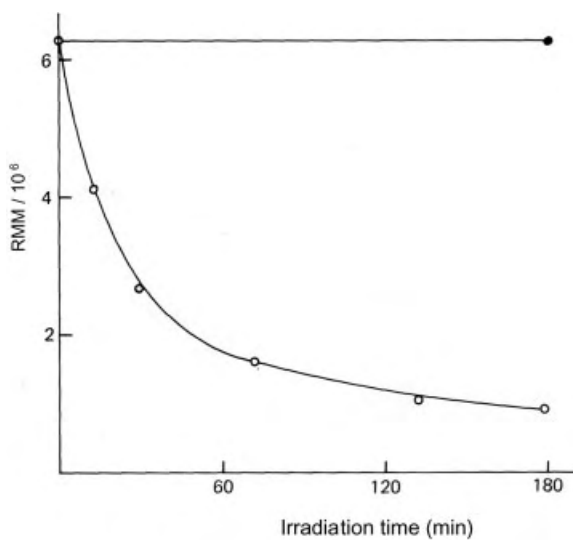


Fig. 5.17. US degradation of an air saturated (O) and degassed (●) polystyrene sample in toluene (0.5 %) at 400 kHz.

Tab. 5.6 Degradation of polystyrene in toluene (1 %) in the presence and absence of a gas.

Irradiation time	[min]	0	30	60	90	120
Flow time (air saturated)	[s]	23.6	19.7	19.0	18.4	18.3
Flow time (degassed)	[s]	23.6	24.0	—	—	23.6

Jellinek has explained this anomaly in terms of the velocity at which the gas filled cavities collapse. The larger the velocity of the cavity collapse, the faster the solvent molecules are swept past the polymer molecule and the faster is the degradation rate. Jellinek's estimate of the average collapse velocity of a cavity when filled with a monatomic gas was approximately 70 % that of a cavity filled with a diatomic gas – i. e. a slower collapse velocity. It may be fortuitous, but the ratio of the degradation rates for argon and oxygen, gases of similar solubility is 0.8 i. e. 80 %, a value close to the 70 % obtained (see Tab. 5.8).

According to Jellinek's deductions the differences in degradation rate expected for the diatomic and polyatomic gases should be smaller. A consideration of Tab. 5.8 shows that this is not observed in practise, the polyatomics having considerably lower rates. In fact, unlike the diatomics, the degradation rates for polyatomics are quite dissimilar, the rates decreasing with increase in solubility. If however solubility

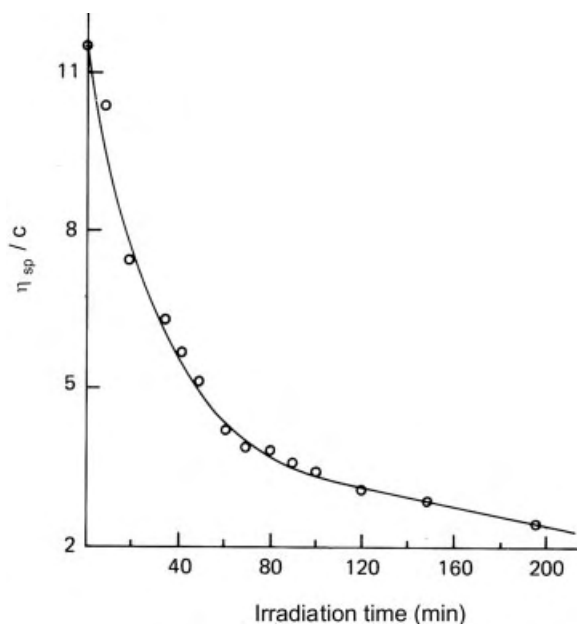


Fig. 5.18. Degradation of a high relative molar mass (R.M.M.) sample of poly(methyl methacrylate) in benzene *in vacuo*.

Tab. 5.7 Intrinsic viscosity vs irradiation time of polystyrene in benzene (1 %).

Dissolved gas	Irradiation time [min]						
	0	10	20	40	60	120	240
Air	1.81	1.22	0.95	0.81	0.68	0.60	0.47
N ₂	1.82	–	1.03	–	0.8	–	–
O ₂	1.79	–	1.04	0.82	0.8	–	–
H ₂	1.81	–	1.09	–	0.68	–	–
Ar	1.81	1.30	1.20	0.95	0.77	0.71	0.56
NH ₃	1.81	1.67	1.58	1.28	1.06	–	–
CO ₂	1.80	1.66	1.65	1.50	–	–	–
SO ₂	1.90	–	1.72	–	1.86	–	–

Tab. 5.8 Degradation rate vs gas solubility.

Gas		Air	N ₂	O ₂	H ₂	Ar	NH ₃	CO ₂	SO ₂
Rate	[10 ⁻² min ⁻¹]	47.5	43.0	42.5	40.0	33.7	12.7	8.3	5.0
γ		1.40	1.40	1.40	1.41	1.67	1.31	1.30	1.29
Solubility		0.14	0.11	0.22	0.07	0.24	9.95	2.4	88.0
Conductivity	[10 ² W m ⁻¹ K ⁻¹]	2.23	2.28	2.33	15.9	1.58	2.00	1.37	0.77

was the only other contributing factor to degradation a solution saturated with hydrogen ought to degrade faster and to a greater extent than one saturated with any of the other diatomic gases. This is not the case as Tab. 5.8 shows.

It may be however that the thermal conductivity of the gas plays some role. The value for hydrogen is somewhat higher than those for the other diatomics indicating that more heat (formed in the bubble during collapse) will be dissipated in the surrounding liquid effectively decreasing the maximum temperature, T_{\max} , attainable in the bubble. That is not to say that degradation in the presence of cavitation is thermal in origin as work by Melville has shown. Melville carried out both ultrasonic and thermal degradation of two samples of copolymer of polymethyl methacrylate and acrylonitrile, (molar ratio of methacrylate to acrylonitrile 411:1 and 40:1) and observed that whereas the latter copolymer had the faster thermal degradation rate, in the presence of ultrasound both copolymers showed practically the same rate of degradation. Further, a sample of polymethyl methacrylate had the same ultrasonic degradation rate as both of the copolymers (Fig. 5.20).

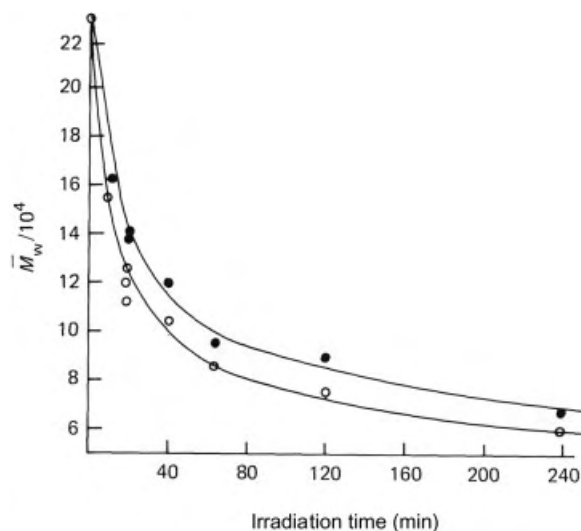


Fig. 5.19. Degradation of polystyrene in benzene with argon (●) and air (○).

5.3.5

Intensity

In Chapter 2 we explained why there existed a cavitation threshold i. e. a limit of sound intensity below which cavitation could not be produced in a liquid. We suggested that only when the applied acoustic amplitude (P_A) of the ultrasonic wave was sufficiently large to overcome the cohesive forces within the liquid could the liquid be torn apart and produce cavitation bubbles. If degradation is due to cavitation then it is expected that degradation will only occur when the cavitation threshold is exceeded. This is confirmed by Weissler who investigated the degradation of hydroxycellulose and observed that the start of degradation coincided with the onset of cavitation (Fig. 5.21).

It has also been suggested (Chapter 2) that there is an optimum power which can be applied to a system to obtain the most beneficial effect. Qualitatively it may be suggested that the number of bubbles produced at very high intensities serve to reduce power dissipation by reflecting the sound wave and creating a non linear response to the increase in intensity. Quantitatively we can argue that at high intensities (i. e. large P_A values) the cavitation bubbles have grown so large on rarefaction that there is insufficient time available for collapse during the compression cycle (see Section 2.6.6). Mark has observed this phenomenon for a sample of polystyrene in toluene. Using a sample of initial R.M.M. 300 000 he observed that the relative viscosity of the solution after 90 min irradiation showed very little reduction beyond an input power of 10 W cm^{-2} (Fig. 5.22).

Others workers who have investigated the effect of intensity on degradation are Melville [26], Wada and Nakane [42] and more recently Chen Kequiang et al. [43], Price [39], and Lorimer et al. [4].

Melville investigated the effect of intensity, as measured by the anode current supplied to the oscillator, and observed that the degradation rate and extent of degradation for polystyrene in benzene increased with increase in intensity (Fig. 5.23).

Similar behaviour has been observed in other polymer systems e. g. Wada and Kanane for the degradation of polymethyl methacrylate in chloroform (Fig. 5.24) and

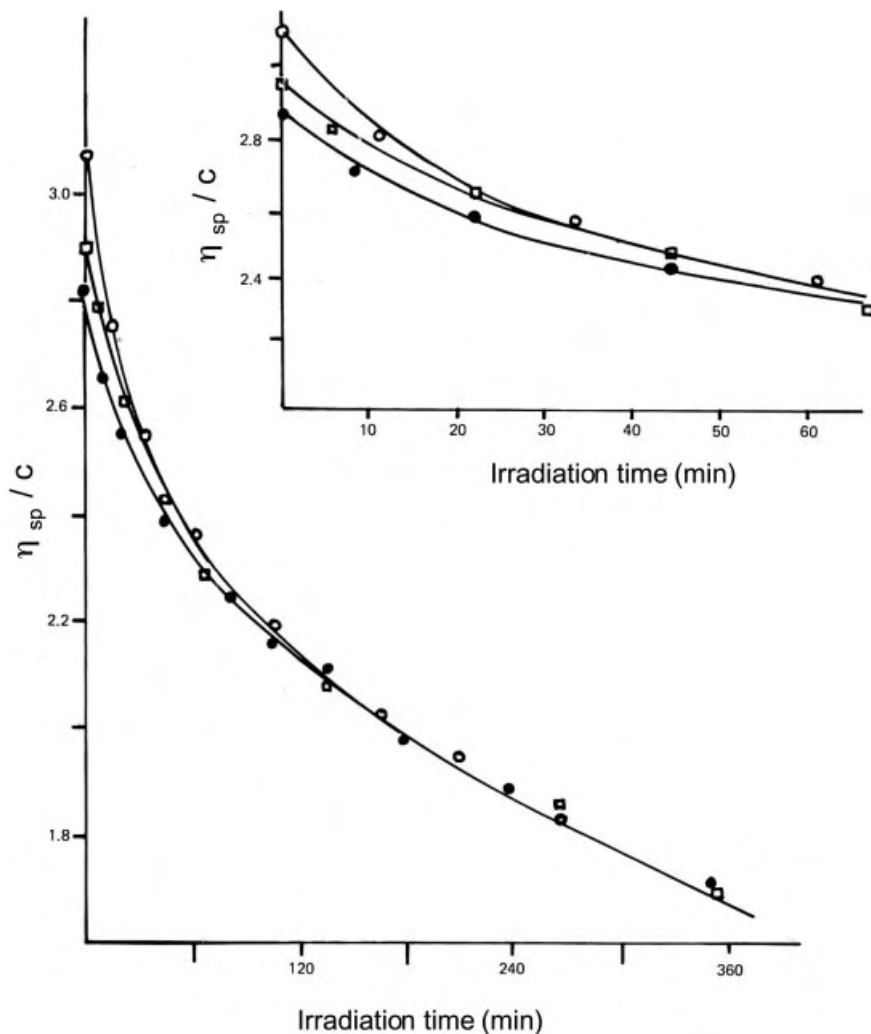


Fig. 5.20. Effect of polymer composition (1% in benzene) on degradation rate.

Chen Kegiang for the degradation of hydroxyethylcellulose (Fig. 5.25) and polyethylene oxide (Fig. 5.26) in aqueous solution.

In all the above cases, degradation is clearly faster at higher intensities. It is possible to show [30] for all the above that the (initial) rate constant (k') is a linear function of intensity (Fig. 5.27).

Similar increases in k' with ultrasonic intensity have been found for other polymers such as polystyrene [44], poly(methyl methacrylate) [45], poly(dimethylsiloxane) [46], poly(ethyleneoxide), hydroxyethyl cellulose, poly(vinyl acetate), poly(acrylamide) [47, 48] and hydroxypropyl cellulose [49].

Figures 5.24, 5.25 and 5.26 also show that the limiting molar masses are lower the higher the intensity. Whilst Okuyama [50] and Thomas et al. [51] predicted, and several workers observed [52], that the limiting molar mass is invariant with intensity, most workers now agree that P_L decreases with increase in ultrasonic intensity. Price [39] found that the results of the ultrasonic degradation of polystyrene in toluene fitted equation (Eq. 5.22).

$$M_{\text{lim}} = 41800 - 90.8 I \quad (5.22)$$

where I was given in W cm^{-2} .

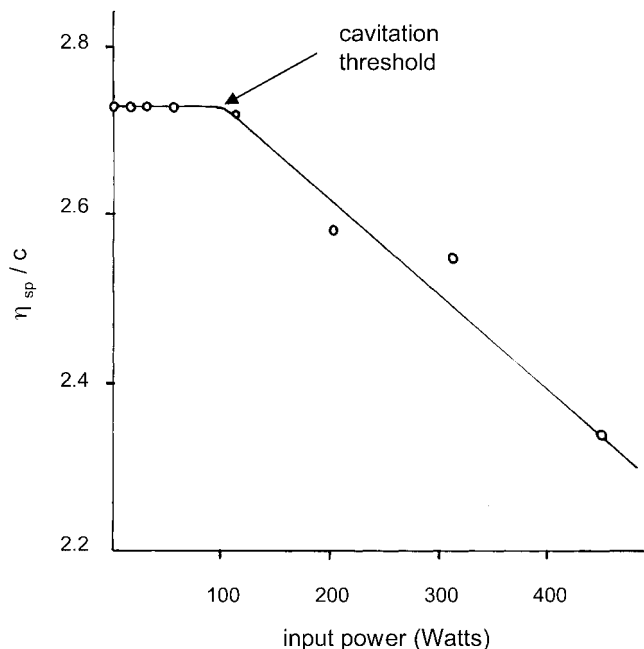


Fig. 5.21. Degradation of hydroxycellulose (0.8%; $f = 400$ kHz) as function of input power.

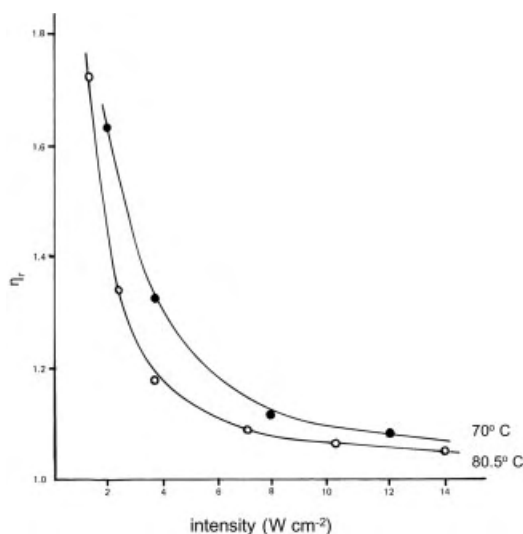


Fig. 5.22. Effect of intensity on degradation of polystyrene in toluene; initial R.M.M. = 300 000; irradiation time 90 min.

This variation in limiting molar mass with intensity can be predicted if we accept Schmid's hypothesis that a modified Stoke's equation can be applied to polymer degradation.

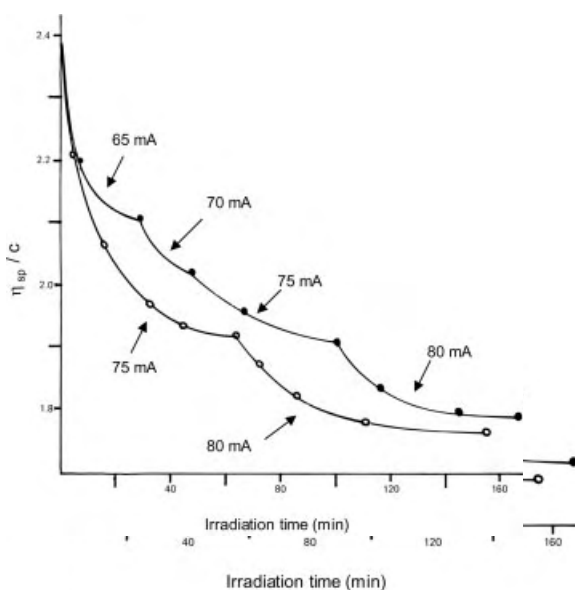


Fig. 5.23. Effect of intensity on the extent and rate of degradation of polystyrene in benzene.

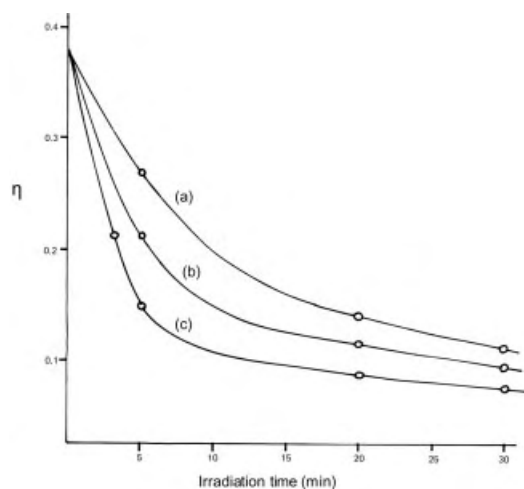


Fig. 5.24. Degradation of PMMA in chloroform (0.1%) at various irradiation intensities; (a) 0.8 W cm^{-2} ; (b) 1.3 W cm^{-2} ; (c) 2.2 W cm^{-2} .

For example, we showed in Chapter 2 that that the solvent velocity, V , was proportional to the acoustic pressure, P_a , (Eq. 2.11), and that the acoustic pressure was proportional to the ultrasonic intensity, I (Eq. 2.13).

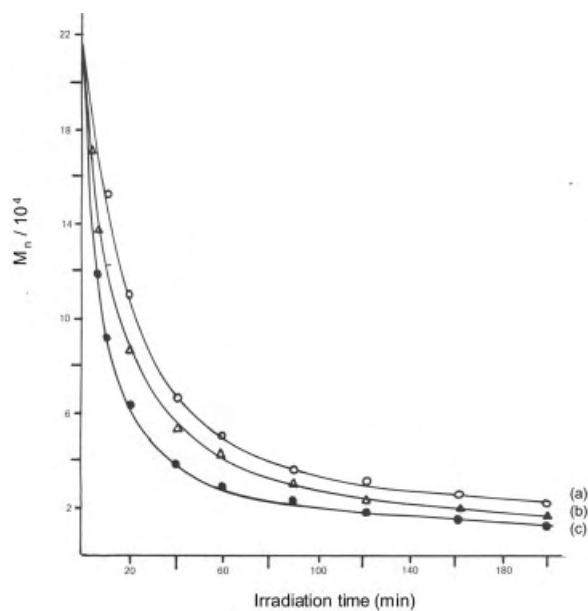


Fig. 5.25. Degradation of an aqueous solution of hydroxyethyl cellulose (0.5%) at various sonic intensities ($T = 25^\circ\text{C}$); (a) 1.5 A; (b) 2.0 A; (c) 2.5 A.

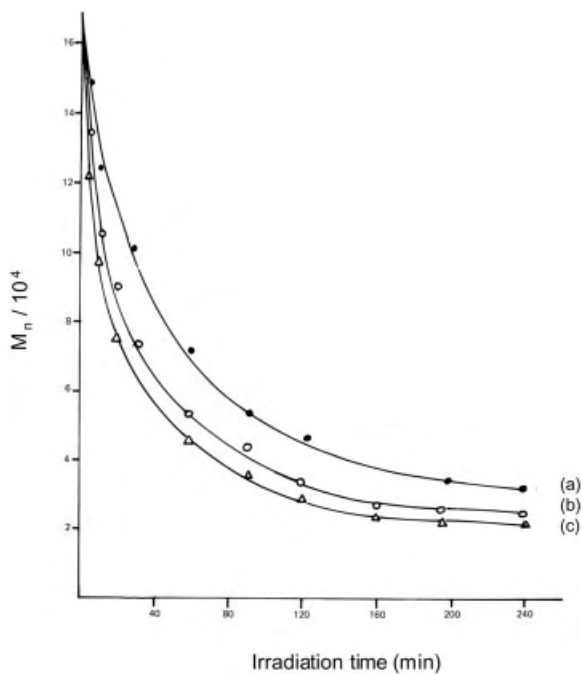


Fig. 5.26. Degradation of aqueous polyethylene oxide (0.5%) at various sonic intensities ($T = 25^\circ\text{C}$); (a) 1.5 A; (b) 2.0 A; (c) 2.5 A.

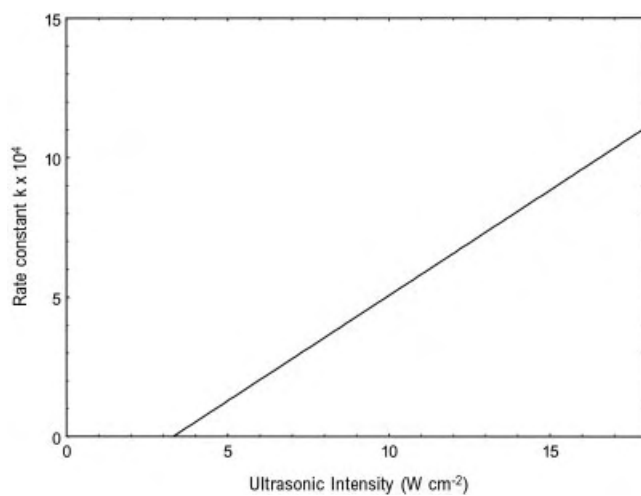


Fig. 5.27. Effect of ultrasound intensity on the degradation of polystyrene.

$$\frac{P_a}{V} = \rho c \quad (2.11)$$

$$I = \frac{P_A^2}{2\rho c} \quad (2.13)$$

where ρ and c are the density and velocity of sound in the fluid. Combining Eqs. 2.11 and 2.13 gives Eq. 5.23 which on substitution into Eq. 5.8 (taking F as 4.5×10^{-9} N) and using the example of polystyrene in benzene yields Eq. 5.24.

$$V = \left(\frac{2I}{\rho c} \right)^{1/2} \quad (5.23)$$

$$n = \frac{1.1 \times 10^6}{I^{1/2}} \quad (5.24)$$

Thus for an intensity of 10 W cm^{-2} (10^5 W m^{-2}), $n = 3480$ (e.g. a limiting R.M.M. of approx. 362 000) whilst the application of 50 W cm^{-2} gives an n value = 1556 (e.g. a limiting R.M.M. of 162 000).

5.3.6

External Pressure

Several workers have investigated the effect of pressure on ultrasonic degradation and obtained contradictory results. For example, whereas Schmid and Rommel observed that 5 and 8 atm respectively of excess pressure slowed and eventually stopped the ultrasonic degradation of nitrocellulose, the application of higher excess pressures, 8 and 15 atm, only resulted in a slowing down of the degradation rate for styrene, and then to the same extent for both pressures (Fig. 5.28). In contrast, Mark, although employing a lower molar mass polystyrene sample than Schmid, (140 000 compared with 850 000), had observed increases in the degradation rate with increases in pressure (Fig. 5.29).

Since both authors employed intensities equivalent to a pressure amplitude (P_A) of approximately 5 atm it was anticipated that if cavitation were the cause of degradation then the extent of degradation and its rate ought to have ceased completely at 15 atm (approx. P_h) since P_h was larger than P_A (see Section 2.6.5).

Melville and Murray have investigated the degradation of polystyrene in toluene, albeit *in vacuo* and at a slightly lower insonation frequency (213 kHz) and compared their results with those obtained by Schmid (300 kHz) at 15 atm (Tab. 5.9).

Apart from the initial values, there is a reasonable similarity between the results, i.e. initial rapid polymer breakdown merging into slower rates as the degradation pro-

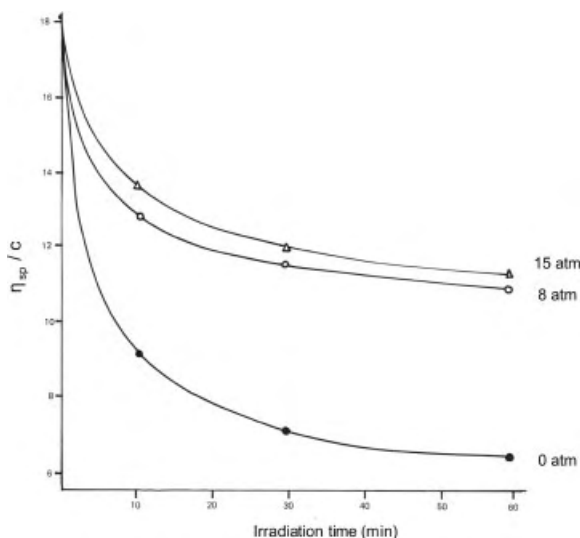


Fig. 5.28. Degradation of polystyrene in toluene at various applied pressures; Δ 15 atm; \circ 8 atm; \bullet 0 atm.

ceeds. If we are to conclude that cavitation is absent in the absence of a gas, or in the presence of a large overpressure, the above data suggests that degradation can still be accomplished by ultrasonic waves even in the absence of cavitation. One possible explanation is that shear forces are set up by the collapsing bubbles, the magnitude of which increases with increasing intensity of the wave. It is these shear forces which result in the stretching of the chain to breaking point and are therefore responsible for the observed degradation. In the presence of a gas, the forces will contain an added contribution from cavitation. The values for the limiting R.M.M.'s found by Melville, Schmid and Mark are given in Tab. 5.10.

Tab. 5.9 Degradation of polystyrene in toluene at various applied pressures
($T = 20^\circ\text{C}$; $f = 300\text{ kHz}$; intensity = 10 W cm^{-2}).

Irradiation time [min]	Melville (vacuo) η_{sp}/c	Schmid (15 atm) η_{sp}/c
0	2.72	15.7
5	2.38	2.5
20	2.03	2.0
60	1.41	1.8
100	1.14	—
120	—	1.6

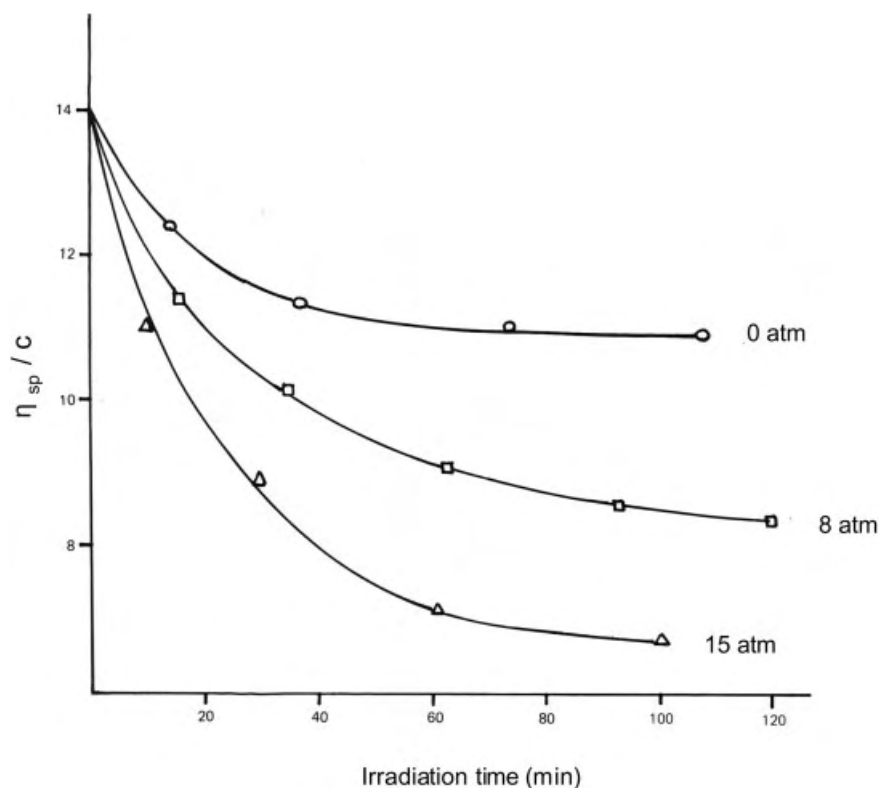


Fig. 5.29. Degradation of polystyrene in toluene at various applied pressures; $T = 20^\circ\text{C}$; $f = 300\text{ kHz}$; intensity $= 10\text{ W cm}^{-2}$.

Tab. 5.10 Limiting R.M.M. for polystyrene in toluene.

R.M.M.	Melville		Schmid		Mark	
Initial	700 000		850 000		140 000	
	Vacuo	1 atm	15 atm	1 atm	15 atm	1 atm
Final	226 000	47 000	121 000	28 000	70 000	10 000

Whereas the work of Melville and Schmid seems to confirm the importance of cavitation in polymer degradation, (i. e. less degradation in degassed or pressurised systems), Mark's value for the pressurised system is somewhat difficult to explain.

5.3.7

R.M.M. and Concentration

Schmid and Rommel, and separately Mostafa, have studied the degradation of a number of polystyrene samples of differing R.M.M. All authors found that the degradation rate (Fig. 5.10) was highest for the sample with the largest R.M.M. and that the curves for all samples converged in the later stages, apparently reaching the same final relative molar mass. Schmid and Rommel also found similar relationships in their investigations of polyvinyl acetate, polymethyl acrylate and nitrocellulose. Basedow [53], investigating the effect of ultrasound (20 kHz, 10 W cm⁻²) on the degradation of dextran, observed that for molar masses (M) higher than the limiting value the degradation rate was proportional to $M^{4/3}$; for molar masses below the limiting value the rate constant was proportional to $M^{5/6}$.

Several authors [21, 24, 33, 54–56] have also investigated the effect of solution concentration on degradation. In every case, the rate and extent of degradation have been found to decrease with increase in concentration (Fig. 5.30).

Such observations have been interpreted in terms of the increase in viscosity of the solution – i.e. the higher the viscosity the more difficult it becomes to cavitate the solution, at a given intensity, and the smaller is the degradation effect.

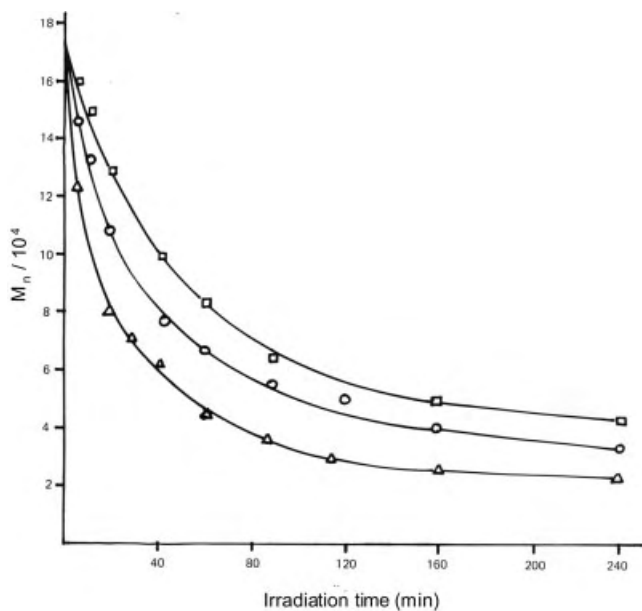


Fig. 5.30. Degradation of aqueous poly(ethylene oxide) at various concentrations (intensity = 2.5 A; $T = 25^\circ\text{C}$); $\square = 1.5\%$; $\circ = 1.0\%$; $\triangle = 0.5\%$.

Tab. 5.11 Rate constants and limiting molar masses for ultrasonic degradation of polystyrene at various concentrations in toluene.

Concentration [mass %]	Rate constant [$\text{min}^{-1} \times 10^{10}$]	Limiting molar mass
0.10	2.40	55 000
0.50	5.45	105 000
0.75	4.15	195 000
1.00	0.98	203 000

Price et al. [56] have fitted their degradation data for polystyrene in toluene to Eq. 5.12 and have shown, over a limited sonication time interval, that the value of the limiting molar mass increased with increase in concentration. (Tab. 5.11).

We have also shown that the rate constants for the degradation of aqueous (native) dextran, at a given intensity (variable temperature) or a given temperature (variable intensity), appear to be dependent on the solution concentration (Tab. 5.12a). However the limiting molar mass appears to be less dependent (Tab. 5.12b), especially at low power or high temperature where the mechanical/cavitation effects are less pronounced. This suggests that experimentally observed limiting molar mass is a function of both the total irradiation time and ultrasonic intensity.

Tab. 5.12a Rate constant and limiting molar masses (after 8 h ultrasonic irradiation) for the ultrasonic degradation of aqueous dextran; (a) at 30 °C and variable ultrasonic power; (b) at an ultrasonic power input of 60 W and variable temperature.

(a)

Concentration [mass %]	Rate constant [$\text{s}^{-1} \times 10^{10}$]			Limiting molar mass		
	20 W	35 W	60 W	20 W	35 W	60 W
2	4.4	5.3	10.5	50 000	45 000	45 000
5	3.2	3.5	8.3	200 000	110 000	80 000
10	1.1	1.5	3.9	230 000	170 000	60 000

(b)

Concentration [mass %]	Rate constant [$\text{s}^{-1} \times 10^{10}$]			Limiting molar mass		
	30 °C	50 °C	70 °C	30 °C	50 °C	70 °C
2	10.6	6.5	3.8	45,000	45,000	40,000
5	8.3	3.4	3.5	80,000	80,000	60,000
10	3.9	3.3	2.7	60,000	60,000	70,000

5.3.8

Nature of the Polymer

There is much contradictory evidence as to whether the degradation rate is influenced by the chemical nature of the backbone. For example, Garcia Alvarez et al. [57] investigating the degradation of polyaspartates and polyglutamates observed that whilst the degradation rate increased slightly with increase in the concentration of the amide groups within the main chain, similar limiting molar mass values were obtained. The authors also found that the rate of degradation was influenced by the “effective” diameter of a polymer chain, after taking account of the size of the side groups [27]. For example poly(*n*-dodecyl-L-aspartate) degraded faster than the *n*-propyl derivative. A similar effect has been observed for the poly(methacrylates), where poly(lauryl methacrylate) has been found to degrade four times faster than poly(methyl methacrylate). This view is supported by Thomas [58] who found that while poly(styrene) and poly(methyl methacrylate) degraded at similar rates, poly(lauryl methacrylate) degraded approximately three times faster. On the other hand, Malhotra [59] has degraded a series of alkyl methacrylates and observed similar kinetic results. Schoon and Reiber [52] have studied the degradation of a wide variety of polymers (e. g. poly(styrene), poly(styrene-butadiene) copolymer, poly(dimethyl siloxane) and natural rubber) and have found that under similar conditions all polymers gave similar results suggesting that the chemical nature of the polymer was relatively unimportant.

All the above factors may be summarised by Tab. 5.13.

In an attempt to explain these observations several models, based upon kinetic or molecular considerations, have been reported.

Tab. 5.13 Factors which increase the rate and extent of degradation.

-
- (a) Saturation of the polymer solution with a gas.
 - (b) Employing a gas with a low solubility.
 - (c) Using a solvent with a low vapour pressure.
 - (d) Reducing the experimental temperature.
 - (e) Reducing the insonation frequency.
 - (f) Increasing the intensity of irradiation.
 - (g) Decreasing the solution concentration.
 - (h) Increasing the R.M.M. of the polymer.
-

5.4

Degradation Mechanisms

Jellinek's model for polymer breakdown is simply an extension of the concepts identified by Schmid except that the frictional and impact forces were considered to be a consequence of cavity collapse. Using equations developed by Noltingk and Neppiras, Jellinek deduced that the velocity of a solvent molecule in the vicinity of a collapsing bubble, containing a monatomic gas, was approx. 300 cm s^{-1} . By employing a modified Stokes formula (Eq. 5.8) he was able to show that this velocity produced a frictional force of $3.2 \times 10^{-8} \text{ N}$ per bond, an order of magnitude larger than that necessary to break a C-C bond. Further, it is possible to deduce from Eq. 5.8 that for a solvent velocity of this magnitude (300 cm s^{-1}) a polystyrene molecule with a degree of polymerisation less than 430 (i. e. $M_n = 43000$) ought not be degraded – i. e. there is a lower limit of R.M.M.

Doulah [27], on the other hand, has suggested that it is the shock wave energy, released as the cavity collapses, not the shear force which is responsible for the degradation. The suggestion is that the bubble, in the cavitation field, acts as a power transformer converting the acoustic energy into hydrodynamic energy. By considering the shock waves to give rise to a series of eddies and that the macromolecule, suspended in the cavitation field, will experience motions of various amplitude and intensity due to the eddy motion, he was able to calculate the dynamic force set up across the length of the macromolecule. The results of his calculations indicated that the degradation rate was dependent upon (a) acoustic intensity, (b) the size of the macromolecule, and (c) suggested that there would be a minimum chain length below which degradation would not occur. All three deductions have been confirmed experimentally. However, what neither of the above two theories could predict was the point, or points, in the macromolecule where bond breakage would occur. Although it might be expected that ultrasonic degradation, like chemical or photodegradation, occurs at the points of inherent weakness in the polymer's backbone, work by Melville seems to refute this suggestion. For example, Melville has shown that the degradation of two separate polymethyl methacrylate (A) – polyacrylonitrile (B) copolymers (molar ratios

Tab. 5.14 Comparison of effect of irradiation ($\sim 6 \text{ h}$) on R.M.M. of various polymers.

Polymer/copolymer	Initial R.M.M.	Final R.M.M.
Methyl methacrylate	725 000	544 000 \pm 40 000
Methyl methacrylate*	725 000	460 000 \pm 40 000
Methyl methacrylate-acrylonitrile	615 000	385 000 \pm 25 000
Methyl methacrylate-acrylonitrile*	615 000	395 000 \pm 25 000

* Repeat determination of R.M.M.

of A:B of approximately 40:1 and 400:1 respectively) yielded almost identical final molar masses, as determined by osmometry, after irradiation with ultrasound (Tab. 5.14).

If it is assumed that the A-B linkages are appreciably weaker than the corresponding A-A or B-B linkages, then appreciably different molar masses ought to have been obtained as is the case for thermal degradation. For example we might expect that the R.M.M. would fall to the average value of the methyl methacrylate chains which for the 40:1 copolymer (initial R.M.M. 547 000) would be 4000 ($= 40 \times 101$), whilst for the copolymer of R.M.M. 615 000 this would be 41 000 ($= 411 \times 101$). Further confirmation that degradation is not taking place selectively at the A-B linkages is afforded by Fig. 5.19 where it can be seen there is no appreciable difference in the rate of degradation of the two copolymers. If scission does not take place at the weak spots within the macromolecule we are left to conclude that scission is either a random process or that it takes place at the midpoint of the polymer chains.

Elegant work by Van der Hoff [60] seems to suggest that it is the latter, or more correctly there is a Gaussian distribution about the midpoint of a chain. However, as to whether the main chains are primarily broken by ultrasonic action is still open to question since it is possible that the main chain scissions are secondary effects due to chemical reactions initiated by unstable intermediates, such as free radicals or ions, produced by sonication. For example McKay [61] has shown that hydroxyl radicals, generated by the oxidation of Fe^{2+} by H_2O_2 , are the cause of chain scission in polyacrylamide molecules in aqueous solution.

Cleavage of a covalent bond may occur either homolytically or heterolytically and both possibilities have been observed during polymer degradation. Homolytic cleavage is the most common with the depolymerisation resulting in the breakage of a carbon-carbon atomic bond in the macromolecule to produce long chain radical entities [62]. The existence of these radical entities has been established by investigating the depolymerisation process in the presence of various radical scavengers such as diphenyl picrylhydracyl (DPPH). Spectroscopic analysis of the loss of DPPH

Tab. 5.15 Ultrasonic degradation (20 kHz, 70 W, 27 °C) of various polyacrylates (PRMA) in toluene.

Irradiation time [min]	Heterogeneity index M_w/M_n				
	R =	Methyl	Ethyl	<i>n</i> -Butyl	Cyclohexyl
0		4.20	2.80	2.66	2.40
60		2.07	1.80	1.80	1.68
120		1.77	1.64	1.72	1.58
180		1.58	1.62	1.90	1.50
240		1.46	1.48	1.80	1.49
360		1.45	1.54	1.66	1.46
480		1.38	1.43	1.62	1.45

($\lambda_{\text{max}} = 525 \text{ nm}$) has allowed both a determination of the depolymerisation rate and the number of break points (i. e. 2 DPPH molecules per bond breakage). Evidence for the formation of macroradicals in the degradation of polymethyl methacrylate, polystyrene and polyvinylacetate has also been provided by Tabata [63] using spin trapping and esr techniques. Taranukha [64] has also used spin traps to study the degradation of aqueous polyacrylamide.

Obviously in the absence of radical scavengers the molecular fragments are free to recombine by the usual termination mechanisms. Combination termination will produce macromolecules of the same, or differing lengths, as those existing just prior to bond breakage, depending upon whether the combining molecular fragments are from the same or differing polymer chains. Disproportionation termination between fragments no matter what their origin must result in smaller macromolecules. Thus in the long term it might be anticipated that degradation will take place with a decrease in R.M.M. What perhaps is not expected is the observed reduction in polydispersity (i. e. ratio of $M_w : M_n$) with the passage of time (Tab. 5.15).

This reduction has significant consequences, since although the absolute magnitude of a polymer's relative molar mass (M_w or M_n) is important, there is a whole series of physicochemical properties (e. g. film formation, chemical stability, solution flow etc.) which depend upon the degree of polydispersion. In hindsight the reduction in polydispersity can be explained using the ideas of Glynn and Jellinek. For example, according to Jellinek the larger the polymer the greater is the expected frictional force and the more likely that bond breakage will occur. If scission is Gaussian (Glynn), then breakage will produce molecular fractions of slightly different size and if the larger fractions, from two separate chains, recombine the resultant polymer will still be sufficiently large to be further degraded. Combination of the smaller fractions, however, will lead to a decrease in molecular size and the chains will have a lower probability of further degradation. With the passage of time there will be a higher proportion of the smaller R.M.M. material in the system and the sample will become more homogeneous. Although most of the reported literature seems to infer that degradation of a macromolecule takes place by main chain scission, we should not rule out the possibility of C-H scission since the bond energy for the latter (412 kJ mol^{-1}) is only some

Tab. 5.16 Degradation of PNVK in benzene as a function of irradiation time ($HI = \frac{M_w}{M_n}$).

		Irradiation time [min]					
		0	10	20	30	60	120
M_n	$[10^3]$	296	326	245	245	183	143
M_w	$[10^3]$	715	555	415	398	276	211
HI		2.42	1.71	1.69	1.63	1.51	1.48

20 % higher than that for the former (350 kJ mol^{-1}). The consequence of such a scission would, on termination by combination lead to branched structures.

Interestingly, our own studies have revealed that both the shape of the macromolecule and the glass transition temperature, T_g , change with irradiation time. For example, the irradiation of a bimodal commercial sample of polyvinylcarbazole (PNVK) (Fig. 5.31a) in dichloromethane occurred with an initial increase in (the number average) molar mass (M_n) and an apparent loss in the bimodal nature of the polymer (Tab. 5.16, Fig. 5.31b). A similar initial increase in M_n has been observed by Price [39] during a sonically induced polymerisation.

The shapes of the degradation curves (Fig. 5.31b), and the increase in M_n can be rationalised in terms of a higher probability and more rapid degradation of the larger R.M.M. sample (peak B, Fig. 5.31a) giving rise to molecules with a higher R.M.M. than the average for peak A (i.e increase in $\bar{M}_n = \frac{\sum N_i \times M_i}{\sum N_i}$) but lower than average for peak B (i.e lower $\bar{M}_w = \frac{\sum w_i \times M_i}{\sum w_i}$). (Similar behaviour was observed with a sample prepared in our laboratories by a free radical mechanism and subsequently sonicated in benzene).

For each sample, the Flory Huggins constants (k' , Eq. 5.25) were also determined (by viscosity measurements) as function of sonication time and are given in Tab. 5.17.

$$\eta_{sp}/c = [\eta] + k'[\eta]^2 c \quad (5.25)$$

Whilst not all workers agree as to the relevance of individual k' values, all agree that for two polymers with similar \bar{M}_n values, then the polymer with the lowest limiting viscosity value will be the more branched. Price [65, 66] has observed a similar trend in molar mass with irradiation, albeit in a sonochemically polymerising system.

It is well known that the structure, physical and physicochemical characteristics of macromolecules depend not only on the nature of the monomer (homopolymer) or monomers (copolymer) from which they are synthesised but also on the method of production (e. g. graft, block or random copolymers). For instance, whereas random copolymerisation of two monomers A and B produces a polymer with a property (e. g. solubility, polarity) which is the weighted average of the two constituent monomers, block (or graft) copolymers have properties which are the sum of those of the two homopolymers. For example a graft copolymer consisting of water soluble (polyethylene oxide) and oil soluble (polystyrene) components is capable of dissolving in both solvent types. The preparation of graft copolymers can be accomplished by irradiating a mixture of two homopolymers with either γ or X-rays, or by polymerisation of a monomer (A) from initiation sites along the polymer chain of monomer B. Alternatively the copolymer can be prepared by a mechanical blending of the two homopolymers. To effect the latter type of process and produce a genuine graft copolymer rather than a simple mixture of the two homopolymers the two components are

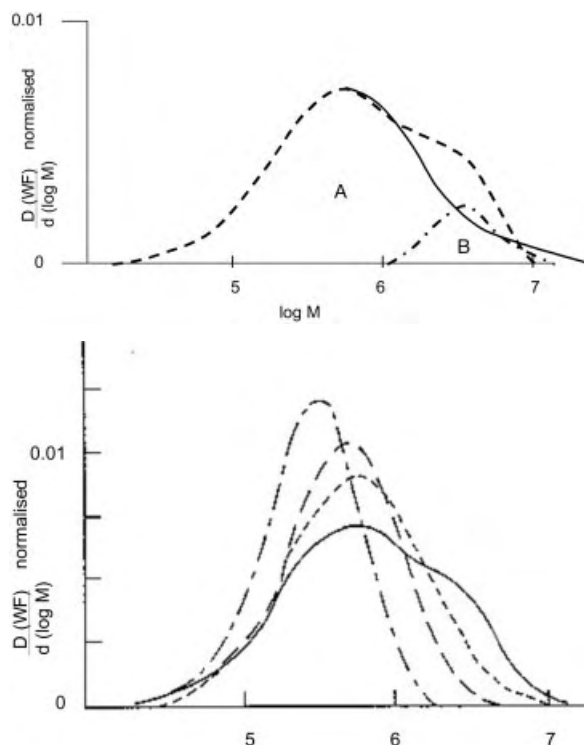


Fig. 5.31. R.M.M. distribution function (a) initial sample; (b) PNVK in dichloromethane; irradiation times: solid curve = 0 min; dotted curve = 5 min; dashed curve = 15 min; chain curve = 20 min; (WF = weight fraction)

milled or masticated together. The mechanical shearing during the milling process results in homolytic cleavage of the bonds and subsequent cross combination between the different polymer fragments then results in a graft copolymer. Block copolymers

Tab. 5.17 Degradation of PNVK in benzene as a function of irradiation time.

	Irradiation time [min]					
	0	10	20	30	60	120
$\eta[10^2 \text{ dm}^3 \text{ g}^{-1}]^a$	6.76	6.08	4.92	4.24	3.52	3.56
k'^b	0.62	0.63	0.90	1.34	1.84	0.52
$T_g[\text{K}]^c$	500	503	502	501	497	503
$M_n[10^3]$	296	326	245	245	183	143

^a $[\eta]$ is limiting viscosity obtained from Eq. 5.25

^b k' is slope of Eq. 5.25

^c T_g is glass transition temperature

on the other hand are often produced *via* anionic mechanisms. The process utilises the fact that the anionic chain ends often remain “alive”, particularly at low temperature, even though the monomer has been consumed and that chain growth can be restarted by addition of more of the same monomer, to give a homopolymer, or addition of a different monomer to give the block copolymer. In practise some restrictions exist with respect to the type of monomers which can be used in a block copolymerisation reaction in that the monomers should have similar electron affinities if mutual reinitiation is to take place. However as with graft copolymer production milling of a mixture of homopolymers can also be used to prepare the block copolymer. This technique alleviates many of the hazardous experimental difficulties which may be experienced using the anionic technique.

We have already seen in this section how ultrasound, like milling, is capable of producing chain scission and thus give rise to macroradicals. It is therefore not surprising that the application of ultrasound to the synthesis and modification of polymers has attracted, and continues to attract, the attention of many investigators.

5.5 Polymer Synthesis

Early investigations into the use of ultrasound in polymer synthesis involved sonicating solutions containing a polymer and a monomer [67]. Polymerisation was thought to be affected by utilising the shock wave energy, released on bubble collapse, to homolytically break a carbon-carbon bond in the polymer’s backbone thereby producing a radical entity which could attack the monomer and polymerise by a conventional mechanism. Driscoll using polystyrene as the “initiating” species was able to polymerise styrene in toluene/acetone as solvent at a rate of 1 % per hour at 60 °C. This conversion rate suggests that the ultrasonic degradation of polystyrene is providing approximately $5 \times 10^{-8} \text{ mol dm}^{-3} \text{ s}^{-1}$ of radicals. To obtain this rate, at a similar temperature, with a conventional initiator (e. g. AZBN) would require approximately 0.4 g/L of initiator, an order of magnitude less than used industrially.

In principle ultrasound can be used to prepare both block (Fig. 5.32) and graft copolymers (Fig. 5.33).

Graft polymers are produced by sonicating a mixture of a polymer and a dissimilar monomer. The graft is produced by breaking a side chain bond to produce the macro-radical (Fig. 5.33) which then reacts with the monomer.

Keqiang [43] has successfully produced block copolymers, based upon cellulose, while Henglein has been able to produce both graft and block copolymers using polystyrene and polymethyl methacrylate. Price [68] has shown that the irradiation of mixtures of polystyrene and poly(*cis*-butadiene) and separately polystyrene and

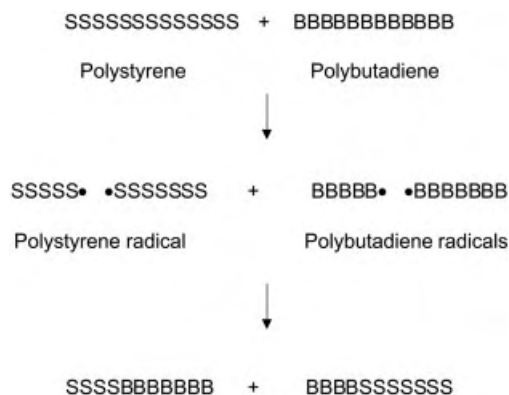


Fig. 5.32. Production of a block copolymer by the ultrasonic irradiation of two homopolymers.

poly(methyl phenyl silane) in toluene led the formation of block copolymers and to the compatibilisation of otherwise immiscible polymer mixtures.

Malhorta [7] has employed a variety of homopolymers (rigid and flexible) in the synthesis of block copolymers but met with only limited success. Homopolymers with bulky substituents, although able to undergo chain scission did not result in scrambled copolymers in the presence of polystyrene. In all of the above syntheses, degradation of the homopolymers by ultrasound was the first step in the production of long chain radicals of each component which then terminated by cross combination. Obviously to ensure production of the macroradical, the homopolymers employed must have degrees of polymerisation greater than P_L . We have already seen (Tab. 5.2) that polystyrene samples of approx. 200 000 are degraded to give polymers with final R.M.M. values of approximately 70 000. If Glynn's gaussian distribution mechanism is correct, this implies only 2 C-C bonds are broken overall i.e. 200 000 to 100 000 and then 100 000 to 50 000. A similar deductions can be made from Tab. 5.10. However this is an overall resultant value for chain scission and

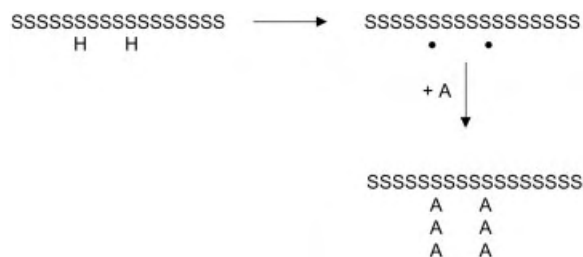


Fig. 5.33. Production of a graft copolymer.

does not take into account that bonds are being remade due to combination termination. Malhorta has deduced from GPC analysis that the rate of bond scission in a polystyrene sample (2 % in THF), at 27 °C, after 30 min irradiation (20 kHz, 70 W) is 0.032 scissions per minute (i. e. 1 bond in 30 min) whilst after 8 h it is 0.014 scissions per minute – i. e. a total of 7. At a lower temperature (– 20 °C) the number is increased considerably, as expected, being 0.116 scissions per minute after 30 min and 0.053 scissions per minute after 4 h. What may be surprising therefore is the high yield of block copolymers produced, often as high as 90 %, which results from the breakage of only a limited number of bonds in the macromolecule. This prompted Berlin [69] to suggest that the macroradical is also capable of degrading a stable macromolecule.

In principle block copolymers can also be produced by irradiating solutions containing a homopolymer (from monomer type A) and a monomer (type B) (Fig. 5.34). In such cases, polymerisation resembles that of graft polymerisation where the monomer (B) is thought to be initiated by the macroradical produced by the ultrasonic degradation of the homopolymer. In those cases where polymer was deliberately absent, polymerisation was either not observed to occur or proceeded at a similar rate to that in the presence of polymer.

For example, Melville [26] studied the ultrasonically induced polymerisation of monomers such as styrene, methyl methacrylate and vinyl acetate in the presence and absence of polymethyl methacrylate and found that the polymerisation rates ($\sim 1\%$ conversion/h) were not substantially increased by the presence of polymer. He concluded, in contrast to Driscoll, that the degradation of polymer was not the major source of radical production. Using hydroquinone as an inhibitor, he was able to deduce, from retardation times, that the rate of radical production was $\sim 2 \times 10^{-9} \text{ mol dm}^{-3} \text{ s}^{-1}$. A typical value for radical production using as an example the thermal initiation of AZBN ($10^{-3} \text{ mol dm}^{-3}$) at 60 °C is $\sim 2 \times 10^{-8} \text{ mol dm}^{-3} \text{ s}^{-1}$ – i. e. an order of magnitude greater.

Prior to 1972 there had been only a few reports of the direct sonochemical initiation of monomer. Lindstrom and Lamm [70] had reported the aqueous polymerisation of acrylonitrile, while Henglein [62, 71] reported the polymerisation of acrylamide in water. By assuming the initiating species were either H^\bullet or $\bullet\text{OH}$ (or both), produced

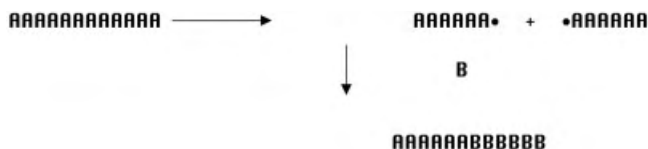
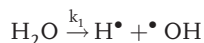


Fig. 5.34. The production of block copolymers from homopolymer A and monomer B.

during the cavitation process, or radicals produced as a result of polymer (P) degradation, Lindstrom and Lamm proposed the following mechanism:



On applying the stationary state (i.e. rate of initiation = rate of termination), the authors deduced that the radical concentration $[\text{R}^\bullet]$ and propagation rate, R_p , were given respectively by:

$$[\text{R}^\bullet] = \left[\frac{(k_1 + k_2[\text{P}])}{k_4} \right]^{1/2} \quad (5.26)$$

$$R_p = -\frac{d[\text{M}]}{dt} = k_3[\text{M}] [\text{R}^\bullet] \quad (5.27)$$

On expressing both the polymer and monomer concentrations in terms of the fraction polymerised (or extent of reaction, $p = \left[\frac{([\text{M}]_0 - [\text{M}])}{[\text{M}]_0} \right]$), they reduced Eq. 5.27 to

$$\frac{dp}{dt} = (1 - p)k_3 \left[\frac{k_1 + [\text{M}]_0 k_2 p/n}{k_4} \right]^{1/2} \quad (5.28)$$

where n was the average number of monomers in the polymer i.e. $[\text{P}] = \frac{([\text{M}]_0 - [\text{M}])}{n}$. For this particular polymerisation reaction, the extent of reaction over the time interval investigated never exceeded 0.02. By making the assumption that $(1 - p)$ could be approximated to unity, integration of Eq. 5.28 yielded Eq. 5.29, a relationship which the authors found fitted the data extremely well:

$$t = c_1[(1 + c_2 p)^{1/2} - 1] \quad (5.29)$$

In the above, $c_1 = \frac{2n k_1^{1/2} k_4^{1/2}}{k_2 k_3 [\text{M}]_0}$ and $c_2 = \frac{k_2 [\text{M}]_0}{k_1 n}$.

This early investigation of Lindstrom and Lamm was also particularly important in that it proved there had to be a threshold intensity of ultrasound before polymerisation took place.

Berlin [69] also confirmed the importance of the presence of $\bullet\text{OH}$ radicals in his investigation of the polymerisation of polystyrene in the presence of styrene monomer when he found the addition of water to the reaction solvent (benzene) greatly enhanced the yield of polymer. However, latterly it has been argued for these systems that the appearance of water decomposition products (e. g. H_2O_2) led to oxidation of the various impurities, which previously, may have acted as inhibitors in the polymerisation process.

Ultrasonic waves have also been found to increase the rates of emulsion and suspension polymerisations. For example, Hatate [72] has investigated the suspension polymerisation of styrene under ultrasonic irradiation in both batch and continuously stirred reactors. For both processes he was able to confirm that irradiation was an effective method of preventing both agglomeration between the droplets and the sticking of droplets to the reactor wall. Both these factors can lead to serious problems such as heat build up and the formation of large masses and make it impossible to carry out prolonged operations. In the case of the batch reactor, the effects of ultrasound on the conversion and the average R.M.M. were found to be negligibly small. Hatate's suggestion was that the ultrasonic energy supplied to the monomer phase (500 W), whilst sufficient to prevent agglomeration, was not great enough to effect the polymerisation rate. Unfortunately it was not possible to quantify the effect of ultrasound in the continuous process due to the extreme difficulty in the absence of ultrasound in realising the steady state due to agglomeration and sticking of the droplets.

For the thermally initiated (potassium persulphate) emulsion polymerisation of styrene, we have observed [73] a twofold increase in the initial polymerisation rate in the presence of ultrasound (20 kHz), the increase being dependent upon the level of surfactant employed. Several workers have suggested that possible explanations for the observed increase in rate are:

1. the oxidation of impurities e.g. inhibitors,
2. the removal of oxygen (known to inhibit radical reactions) by ultrasonic degassing, and
3. ultrasonic degradation of the polymer to provide more active sites (i. e. autocatalysis).

Since we still observed increased rates in the absence of inhibitor and in the presence of ultrasound (Fig. 5.35) we have explained the reduction or lack of an induction period in the presence of ultrasound in terms of two factors; namely, a greater radical production both from enhanced initiator breakdown [74], and/or degradation of the polymer, and also from the creation of a far more stable emulsion. This latter point was confirmed visually. Depending upon the irradiation power and surfactant level employed, we were able to observe up to 40 % increase in initiator breakdown and a de-

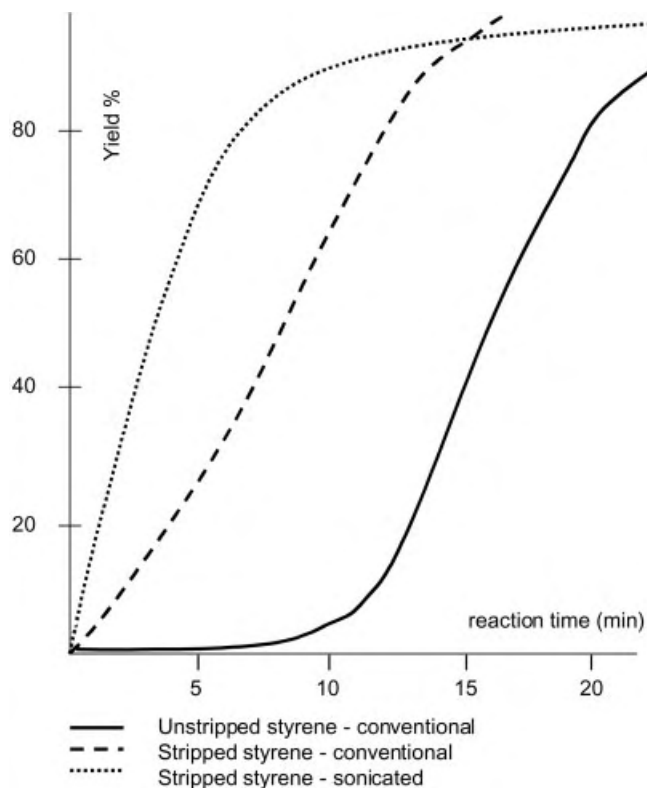


Fig. 5.35. Emulsion polymerisation in the presence and absence of inhibitor and in the presence and absence of ultrasound (Conditions: 8 % styrene (w/v), 0.8 % surfactant (w/v), potassium persulphate, $T = 70^{\circ}\text{C}$).

crease of one order of magnitude in molar mass (12×10^6 to 1×10^6) in the presence of ultrasound. And, since irradiation only appeared effective during the initial part of the process (< 25 min), we also investigated the effect of applying ultrasound for an initial 30 min period before allowing the reaction to proceed conventionally. The result was an improved yield in the early period of the reaction, when compared to conventional polymerisation, followed by a slightly improved yield in the latter stages when compared to the continuously sonicated reaction.

Recently Biggs [74] has investigated the emulsion polymerisation of styrene using ultrasonic irradiation as the initiation source (i. e. in the absence of a chemical initiator). Similar to Lorimer and Mason using a thermally initiated system, Biggs found both a marked increase in monomer conversion rate as a function of time as the ultrasonic intensity was increased but remarkable constancy in the resultant latex particle

size (40–50 nm). Work at different temperatures and surfactant concentrations confirmed Lorimer and Mason's findings that the higher the temperature or surfactant concentration the faster the rate for a given ultrasonic intensity.

Until the work by Kruus [76], few workers had systematically investigated the effects of varying such parameters as intensity, frequency, temperature and the nature of the gas on the polymerisation process.

Berlin [69] had shown that for the block copolymerisation of polymethyl methacrylate with acrylonitrile, the time required to produce a given amount of polyacrylonitrile in the block decreased with increasing intensity.

Miyata and Nakashio [77] studied the effect of frequency and intensity on the thermally initiated (AIBN) bulk polymerisation of styrene and found that whilst the mechanism of polymerisation was not affected by the presence of ultrasound, the overall rate constant, k , decreased linearly with increase in the intensity whilst the average R.M.M. increased slightly. The decrease in the overall value of k they interpreted as being caused by either an increase in the termination reaction, specifically the termination rate constant, k_t , or a decrease in the initiator efficiency. The increase in $k_t (= k_t^0/\eta)$ is the more reasonable in that ultrasound is known to reduce the viscosity of polymer solutions. This reduction in viscosity and consequent increase in k_t could account for our observed reductions [78] in initial rate of polymerisation of *N*-vinylpyrrolidone in water. However this explanation does not account for the large rate increase observed for the pure monomer system.

Unfortunately little can be learned from Myata's and Nakashio's work at different frequencies. Employing a constant output power from the sound generator, and operating at 200, 400, 600 and 800 kHz, they observed a maximum for the value of k at 400 kHz. Whether the maximum is meaningful is uncertain because of the experimental conditions employed. It has already been suggested that larger input intensities are necessary, at the higher frequencies, if equivalent sonochemical effects are to be produced. However, it is important to recognise that frequency is a factor which determines cavitation threshold, size of bubble and the time scale of bubble growth and collapse. Therefore it is anticipated that changing frequency will alter the polymerisation process.

Kruus [76] investigated the homopolymerisation of methyl methacrylate (MMA) at different temperatures and different acoustic intensities in the absence of solvent (i. e. bulk polymerisation), polymer and initiator. The work showed that although intense ultrasound could be used to initiate polymersiation, the yields were too small (< 4 % per hour) to suggest that the technique could provide a commercial alternative to the conventional methods (Fig. 5.36).

To explain his observed variations of polymerisation rate with time, reaction volume and acoustic intensity, Kruus adopted the following reaction mechanism in which he regarded cavitation bubbles as a "reactant" and represented their concentration as $[C]$.



By applying the steady state analysis (i. e. rate of production of radical = rate of loss of radicals) gives Eq. 5.35, and assuming the concentrations of the cavitation bubbles $[C]$ could be expressed as

$$[C] = \frac{N_c}{V} = \frac{FI}{V}$$

where N_c is the number of cavitation bubbles, V is the reaction volume, I is the acoustic intensity and F is a proportionality constant, Kruus was able to deduce that the rate of polymerisation was inversely proportional to the square root of the acoustic intensity (Eq. 5.36) provided all other parameters were kept constant.

$$[R^\bullet] = \left(\frac{k_1[M][C] + k_3[P][C]}{k_t} \right)^{1/2} \approx \left(\frac{k_1[M][C]}{k_t} \right)^{1/2} = \left(\frac{k_1[M][FI/V]}{k_t} \right)^{1/2} \quad (5.35)$$

$$R_p = \frac{-d[M]}{dt} = k_p[M][R^\bullet] = K[M]^{3/2} \left(\frac{FI}{V} \right)^{1/2} \quad (5.36)$$

This dependence of the rate (R_p) on the square root of the acoustic intensity (Eq. 5.36, Fig. 5.37) is very similar to that observed for photoinitiated polymerisations where the propagation rate is proportional to the square root of the light intensity.

Fig. 5.37 also implies that there exists a cavitation threshold for this system, since polymerisation only occurs when the intensity is greater than 2 W cm^{-2} . This is in agreement with earlier work by Lindstrom and Lamm and ourselves.

Kruus also carried out several polymerisations at constant intensity (20 W cm^{-2}) in the temperature range -17°C to $+40^\circ\text{C}$ (Fig. 5.36). The Arrhenius plot yielded an activation energy of 19 kJ mol^{-1} , a value which was in good agreement with that reported ($17-20 \text{ kJ mol}^{-1}$) for the bulk polymerisation of MMA when the contribution from initiation is excluded. This suggests that initiation by ultrasound is independent of temperature, or has a small to negligible activation energy, and in this respect resembles photopolymerisation.

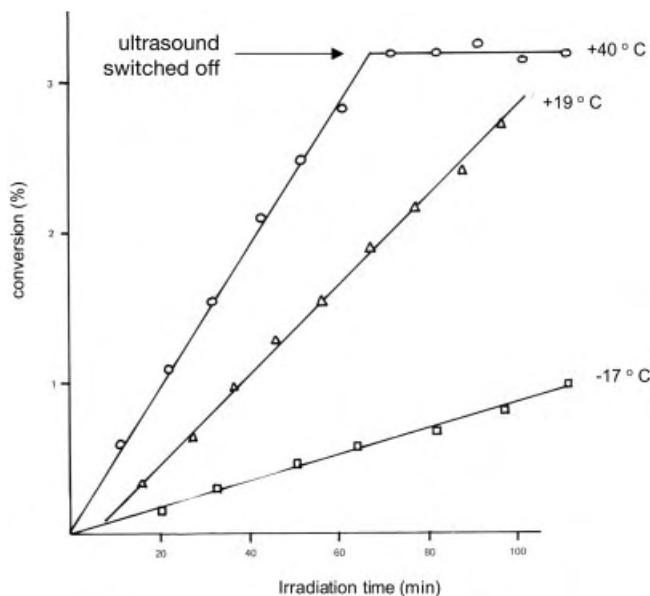


Fig. 5.36. Bulk polymerisation of polymethyl methacrylate (PMMA) in the presence of ultrasound (intensity = 20 W cm^{-2} , $f = 20 \text{ kHz}$); $\circ = +40^\circ\text{C}$, $\triangle = +19^\circ\text{C}$; $\square = -17^\circ\text{C}$.

Kruus also conducted experiments in the presence of the radical scavenger diphenylpicrylhydrazyl (DPPH) and observed induction periods which were roughly proportional to concentration of DPPH employed. This clearly demonstrates the free radical nature of the polymerisation. By assuming that each of the monomer radicals produced by the cavitation process (Eq. 5.30) reacted with one DPPH molecule, he was able to deduce the following kinetic relationship:

$$-\frac{d[\text{DPPH}]}{dt} = 2f k_1 [\text{M}]_0 \left(\frac{FI}{V} \right) \quad (5.37)$$

which on integration yields:

$$[\text{DPPH}]_0 - [\text{DPPH}]_t = 2f k_1 [\text{M}]_0 \left(\frac{FI}{V} \right) t \quad (5.38)$$

Excellent correlations were obtained (> 0.97) for plots of the consumed DPPH with time (t), intensity (I) and reciprocal volume ($1/V$).

Experiments were also performed at various temperatures in the presence of DPPH. Although the data fitted the conventional Arrhenius relationship (Eq. 5.39), it gave an activation energy which was negative i.e. inverse Arrhenius behaviour.

$$\ln k = \ln A - \frac{E}{RT} \quad (5.39)$$

(In the above equation, k is the rate constant, A is the pre-exponential or Arrhenius factor, E is the activation energy, R is the gas constant ($8.314 \text{ J mol}^{-1} \text{ K}^{-1}$) and T is the reaction temperature in Kelvin.)

This work was also particularly important in that it showed that polymerisation ceased in the absence of ultrasound (Fig. 5.36 at $T = 40^\circ\text{C}$). Although this phenomenon has not been utilised it does offer the possibility of controlling runaway exothermic reactions.

Driscoll [67], Lorimer and Mason [79] and Price [65] have also obtained inverse Arrhenius temperature dependencies for reactions performed in the presence of ultrasound. For example Driscoll has investigated the polymerisation of styrene and methyl methacrylate in the presence of their respective homopolymers and observed that the lower the reaction temperature the faster was the reaction rate and the higher the final polymer yield (Figs. 5.38 and 5.39). Price on the other hand using a non polymer system has sonicated methyl butyrate (MeOBu) and compared the rates of radical production in the absence and presence of the initiator azobisisobutyronitrile (AIBN) (Tab. 5.18).

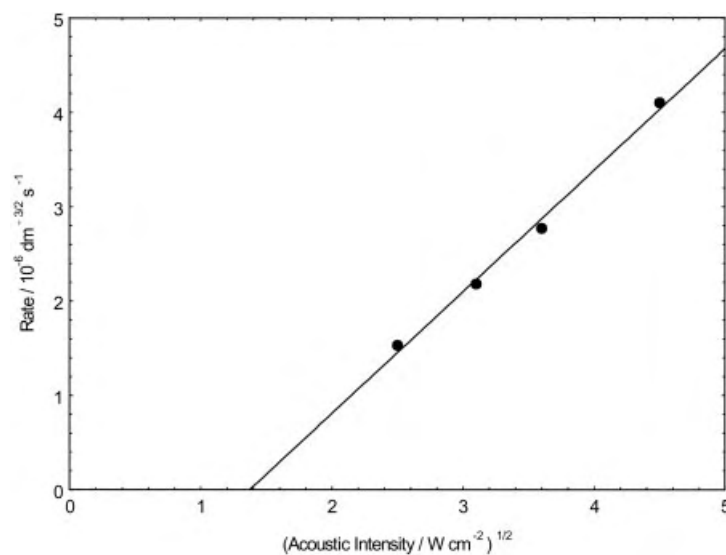


Fig. 5.37. Polymerisation rate of PMMA as a function of the square root of acoustic intensity.

Tab. 5.18 Radical production in the absence and presence of ultrasound.

System	Temperature [°C]	Rate constants [s ⁻¹]	
		Ultrasound	Conventional
MeOBu	– 10	6.35×10^{-5}	
MeOBu	25	2.21×10^{-5}	1×10^{-15}
MeOBu	60	1.03×10^{-5}	
MeOBu + 0.1 % AIBN	25	9.13×10^{-5}	2×10^{-8}
MeOBu + 0.1 % AIBN	70	–	3.1×10^{-5}

By sonically inducing the polymerisation of methyl methacrylate (MMA), Price [65] has extended the work of Kruus and studied the effect of the absence and presence of the initiator azobisisobutyronitrile (AIBN). Similar conversions to Kruus (2–3 % per hour) were obtained in the absence of initiator at 25 °C. However considerable improvements in the polymerisation rate were observed when 0.1 % of initiator were used (Fig. 5.40), the reaction appearing to become autocatalytic. This no doubt is due to the faster production of polymer in the initiated system (faster initiation due to enhanced initiator breakdown) which is then available for degradation to produce more free radical entities.

Price was also to confirm the dependence of the initial rate of polymerisation on the square root of the ultrasound intensity as have other workers, working in initiator free systems.

Studying the sonically induced polymerisation of bulk (pure) MMA over a six hour insonation period, workers have found, at a given intensity but at different temperatures, that lower molar masses were produced at the lower temperatures (where greater degradation can take place (Tab. 5.19) whilst sonication at a given temperature, but at different intensities, led to the discovery that lower molar masses were obtained for the larger intensities (Tab. 5.20).

Tab. 5.20 appears to confirm the prediction of Eq. 5.24.

We [80] have investigated the solution polymerisation of N-vinylcarbazole (NVC) in benzene in the presence and absence of both initiator and high intensity 20 kHz ultrasound (500 W cm⁻²) (Tab. 5.21).

We noted in Section 5.1, that for conventional polymersiation the propagation rate and molar mass (M_n) were dependent on the initiator and monomer concentrations according to equations

$$R_p = K[M][I_0]^{1/2} \quad (5.4)$$

$$M_n = K[M]/[I_0]^{1/2} \quad (5.5)$$

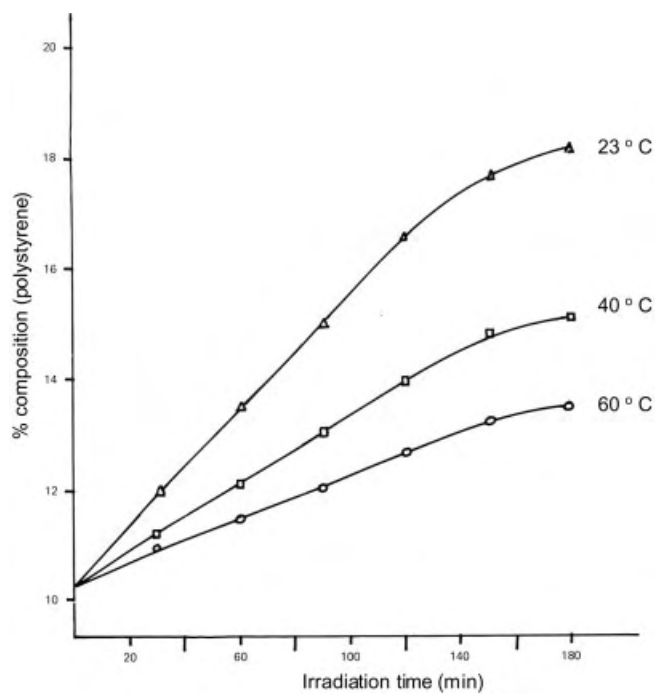


Fig. 5.38. Continuous polymerisation of styrene.

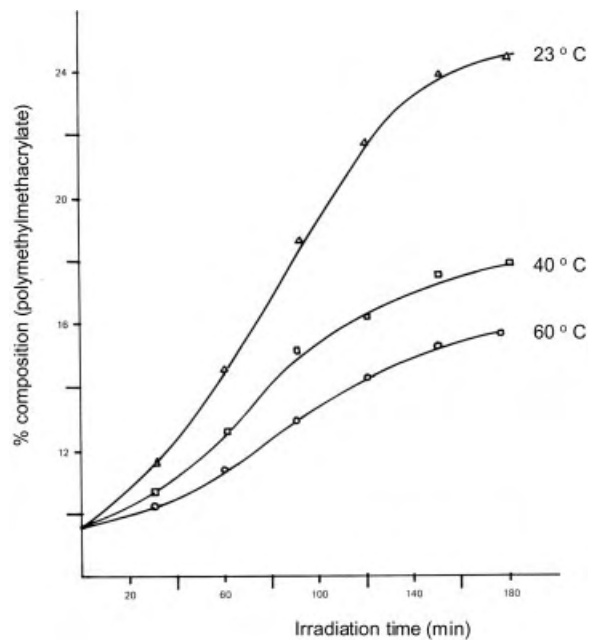


Fig. 5.39. Continuous polymerisation PMMA.

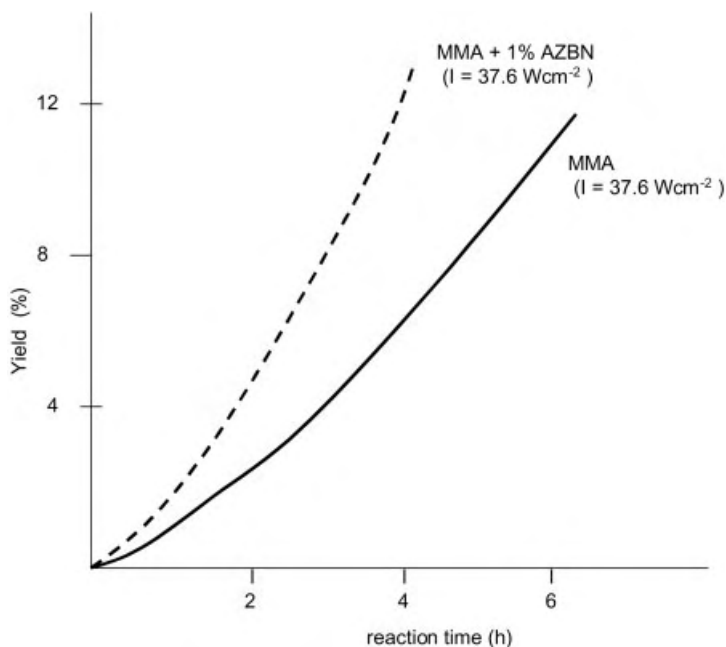


Fig. 5.40. Bulk polymerisation of MMA ($T = 25\text{ }^{\circ}\text{C}$; reaction volume = 50 cm^3); (a) AZBN = 0% (w/v); intensity = 37.6 W cm^{-2} ; (b) AZBN = 0.1% (w/v); intensity = 37.6 W cm^{-2} .

We observed that in the absence of ultrasound (C), but the presence of initiator (reaction number 1 and 2), the rate (or yield (Y) per unit time) and molar mass data (M_n) conformed approximately, as expected, to that for conventional polymerisation – i. e. quadrupling the initiator concentration led a doubling of the yield (Eq. 5.4) and a halving of the molar mass (Eq. 5.5).

Using a value of K (derived from Eq. 5.5) suggested that in the presence of ultrasound, and the absence of initiator, ultrasound was able to provide an “equivalent” initiator concentration of $6 \times 10^{-4}\text{ mol dm}^{-3}$. In general the work was important in that it showed a reciprocal volume dependence rather than a $(1/V^{1/2})$ dependence as shown by Kruus. It also showed that in the absence of initiator, it was possible to

Tab. 5.19 Limiting molar mass values as a function of temperature (intensity = 25 W cm^{-2})

Temperatures [$^{\circ}\text{C}$]	R.M.M.
– 10	107 000
0	119 000
+ 25	147 000
+ 40	241 000
+ 60	356 000

Tab. 5.20 Limiting molar mass values as a function of intensity ($T = +25\text{ }^{\circ}\text{C}$).

Intensity [W cm^{-2}]	R.M.M.
13	144 000
29	131 000
35	97 000
58	35 000

produce polymer with molar masses which were significantly larger than those produced by conventional polymerisation, whereas in the presence of initiator the converse was true.

Stoffer et al. [81] have investigated the sonochemical polymerisation of both methyl methacrylate and acrylamide. No polymerisation was observed in the absence of an initiator. However in the presence of initiator and ultrasound, polymerisation conformed to the usual radical kinetics. Orszulik [82] has also been able to show that whilst polymerisation and copolymerisation of acrylic monomers did not occur in the absence of the initiator, in the presence of AZBN as initiator moderately high yields were produced after prolonged sonication (17 h).

We [83] have also investigated the effect of ultrasound on the aqueous polymerisation of *N*-vinyl pyrrolidinone (NVP). This particular monomer does not follow the normal rate (R_p)-monomer (M) dependence ($R_p = K[M]$, Fig. 5.41c), but exhibits a maximum in the rate at 80 % monomer (v/v) of monomer to water (Fig. 5.41a).

This maximum is thought, from viscosity and enthalpy of mixing studies (Fig. 5.42), to be due to the formation of a H-bonded monomer-water complex. Previous investigations of the solvolysis of 2-chloro-2-methylpropane had led us to conclude that low intensity ultrasound ($< 2\text{ W cm}^{-2}$) was capable of destroying H-bonds and if this were

Tab. 5.21 The effect of initiator (AZBN) on the sonically induced polymerisation of NVC in benzene (U – ultrasonic; C – non ultrasonic).

Reaction number	Type	Reaction temperature [$^{\circ}\text{C}$]	[AZBN] [10^3 mol dm^{-3}]	Reaction time [min]	Reaction volume [cm^3]	Yield [%]	M_n [10^3]	M_w [10^3]	HI
1	C	60	10.0	30	25	31	285	700	2.5
2	C	60	2.5	30	25	13	530	1300	2.5
3	U	54–69 (62)	10.0	8	25	18	281	671	2.4
4	U	63–79 (71)	10.0	12	25	32	246	566	2.3
5	U	58–69 (64)	10.0	18	25	45	164	385	2.3
6	U	61–72 (66)	0.0	30	25	11	1150	2600	2.3
7	U	58–78 (68)	0.0	60	50	10	1100	2200	2.0

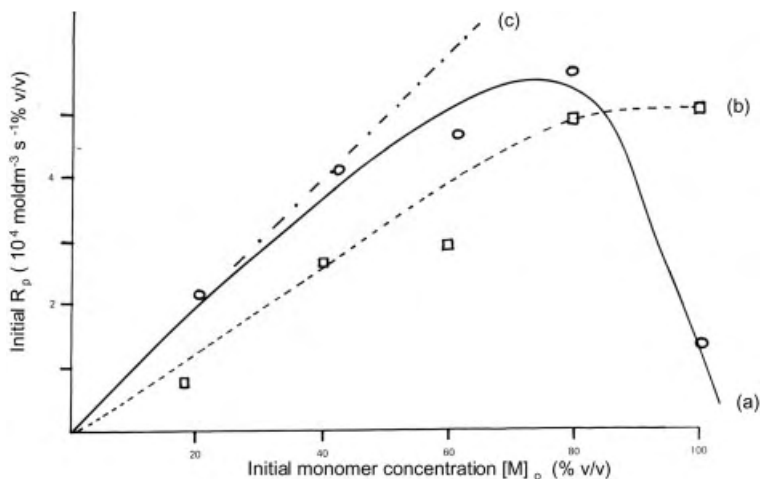


Fig. 5.41. Effect of ultrasound on the aqueous polymerisation of N-vinyl pyrrolidinone (NVP); (a) R_p versus $[M]_0$ dependence without ultrasound; (b) R_p vs $[M]_0$ dependence with ultrasound; (c) R_p versus $[M]_0$ dependence theoretical.

so then the application of ultrasound to the NVP system ought to lead to a destruction of the complex and a decrease in the propagation rate (R_p). Except for the pure monomer system, where there could not be H-bonding since water was absent, all R_p values

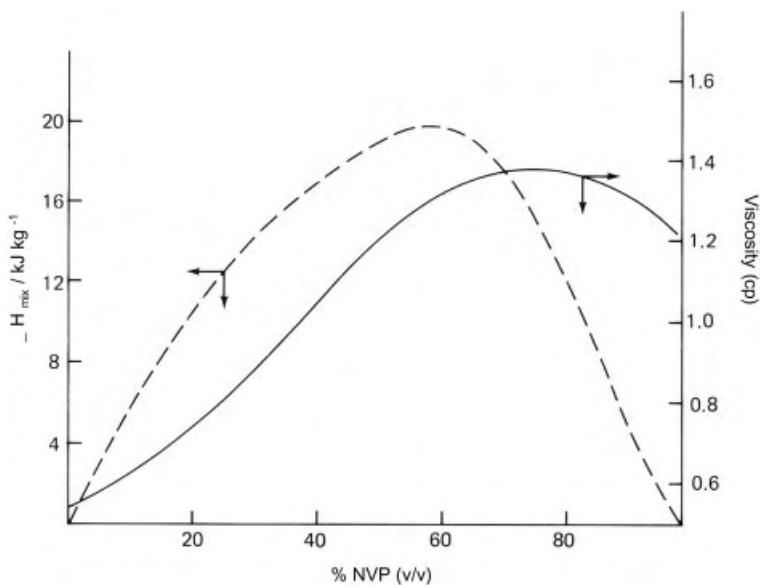


Fig. 5.42 (4.24). Heat of mixing (—) and viscosity (---) for aqueous N-vinyl pyrrolidinone mixtures.

were decreased in the presence of ultrasound (Fig. 5.41b). It can only be assumed that some other effect, perhaps chemical rather than physical, is operating in the pure monomer system since the R_p value increased in the presence of ultrasound.

Henglein [71] has used pulsed ultrasound and has shown that the degree of polymerisation decreases when the duration of pulsed ultrasound is decreased. The growth and collapse of cavitation bubbles require a finite time – they are not instantaneous. Henglein has also shown that the rate (and degree of polymerisation) depends upon the nature of the gas used to saturate the system. For the polymerisation of methacrylic acid in aqueous solution, a 15 min irradiation yielded 10.7 % conversion in the presence of N_2 , 1.8 % conversion in the presence of O_2 (low presumably due to inhibition) and no polymerisation in a degassed solution).

Toppare [84] and Ito [85] have studied the effect of ultrasound on electroinitiated chain polymerisation. Although more detailed discussion is reserved for Chapter 6, for the sake of completeness brief mention will be made here.

Toppare and Akbulut has investigated the effect of ultrasound (25 kHz bath) on both the polymerisation rate and composition of the copolymers produced by the electro-initiated cationic polymerisation of isoprene with (α -methylstyrene). In the absence of ultrasound the yield of copolymer was found to decrease with increase in the applied polymerisation potential due to the formation at the electrode of a polymer film. These films created a resistance to the passage of current into the bulk media with consequent reduction in rate and yield. In the presence of ultrasound however, the total conversion was found to exhibit a slight increase with increase in the polymerisation potential (E_{pol}). This increase was attributed to both increased mass transfer to the electrode and to a “sweeping clean” of the electrode surface by the ultrasound. The authors also noted that both the proportion of isoprene incorporated into the polymer and the reactivity ratios were affected by the polymerisation potential. Toppare has also investigated the polymerisation of butadiene sulfone in the presence of ultrasound and compared it to the radically initiated conventional reaction and again found a faster rate in the presence of ultrasound which he again attributed to greater mass transfer.

Ito [85] investigated the sonoelectropolymerisation of thiophene (0.3 mol dm^{-3}) in nitrobenzene using tertiary butyl perchlorate as the electrolyte, platinum electrodes

Tab. 5.22 Comparison of the film properties from the polymerisation of thiophene.

Properties	Conventional	Ultrasonic
Film	brittle [$> 5 \text{ mA cm}^{-2}$]	flexible/tough [$> 10 \text{ mA cm}^{-2}$]
SEM	irregular	regular
Modulus	1.8 GPa	3.2 GPa
Strength	50 MPa	90 MPa
Conductivity	low	high

Tab. 5.23 The effect of current density of the yield and conductivity of polythiophene.

Current density [mA cm^{-2}]	Polymer yield [%]		Conductivity [S cm^{-1}]	
	Non ultrasonic	Ultrasonic	Non ultrasonic	Ultrasonic
0.7	84	96	15	25
3.0	63	95	40	80
5.0	52	93	60	90

and employing a cleaning bath (45 kHz, 35 W) as the source of ultrasound. He found significant improvements in the both the strength and conductivity of the films produced (Tabs. 5.22 and 5.23.)

Sonopolymerisation is not only restricted to the polymerisation of vinyl monomers. The use of ultrasound in ring opening polymerisation, condensation polymerisation and polymerisation by coupling reactions have all been reported.

Ragaini [86] has reported that the ring opening polymerisation of ϵ -caprolactam (nylon 6, Fig. 5.43), in the presence of ultrasound, takes place without the need for added water and yields larger molar masses in shorter reaction times and at lower reaction temperatures than conventional polymerisation.

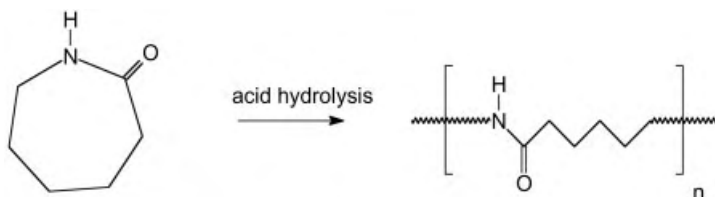


Fig. 5.43. Ultrasonic polymerisation of nylon 6.

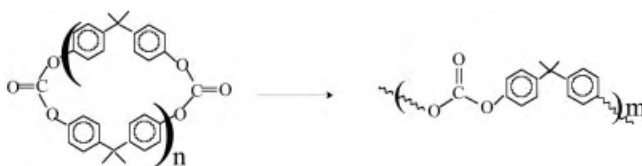


Fig. 5.44. Ring opening polymerisation of polycarbonates.

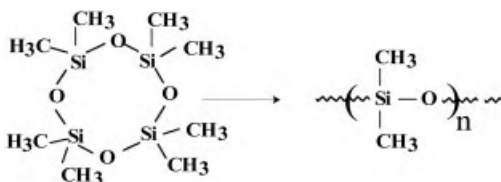


Fig. 5.45. Polymerisation of poly(dimethylsiloxane).

Stoessel [87] has reported using ultrasound to promote the ring opening of polycarbonate rings (Fig. 5.44) whilst Price [88] has studied the ring opening polymerisation of poly(dimethylsiloxane) (Fig. 5.45). Price found that in the presence of ultrasound, and the presence of sulphuric acid at room temperature, faster polymerisation rates and higher molar masses were obtained.

Watanabe [89] has used ultrasound in the synthesis of aromatic polyformals. Using a condensation reaction between a dihaloalkane and diphenol (Fig. 5.46) he was able to show that in the presence of ultrasound higher yields and larger molar masses were obtained.

Rehmann [90] has employed ultrasound to improve the yield of polyphenylene, thought at one time to have a future as a conducting material. Using dibromobenzene and a nickel complex catalyst he investigated both bath and probe systems and found that sonication led to improved yield when compared to the conventional synthesis (i. e. reflux) and also had the advantage of allowing the use of a lower temperature (20 °C).

Several workers [88, 91–95] have investigated the use of ultrasound in the synthesis of poly(organosilanes) (Fig. 5.47).

In general they found both enhanced reaction rates and polymers with lower polydispersities in the presence of ultrasound provided by both bath and probe systems. Higher ultrasonic intensities resulted in narrower molar mass distributions.

More recently Kashimura et al. [96] has investigated the effect of ultrasound on the electroreductive synthesis of polysilanes, polymer germanes and related polymers using magnesium electrodes. They found that the presence of ultrasound greatly facilitated the reactions.

Very little is reported regarding the effect of ultrasound on Ziegler-Natta polymerisation. The first report was by Mertes [97] who obtained a more uniform poly(ethene) in the presence of ultrasound. It was suggested this was as the result of a better dispersion of the catalyst and the prevention of catalyst deactivation (sweeping clean) in the presence of ultrasound.

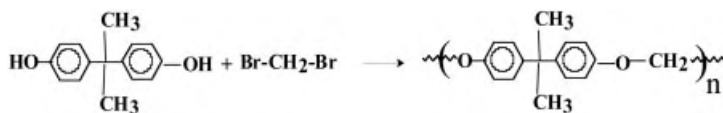


Fig. 5.46. Synthesis of polyformal.

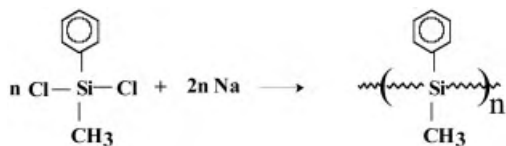


Fig. 5.47. The synthesis of poly(organosilanes).

Tab. 5.24 Effect of ultrasound on Ziegler-Natta polymerisation of styrene.

Conditions	Temperature [°C]	Yield [%]	M _n	HI
Stirred	30	5	53 650	11.9
Ultrasound	30	24	45 700	2.5
Stirred	60	20	8100	40.5
Ultrasound	60	56	39 800	2.6

More recently Price [98] has employed Ziegler-Natta techniques to polymerise styrene. Using an ultrasonic bath (35 kHz, 110 W) he was able to increase yields and improved polydispersities when compared to conventional polymerisation (Tab. 5.24).

5.6

Ultrasonic Processing of Polymers

Although the word “processing” is normally reserved for the method of manufacture of any finished article it is important to recognise that the word can also describe the preparation or synthesis of the material. Thus in the polymer field it can range from improved methods of synthesis of polymers with “tailor made” properties (see Section 5.5) to improved methods of dispersion or improved methods of extrusion. Typical technological uses are shown in Tab. 5.25.

5.6.1

Treatment of Plastics

There are at present only a few commercial applications of ultrasound in the plastics industry. The best known is probably the welding of thermoplastics, a process which now lends itself readily to automation. In common with the welding of metals, the ultrasonic welding of plastics is primarily a hot stage. In the process ultrasound is applied to two layers of plastic, heat is generated at the interface causing the material

Tab. 5.25 Technological uses of ultrasound in polymers.

Power ultrasound in polymer technology	
Treatment of polymers	Treatment of plastics
Molecular weight reduction	Surface treatment
Enhanced radical production	Reduction in viscosity in molding
Copolymerisation	Mixing of additives

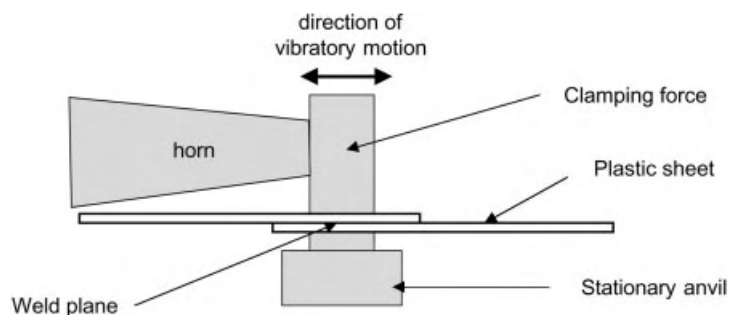


Fig. 5.48. Vibratory shear welding.

to soften, and flow, and the two layers are subsequently glued or joined together (Fig. 5.48) is a schematic representation of a vibratory welder.

Provided the ultrasonic heat is applied selectively at the interface only, it will cause minimum distortion and degradation of the material. Obviously in order that a good weld may be obtained, the plastic must have characteristics which make it suitable for welding. These include:

1. the ability to transmit and absorb the vibrational energy;
2. a relatively low melting/softening temperature;
3. a low thermal conductivity to facilitate local build-up of heat;
4. a low proportion of lubricant, plasticiser or trapped moisture, which tend to have adverse effects on weldability.

Crystalline polymers with high melting temperatures and a very narrow melting range are generally difficult to weld ultrasonically, whereas the rigid amorphous plastics (e. g. polycarbonate or polystyrene) are best.

A typical ultrasonic welder consists of a high-frequency electrical power supply, an electromechanical transducer and a mechanical, usually pneumatically powered, press for clamping the parts during welding. Although welding times of the order of 1/10 of a second are common, most welds are accomplished in about a second or so. This allows, on completion of the ultrasonic exposure, a short delay before retraction of the horn to enable the plastic time to solidify. Although it is quite possible to use either 10 or 40 kHz instruments, most ultrasonic welders now in use operate at 20 kHz with a power density (i. e. intensity) of 1000 W cm^{-2} . The choice of 20 kHz represents a compromise in equipment cost, noise and the ability to handle the particular application. Whereas lower frequencies can sustain greater intensities, e. g. 10 kHz this frequency is now in the audible range.

With the improvement in equipment design and the manufacture of higher-powered instruments have come the welding-related applications such as staking, metal-in-plastic insertion and spot-welding.

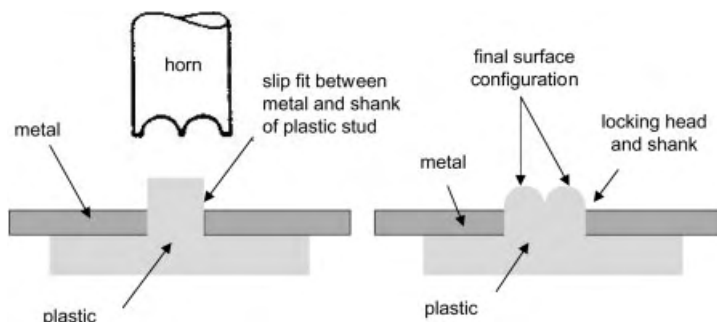


Fig. 5.49. Ultrasonic plastic staking.

Ultrasonic staking (Fig. 5.49) i.e. the enclosure of another material in plastic, takes place by inducing an ultrasonic stress in the plastic causing the stud to yield and eventually conform to the shape of the horn. The advantages of the technique are that:

- tight joints are obtained;
- the lower temperatures minimise the extent of degradation and allow the use of crystalline materials.

In contrast ultrasonic insertion Fig. 5.50 is where a hole is pre-moulded in the plastic (slightly smaller than the metal insert) and the horn is used first to melt the plastic before driving the insert into place.

Ultrasonic spot welding is a process which is being used increasingly as an alternative to adhesion, riveting and stapling in the automobile and furniture industries. Using specially designed projection tips, enhanced weld strength (and good appearance) is produced in such plastics as ABS (acrylonitrile-butadiene-styrene), poly(ethene), poly(propene) and PVC (poly(chlorethene))

Other applications are compression and injection molding. In order to mould it is necessary to heat the polymer to a temperature at which it will flow easily so that it can be introduced to the mould. Quite often this temperature needs to be quite high and often leads to charring and a poor product.

Paul and Crawford [99], using low frequency high-intensity ultrasound (20 kHz; 150–900 W) and solid phase compaction have shown that it is possible to mould poly(propene) without the use of external heat. By varying the compaction pressure (0.5–4 MPa), the sonication time (0.1–6 s), the amount of the charge (0.5–1.5 g), the size of the charge (84–250 μm) and the “hold time” (time after the application of ultrasound), they were able to show that the smaller the particles employed ($\sim 150 \mu\text{m}$) and the longer the dwell time (up to 6 s) the greater was the tensile strength of the material produced. They also observed that polypropene moulded ‘ultrasonically’ had 85 % of the strength obtainable by conventional injection mould-

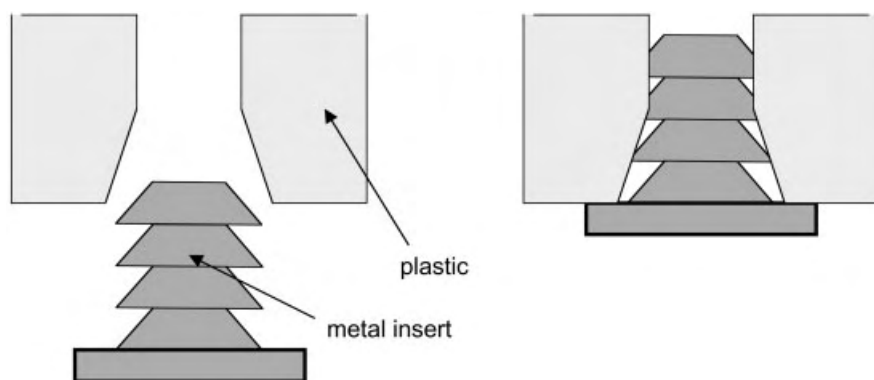


Fig. 5.50. Ultrasonic insertion of metal in plastic.

ing. Unfortunately there was a trade-off in ductility, with the ultrasonically moulded material having only 15 % extension to break as compared with the 'norm' of 300 %.

Fairbanks [100] has also used ultrasound (75 W) to compression mould both thermoplastic powders (acrylics and vinyls) and thermoset powders (phenolics and allylics). The optimum conditions to produce maximum fusion are given in Tab. 5.26.

The overall conclusion for thermoplastics was that ultrasonic intensity was more influential than time in promoting fusion and that the depth of fusion increased with increase in pressure. For thermosets ultrasonic intensity and time have equal influence in promoting fusion and the depth of fusion decreased with an increase in pressure.

Fairbanks has also studied the effect of ultrasonic energy on the flow characteristics of a poly(methyl methacrylate) melt in a simulated injection moulder. Initially the ultrasound (20 kHz, 0–105 W) was applied either simultaneously or independently to both the extruder tube and the cylinder of the moulder. However, since no discernible effect was observed when ultrasound was applied at the extruder tube, further work with the horn in this position was discontinued.

Applying ultrasound to the cylinder, no matter what the position, led to a significant decrease in the melt viscosity (0–60 %), and increase in flow rate, the magnitude of

Tab. 5.26 Optimum conditions for ultrasonic compression moulding of thermosets and thermoplastics.

Variable		Thermoplastic	Thermoset
Ultrasonic intensity	[W cm ⁻²]	35.5	94.5
Static pressure	[kg cm ⁻²]	0.5	1.2
Duration of the process	[s]	65.0	40.0
Maximum length of fusion	[cm]	0.8	1.0

Tab. 5.27 Viscosity reduction as a function of ultrasonic intensity.

Temperature [°C]	Pressure [MPa]	Power level [W]		
		45	75	105
		η_{ult}/η_{init}^*		
185	10.14	0.58	0.45	0.39
190	10.14	0.59	0.41	0.35
195	10.14	0.70	0.43	0.39
200	3.04	1.00	0.96	0.82
200	5.07	0.91	0.85	0.69
200	6.08	0.92	0.77	0.57

which was dependent on the melt temperature, the ram pressure and the ultrasonic power level (Tab. 5.27).

As Tab. 5.27 shows, the ease of extrusion increases with:

1. increase in ultrasonic power at constant temperature and ram pressure, and
2. increase in ram pressure at constant temperature and power.

Fairbanks' suggestion was that the reductions in viscosity were due to one of the following:

1. Creation of a slip flow at the wall of the cylinder and the entrance to the extruder tube. No doubt this is due to the preferential absorption of the ultrasonic energy at the melt-metal interface which then appears as heat, thereby reducing the viscosity at the wall.
2. Reduction in the apparent bulk viscosity due to a change in polymer rheology. It is well known that ultrasound can lead, *via* degradation, to a reduction in polymer solution viscosity. Although Fairbrother did not investigate whether degradation of the polymer, and subsequent reduction in R.M.M. and hence viscosity had occurred, it seems reasonable to assume that the polymer melt with an initial viscosity of 30 000–100 000 poise would certainly have resisted cavitation and thus degradation.

One disadvantage of the use of ultrasound in the process was that it proved extremely difficult, unless external heat was supplied, to remove the remaining polymer slug from the cylinder. This seems to indicate that ultrasound had also increased the magnitude of the polymer-to-metal bond.

Another application based on a polymer's increased ease of flow in the presence of ultrasound is the atomisation of polymers. Here the particles are fed through an extruder then atomised (Fig. 5.51). The size of droplets (D) are governed by Eq. 5.44, where λ is the surface tension, ρ is the density and F is the exciting frequency.

$$D = 0.34 \left(\frac{8\pi\lambda}{\rho F^2} \right)^{1/3} \quad (5.44)$$

An application which utilises both the ability of ultrasound to generate heat and a polymer's poor thermal conductivity is in the vulcanisation of rubber [101]. Because of rubber's poor thermal conductivity, the conventional process is slow and energy-intensive and typically several hours may be required to vulcanise thick sections of material even at temperatures and pressures of 205 °C and 14.3 MPa. Even under these extreme conditions, poor bonding between the non-polar rubber and the various polar reinforcements (e.g. cord, fabric or metal) often results, leading to interfacial failure. Any attempt to counteract these problems, such as the use of various additives to accelerate the cure process, or special surface treatments to improve the bonding, simply serve to increase the manufacturing costs. There is also the further problem that the additives often cause scorching during the moulding stage. However, the use of ultrasound largely overcomes many of these disadvantages. For example, the poor thermal conductivity, a major problem in the conventional process, becomes an advantage in the ultrasonic process. In the conventional process, poor conductivity resists the penetration of the heat, which is applied externally and often leads to charring.

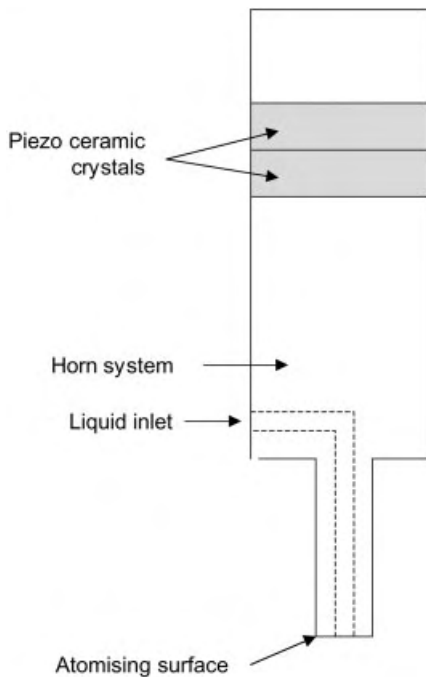


Fig. 5.51. Ultrasonic atomisation.



Fig. 5.52. Coating of a pigment during conventional emulsion polymerisation.

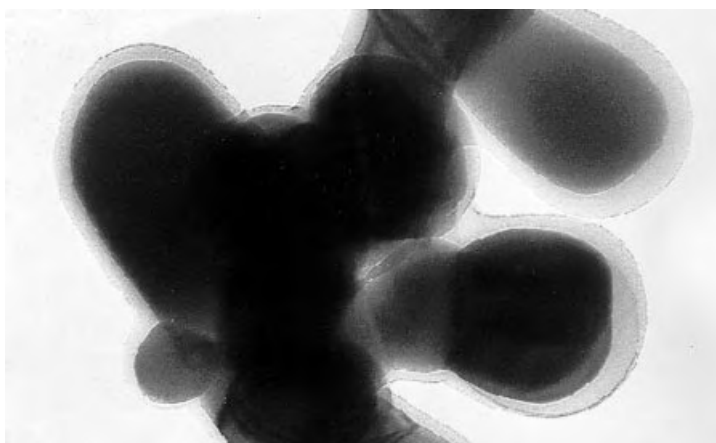


Fig. 5.53. Coating of a pigment during emulsion polymerisation in the presence of ultrasound.

In the ultrasonic process, the heat is generated internally and is stopped from escaping. It also allows a more uniform internal build-up of temperature.

Ultrasonic vulcanisation also tends to change the interfacial property of the rubber and the reinforcing materials to improve bonding. Improved wetting and flow characteristics produced by ultrasonic vulcanisation have the potential to increase the interfacial bond strength between the rubber and the reinforcing materials currently used.

Using frequencies of 10–100 kHz has led to more than 100 % increase in the production rate; better than 50 % energy saving; potential of improved bond qualities resulting in better mechanical and ageing properties of the final product; reduced raw material cost resulting from reductions or elimination of costly additives such as accelerators, activators and coupling agents; lower mould temperatures and accelerated degassing. It does require, however, that the process is performed at an overpressure of 500–1000 psi to inhibit cavitation and possible degradation.

Another application of ultrasonic technology is in the area of polymer blending (see Chapter 7, Fig. 7.2) The major difficulty encountered in blending is the production of a homogeneous mixture with complete dispersion of the added component. Scott-Bader UK, using a whistle reactor, have achieved considerable improvement in the blending of pyrogenic silica with various polyester resins. The whistle reactor is capable of processing 12 000 L/h, requires 40 % less silica than conventional methodology, provides the correct thixotropic characteristics no matter what resin is employed, and is capable of also dispersing pigment into the resin to produce the gel coat used as the final layer in building up the glass fibre components.

Another application which combines ultrasound's ability to disperse material and to provide enhanced radical production is in the production of paints. Most paint formulations contain TiO_2 pigment particles produced by ball milling. Unfortunately during storage there is a problem with the re-agglomeration of the TiO_2 pigment which ultimately leads to poor coverage and a patchy appearance of the final paint product. By applying ultrasound to TiO_2 pigment in an emulsion system (water, surfactant and monomer) we were able to show [102] that it was possible to produce the "ideal" pigment for formulation purposes where each particle was separated from its neighbour and was totally covered with polymer and had no tendency to reaggregate (see Figs. 5.52 and 5.53).

Currently there is much interest in modifying the surfaces of commodity polymers with a view to either functionalising the surfaces to provide for more exotic materials or subjecting the treated surface to electroless or electrolytic plating to produce, for example, printed circuit boards.

References

1. E.W. Flösdorf and L.A. Chambers, *J. Am. Chem. Soc.*, 1933, **55**, 3051.
2. A. Szalay, *Z. Phys. Chem. A.*, 1933, **164**, 234.
3. A.S. Gyorgi, *Nature* (London), 1933, **131**, 278.
4. J.P. Lorimer, T.J. Mason, T.C. Cuthbert, and E.A. Brookfield, *Ultrasonics Sonochemistry*, 1995, **2**, 55.
5. G. Schmid and O. Rommel, *Z. Phys. Chem.*, 1939, **A185**, 97; *Z. Elektrochem.*, 1939, **45**, 659; G. Schmid and E. Beuttenmüller, *Z. Elektrochem.*, 1943, **49**, 325; *ibid.*, 1944, **50**, 209; G. Schmid, *Phys. Z.*, 1940, **41**, 326; *Z. Phys. Chem.*, 1940, **186A**, 113; G. Schmid, P. Paret, and H. Pfeleider, *Kolloidn. Zh.*, 1951, **124**, 150; G. Schmid and W. Poppe, *Z. Elektrochem.*, 1949, **53**, 28.
6. H.F. Mark, *J. Acoust. Soc. Am.*, 1945, **16**, 183.
7. S.L. Malhotra, *J. Macromol. Sci. Chem.*, 1982, **A18**, 1055.
8. A. Basedow and K.H. Ebert, *Makromol. Chem.*, 1975, **176**, 745; *Polymer Bulletin*, 1979, **1**, 299.
9. D.W. Ovenall, G.W. Hastings, and P.E.M. Allen, *J. Polymer. Sci.*, 1958, **33**, 207.
10. G. Gooberman and J. Lamb, *J. Poly. Sci.*, 1960, **42**, 35.
11. B. S. El'tseton and A. A. Berlin, *Polym. Sci. USSR*, 1964, **5**, 668.
12. K. Goto and H. Fujiwara, *Kobunshi Kagaku*, 1966, **23**, 827.
13. T. Sato and D.E. Nalepa, *J. Appl. Polymer Sci.*, 1978, **22**, 865.
14. K. Chen, S. Chen, and X. Xu, *33rd IUPAC Symposium on Macromolecules, Conference Proceedings*, 1990.
15. G.R.J. Thomas, *J. Phys. Chem.*, 1959, **63**, 1725.
16. X. Hu and X. Hu, *Huagong Xuebao*, 1982, 310.
17. G. Madras, S. Kumar, and S. Chatopadhyay, *Polymer Degradation and Stability*, 2000, **69**, 73.
18. W. Gaertner, *J. Acoust. Soc. Am.*, 1954, **26**, 977.
19. R.O. Prudhomme and P. Graber, *J. Chim. Phys.*, 1949, **46**, 667; R.O. Prudhomme, *ibid.*, 1950, **47**, 795.
20. H.H. Jellinek and G. White, *J. Poly. Sci.*, 1951, **6**, 745; *ibid.*, 1952, **6**, 757.
21. H.H. Jellinek and G. White, *J. Poly. Sci.*, 1951, **7**, 33; H.H. Jellinek and G. White, *ibid.*, 1954, **13**, 441; H.H. Jellinek, *Degradation of Vinyl Polymers*, Academic Press, 1955.
22. A. Weissler, *J. Appl. Phys.*, 1950, **21**, 171; *J. Chem. Phys.*, 1950, **18**, 1513; *J. Acoust. Soc. Am.*, 1951, **23**, 370.
23. G. Gooberman, *J. Poly. Sci.*, 1960, **42**, 25.
24. G. Gooberman and J. Lamb, *J. Poly. Sci.*, 1960, **47**, 229.
25. F. Gebert, *Angew. Chem.*, 1952, **64**, 625.
26. H.W. Melville and A.J.R. Murray, *J. Chem. Soc. Faraday. Trans.*, 1950, **46**, 996.
27. M.S. Doulah, *J. Appl. Poly. Sci.*, 1978, **22**, 1735.
28. M.A.K. Mostafa, *J. Poly. Sci.*, 1958, **33**, 295; *ibid.*, 1958, **33**, 311; *ibid.*, 1958, **33**, 323; *ibid.*, 1958, **33**, 519.
29. G. Schmid and Poppe, *Z. Elektrochem.*, 1949, **53**, 28;
30. H.H. Jellinek, *J. Poly. Sci.*, 1959, **37**, 485.
31. B.E. Noltingk and E.A. Neppiras, *Proc. Phys. Soc. B (London)*, 1950, **63B**, 674; *ibid.*, 1951, **64B**, 1032.
32. M.A.K. Mostafa, *J. Poly. Sci.*, 1958, **33**, 311.
33. G. Schmid and O. Rommel, *Z. Phys. Chem.*, 1939, **A185**, 97; *Z. Elektrochem.*, 1939, **45**, 659.
34. G. Schmid and E. Beuttenmüller, *Z. Elektrochem.*, 1943, **49**, 325; *ibid.*, 1944, **50**, 209; G. Schmid, *Phys. Z.*, 1940, **41**, 326; *Z. Phys. Chem.*, 1940, **186A**, 113;

- G. Schmid, P. Paret, and H. Pfeleider, *Kolloidn. Zh.*, 1951, **124**, 1 50.
35. H.A. Leub and T.G. Schoon, *J. Poly. Sci. Symp.*, 1949, **A199**, 39.
 36. S.V. Golubev, Z.A. Tikhonova, Y.D. Semchikov, and I.V. Vyskomol, *Soedin. Ser. A*, 1987, ²⁹, 2393.
 37. S.L. Malhorta, *J. Macromol. Sci. Chem.*, 1982, **A17**, 601.
 38. P. Alexander and M. Fox, *J. Polym. Sci.*, 1954, **12**, 533.
 39. G.J. Price, P.J. West, and P.F. Smith, *Ultrasonics Sonochemistry*, 1994, **1**(1), S51.
 40. H.H. Jellinek and H.W. Brett, *J. Poly. Sci.*, 1956, **21**, 535.
 41. S.L. Malhorta, M. Breton, and J.M. Gauthier, *J. Macromol. Sci. Chem.*, 1982, **A18**, 1151.
 42. E. Wada and H. Nakane, *J. Sci. Res. Inst. (Tokyo)*, 1951, **1**, 45.
 43. C. Keqiang, S. Ye, L. Huilin, and X. Xi, *J. Macromol. Sci. Chem.*, 1985, **A22**, 455; *ibid*, 1986, **A23**, 1415.
 44. M.A.K. Mostafa, *J. Poly. Sci.*, 1958, **33**, 519.
 45. S.V. Goluev and Y.D. Semchikov, *Isv. Vyssh. Ucheb. Saved. Khim. Tekhnol.*, 1983, **26**, 1483.
 46. M.T. Shaw and F.J. Rodriguez, *J. Appl. Poly. Sci.*, 1967, **11**, 335.
 47. K. Chen, Y. Shen, and X. Xu, *Gaofenzi Tongxun*, 1985, **6**, 401.
 48. Z. Cao and X. Xu, *Huanong Xuebao*, 1985, **1**, 56.
 49. S.L. Malhorta, *J. Macromol. Sci. Chem.*, 1982, **A17**, 601.
 50. M. Okuyama, *Z. Elektrochem.*, 1955, **59**, 565.
 51. B.B. Thomas and W.J. Alexander, *J. Poly. Sci.*, 1957, **25**, 285.
 52. T.G. Schoon and G. Reiber, *Angew. Makromol. Chem.*, 1971, **15**, 263; *ibid*, 1972, **23**, 43.
 53. A. Basedow and K.H. Ebert, *Makromol. Chem.*, 1975, **176**, 745; *Polymer Bulletin*, 1979, **1**, 299.
 54. B.B. Thomas and W.J. Alexander, *J. Poly. Sci.*, 1955, **15**, 361.
 55. R.S. Porter, M. Cantow, and J.F. Johnson, *J. Appl. Phys.*, 1964, **35**, 15.
 56. G.J. Price and P.F. Smith, *Polymer International*, 1991, **24**(3), 159.
 57. M. Garcia-Alvarez, F. Lopez-Carrasquero, M. Morriolo, and S. Munoz-Guerra, Ultrasonic degradation of polyasparates and polyglutamates, *J. Poly. Sci., Poly Phys.*, 1997, **14**, 2379.
 58. G.R. Thomas, *J. Phys. Chem.*, 1959, **63**, 1725.
 59. S.L. Malhotra, *J. Macromol. Sci. Chem.*, 1986, **A23**, 729.
 60. P.A.R. Glynn, B.M.E. Van der Hoff, and P.M. Reilly, *J. Macromol. Sci.*, 1972, **A6**, 1653; *ibid*, 1973, **A7**, 1695.
 61. D.K. Ramsden and K. McKay, *Polym. Deg. Stab.*, 1986, **15**, 15.
 62. A. Henglein, *Makromol. Chem.*, 1954, **15**, 15; *ibid*, 1955, **15**, 188.
 63. M. Tabata and J. Sohma, *Chem. Phys. Lett.*, 1980, **73**, 178; *Eur. Polym. J.*, 1980, **16**, 589.
 64. O.M. Taranukha, P.N. Dmitrieva, and T.V. Korzh, *Dpov. Akad. Nauk. Ukr. R. S. R. Ser. B, Geol. Khim. Biol. Nauk.*, 1985, **7**, 47.
 65. G.J. Price, D.J. Norris, and P.J. West, *Macromolecules*, 1992, **25**, 6447.
 66. G.J. Price, P.F. Smith, and P.J. West, *Ultrasonics*, 1991, **29**, 166.
 67. K.F. Driscoll and A.U. Sridhari, *J. Appl. Polym. Sci., Appl. Polym. Symp.*, 1975, **26**, 135.
 68. G.J. Price and P.J. West, *Polymer*, 1996, **37**, 3975.
 69. A.A. Berlin, *Usp. Khim.*, 1960, **29**, 1189; *Khim. Nauka. Prom.*, 1957, **2**, 667.
 70. O. Lindstrom and O. Lamm, *J. Phys. Colloid Chem.*, 1951, **55**, 1129.
 71. A. Henglein, *Z. Naturforsch. B*, 1952, **7**, 484; *ibid*, 1955, **10**, 616; *Makromol. Chem.*, 1954, **14**, 15; *ibid*, 1955, **15**, 188; *ibid*, 1956, **18**, 37.

72. Y. Hatate, T. Ikeura, M. Shinonome, K. Kondo, and F. Nakashio, *J. Chem. Eng. Jpn.*, 1981, **4**, 38.
73. J.P. Lorimer, T.J. Mason, K. Fiddy, D. Kershaw, D. Dodgson, and R. Groves, *Ultrasonics International Conference proceedings*, Butterworth Scientific, 1989, 1283.
74. J.P. Lorimer, T.J. Mason, and K. Fiddy, The enhancement of chemical reactivity by power ultrasound – an alternative interpretation of the hot-spot, *Ultrasonics*, 1991, **29**, 338–343.
75. S.K. Ooi and S. Biggs, *Ultrasonics Sonochemistry*, 2000, **7**, 125.
76. P. Kruus, D.J. Donaldson, and M.D. Farington, *J. Phys. Chem.*, 1979, **83**, 3130.
77. T. Miyata and F. Nakashio, *J. Chem. Eng. Jpn.*, 1975, **8**, 463.
78. J.P. Lorimer, T.J. Mason, and A. Turner, The effect of ultrasound on polymerisation reactions, *Ultrasonics International 87 (proceedings)*, Butterworths, 1987, 762–766.
79. T.J. Mason, J.P. Lorimer, and B.P. Mistry, *Tetrahedron*, 1985, **41**(22), 5201.
80. J.P. Lorimer, T.J. Mason, and D. Kershaw, *Ultrasonics International 89, Conference Proceedings*, Butterworth Scientific, London.
81. J.O. Stoffer, O.C. Sitton, and H.L. Kao, *Polym. Mater. Sci. Eng. Prepr.*, 1991, **65**, 42; J.O. Stoffer, O.C. Sitton, and Y.H. Kim, *Polym. Mater. Sci. Eng. Prepr.*, 1992, **67**, 242.
82. S.T. Orszulik, *Polymer*, 1993, **34**, 1320.
83. J.P. Lorimer and T.J. Mason, *Ultrasonics International 87, Conference Proceedings*, Butterworths, 762.
84. L. Toppare, S. Eren, and U. Akbulut, *Polymer Communications*, 1987, **28**, 36; U. Akbulut, L. Toppare, and B. Yurttas, *Polymer*, 1986, **27**, 803; *British Polymer Journal*, 1986, **18**, 273; S.P. Aybar, B. Hacioglu, U. Akbulut, and L. Toppare, *J. Poly. Sci., Polym. Chem.*, 1991, **29**, 1971.
85. S. Osawa, M. Ito, K. Tanake, and J. Kuwano, *J. Polym. Phys.*, 1992, **30**, 19.
86. V. Ragaini, Italian Patent Appl., 20478-A/90.
87. S.J. Stoessel, *J. Appl. Poly. Sci.*, 1993, **48**, 505.
88. G.J. Price, E.N. Wallace, and A.M. Patel, 1995, In *Silicone Containing Polymers*, R.G. Jones (ed.), p 147, Cambridge, UK: R Soc Chem.
89. S. Watanabe, I. Matsubara, M. Kakimoto, and Y. Imai, *Polym. J.*, 1993, **25**, 989.
90. M. Rehmann, A. Schluter, and W.J. Feast, *Synthesis*, 1988, 386.
91. H.K. Kim and K. Matyjaszewski, *J. Am. Chem. Soc.*, 1989, **110**, 3321.
92. H.K. Kim, D. Greszta, H. Uchida, and K. Matyjaszewski, *Macromolecules*, 1995, **28**, 59.
93. G.J. Price, M.P. Hearn, E.N. Wallace, and A.M. Patel, *Polymer*, 1996, **37**, 2203.
94. G.J. Price and A.M. Patel, *Eur. Polym. J.*, 1996, **11**, 1289.
95. R.D. Miller, D. Thompson, R. Soorijakumaran, and G.N. Fickes, *J. Polym. Sci., Polym. Chem.*, 1991, **29**, 813.
96. S. Kashimura, M. Ishifune, N. Yamashta, H.B. Bu, M. Takabayashi, S. Kitajima, D. Yoshiwara, Y. Kataoka, R. Nishida, S.I. Kawaski, H. Murase, and T. Shona, *J. Org. Chem.*, 1999, **64**, 6615.
97. T.S. Mertes, US Patent, 2899414 (1960).
98. G.J. Price and A.M. Patel, *Polymer*, 1992, **30**, 20.
99. D.W. Paul and R.J. Crawford, *Ultrasonics*, 1981, 23.
100. H.V. Fairbanks, *Ultrasonics*, 1974, 22; P. Khaladkar, J. Sears, and H. Fairbanks, *Proc. M. Va. Acad. Sci.*, 1973, **45**, 412.
101. N. Senapati and D. Mangarj, US Patent, No. 4 548 771 (1985).
102. J.P. Lorimer, T.J. Mason, and D. Kershaw, *Colloid and Polymer Science*, 1991, **269**, 392–397.

6

Sonoelectrochemistry

6.1

Introduction

Sonoelectrochemistry can be considered as the interaction of sound (hence SONO) with electrochemistry which is itself the interconversion of electrical and chemical energies. Whilst this chapter will concentrate on the application of ultrasound to important industrial processes such as electrodeposition (or electroplating) and electro-organic synthesis, it is important to first introduce the concept of electrochemistry, for those who are unfamiliar, so that we will have a better understanding as to what precisely happens in an electrochemical or electroplating process and how the application of ultrasound will be of benefit.

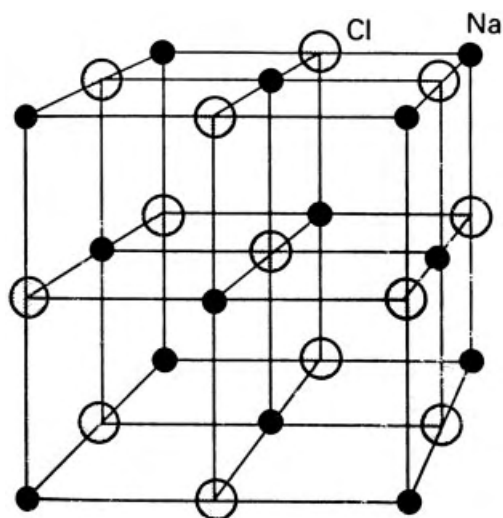


Fig. 6.1. NaCl crystal structure.

In general, any ionic solid can be pictured as a unit cell in which the cations are surrounded by a number of anions and the anions are surrounded by a number of cations. A typical example is that of sodium chloride (Fig. 6.1).

On addition to water, the lattice is destroyed and the solid dissolves to create a conducting solution of solvated sodium and chloride ions in water. Since some short range order still exists between the two ions we may naively picture the solvated solution as follows (Fig. 6.2). So what happens when we insert a piece of metal into solution.

It is known that when individual metal atoms condense to form a solid, the various atomic orbital energy levels broaden and merge. The band of levels corresponding to the merger of bonding molecular orbitals is called the *valence band* (usually completely filled) and the level corresponding to the non bonding molecular orbitals is called the *conduction band* and as such is usually only partially filled and is responsible for the electrical conductivity. Thus, when two metals (dissimilar conducting phases) are connected together electrons will flow from one metal to the other. The direction of flow is from the metal with the highest Fermi level to the one with the lower Fermi level. This electron transfer results in the separation of charge and an electric potential difference across the boundary. The effect of the electric potential difference is to raise the energy of the conductance band of the second metal and lower the energy of the conductance band of the first metal until the Fermi levels are equal in energy.

By analogy, when we immerse a metal in a solution of ions, something happens to set up an electric potential difference between the metal and the solution. The metal and the ions do not exist as independent entities. Let us take the example of immersing a piece of copper metal into aqueous copper sulphate.

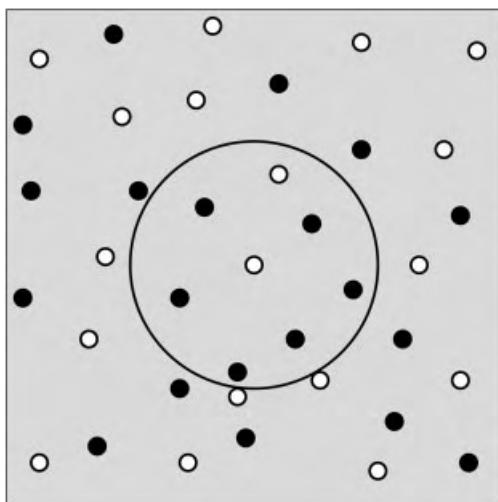


Fig. 6.2. Ions in solution.

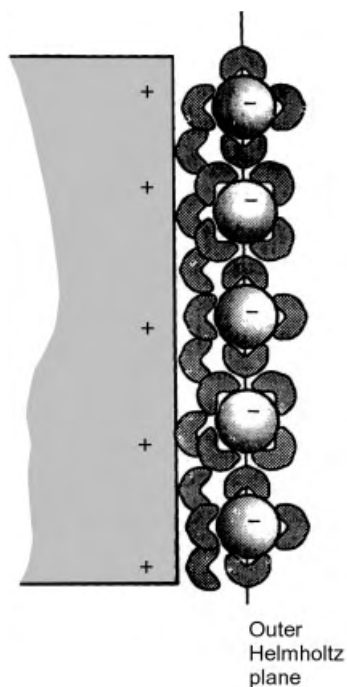


Fig. 6.3. Helmholtz layer.

When we insert the copper metal into the copper sulphate solution, we find that some of the copper ions deposit on the copper metal. They do this by accepting electrons from the metal conduction band thereby leaving the metal with a small positive charge (Eq. 6.1).



In order to preserve electrical neutrality, the solution gains a small negative charge (see Fig. 6.3). This particular process is a *reduction process*.

For a more active metal such as zinc, it may be the other way around; a few zinc atoms spontaneously leave the metal surface as ions, giving the metal a small negative charge and the solution a small positive charge (Eq. 6.2). This process is one of *oxidation*.



So, in general when two conducting phases are brought into contact, an interphase electric potential will develop. The exploitation of this phenomenon is one of the subjects of electrochemistry and we can define electrochemical reactions as ones in which

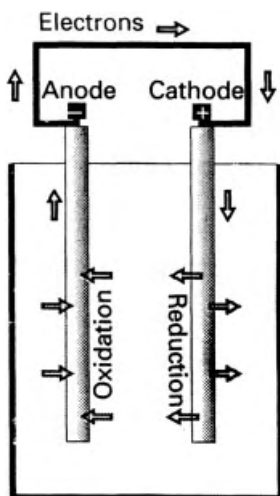


Fig. 6.4. Electrochemical cell with single electrolyte.

the key processes are the transfer of electrons from a substrate to an electrode. The basic apparatus in which this takes place is called an electrochemical cell. Electrochemical cells usually consist of two electrodes and an electrolyte (Fig. 6.4).

By convention, the electrode at which oxidation occurs is called the *anode* and the electrode at which reduction occurs is called the *cathode*. In Fig. 6.4 the two electrodes share the same electrolyte. If the electrolytes are different, then the two compartments will need to be separated perhaps for chemical reasons. (Electrical continuity is preserved by usually employing a salt bridge.)

Let us continue with the example of copper ions in contact with copper metal and zinc ions in contact with zinc metal. This combination is usually referred to as the Daniell cell or zinc/copper couple (Fig. 6.5a). For this electrochemical cell the reduction and oxidation processes responsible for the overall reaction are separated in space; one half reaction taking place in one electrode compartment and the other takes place in the other compartment.

Of the two possible spontaneous oxidation processes (Eqs. 6.2 and 6.3) the conversion



of zinc atoms into zinc ions is the more likely and results in a transfer of electrons to the zinc metal (electrode). At the other electrode, a reduction process occurs in which copper ions are converted to copper metal (Eq. 6.3) by withdrawing electrons from the

electrode thereby leaving it positively charged. The electrons produced on the zinc electrode flow through the external wire from the zinc to the copper to supply the electrons for the reduction process. Provided there is always some zinc metal or copper ions remaining, this cell will continue to spontaneously produce a current. The overall spontaneous cell reaction is given by Eq. 6.4.



For the Daniell cell, the overall (cell) potential, or cell electromotive force (E) is given by the so-called Nernst equation [1] (Eq. 6.5).

$$E = E^0 + \frac{RT}{zF} \ln \frac{[\text{Cu}^{2+}]}{[\text{Zn}^{2+}]} \quad (6.5)$$

where z is the number of electrons transferred in the process, F is the Faraday constant (96 489 C), T is the temperature (K), R is the gas constant ($8.314 \text{ J mol}^{-1} \text{ K}^{-1}$), $[\text{Cu}^{2+}]$ and $[\text{Zn}^{2+}]$ are the concentrations of copper and zinc ions respectively and E^0 is the standard cell potential (obtainable from the literature). When the cell is allowed to run spontaneously (i. e. the two electrodes are connected by a wire), with equal concentrations of the zinc and copper ions, the cell will generate a current, at a potential difference of 1.1 V, in which the zinc electrode is the anode and is negative, since it dissolves to become Zn^{2+} ions, and electrons are transferred to the copper electrode.

However, if an external potential difference of more than 1.1 V is intentionally applied so as to make the zinc the cathode (i. e. negative), then the current flow could, in principle, be reversed as the zinc ions attempted to be deposited to produce zinc metal.

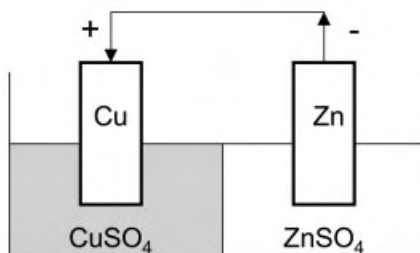
If the cell is exactly balanced against an external potential source ($= 1.1 \text{ V}$), although no net current will flow, there will still be current flows at each electrode but in this they are equal. The point at which this occurs is called the exchange current.

A better example of the term electrochemistry – the interconversion of electrical and chemical energy lead – is the “storage” battery or lead accumulator (Fig. 6.5b). On discharge chemical energy is spontaneously transformed into electrical energy, whilst on “re-charge” electrical energy is transformed non-spontaneously into chemical energy.

Thus in practise, we can recognise two types of electrochemical cell. These are called electrolytic cells and galvanic cells. An electrolytic cell uses an external power source (i. e. a voltage source) to move the electrons and perform the electrolysis. The aim of the electrolysis may be to generate a species in solution, produce a precipitate, produce

Electrochemical Cell Discharge
(interconversion of chemical to electrical energy)

(a) Daniell Cell - copper / zinc couple



(b) Lead Accumulator - lead / lead dioxide couple

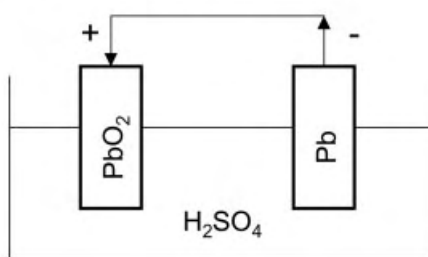


Fig. 6.5. (a) Daniell and (b) lead accumulator cells.

a coating on an electrode or generate some other phase. Examples are electroanalysis and electrosynthesis which loosely include electrodeposition, electroplating and electrochemical corrosion. Other electrolytic techniques include electropolishing, electro-machining and electrochemical etching. In the case of electrosynthesis the electrodes usually have a large area and they use relatively high substrate concentrations. In galvanic cells the electrochemical reaction drives the movement of electrons (e.g. batteries). In the electrolytic cell, the cathode is still the location of reduction but since the process is now no longer spontaneous, electrons must be supplied from an external source i. e. a power supply and therefore the cathode is negative and the anode positive.

Having identified the main features of electrochemistry, the remainder of this chapter will focus on the use of electrolytic cells and will use as examples the electrodeposition (or electroplating) of metals such as copper, zinc, iron, chromium, nickel and silver. The chapter will also consider the electrochemistry of some organic molecules. Electroanalysis will not be considered since a full description is not within the scope of this chapter. For those interested readers, there is a review on the topic [2].

6.2

Electrolytic Discharge

In order to produce current flow through an electrolytic cell for the discharge (or electrodeposition) of any metal, a potential, at least equal to if not greater than the “zero current” or reversible potential must be applied. For zinc ions this would be 0.763 V [3]. The potential at which continuous deposition of material (or discharge of ions) commences is called the discharge or decomposition potential (Fig. 6.6).

Faraday’s first law of electrolysis [4] states that “the mass of any substance liberated by a current is proportional to the quantity of electricity which has passed”. Thus any increase in current (density) ought to lead to an increase in the rate of discharge and a more economical process. However the discharge of the metal ions, to generate metal, is not as straight forward as it seems and there can be several problems associated with the discharge rate.

The first problem is that any ion needs to be brought from the bulk solution to the electrode surface before it can be discharged. On approaching the electrode, the ion needs to cross a boundary layer called the diffusion layer. This layer is about 0.1 mm (or 100 μm) thick and is distinguished from the electrode double layer which is 100 000 times smaller (Fig. 6.7).

On entering the diffusion layer, the ion loses its solvation molecules (all ions in solution are solvated) and approaches the metal surface, where it is adsorbed as a “naked” ion before the electron transfer process takes place. Obviously the wider is this diffusion layer (δ), the longer it will take the ion to diffuse across it and the slower will be the overall process. Anything which can diminish or disrupt this layer (i. e. make it smaller) will improve the speed of the process.

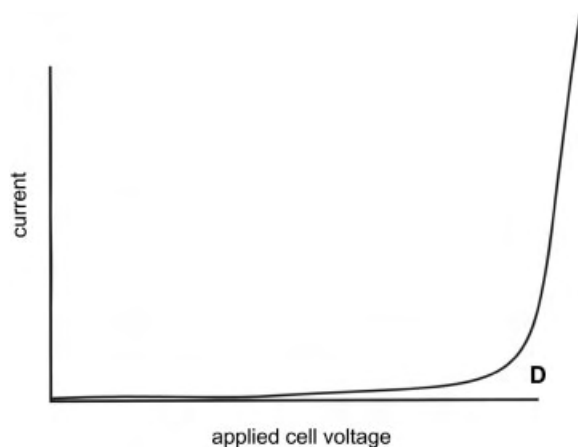


Fig. 6.6. Discharge potential diagram (variation in current with voltage).

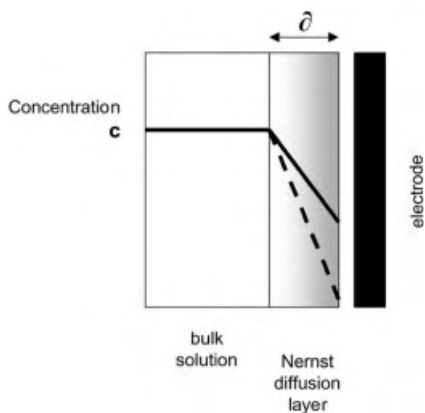


Fig. 6.7. Diffusion layer.

Stirring is one obvious solution and this method is adopted commercially [5]. However the fastest form of stirring is ultrasonic agitation. Applying ultrasound has been found to decrease the thickness of this diffusion layer, and so assist the electrode reaction (Fig. 6.8).

Obviously one of the important economic requirements for electroplating industry is that as much material is plated in as short a time as possible. Therefore industrially the process is run at high currents for maximum discharge rate (Faraday's first law). However higher discharge rates mean that the surface concentration of the ions at the

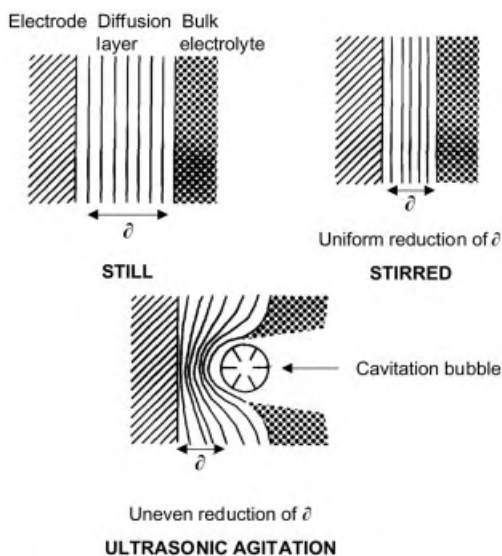


Fig. 6.8. Disturbance of diffusion layer.

cathode tend to decrease because the rate of diffusion from the bulk of the solution is lower than the rate of discharge at the surface. This will cause the deposition rate to fall. However, the application of ultrasound will increase the movement of the metal ions, thereby minimising the concentration effect. (By analogy if we have dissolution at the anode, then the concentration of metal ions increases at high current densities, since their rate of dissolution is greater than the rate of diffusion away from the metal surface into the bulk solution. Hence the process becomes more difficult, and therefore the rate of dissolution tends to decrease.) A further benefit of using ultrasound is that by minimising the difference in concentration around the electrodes, there is also a reduction in the effect of “resistance polarisation” which contributes to the ohmic-drop of the cell.

Another problem in the discharge process arises when the “naked” ion having reached the electrode surface and found a suitable site, combines with an electron and is discharged. All too often the speed it combines with the electrons is rate determining. When the molecule to be discharged is a gas there is also some energy required to dislodge it from the electrode surface – this is often called “activation polarisation”. A similar, but reversed, procedure applies to the dissolution of metals at the anode. An example of ultrasonically assisted gas evolution is from the work of Cataldo [6] who found that the evolution of chlorine, using carbon electrodes, was significantly improved in the presence of ultrasound (30 kHz, 2 W cm⁻², Tab. 6.1).

The final problem encountered in discharge is electrode fouling. This is especially important in electro-organic synthesis, a topic which will be discussed later.

All the problems outlined above are the main reasons why in most cases the potential (E_{app}) required to discharge an ion is considerably higher than the so-called “zero current” or “reversible” potential (E^0). The potential one needs to apply (E_{app}) is in excess of the “reversible potential” by a quantity called the cell overpotential. The overpotential is the sum of the overpotentials of concentration (η^C) and polarisation (η^A) activation plus the ohmic drop ($I \times R$) needed to drive the current through the electrolyte (Eq. 6.6).

$$E_{\text{app}} = E^0 + \eta^C + \eta^A + \eta^R \quad (6.6)$$

Tab. 6.1. Ultrasonic degassing in the sonoelectrolysis of 22 % HCl.

	Conventional	Ultrasonic
Yield H ₂	58.3	59.0
Yield Cl ₂	< 1.0	59.0

The application of ultrasound to an electrolytic solution is beneficial in that it reduces the ohmic, activation and concentration overpotential thereby allowing discharge at lower applied voltage.

Thus in summary, some of the particular advantages which accrue from the use of ultrasound in electrochemistry include:

- degassing at the electrode surface
- disruption of the diffusion layer which reduces depletion of electroactive species
- improved mass transport of ions across the diffusion layer
- continuous cleaning and activation of the electrode surfaces.

All of these effects combine to provide enhanced yield and improved electrical efficiency. Other benefits which will become apparent include increased limiting currents [7, 8], lower overpotentials and improved electrodeposition rates [9]. (Efficiency is defined as the amount metal deposited divided by the amount that should be deposited according to Faraday's laws of electrolysis.)

6.3

Electroplating in the Presence of Ultrasound

Recent studies have demonstrated that simultaneous ultrasonic irradiation of electrochemical systems significantly improve electrochemical reactions [10, 11]. Ultrasound has been used extensively in the electroplating industry for many years, and the literature contains many articles reporting the advantages of ultrasound in electrodeposition and plating which include:

- increased hardness
- increased coating thickness
- improved porosity
- increased reaction efficiency and deposition rates
- use of less toxic electroplating solutions
- greater adhesion
- minimisation of levellers, brighteners and other additives.

Whilst there may be different origins for the variety of these effects, one well-characterised consequence of ultrasonic irradiation is the generation and subsequent collapse of cavitation bubbles within the electrolyte medium and near to the electrode surface of the electrochemical cell. The electrode surface causes asymmetrical collapse of a bubble which in turn leads to the formation of a high velocity jet of liquid

which is directed toward the surface. This jetting is thought to lead to the destruction of the mass transfer boundary layer [12] at the electrode. This improves the overall mass transfer of the system and, as a consequence, the reaction rates at the electrodes.

However there is yet another way that the presence of ultrasound benefits the plating process in that it can be used to provide clean grease free surfaces so that maximum adhesion between the substance being plated and the plating surface can occur. The traditional methods of removing grease and other contaminants is either to use a hot (or cold) organic solvent dip, or to expose the plating surface to the organic solvent vapour. These processes are expensive and Walker has reported [13] that a cheaper alternative exists in which aqueous alkaline solution combined with ultrasound is able to degrease articles 1500 times faster than the use of alkali and mechanical stirring. Other workers have found the use of ultrasound has enabled the use of milder alkaline cleaners, increased cost effectiveness and reduced pollution hazard [14–17].

Let us now discuss examples of the use of ultrasound in the electroplating of such metals as chromium, zinc, iron, copper, silver and nickel (electro and electroless).

6.3.1

Chromium Plating

The electroplating of chromium for hardness, wear resistance and corrosion resistance is a large world wide business. Conventional plating systems employing Cr(VI) are coming under great environmental pressure because of toxicity and reactivity of the metal in this highly oxidised valence state and there is a considerable drive to examine the potential use of Cr(III) since in this state it is much less hazardous and less wasteful of energy requiring three electrons instead of six per metal atom for the reduction process. Unfortunately, there is no satisfactory commercial Cr(III) plating system in use at the time of writing. Such systems which are in use give poor wear resistance, poor crack number densities and poor adhesion all really stemming from the inability to produce sufficiently thick coatings. Typical coatings are 1–3 μm thick compared to Cr(VI) systems which yield 60 μm and more. Consequently Cr(III) is only used on a relatively small scale for decorative finishes i. e. where hard wearing is not envisaged.

Several workers have investigated Cr(III) plating. Fig. 6.9 presents two typical conventional time-coating thickness curves [18, 19].

As can be seen in Fig. 6.9, both the plating rate and the extent of coverage (i. e. thickness) appear to be pH dependent with coverage “plateauing” as time progresses – i. e. a non uniform plating rate. Tu [18] has measured the pH close to the cathode during plating and found it rose to 8.1 in 24 min. He rationalised his findings by suggesting that the increase in pH gave rise to the production of chromic hydro-

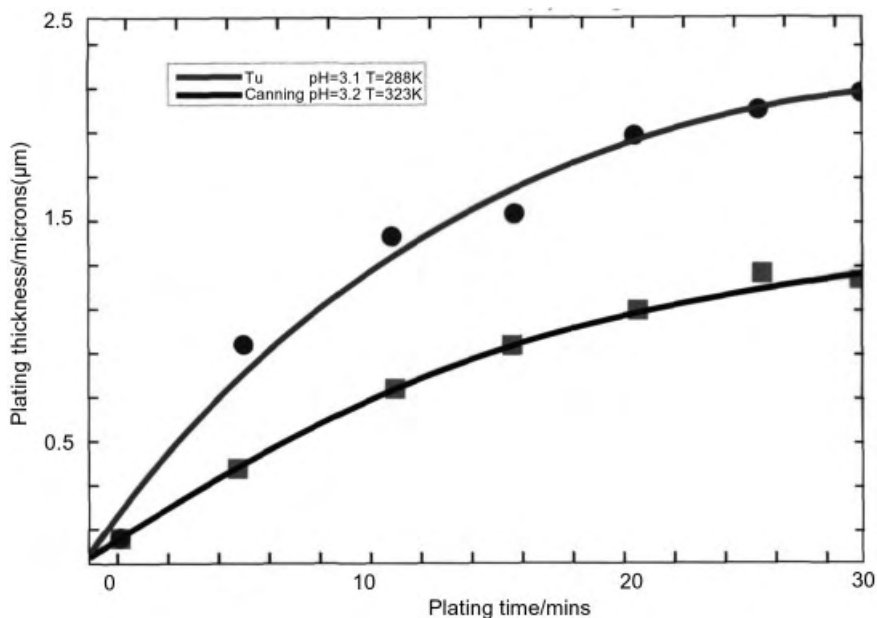


Fig. 6.9. Comparison of Cr thickness.

oxide, or polychromic compounds, which covered the electrode and stopped the deposition – hence the tail off.

At Coventry University [20] we have obtained similar results to Tu under conventional (silent) conditions. Our initial thoughts were that if the effect of the “tail off” was either a consequence of mass transfer to the electrode, or a consequence of some problem with the diffusion layer, then ultrasound might be expected to have an effect and thus improve the plating rate. Investigations in the presence of ultrasound and at various pH values did not significantly affect the plating characteristics i. e. the plateau effect still remained. However, the overall efficiency in the presence of ultrasound was affected (Fig. 6.10).

Fig. 6.10 shows two things:

1. The percentage efficiency observed in both conventional and ultrasonic plating is pH dependent and confirms the findings of Tu who observed maximum efficiency in the absence of ultrasound at pH = 2.1 (Fig. 6.11).
2. There was an improvement in efficiency, when compared to conventional plating, which increased as the pH increased. This latter point identifies a possible small technological benefit to the industry. For example, rather than curtail conventional plating at pH = 2.7, it is possible to continue plating (in the presence of ultrasound) at higher pH values. For example, at pH = 3.1 the efficiency is ap-

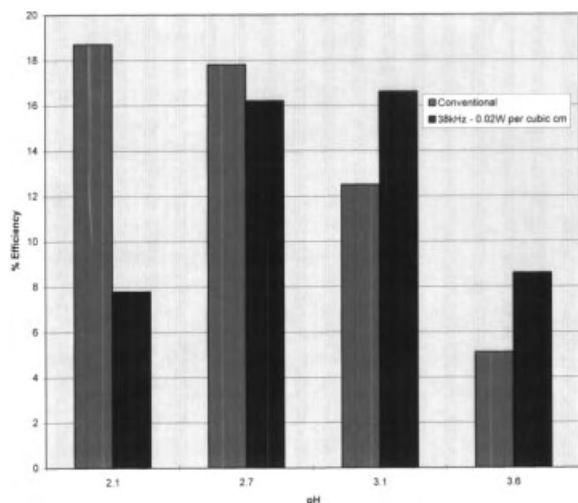


Fig. 6.10. Effect of ultrasound and pH on Cr(III) plating.

proximately 17 % in the presence of ultrasound compared to 12 % in the absence of ultrasound. This value compares favourably with an efficiency of 19 % at pH 2.1 in the absence of ultrasound.

It was suggested previously that one of the obvious variables to change in order to provide for increased plating rates was the current density. The more current applied (in a given time), the faster the coating should develop. Fig. 6.12 compares the effects of increasing the current density (CD) on the plating characteristics for Cr(VI) and Cr(III) [21]. Only for Cr(VI) is the effect as predicted.

We have studied the effect of current density, in the presence of ultrasound, on the plating of Cr(III) (Tab. 6.2).

Tab. 6.2 shows that when compared to conventional plating, there is a significant improvement at higher current density for plating undertaken in the presence of ultrasound. Whilst the tendency towards decreased efficiency (and hence decreased coat-

Tab. 6.2. Effect of current density (CD) on the electroplating of Cr(III); plating time = 5 min; $T = 30\text{ }^{\circ}\text{C}$; frequency = 38 kHz (bath); power = 0.022 W cm^{-3}).

CD [A dm^{-2}]	Thickness [μm]		Efficiency [%]		Cell voltage [V]	
	Conventional	Ultrasonic	Conventional	Ultrasonic	Conventional	Ultrasonic
5	0.30	0.08	4.9	1.0	3.0	2.9
10	1.06	1.14	15.4	16.2	3.9	3.8
20	0.35	0.94	5.0	13.7	4.3	4.2

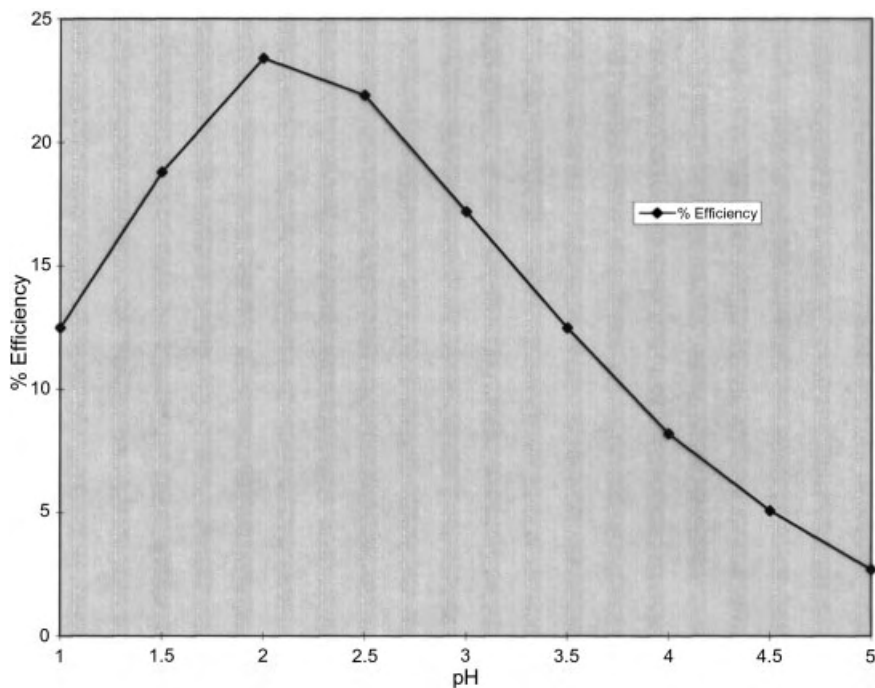


Fig. 6.11. Efficiency vs pH dependence.

ing thickness) at high current density is still apparent in the presence of ultrasound, it is not as dramatic as that observed in conventional plating (Fig. 6.12) – compare the similarity of values obtained at 20 A dm^{-2} and 10 A dm^{-2} .

Work at Coventry University has also shown that applying ultrasound improves the brightness, as measured by reflectance, of the coatings. This increase in brightness is common to many metals electrodeposited in the presence of ultrasound and is thought to be due to the shock waves generated during cavitation which not only harden the surface and remove hydrogen gas bubbles, but also break off any perpendicular growths such as dendrites [22].

Commercially industry uses solutions which contain a stabiliser to keep the Cr(III) in solution and improve the throwing power. Stabilisers are added to stop Cr(III) oxi-

Tab. 6.3. Cr(III) – Effect of stabiliser on the plating efficiency of Cr(III).

Stabiliser [%]	Efficiency [%]	
	Conventional	Ultrasonic
40	10.9	13.6
50	5.4	16.9

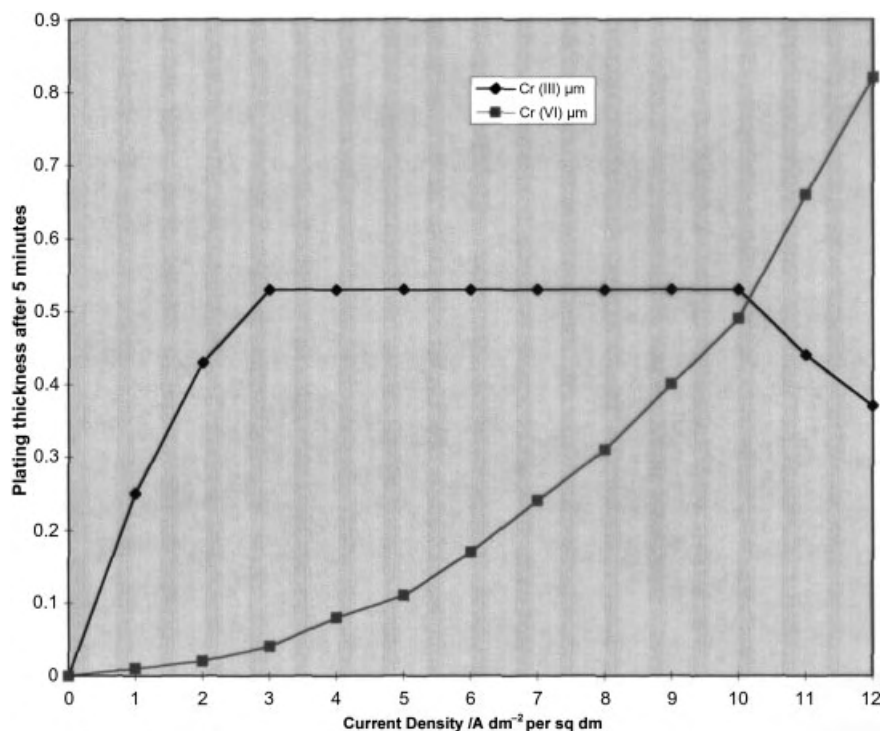


Fig. 6.12. Effect of current density on plate thickness – Cr(III) vs Cr(VI).

dising to Cr(VI). The optimum value is between 65–70 %. Using ultrasound, it is possible to reduce this value to 50 % and yet still obtain nearly a doubling in efficiency (Tab. 6.3).

Improvements in the efficiency of chromium (VI) plating in the presence of ultrasound have been known for some time [23] as has the improvement in adhesion and hardness. At Coventry University, work has centred on pilot scale electroplating (140 L) with a view to scale up. Chrome (VI) solutions are usually prepared by dissolving known masses of chromium (VI) oxide in distilled water and adding concentrated sulphuric acid in the ratio of 1:100 sulphuric. The system is highly acidic and during the electroplating process there is a competition between hydrogen and chromium for displacement at the cathode. Any hydrogen which is evolved erupts at the surface in a stream of bubbles and as the bubble bursts, a mist or vapour is formed which passes into the work place. It is the presence of this vapour which has been linked to the occurrence of cancer of the mouth, nose and throat of plant operators. Normally, the amount of mist is increased if either the concentration of electrolyte or the current density is increased – both of these are requirements for a faster production and hence

Tab. 6.4. The effect of the source of ultrasound on Cr(VI) mist emission (Cr mg m^{-3}).

Conventional	Ultrasonic bath [38 kHz]	Airborne	Bath + airborne
984 ± 131	191 ± 29	65 ± 21	57 ± 14

increased profit. The reduction in mist being vented into the work place are controlled currently by two methods. These are lip extraction and the use of fume suppressants. At Coventry we have identified a third possibility for the control of the level of emissions [24] – the use of ultrasound. For small scale work, ultrasound was effective either when applied through the air above the plating bath or when used in the plating solution itself (Tab. 6.4.)

For large scale (200 L capacity plating tank) it proved impossible to apply airborne ultrasound and therefore the ultrasound was introduced into the plating tank (Fig. 6.13). The transducers consisted of two banks of three mounted in dummy tanks and delivered in total 1.4 kW into 135 L making the overall ultrasonic intensity 0.01 W cm^{-3} . The cathode consisted of a steel bar (5 cm diameter and 20 cm length) and 4 large lead anodes (diameter 3.7 cm and length 39 cm) were used. On sonication

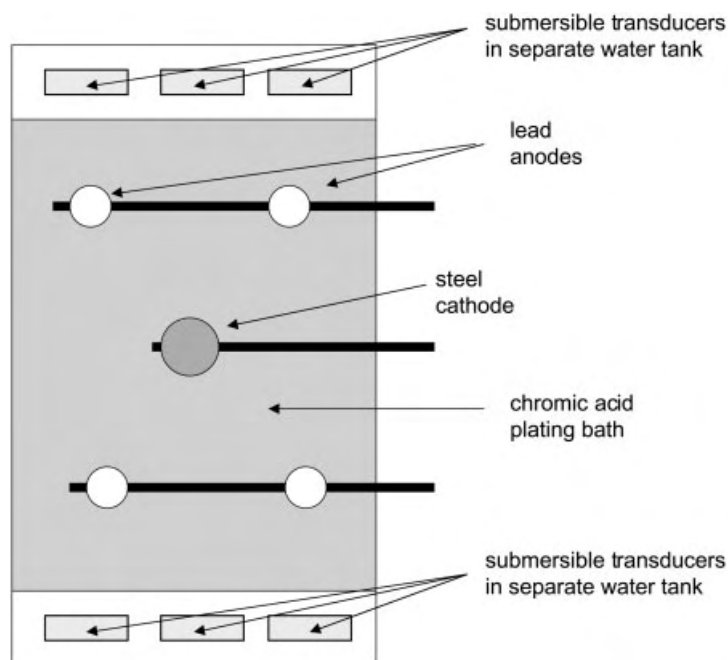


Fig. 6.13. Plan view of pilot Cr(VI) rig showing configuration of transducers.

Tab. 6.5. Effects of ultrasound in Chromium(VI) plating; (a) effect of concentration on plating efficiency; (b) effect of concentration on plating hardness; (c) effect of current density on plating efficiency; (d) effect of current density on mist emission; (e) effect of ultrasonic power on emissions.

(a)

Concentration [g/L]	Conventional plating	Ultrasonic plating	Efficiency change [%]
150	17.6	18.9	7.4
200	18.8	20.6	9.6
250	19.4	21.3	9.8

(b)

Concentration [g/L]	Conventional plating	Ultrasonic plating	Efficiency change [%]
150	972	957	− 1.5
200	972	1020	+ 4.9
250	951	1047	+ 10.1

(c)

Current density [A dm^{-2}]		Efficiency [%]	
	Conventional	Ultrasonic	Efficiency change [%]
15.5	12.2	9.4	− 23
31.0	21.9	17.9	− 18
62.0	23.3	25.1	+ 8
93.0	25.9	26.8	+ 4

(d)

Current density [A dm^{-2}]		Amount of mist [mg m^{-3}]	
	Conventional	Ultrasonic	Decrease in mist [%]
15.5	4.1	0.10	97.5
31.0	6.5	0.14	97.8
62.0	11.7	0.51	95.6
93.0	21.3	0.74	96.5

(e)

Number of transducers	0	2	4	6
Mist emission [mg m^{-3}]	6.6	2.1	0.4	0.14

both the efficiency of the process (Tab. 6.5a) and the hardness of the deposit (Tab. 6.5b) were increased at constant current density. There was also improved efficiency at very high current density (Tab. 6.5c). However what is most dramatic is the reduction in the amount of mist produced at very high current density (Tab. 6.5d) when plating was performed in the presence of ultrasound. Also the reduction in the mist produced was dependent on the applied ultrasonic power (Tab. 6.5e) i. e. the greater the applied power the lower the actual emission value.

Tab. 6.6. (a) Effect of temperature and current density on current efficiency; (b) effect of temperature and current density on microhardness (VHN).

(a)

Temp. [°C]	Current density [A dm ⁻²]					
	20		40		60	
	Conventional	Ultrasonic	Conventional	Ultrasonic	Conventional	Ultrasonic
50	33.1	29.7	42.5	40.0	46.3	44.1
55	31.1	27.0	40.8	38.2	45.0	42.8
60	29.4	25.0	39.4	36.7	43.3	40.1

(b)

Temp. [°C]	Current density [A dm ⁻²]					
	20		40		60	
	Conventional	Ultrasonic	Conventional	Ultrasonic	Conventional	Ultrasonic
50	997	1080	1010	1105	1055	1135
55	980	1040	995	1060	1030	1090
60	955	1005	975	1040	1010	1080

Other workers have studied the effects of varying current density and plating temperature on the hardness and current efficiency and have obtained similar observations (Tab. 6.6), namely that maximum current efficiency occurred at lower temperatures, higher current densities and in the absence of ultrasound (Tab. 6.6a), yet improved hardness occurred at the highest current density and in the presence of ultrasound but at lower plating temperatures (Tab. 6.6b).

Another example of where ultrasound influences the discharge rate of chromium is in the chromium electroplating of steel plates. When cold-rolled steel plate is electrolytically chromated from a silent aqueous solution containing chromates and dichromates, a chrome coating of 13 mg m⁻² is obtained after 1 s, whilst in the presence of ultrasound a coating of 45 mg m⁻² is obtained [25] in the same time. The product is also accompanied with an increase in the brightness of the metal. Similar results have been found by other workers [26].

An alternative method to the irradiation of the plating tank itself is to apply ultrasound directly to the cathode. In a report on hard chromium plating using a steel cathode vibrating at 20 kHz (145 W, magnetostrictive) it was shown that a better quality of plating (e.g. brighter and harder) was obtained when compared with conventional methodology [27].

6.3.2

Zinc Electroplating

Walker [9] has studied the effect of ultrasonic agitation in terms of hardness, quality of deposit and efficiency. Using spent zincate plating baths, he observed that both the efficiency of the zinc recovery process and the maximum current density which could provide for good quality deposits was significantly increased in the presence of ultrasound (Tab. 6.7). He also observed that the improvement was inversely dependent on the bath concentration; the more dilute was the bath (0.5 g dm^{-3} zinc) then the greater the improvement.

Kamat and co-workers [28] have investigated the effects of sodium hydroxide and zinc oxide concentration, temperature and ultrasonic agitation in an attempt to define the best conditions (i. e. a high rate of plating yet still giving an adherent and uniform coating) for a noncyanide alkaline zinc electroplating bath used in the wire industry. They found that in the presence of mechanical agitation a current density of $4\text{--}5 \text{ A m}^{-2}$ was achieved, giving an anodic current efficiency of approximately 100 % and a cathodic current efficiency of 97 to 99 %. In the presence of ultrasound (25 kHz and 250 W), a current density as high as $22\text{--}26 \text{ A m}^{-2}$ was observed at a cathodic current efficiency of 94 to 96 %. A comparison of the salient features of this noncyanide bath and the commonly used acid sulphate bath showed that the noncyanide bath was superior with respect to throwing power and metal distribution, brightness, cathodic current efficiency and limiting cathodic current density in the presence of the ultrasonic field.

Prasad and co-workers [29] have compared the properties of deposits obtained from several still and ultrasonically agitated plating baths. They showed that the use of ultrasound during electrodeposition of zinc (and several other metals) produced smoother and harder deposits [30]. Ultrasonic agitation was originally considered to produce harder deposits because it formed a smaller grain size [31] and the deposits contained more material [32]. It is now generally accepted that these explanations are not entirely satisfactory because very many exceptions have been observed, and the increase in hardness is now considered to be due to a combination of factors resulting from cavitation e. g. a reduction in porosity [33, 34].

Tab. 6.7. Effect of ultrasound on zinc plating (10 g dm^{-3} of Zn).

		Still	Stirred	Ultrasound
Thickness of diffusion layer	[μm]	100	30	13
Maximum cathodic current density to provide a good deposit	[A dm^{-2}]	120–150	550–650	1200–1500
Cathodic current efficiency at 200 A dm ⁻²	[%]	87	98	99

Porosity is particularly important in thin coatings since it can lead to corrosion or the formation of corrosion products on the surface, which in turn have a detrimental effect. The common cause of porosity is the formation of hydrogen bubbles on the cathode surface during plating. These bubbles shield the plating surface from the substrate and prevent deposition on “local sites” below the bubble. Ultrasonic agitation of the solution assists in the removal of these bubbles so enabling a more uniform deposition to occur. Grain coalescence and two-dimensional growth are also encouraged so denser deposits are formed. This improvement in quality, due to the reduction in porosity with ultrasound, has been reported for several metals [35–39].

6.3.3

Iron Electroplating

In the case of iron, the use of ultrasound has been found to improve the hardness of the deposit (Tab. 6.8). The extent of the improvement was found to be dependent on the type of bath employed, the plating temperature and plating current [40].

When the technique of electroplating is used to deposit a layer of iron on another metal surface, it is usual to employ a sacrificial iron anode and a solution of a ferrous salt e.g. ferrous sulphate. (This is the usual technique for silver plating.) The typical anodic (Eqs. 6.7 and 6.8) and cathodic reactions (Eqs. 6.9–6.12) are given below.



Tab. 6.8. Hardness (HV) of electrodeposited iron.

Hardness (HV) of electrodeposited iron				
Conditions	Bath Type			
	Ferrous sulphate 30 °C; 4 A dm ⁻²	Ferrous sulphate 60 °C; 10 A dm ⁻²	Ferrous ammonium sulphate 60 °C; 4 A dm ⁻²	Ferrous sulphamate 55 °C; 12 A dm ⁻²
Still	148	84	165	203
Stirred	152	103	191	201
Sonicated	178	163	203	221
Increase [%] stirred/still	2.7	22.6	15.8	0.0
Increase [%] us/stirred	17.1	58.3	6.3	8.9



The reactions marked with an asterisk (*) lead to lower efficiencies. (The conversion of ferrous to ferric, Eq. 6.8, usually takes place because of dissolved oxygen.) In order for the bath composition to remain constant, the rate of dissolution (Eq. 6.7) must equal the rate of deposition (Eq. 6.9). If they do not occur at the same rate this will lead to concentration polarisation which will act as a barrier to the electrode reactions. We have seen previously (Section 6.2) that ultrasound is able to reduce concentration polarisation.

Ultrasound has also been used to effect changes in the composition of a deposit during plating. For example it is particularly advantageous to increase the proportion of iron in nickel-iron alloy deposits thereby giving cheaper coatings. For a deposit produced in the presence of 24.8 kHz ultrasound, the deposit increased from 3.5 % for the silent system to 19.2 %. Using 37.9 kHz ultrasound, the deposit was 18.8 % [41].

6.3.4

Copper Electroplating

Ultrasound has been used to improve the quality of copper during the industrial electrodeposition [22]. Using 20 kHz ultrasound (0.34 W cm^{-2}) and employing a copper anode (foil) and a copper cathode (sheet) led to less powdery brighter deposits. There was also a significant improvement in the current density from 60 A dm^{-2} in the absence of ultrasound to 500 A dm^{-2} in the presence. Work by Smirnov [42] has shown that coatings produced in the presence of ultrasound were smoother and harder.

Chiba [43] has found that the electrodeposition of copper from a cupric-EDTA bath, in the presence of ultrasound, gave increased limiting current densities and increased cathodic efficiencies while at the same time reducing the grain size. Walker [44, 45] has shown that deposits obtained from sulphate baths in the presence of ultrasound show increased hardness.

Drake [35] has measured the thickness of the diffusion layer during the electrodeposition of copper from an acidic-sulphate system. He obtained a value of approximately $200 \mu\text{m}$ for the silent system and values of $34 \mu\text{m}$ and $3.4 \mu\text{m}$ for ultrasonic frequencies of 1.2 MHz and 20 kHz respectively. The corresponding values of the limiting-current density were from 8 A m^{-2} (silent) to 50 A m^{-2} (1.2 MHz) to 500 A m^{-2} (20 kHz), indicating a significant increase in the rate of deposition.

6.3.5

Electrolytic Removal of Silver

The major use of silver metal is in the photographic industry. However, only a proportion of this expensive raw material is found in the end product (i. e. the photograph). For example, during the development process, unreduced silver (usually a silver halide salt) is dissolved out by immersion in a bleach fix bath. These baths are mainly composed of sodium thiosulphate. In order to improve the life-time of the bath or to have the possibility of re-using the bath, and consequently improve the economy for large scale operations, the dissolved silver has to be removed from the bath. This step will lead to the recovery and conservation of a very expensive noble metal. A second source of silver for recovery is in the development of the photograph. This requires a washing process to stabilise the photograph. This wash water will also contain silver.

Industrially, the silver is recovered from either the wash water, or the bleach fix separately or from a mixture of the two using electrolysis employing a stainless steel cathode cylinder and an anode of stainless steel mesh. A typical wash solution composition contains silver (4 g L^{-1}), sodium thiosulphate (220 g L^{-1}), sodium bisulphite (22 g L^{-1}) and sodium ferric EDTA (4 g L^{-1}). At Coventry we have used a scaled down version of the industrial process employing 250 mL samples [46]. Electrolysis experiments were performed at ambient temperature with both wash and bleach fix solutions and in which the potential applied to the cathode and the speed of rotation of the cathode were varied. The sonic energy (30 W) was supplied by a 38 kHz bath. The results are given in Tab. 6.9. The table shows that the recovery of silver on sonication of the wash or bleach fix solutions is much improved especially if the electrode is rotated while ultrasound is applied. Yields with bleach fix (which contains ferric ions) are less since Fe^{3+} and Ag^+ compete for discharge (Eqs. 6.13 and 6.14).



Tab. 6.9. Effect of ultrasound on silver removal.

Rotation speed of electrode [rpm]	Wash solution – silver removed [%]		Bleach fix – silver removed [%]	
	Conventional	Ultrasonic	Conventional	Ultrasonic
0	4	21	2	13
2000	95	100	33	82

One possible reaction which hinders the total removal of the silver is the formation of a complex between silver and thiosulphate ions (Eq. 6.15). Whilst the removal of such a large quantity of sodium thiosulphate (220 g L^{-1} prior to discharge of silver is not economically feasible, removal (discharge) of thiosulphate is improved in the presence of ultrasound (Tab. 6.10).

6.3.6

Nickel Electroplating

The effect of ultrasound has been extremely beneficial in improving the hardness of nickel deposits (Tab. 6.11). Using a variety of plating solutions it has been shown that the presence of ultrasound improves the hardness of the coating with the magnitude dependent on the particular bath composition employed [9, 12].

It is thought that the increased hardness (Tab. 6.11) is due in part as a result of the reduced pore density and the increase in dislocation density caused by work hardening. It is well known that raising the temperature of a metal work hardens that metal and it is thought that the implosion of cavitation bubbles close to the electrode raises the microscopic temperature. In addition collapse will produce surface impacts by solvent also generating work hardening.

At Coventry we have investigated the effect of frequency and power on the plating thickness and hardness of a “proprietary” plating mixture (nickel sulphamate, $\text{pH} = 4.1$) using equivalent apparatus to that used commercially (i. e. carbon rod cathode and nickel pellets as anode). Tab. 6.12 shows that electroplating (total electrolysis time of 3 h) using 20 kHz ultrasound whilst not improving the thickness of the deposit significantly compared to that in the absence of ultrasound, leads to a significant improvement in the hardness.

Also there appears to be frequency effect in that 38 kHz gives both good coverage, at lower ultrasonic power, and a harder material. The improvement in coverage is a direct result of ultrasonic degassing of the system. For example, during conventional plating the hydrogen gas produced tends to stick to the metal surface. This action is known as

Tab. 6.10. The effect of ultrasonic power (20 kHz probe) on the loss of thiosulphate.

Percentage ultrasonic power	Percentage sodium thiosulphate remaining		
	40 mA (30 min)	100 mA (30 min)	100 mA (60 min)
0	1	3	7
20	3	5	12
40	4	7	13
60	6	30	40

Tab. 6.11. Mechanical effects of ultrasonic agitation.

Bath type	Hardness (hv) of electrodeposited nickel			
	Chloride	Sulphamate	Watts*	Sulphate
Still	193	183	151	151
Ultrasound	305	353	317	407
% Increase in hardness	58	93	110	170

* Composition of Watts bath: NiSO_4 (240 g dm^{-3}); NiCl_2 (45 g dm^{-3}); boric acid (30 g dm^{-3}).

polarisation and leads to a reduction in the plating rate and less uniform coverage of the surface. Although this can be remedied by using higher current densities for plating this, in turn, can lead to “burning” and it is still beneficial to use ultrasound to degas.

Nowack and Habermehl [47] observed a significant drop in cathodic efficiency (90 % to 20 %) as the current density in a silent system was changed from 100 to 200 A m^{-2} . In contrast ultrasound was highly beneficial and the efficiency remained very high (70 %) even at a current density of 800 A m^{-2} .

When it comes to plating inside small apertures or in recesses or crevices, conventional electroplating fails and there is a need to employ electroless chemical plating. For these systems, as the name implies, there is no passage of current. In order to get the nickel to plate in the absence of an applied current, it is necessary to engineer the system so that it supplies its own electrons. This can be accomplished by using a reducing agent such as sodium hypophosphite. Independent investigations by Rich [48], Mallory [49] and Matsuoka [50] have shown increases in deposition rates and decreases in phosphorus content in the presence of ultrasound. However it important for a successful plating operation that the free nickel concentration is kept as low as possible so that it does not impede the movement of the reductant to the material to be plated. At Coventry Univesity, we have investigated the effect of nickel concentration and have found that at all concentrations the presence of ultrasound increases the plating rate quite significantly (Fig. 6.14).

Tab. 6.12. Effect of power and frequency on the thickness and hardness of nickel; conditions: 1.90 V; 139 mA ($= 2 \text{ A dm}^{-2}$); 25°C .

Conditions	Silent	20 kHz	20 kHz	38 kHz	500 kHz	Silent
		8 W	10 W	4 W	6 W	40°C
Thickness [μm]	73.5	90.0	94.3	166.0	116.9	83.1
Hardness VHN	79.9	167.3	124.1	166.1	151.7	96.3

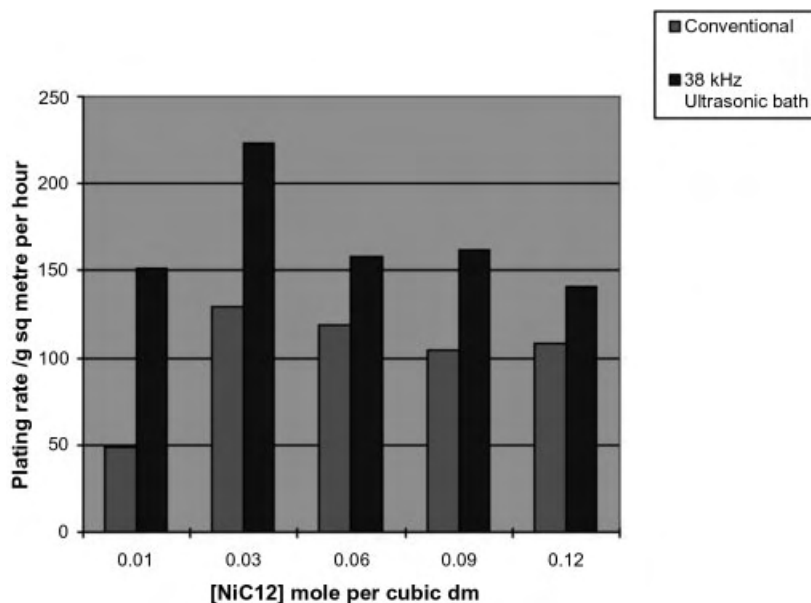


Fig. 6.14. Effect of nickel concentration on the electroless plating rate.

6.4

Sonoelectroorganic Synthesis

The study of electrosynthetic reactions is not a new phenomenon. Such reactions have been the study of investigation for more than a century and a half since Faraday first noted the evolution of ethane from the electrolysis of aqueous acetate solutions. This reaction is more well known as “the Kolbe electrolysis” [51]. Since the report of Kolbe, chemists have had to wait nearly a century until the development, in the 1960’s, of organic solvents with high-dielectric which have been able to vastly increase the scope of systems that could be studied [52]. Added to this more recently is the synergistic effect that ultrasound should be able to offer in the improvement of the expected reactions by virtue of its ability to clean of surfaces, form fresh surfaces and improve mass transport (which may involve different kinetic and thermodynamic requirements)

In this section we will focus on electroreductive and electrooxidative synthesis and touch briefly on the electrosynthesis of selected organometallics and electroinitiated chain polymerisation, previously introduced in Chapter 5.

6.4.1

Electrooxidative Syntheses

Prior to our own studies in the late 1980's, the possibility that ultrasound could be deliberately employed to alter the course of a reaction had not really been addressed. It had simply been used to improve reactivity.

The reaction we chose was the electrooxidation of carboxylate anions. Although the reaction had been regularly reviewed [52–54], and was the subject of a wealth of empirical data, there still remained mechanistic controversy [66]. In general the mechanism breaks down into a pathway involving one-electron per molecule of starting material, giving products from the radical intermediate, for example the dimer [R-R] (which is the actual Kolbe reaction) and a two-electron pathway per starting molecule, giving products from an intermediate cation (Fig. 6.15).

We chose to examine a system where both pathways operate [56] in order to best identify any sonoelectrochemical effect on mechanism [57]. Tab. 6.13 shows product ratios from the electrooxidation of partially-neutralised cyclohexanecarboxylate in methanol at platinum, at a current density of 200 mA cm^{-2} in the presence and absence of ultrasound.

In the absence of ultrasound, the results show a substantial amount (49 %) of the dimer bicyclohexyl from the one-electron pathway, together with cyclohexylmethyl-ether, cyclohexanol and other products from the two-electron pathway (approx. 30 %). The methyl cyclohexanoate ester (17 %) can be thought to arise from the acid catalysed chemical esterification of the starting material with the solvent methanol. (As a result of the high current densities needed, (parasitic) discharge of the solvent methanol produces a large quantity of protons around the anode as a competitive reaction [54].)

The table shows the effect on product ratio of ultrasonic irradiation (Kerry Pulsatron cleaning bath; 35 kHz; 50 W) during electrolysis. Here there is only 8 % of the bicyclohexyl dimeric one-electron product, with approximately 41 % of the two-electron product from nucleophilic capture of the intermediate carbocation. The preponderance of cyclohexene (32 %) over cyclohexane (> 3 %) shows its formation is by proton loss from the carbocation intermediate, since free-radical routes to cyclohexene (i. e. hydrogen atom abstraction) also produce cyclohexane in equal if not greater amounts

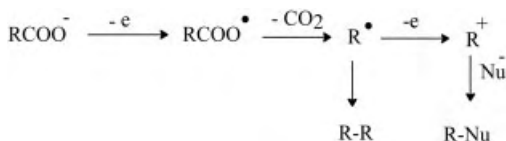


Fig. 6.15. Kolbe reaction.

Tab. 6.13. Electrolysis of cyclohexanecarboxylate.

Product	Silent conditions	Ultrasonic conditions
Bicyclohexyl	49.0	7.7
Cyclohexane	1.5	2.6
Cyclohexene	4.5	32.4
Methoxycyclohexane	24.9	34.3
Methyl cyclohexanoate	17.0	2.5
Cyclohexanol	2.1	6.8

[54, 57]. It is also noted that the formation of methyl cyclohexanoate ester is less in the presence of ultrasound, suggesting enhanced adsorption of carboxylate with concomitant suppression of solvent discharge. This has precedent since ultrasound is thought to enhance adsorption phenomena in some dissolving-metal chemical reactions [58].

We also found that in the presence of ultrasound that not only was there a drop in overall cell voltage from 8.3 V to 7.3 V but the reaction approached completion in a shorter timescale despite the apparent switch to the two-electron process. Overall, ultrasound appeared to favour the two-electron mechanism, and the greatest effect of sonication upon product distribution was the substantial enhancement of alkene formation.

We have also investigated the electrooxidation of phenylethanoate, a system where there is no proton-loss pathway from the intermediate carbocation. Tab. 6.14 shows relative product ratios for phenylacetate in similar conditions to those used for cyclohexane carboxylate, but employing 100 mA cm^{-2} current density [59, 60].

We found that conventional electrolysis (of the partially-neutralised salt) in methanol produced a very rapid increase in applied cell-voltage and the attainment of no effective product (Column I). This was due to the production of a pale coloured coating at the anode which caused the reaction to cease. This is a well known occurrence in electroorganic chemistry [61] and the remedy is to add pyridine to keep the electrode clean, presumably by solubilising the inhibiting layer. Column II shows the product ratios from the silent reaction in the presence of 13 % (v/v) of pyridine. Here there is 60 % of

Tab. 6.14. Electrolysis of phenylacetate.

Product	Silent		Ultrasonic	
	I 0 % pyridine	II 13 % pyridine	III 0 % pyridine	IV 13 % pyridine
Bibenzyl	0	59.8	52.7	51.3
Toluene	0	0.4	3.1	1.5
Benzyl methyl ether	0	21.1	32.3	27.8
Methyl phenylethanoate	0	10.2	6.2	4.2

the Kolbe dimer bibenzyl (one-electron product), 21 % of the two-electron product (methyl ether) and some 10 % of the (parasitic) methyl ester. A major component of the remaining (8 %) material is benzaldehyde, a persistent by-product of arylacetate electrooxidations.

Column III shows the effect of ultrasound upon the product ratio with methanol as solvent. As can be seen there is now 53 % bibenzyl, 32 % of methyl ether and 6 % of methyl ester (with a total of 5 % of other products) suggesting a slight shift towards the two-electron products, but with an overall diminution of solvent discharge (approx. 6 % ester) and side-reactions (approx. 6 %). This result confirms the fact the phenyl acetate electrooxidation favours the one-electron route (to bibenzyl) in a wide range of conditions [61], and is much less sensitive to mechanistic switches by manipulation of parameters (e. g. ultrasound) than is cyclohexane carboxylate electrooxidation [54].

Column IV shows the product ratios in the presence of ultrasound and in the presence of pyridine. Overall there is the same trend with sonication, namely a slight shift from one-electron towards two-electron pathway, though here there is a higher yield of benzaldehyde derived by-products (approx. 16 %).

The most significant factor is that there is no evidence of electrode fouling for reactions in the presence of ultrasound and the reactions maintain current density at a steady and lower voltage. In addition, a fine white powder formed during the electrolysis (yield 14 % by weight) in the presence of ultrasound was subsequently shown to be a polymer of moderate R.M.M. which contained aromatic rings and also two types of methylene group (from NMR) and an aliphatic ester carbonyl ($1,735\text{ cm}^{-1}$ in the IR). This suggested a structure incorporating $\text{-C}_6\text{H}_4\text{-CH}_2\text{-}$ units and $\text{-C}_6\text{H}_4\text{CH}_2\text{COO-}$ units. It may be supposed that enhanced mass transport under ultrasound and the abrasion effect near the electrode surface has swept the inhibiting species into solution, thus keeping the electrode clean. There was much less powder in the presence of ultrasound and in the presence of pyridine, suggesting that it was indeed solubility factors that demanded the use of the cosolvent in silent conditions.

Again a further feature was the lowering of the applied cell voltage from 7.9 V to 6.6 V under ultrasound, representing an energy saving. But the perhaps the more important environmental and economic consequence was the non-requirement to add pyridine under ultrasound. This represents a significant procedural enhancement in that the presence of pyridine considerably hampers work-up and also causes problems on environmental and economic grounds.

Ogashasa and Mataka [62] have employed crossed Kolbe electrolyses of deuterated phenylacetates and succinates to produce derivatives of 4-phenylbutyric acids. In control experiments to produce deuterated bibenzyls from phenylacetate without the presence of succinate, they obtained 11 % of dimer with pyridine present, under normal conditions, and 41 % of dimer with an ultrasonic cleaning bath. This increase in yield was ascribed to a "sweeping clean" of the electrode by ultrasound.

We have also examined the use of higher ultrasonic frequencies (500 kHz and 800 kHz) and found the trend in product distribution from carboxylate electrooxidation at platinum electrodes in methanol to be the same as under sonication in the 20 kHz to 40 kHz frequency range. However, we obtained better yields in spite of the usual reduced cell voltage requirements in the presence of ultrasound. There also seemed to be fewer of the numerous low-yield methoxylated species and other side-products.

Other sonoelectrochemical examples where the frequency of ultrasonic irradiation is important is in the electrooxidation of alkylaromatics. A number of possible products may occur which are dependent upon the substrate and the reaction conditions. For hexamethylbenzene, with no free ring-position, side-chain substitution occurs. However in acetonitrile, with some 1% of acetate ion, a competition occurs which leads to either the acetamide derivative $\text{RCH}_2\text{NHCOCH}_3$ or the acetate ester $\text{RCH}_2\text{OCOCH}_3$ [52, 63]. The reaction is known to be affected by the nature of the electrolyte salt in the silent system. Walton et al. repeated the work under ultrasonic conditions with the ultrasound being supplied from either a 38 kHz bath or an 800 kHz bath. The authors employed a platinum anode in $\text{MeCN}/\text{CH}_2\text{Cl}_2$ as solvent containing either Bu_4NBF_4 or Bu_4NClO_4 as electrolyte. Although they noticed some small effect of electrolyte salt, as previously reported, they observed no major effect of sonicating at either frequency [64]. However, for pentamethylbenzene, with a free ring position, a much larger effect was seen. In this case there was an opportunity for nuclear substitution by another ring, leading to a mixture of products (Fig. 6.16) the major one being a diphenylmethane derivative, produced in an overall one-electron process in which a reactive intermediate centred on a methyl group attacked the free ring position of another molecule, since this was statistically favoured over dimerisation *via* the free ring positions on two adjacent species. Alternatively, attack by a nucleophile leads to a two electron product.

Tab. 6.15 shows the percentage product ratios after the passage of 0.3 Faradays mol^{-1} (i.e. not to completion), under potentiostatic control at +1.6 V (*vs* SCE) for silent, stirred and sonicated conditions. Although the use of 38 kHz ultrasound favours the acetamide product, this was also the major product in a solution mechanically stirred. Overall there was very little shift in the total amount of two-electron *vs* one-electron products using 38 kHz ultrasound. However, the use of 800 kHz gave a

Tab. 6.15. Electrooxidation of pentamethylbenzene.

Product	Silent	Mechanical stirring	Ultrasound 38 kHz bath	Ultrasound 800 kHz bath
A	2	8	9	7
B	62	14	14	43
C	20	42	62	24

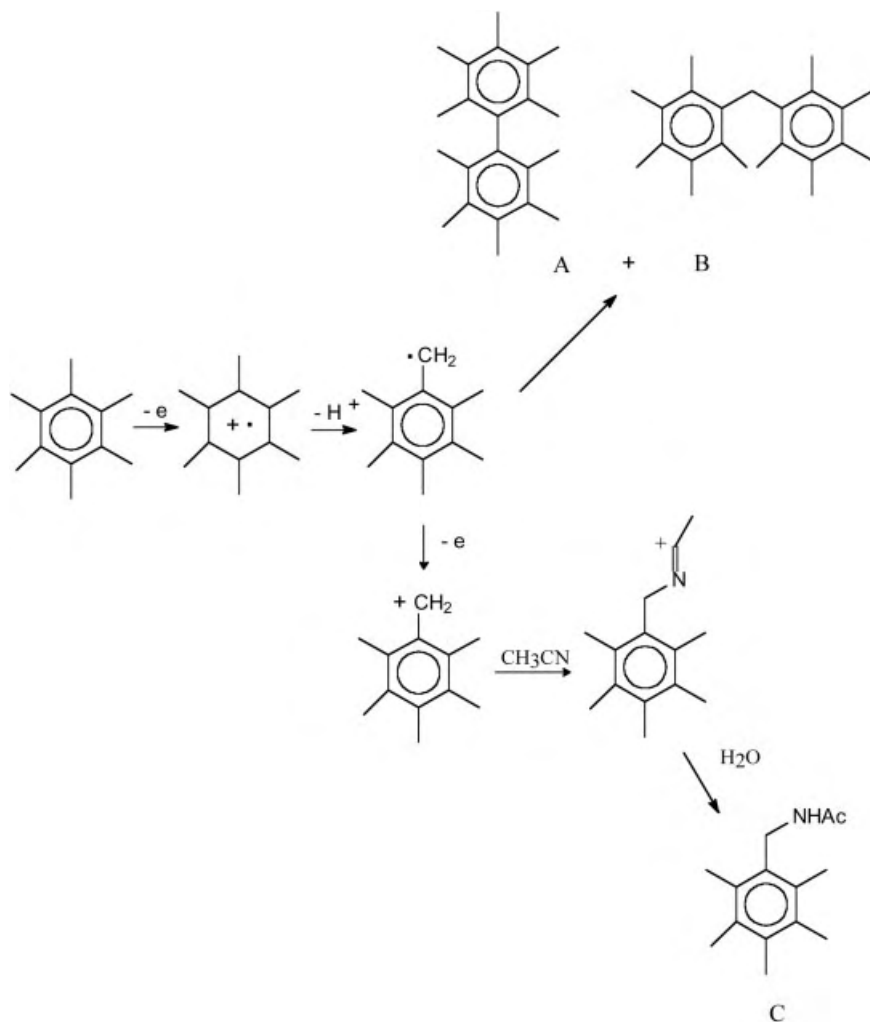


Fig. 6.16. Electrooxidative routes for pentamethylbenzene.

much greater affect in that compounds of diphenylmethane (B) became the major product in a switch to the one-electron mechanism. Thus sonication at different frequencies, at equivalent power, have provided different effects upon the reaction.

Table 6.15 shows the product mixture from an unstirred (silent) reaction in which the only mixing is by convection, an arrangement not normally used in electrosynthesis. (All electrosyntheses are normally agitated mechanically in some way and therefore 'still' conditions cannot practically be achieved.) For these conditions, the major product was the isomeric mixture of diphenyl methane derivatives. This was similar to the product mix obtained at 800 kHz. Thus the use of high frequency ultrasound

(800 kHz) produces less of a product switch than does mechanical stirring. This is an interesting observation which could be significant in other multipathway electrochemical systems. The use of high frequency ultrasound may offer a route to a different hydrodynamic regime.

6.4.2

Electroreductive Syntheses

One of the earliest sonoelectroreductive investigations was the conversion of nitrobenzene into p-amino phenol [65]. Ultrasound (2.375 kW) was applied to a divided cell in which the catholyte consisted of 30 % aqueous H_2SO_4 containing some 0.5 % of SnCl_2 and 0.01 % of the non-ionic surfactant poly (ethyleneglycol) nonyl phenyl ether and the anolyte contained a more dilute 8 % solution of H_2SO_4 . Ultrasound was applied for some 16–30 h during which time the cell temperature rose to 80–90 °C. Using a current density of 50 mA cm^{-2} gave 70 % yield of product.

Work by Ono et al. [66] has been specifically directed at ultrasonic control of product-selectivity in electroreductions. Using a lead cathode, in dilute methanolic sulphuric acid, at a constant current of 20 mA cm^{-2} , Ono electroreduced benzaldehyde under stirred, unstirred and ultrasonic conditions (Fig. 6.17). In an unstirred system, benzyl alcohol (two-electron process) was the major product, while mechanical stirring reversed the position in favour of the hydrodimer (one-electron product). Ultrasonic irradiation from a cleaning bath (100 W, 36 kHz) so strongly favoured the hydrodimer that the alcohol was barely evident (Tab. 6.16).

These authors, using a horn system, also noted less striking but still significant switches towards the one-electron products in other sonoelectrochemical reductions [66] including dimethylmaleate at a lead cathode in an aqueous mixed-phosphate buffer, and benzyl bromide at a lead cathode in methanolic tetraethylammonium bromide solution (Tab. 6.16).

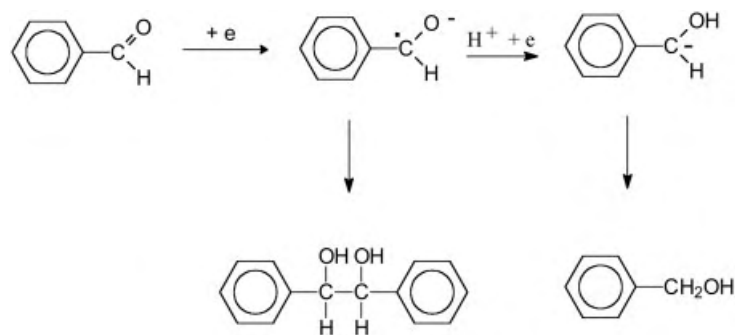


Fig. 6.17. Electroreduction of benzaldehyde.

Tab. 6.16. Electroreduction of benzaldehyde, dimethyl maleate and benzyl bromide.

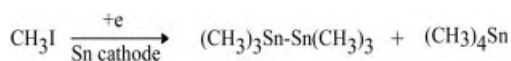
System	Conditions	Product ratio one-electron/two-electron
Benzaldehyde	still solution	0.6
	mechanical stirred	2.5
	ultrasound	3.4
Dimethyl maleate	still solution	0.0
	mechanical stirred	0.3
	ultrasound	0.4
Benzyl bromide	still solution	0.0
	mechanical stirred	0.3
	ultrasound	0.9

The reduction of benzoic acid at a lead cathode in aqueous sulphuric/citric acids yields the two-electron products benzaldehyde and the four-electron product benzyl alcohol rather than one-electron hydrodimer. In all cases studied by the authors they found that ultrasound favoured the process involving the smaller number of electrons per molecule. This is the opposite of the sonoelectrochemical effect seen in carboxylate electrooxidation [57, 59, 60] where the process involving the greater number of electrons was favoured by ultrasound.

Atobe and Nonaka [67] have used a 20 kHz (titanium-alloy) sonic horn as the electrode (called sonoelectrode) for electroreductions of various benzaldehyde derivatives. This they did after insulating the submerged metal part of the horn-barrel with heat-shrink plastic. They found an improvement in current efficiency with insonation, but in addition noted some change in product selectivity towards one-electron-per-molecule products. Although the authors quote enhanced mass transfer across the electrode interface as the origin of the sonoelectrochemical trend towards products from the lesser amount of electrons per substrate molecule, the involvement of surface species on the reactive electrode provides a complication.

Work at Coventry has shown the same switch from a two-electron to a one-electron pathway is occurring at higher insonation frequency in that the electroreduction of benzaldehyde at 800 kHz gives almost entirely the pinacol. A major benefit of the use of the higher frequency however is that there is little weight loss of the lead cathode compared to lower frequency (20 kHz) where it is substantially abraded away.

The electroreduction of methyl iodide at a reactive tin cathode has been examined by Atobe, Matsuda and Nonaka [68]. For the electroreduction (10 mA cm^{-2}) in DMF/ Bu_4NClO_4 at room temperature (Fig. 6.18) in an unstirred reaction, a 1:10 ratio of

**Fig. 6.18.** Electroreduction of methyl iodide at a tin cathode.

dimeric distannane (three-electron product) to tetramethyl stannane (four-electron product) was obtained. Mechanical stirring slightly improved the ratio, while ultrasound from a 20 kHz probe increased the dimer to give a 1:5 ratio. A similar trend was observed for methyl bromide in the same solvent system.

6.4.3

Organometallic Systems

Organoselenium and organotellurium

One of the first series of reports on ultrasonically-enhanced electrosynthesis was by Gautheron, Tainturier and Degrand [69] who used the technique to explore routes to organoselenium and tellurium derivatives. Instead of employing a sacrificial cathode of elemental selenium, their procedure allowed the direct use of selenium powder with carbon cloth as cathode to produce Se_2^{2-} and Se^{2-} . A further benefit was that this method also allowed production of the corresponding tellurium anions. These species could be employed in situ in aprotic solvents such as DMF, THF and MeCN for the synthesis of selenides and tellurides by nucleophilic displacement from haloalkanes.

The system was extended to the electroreductive synthesis [70] of dicyclopentadienyl titanium pentaselenide $(\text{R-C}_5\text{H}_4)_2\text{TiSe}_5$ from selenium powder and $(\text{R-C}_5\text{H}_4)_2\text{TiCl}_2$. When R was methyl, the optimised process gave a 70 % yield. The same authors have investigated the formation of unsymmetrical diaryl chalcogenides [71]. Electroreduction of a symmetrical diaryl chalcogenide at a carbon cloth cathode gave firstly the PhSe^- anion, which on addition of bromobenzonitrile and further electroreduction in the presence of ultrasound, led to a 57 % yield of $\text{PhSe}(\text{C}_6\text{H}_4\text{CN})$ and a 42 % yield of $\text{PhTe}(\text{C}_6\text{H}_4\text{CN})$ with some of the corresponding symmetrical functionalised dichalcogenide as side product.

This mechanism has been further exploited for the production of a number of unsymmetrical phenyl seleno benzophenones and their tellurium analogues [72], again by a two-step electroreductive process, both steps being performed under ultrasound. Having formed the PhSe^- anion, the potential was made more negative before adding the haloketone. Although $\text{PhCOC}_6\text{H}_4\text{SePh}$ could be prepared in 49 % yield, the production of the tellurium analogue was less efficient, giving only 17 % isolated, with symmetrical species such as $\text{PhCOC}_6\text{H}_4\text{TeC}_6\text{H}_4\text{COPh}$ as byproducts.

The use of a redox mediator such as azobenzene has introduced a further sophistication in that it has allowed the cathodic potential in the second step of the procedure to be substantially reduced, until only the mediator remained electroactive. Thus the first step is the electroreductive generation of RSe^- or RTe^- ; then the haloketone, the acidic species such as fluorene, and the azobenzene redox mediator are added and the potential reduced for the second step. By this means isolated yields of 86 %

$\text{PhCOC}_6\text{H}_4\text{SePh}$ and 45 % for the tellurium analogue are obtained. Interestingly, the isolated yield for the tellurium derivative under mechanical stirring was 44 %. Such a little difference between the mechanical stirred yield and the sonoelectrochemical yield, makes the role of ultrasound in such complex systems difficult to ascertain.

Organosilicon and organogermanium

A number of investigations have centred on the use of ultrasound to enhance the production of polysilanes or polygermanes. Using magnesium or aluminium (sometimes copper) as a sacrificial anode, an undivided cell, lithium perchlorate as electrolyte salt and tetrahydrofuran (THF) as solvent, polysilanes of relative molar mass of approx. 3000 in 22 % yield [73] have been prepared from dichlorosilanes such as PhMeSiCl_2 . This contrasted earlier work using mercury cathodes, again in divided cells, where Si-O-containing polymers and cyclotetrasilanes had been obtained [74, 75]. Simultaneous ultrasonic irradiation (47 kHz) increased the yield of polysilane to 33 % without any obvious effect on molar mass or the polydispersity of the system. This procedure has been the subject of a number of patent applications for disilanes obtained from $\text{R}^1\text{R}^2\text{R}^3\text{SiX}$ for a variety of R groups [76] and also digermanes similarly [77].

Other variations concern the electrosynthesis of germane polymers [78] or silane-germane copolymers [79] from dihalo derivatives. Alternatively the use of trihaloderivatives (RSiX_3) allows the formation of network polysiloxanes [80].

6.4.4

Electroinitiated Polymerisations

Chain polymerisation

There are two techniques employed to investigate electroinitiated chain polymerisation. They are potentiostatic control (constant potential) and the more usual galvanostatic control (constant current).

Investigations into the effect of ultrasound upon these polymerisation processes began in the mid 1980's when Akbulut and Toppare [81] examined the potentiostatic control of a number of copolymerisations. In such copolymerisations initiation takes place once a potential in excess of the oxidation potential of either monomer has been applied. However, often potentials even higher than these are required due to the formation at the electrode of a polymer film. These films create a resistance to the passage of current in the bulk medium with consequent reductions in the possible electrochemical reactions and therefore reductions in the rate and the yield. The use of ultrasound has been rationalised in terms of its removal of this layer in a

'sweeping clean' manner, thus allowing the true reactivity ratio of the monomers to operate throughout the electrolysis.

Fig. 6.19 shows the effect of ultrasound (25 kHz cleaning bath) upon the electroxidatively initiated copolymerisation of isoprene with α -methyl styrene, in $\text{CH}_2\text{Cl}_2/\text{Bu}_4\text{NBF}_4$ at -30°C using platinum electrodes in a divided cell [81]. With ultrasound the copolymerisation proceeds effectively at lower potentials, with some curvature in the dependence of composition upon potential. Fig. 6.20 gives the overall conversion of the system in the absence and presence of ultrasound.

In the presence of sonication there is an overall increase in conversion with increase potential, whilst the opposite is true for copolymerisation performed in silent conditions. The lower degree of conversion at the lower potential is not without precedent, since simple mechanical stirring retards styrene polymerisation [82].

In addition, the molar mass (which is proportional to the intrinsic viscosity, $[\eta]$, Tab. 6.17) of the copolymer decreases with increasing potential in the silent system, whereas in the sonicated case it is effectively constant. Overall ultrasound also appears to produce a more uniform reaction system in that in the silent system the reactivity ratio (determined by infra red spectroscopy) increases with electrode potential, whilst under sonication it remains fairly constant.

Akbulut and Toppare also found very similar effects upon copolymer composition, total conversion and R.M.M. control in the styrene-isoprene copolymer system [83] with the analogous traces to Figs. 6.19 and 6.20 shifted to slightly more anodic values and with a better total conversion at high potential in the presence of 25 kHz ultrasound.

The same workers [84] have also examined the copolymerisation of α -methylstyrene and 4-bromostyrene again with similar effect using 25 kHz probe system. In the absence of an electrical potential but in the presence of ultrasound, they failed to produce any sonochemically-induced polymerisation of the monomer over a 24 h period. This is an important experiment since ultrasound is well known to produce radical species which could themselves influence polymerisation.

Akbulut has also reported the effect of ultrasound upon the electronitiated homopolymerisation of butadiene sulfone (Fig. 6.21) in $\text{MeCN}/\text{Bu}_4\text{NBF}_4$ using platinum electrodes [84]. Interestingly ultrasound did not completely clear the electrode of a polymer film, although it did produce an improvement in the percentage conversion versus time characteristics of the polymerisation.

At Coventry we have electropolymerised styrene in the presence and absence of ultrasound (38 kHz) at 0°C and at two different currents (100 mA and 400 mA). We used bright platinum electrodes, dichloromethane as solvent and tetrabutyl ammonium boron hexafluoride (TBABF_6) as the electrolyte. At 400 mA we obtained complete conversion in 150 min with a resultant molar mass of 100 000 compared with 70% conversion and a molar mass of 314 000 in the absence of ultrasound.

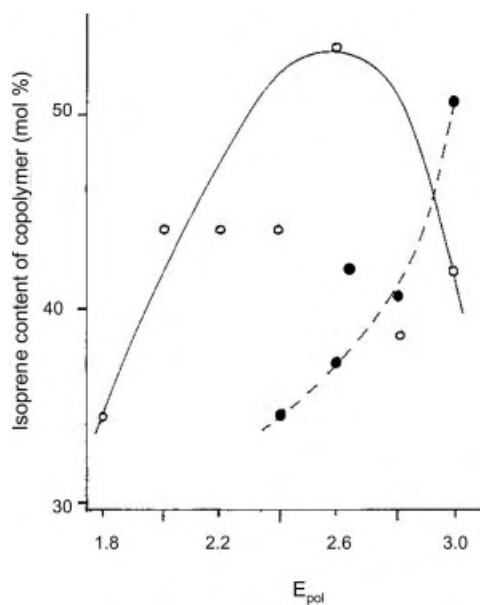


Fig. 6.19. Effect of polymerisation potential (E_{pol}) on the isoprene content (mol %) of electrochemically obtained isoprene- α methylstyrene copolymers; ○ with ultrasound; ● without ultrasound.

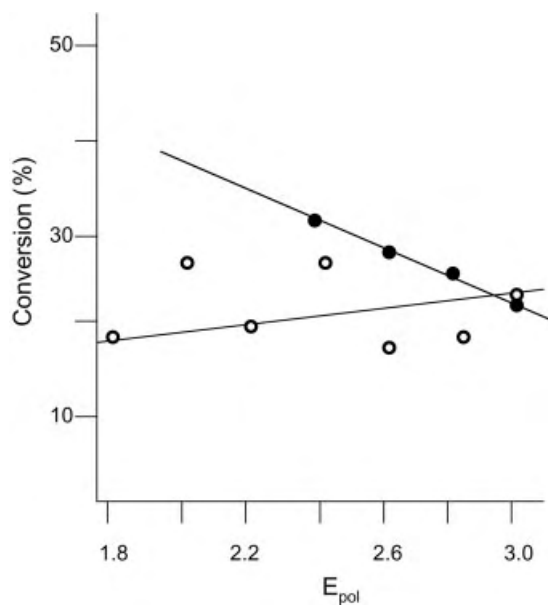


Fig. 6.20. Effect of polymerisation potential (E_{pol}) on the percentage conversion in electrochemically initiated copolymerisation of isoprene with α -methylstyrene; ○ with ultrasound; ● without ultrasound.

Tab. 6.17. Effect of polymerisation potential on molar mass and reactivity ratio.

E_{pol} [V]	Reactivity ratios		
	Isoprene	α -Methyl styrene	$[\eta]$
2.4	0.26 (0.81)	0.19 (0.78)	0.112 (0.049)
2.4	0.36 (0.77)	0.23 (0.77)	0.110 (0.057)
2.6	0.48 (0.70)	0.50 (0.98)	0.098 (0.045)
3.0	0.80 (0.97)	0.75 (0.97)	0.044 (0.050)

Figures in parentheses are in the presence of ultrasound.

The lower molar mass in the presence of ultrasound and the faster kinetics ($k_{\text{ult}}/k_{\text{non}} = 3$) is indicative of chain fragmentation to yield an increase in radical concentration.

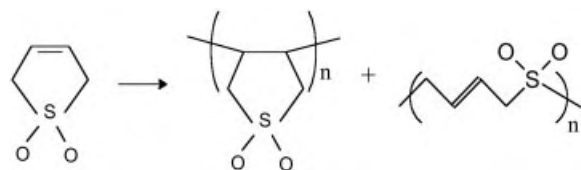
Electrically-conducting polymers

Conducting polymers are quite different systems to the electroinitiated chain polymerisations discussed above being formed by a step-growth mechanism involving stoichiometric transfer of electrons.

The polymers are obtained directly in a conductive polycationic form in which charge-compensating counter anions from the electrolyte system are intercalated into the polymer matrix [85].

The electropolymerisation of the electrically conducting polymers thiophene (mentioned briefly already in Chapter 5) and polypyrrole are thought to be produced by a scheme to that given in Fig. 6.22. (The scheme shows polypyrrole formation. Polythiophene is similar in that NH is replaced by S.)

Polypyrrole readily forms acceptable films under a wide variety of conditions [86] though there are subtle distinctions in behaviour as a result of exact preparation procedure [87]. Ultrasound at 20 kHz at sufficient intensity impedes polypyrrole formation and removes the polymer coating from the electrode [88]. At higher ultrasonic frequencies (e.g. 800 kHz) a free-standing film is produced which can be peeled from the electrode. This film has the interesting feature that the imprint of the wave-

**Fig. 6.21.** Polymerisation of butadiene sulfone.

form can clearly be seen across the surface [89]. X-ray diffraction data has shown minor differences between sonicated and silent films. Results have also shown that one can alter the anion ratio depending on the electrolyte employed. Workers in the field acknowledge that polymers of this type are particularly sensitive to exact preparation protocol and that ultrasound may offer another method of influencing polymer properties.

Polythiophene is less tolerant of preparation conditions than polypyrrole. It also has less two-dimensional cohesion and cannot so easily be peeled from the electrode as a free-standing film. However, it has been shown that the quality of polythiophene films deposited on an electrode can be enhanced by the use of ultrasound. For example, using nitrobenzene as solvent and tertiary ammonium perchlorate as electrolyte, films prepared by conventional methodology (i. e. absence of ultrasound) became brittle as the electrolysis current exceeded 5 mA cm^{-2} . However using ultrasound (35 kHz cleaning bath) produced flexible and tough films (tensile modulus 3.2 GPa and strength 90 MPa) with a high conductivity even at high current density in excess of 10 mA cm^{-2} [90, 91]. Without ultrasound, increases in current density produced an increase in the effective electrode potential giving a low polymer yield and macroscopically inhomogenous films. In the presence of ultrasound, increasing current density did not similarly influence the effective potential and there was a higher yield of better quality film. The sonochemical benefits were especially marked at low temperature (5°C), relatively low monomer concentration (0.1 mol dm^{-3}) and at high current density (up to 10 mA cm^{-2}). The best polymer conductivities obtained were $100\text{--}150 \text{ S cm}^{-1}$ and the sonoelectrochemical enhancement was attributed to the effect upon the diffusion layer during electrode polymerisation.

Another useful commercial polymer is poly *N*-vinyl carbazole which is of interest in reprographic systems due to its photoactive properties. Here there is competition be-

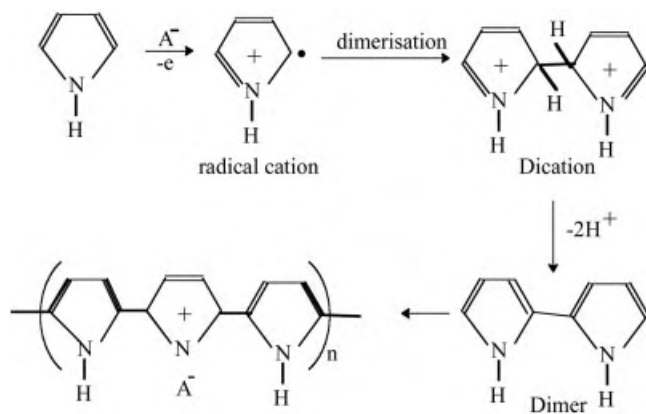


Fig. 6.22. Electrochemical formation of polythiophene.

tween chain polymerisation at the vinyl unit to give a soluble product and cross-linking in the aromatic rings leading to an insoluble and infusible material. Using 20 kHz ultrasound has produced a significant decrease in the polydispersity and increased solubility. Surprisingly a coating of cross-linked species still remained on the electrode, which up to a point did not interfere with its operation. This coating was more adherent than normal, suggesting once again that ultrasound does not always diminish electrode fouling [89].

6.5

Summary

Thus in summary, ultrasonic irradiation produces a number of significant benefits to a wide range of electrochemical systems. Diminution of the diffusion layer has led to faster plating rates, improved hardness and brighter metal deposits. The latter two points are thought to be due to the impingement of cavitation bubbles or shock waves onto the electrode surfaces. In electroorganic synthesis, ultrasound can produce altered product ratios, greater efficiencies, lessened cell power requirements and a diminution of detrimental electrode fouling. If there is an electrodeposition reaction ultrasound alters the properties of the product coating, be it a metal deposited, a semiconductor, a polymer, or some other electrogenerated material. Ultrasound can influence multiphase systems, useful for reactions involving immiscible materials. This effect has been particularly exploited for several applications in environmental science and is of particular interest in view of the drive towards 'clean technology' and the development of microemulsions and similar systems for the replacement of organic solvents by aqueous media.

References

1. G.M. Barrow, *Physical Chemistry*, McGraw-Hill Book Company.
2. J.C. Ball and R.G. Compton, Application of ultrasound to electrochemistry measurements and analyses, *Electrochemistry*, 1999, **67**, 912.
3. *Handbook of Chemistry and Physics*, Chemical Rubber Publishing Company.
4. M. Faraday, *Phil. Trans. Roy. Soc.*, 1834, **124**, 77.
5. D. Fletcher and F.C. Walsh, *Industrial Electrochemistry*, Blackie Academic and Professional, Glasgow, 1993, 49.
6. F. Cataldo, *J. Electroanal. Chem.*, 1992, **332**, 335.
7. J.P. Lorimer, B. Pollet, S.S. Phull, T.J. Mason, D.J. Walton, and U. Geissler, *Electrochimica Acta*, 1996, **41**, 2737.
8. J.P. Lorimer, B. Pollet, S.S. Phull, T.J. Mason, and D.J. Walton, *Electrochimica Acta* 1998, **43**, 449.
9. R. Walker, *Chem. Britain*, 1990, **26**, 251.
10. R.G. Compton, J.C. Eklund, S.D. Page, G.H.W. Sanders, and J. Booth, *J. Phys. Chem.*, 1994, **98**, 12 410.
11. T.J. Mason, J.P. Lorimer, and D.J. Walton, *Ultrasonics*, 1990, **28**, 333.
12. J.K. Klima, C. Bernard, and C. Degrand, *J. Electroanal. Chem.*, 1994, **367**, 297.
13. R. Walker, *Plating Surf. Finish.*, 1985, **72**, 63.
14. K. Emst, *Ind.-Ant.*, 1990, **112**, 12.
15. I. Savioli, *Tecnol. Filo*, 1988, **6**, 26.
16. D.J. McDonald, *Wire Ind.*, 1988, **55**, 78.
17. E. Burnstein, *Products Finishing*, 1989, **53**, 60.
18. Zhemi Tu, *Plating and Finishing*, 1993, 79.
19. Cannings Plating Company, Private communication.
20. D. Pflingsten, MSc by Research Thesis, Coventry University, 1999.
21. P. Crowther, *Electroplating and Metal Finishing*, 1975, **28**, 6.
22. R. Walker and C.T. Walker, *Ultrasonics*, **79**, 1975.
23. J. Dereska, E. Jaeger, and F. Hovorka, *J. Acoust. Soc. Am.*, 1957, **29**, 69.
24. T.J. Mason, J.P. Lorimer, S. Saleem, and L. Paniwnyk, *Environmental Science and Technology*, 2001.
25. M. Kamata, S. Higuchi, and Y. Tsukamoto, *Jpn. Kokai Tokyo Koho*, 1979, 6.
26. D. Ciofica, *Cercetari Metalurgice*, 1979, **20**, 487.
27. E. Mangoong and J.S. Chun, *Thin Solid Films*, 1984, **120**, 153.
28. J.T. Kamat, P.S. Kinnerkar, and D.L. Roy, *Trans. Indian Inst. Met.*, 1975, **28**, 173.
29. P.B.S.N. Prasad, R. Vasudevan, and S.K. Seshadri, *Trans. Indian. Met.*, 1993, **46**, 247.
30. P.B.S.N. Prasad, R. Vasudevan, and S.K. Seshadri, *Indian J. Eng. Mat. Sci.*, 1994, **1**, 178.
31. S.M. Kochergin and G.Ya. Vyaselsa, *Electrodeposition of Metals in Ultrasonic Fields*, Consultants Bureau, New York, 1966.
32. F. Muller and K. Huss, *Helv. Chim. Acta*, 1950, **33**, 217.
33. C.T. Walker and R. Walker, *Nature*, 1973, **244**, 141.
34. C.T. Walker and R. Walker, *Nature*, 1974, **250**, 410.
35. M.P. Drake, *Trans. Inst. Met. Finish*, 1980, **58**, 67.
36. Y. Aramaki, T. Yamashita, and Y.T. Aramaki, *Surface Finish Soc. Japn.*, 1989, **40**, 701.
37. N.P. Moreva, V.A. Pokoev, and G.A. Strlkov, *Fig. Strukt. Sveist. Tverd. Tel.*, 1979, **3**, 81.
38. R. Walker and J.F. Clements, *Met. Finish*, 1970, **16**, 100.
39. R. Walker, *Trans. Met. Finish*, 1975, **53**, 40.
40. R. Walker, *Plating and Finishing*, 1984, 77.
41. R. Walker and S.A. Haglan, *Plating. Surf. Finish*, 1985, **72**, 68.

42. Y. Smirnov, N.N. Khavskii, F.M. Zainutdinov, and N.A. Panov, *Zh. Met.*, 1972, Abstr. No. 5-368.
43. A. Chiba and W.C. Wu, *Plat. Surf. Finish*, 1992, **79**, 62.
44. R. Walker and R.C. Benn, *Plating*, 1971, **58**, 476.
45. R. Walker and R.C. Benn, *Electrochim. Acta*, 1971, **16**, 1081.
46. B. Pollet, PhD Thesis, Coventry University, 1999.
47. N. Nowack and S.K. Habermehl, *Metall-oberfläche*, 1981, **41**, 67.
48. S.R. Rich, *Proc. Am. Electroplat. Soc.*, 1955, **42**, 137.
49. G.O. Mallory, *Trans. Inst. Met. Finish.*, 1978, **56**, 81.
50. M. Matsuoka and T. Hayashi, *Metal Finish*, 1986, **84**, 27.
51. W. Kolbe, *Ann.*, 1849, **69**, 257.
52. M.M. Baizer and H. Lund (eds.), *Organic Electrochemistry*, 3rd Ed., Marcel Dekker, 1991.
53. S. Torii, *Electroorganic Syntheses Part I. Electrooxidations*, Kodansha, 1985; *Part 2 Electroreductions*, Kodansha, 1986.
54. L. Ebersson and J.H.P. Utley, *Organic Electrochemistry*, M.M. Baizer and H. Lund (eds.), 2nd Ed., Marcel Dekker, 1982.
55. Y.B. Vassiliev and V.A. Grinberg, *J. Electroanal. Chem.*, 1991, **1**, 308.
56. G.E. Hawkes, J.H.P. Utley, and G.B. Yates, *J. Chem. Soc., Perkin Trans. 2*, 1976, 1709.
57. D.J. Walton, A. Chyla, J.P. Lorimer, T.J. Mason, and G. Smith, *J. Chem. Soc., Chem. Commun.*, 1989, 603.
58. S.L. Luche, C. Einhorn, and J. Einhorn, *Tetrahedron Lett.*, 1990, **31**, 4125.
59. D.J. Walton, A. Chyla, J.P. Lorimer, and T.J. Mason, *Ultrasonics International, Conference Proceedings*, 1241, Butterworths, 1989.
60. D.J. Walton, A. Chyla, J.P. Lorimer, and T.J. Mason, *Synthetic Commun.*, 1990, **20**, 1843.
61. J.P. Coleman, R. Lines, J.H.P. Utley, and B.C.L. Weedon, *J. Chem. Soc., Perkin Trans. 2*, 1974, 1064.
62. M. Tashino, W. Tsuzuki, H. Goto, S. Ogashasa, and S. Mataka, *Journal of Labelled Compounds and Radiopharmaceuticals*, 1991, 475.
63. A.J. Fry, *Synthetic Organic Electrochemistry*, Harper and Row, 1972.
64. D.J. Walton, U. Geissler, and A. Durham, *Proceedings of World Congress on Ultrasonics, Berlin*, 1995, 659.
65. S. Gigi, V. Paucescu, and S. Jurth, Romanian Patent RO 72382 (1980).
66. Y. Ono, Y. Mishiki, and T. Nonaka, *Chem. Lett.*, 1994, 1623.
67. M. Atobe and T. Nonaka, *Chem. Lett.*, 1995, 669.
68. M. Abobe, K. Matsuda, and T. Nonaka, *Denki Kagaku Oyobi Kogyo Butsuri Kagaku*, 1994, **62**, 1298.
69. B. Gautheron, G. Tainturier, and C. Degrand *J. Am. Chem. Soc.*, 1985, **197**, 5579.
70. B. Gautheron, G. Tainturier, and C. Degrand, *Organometallics*, 1986, **5**, 942.
71. C. Degrand, *J. Chem. Soc., Chem. Commun.*, 1986, 1113.
72. C. Degrand, R. Prest, and P.L. Compagnon, *J. Org. Chem.*, 1987, **52**, 5229.
73. T. Shono, S. Kashimura, M. Ishifune, and R. Nishida, *J. Chem. Soc., Chem. Commun.*, 1990, 1160.
74. E. Hengge and H. Firgo, *J. Organomet. Chem.* 1981, **212**, 166.
75. E. Hengge and G. Latscher, *Monatsch. Chem.*, 1978, **109**, 1217.
76. T. Shono, S. Kashiwamura, and P. Nishida, Jpn. Kokai Tokkyo Koho JP 03264683 (1991) assigned to Osaka Gas Co. Ltd.
77. T. Shono, S. Kashiwamura, P. Nishida, and H. Murase, Jpn. Kokai Tokkyo Koho JP 05306483 (1993) assigned to Osaka Gas Co. Ltd.

78. T. Shono, S. Kashiwamura, P. Nishida, and H. Murase, Jpn. Kokai Tokkyo Koho JP 05306340 (1993).
79. T. Shono, S. Kashiwamura, P. Nishida, and H. Murase, Jpn. Kokai Tokkyo Koho JP 05306342 (1993).
80. T. Shono, S. Kashiwamura, P. Nishida, and S. Kawasaki, Jpn. Kokai Tokkyo Koho JP 05230317 (1993).
81. U. Akbulut, L. Toppare, and B. Yurttas, *Polymer*, 1986, **27**, 803.
81. U. Akbulut, R.L. Birke, and J.E. Fernandez, *J. Poly. Sci., Chemistry*, 1975, **13**, 133.
82. U. Akbulut, L. Toppare, and B. Yurttas, *British Polymer Journal*, 1986, **18**, 273.
83. S. Eren, L. Toppare, and U. Akbulut, *Polymer Commun.*, 1987, **28**, 36.
84. Aybar S.P., Hacıoglu B., and Akbulut U. *J. Poly. Sci. Part A Polymer Chemistry*, 1991, **29**, 1971.
85. T.A. Skotheim (ed.), *The Handbook of Conducting Polymers Vols. 1 and 2*, Marcel Dekker, New York, 1986.
86. D.J. Walton, *Electronic Materials – From Silicon to Organics*, L.S. Miller and J.B. Mullin (eds.), Plenum Press, 1991.
87. D.J. Walton, C.E. Hall, and A. Chyla, *The Analyst*, 1992, **117**, 1305.
88. A. Benahcene, C. Petrier, and G. Reverdy, *New J. Chem.*, 1995, **19**, 989.
89. D.J. Walton, U. Geissler, S. Ryley, C. Campbell, and J. Evans, *Presentation to ISE 47th Meeting*, Balatonfured, Hungary, September 1996.
90. S. Osawa, M. Ito, K. Tanaka, and J. Kuwano, *Synthetic Metals*, 1987, **18**, 145.
91. S. Osawa, M. Ito, K. Tanaka, and J. Kuwano, *J. Poly. Sci. Part B Polymer Physics*, 1992, **30**, 19.

7

Ultrasonic Equipment and Chemical Reactor Design

With so many chemists turning to ultrasound as a source of energy for the acceleration or modification of chemical reactivity it becomes increasingly important that some of the electrical engineering principles which underpin the whole topic of sonochemistry are understood. The first part of this chapter is intended to provide an introduction to the principles of generation of ultrasound for the non-specialist. It is to be hoped that a chemist, armed with this information, will be in a much better position to decide on the type of equipment most appropriate for the intended laboratory application.

7.1

Methods for the Generation of Power Ultrasound

Whatever application of sonochemistry is to be studied or developed there are two essential components, a medium into which the sound must pass and a source of high-energy vibrations. In general the medium used will be a liquid because sonochemistry is driven by acoustic cavitation which can only occur in liquids. The source of the vibrational energy is a transducer, a device capable of converting one form of energy into another, a simple example being a loudspeaker which converts electrical to sound energy.

Ultrasonic transducers are designed to convert either mechanical or electrical energy into high frequency sound and there are three main types: gas driven, liquid driven and electromechanical. All three types have been in use for many years but there have been some recent developments in electromechanical transducers which have improved their performance. A fourth type of transducer, the magnetically-driven vibrating bar, has been introduced which generates very high power vibrations but in the audible range. This has some potential for heavy duty processing and so has been included in the overview below.

7.1.1

Gas-Driven Transducers

These are, quite simply, whistles with high frequency output (the dog whistle is a familiar example). The history of the generation of ultrasound via whistles dates back 100 years to the work of F. Galton who was interested in establishing the threshold levels of human hearing [1]. He produced a whistle which generated sound of known frequencies and was able to determine that the normal limit of human hearing is around $16\,000\text{ cycles s}^{-1}$ (16 kHz). This figure is generally true for older people (> 50 years) however teenagers and young adults are normally quite capable of detecting sound at 20 kHz. This is one of the reasons why ultrasonic devices such as cleaning baths commonly use higher frequencies of around 40 kHz which is certainly not audible to humans. Galton's whistle was constructed from a brass tube with an internal diameter of about two millimetres (Fig. 7.1) and operated by passing a jet of gas through an orifice into a resonating cavity. On moving the plunger the size of the cavity could be changed to alter the "pitch" or frequency of the sound emitted.

An alternative form of gas generated ultrasound is the siren. When a solid object is passed rapidly back-and-forth across a jet of high-pressure gas it interferes with the gas flow and produces sound of the same frequency at which the flow is disturbed. A siren can be designed by arranging that the nozzle of a gas jet impinges on the inner surface of a cylinder through which there are a series of regularly spaced perforations. When the cylinder is rotated the jet of gas emerging from the nozzle will rapidly alternate between facing a hole or the solid surface. The pitch of the sound generated by this device will depend upon the speed of rotation of the cylinder.

Neither type of transducer has any significant chemical application because it is not possible to achieve a sufficiently high intensity in airborne ultrasound by this method. Despite this, applications do exist for airborne ultrasound but the source must be very powerful – usually a sonic horn. In this way one can obtain intensities of a fraction of a

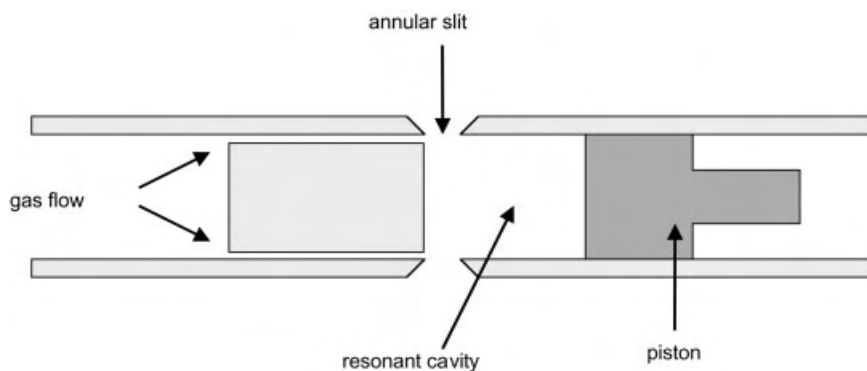


Fig. 7.1. Gas driven transducer – the Galton whistle.

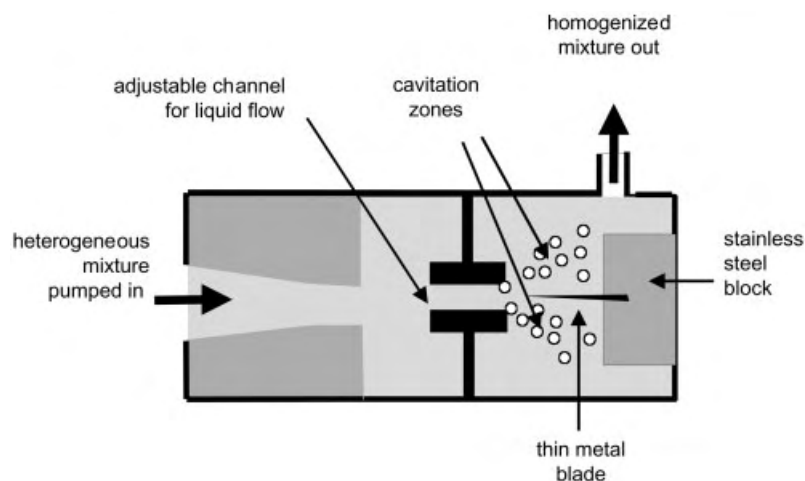


Fig. 7.2. The liquid whistle.

watt per square centimetre in gases and at this level it is possible to use the ultrasound to break down foams, to agglomerate fine dusts and to accelerate drying processes [2].

7.1.2

Liquid-Driven Transducers

In essence this type of transducer can be considered as a “liquid whistle” and it is particularly useful in applications where homogenisation and efficient mixing are important (Fig. 7.2). Process material is forced under pressure generated by a powerful pump through an orifice from which it emerges, as a jet, into a mixing chamber. The jet impacts upon a thin steel blade which is caused to vibrate and thereby produce mixing of the process material flowing over it. Additional mixing is produced through the Venturi effect as the liquid rapidly expands into a larger volume on exiting the orifice. With no moving parts, other than a pump, the system is rugged and durable.

7.1.3

Electromechanical Transducers

The two main types of electromechanical transducers are based on either the piezoelectric or the magnetostrictive effect. The more commonly used of which are piezoelectric transducers, generally employed to power the bath and probe type sonicator systems. Although more expensive than mechanical transducers, electromechanical transducers are by far the most versatile and widely used.

Piezoelectric transducers

These days the most common method employed for the generation and detection of ultrasound utilises the piezoelectric properties of certain crystals one of which is quartz [3]. A simplified diagram of a crystal of quartz is reproduced (Fig. 7.3) which shows three axes defined as x , y and z . If a thin section of this crystal is cut such that the large surfaces are normal to the x -axis (x -cut quartz) then the resulting section will show the following two complementary piezoelectric properties:

1. The direct effect – when pressure is applied across the large surfaces of the section a charge is generated on each face equal in size but of opposite sign. This polarity is reversed if tension is applied across the surfaces.
2. The inverse effect – if a charge is applied to one face of the section and an equal but opposite charge to the other face then the whole section of crystal will either expand or contract depending on the polarity of the applied charges.

Thus on applying rapidly reversing charges to a piezoelectric material fluctuations in dimensions will be produced. This effect can be harnessed to transmit ultrasonic vibrations from the crystal section through whatever medium it might be in. However it is not possible to drive a given piece of piezoelectric crystal efficiently at every frequency. Optimum performance will only be obtained at the natural resonance frequency of the particular sample – and this depends upon its dimensions. In the

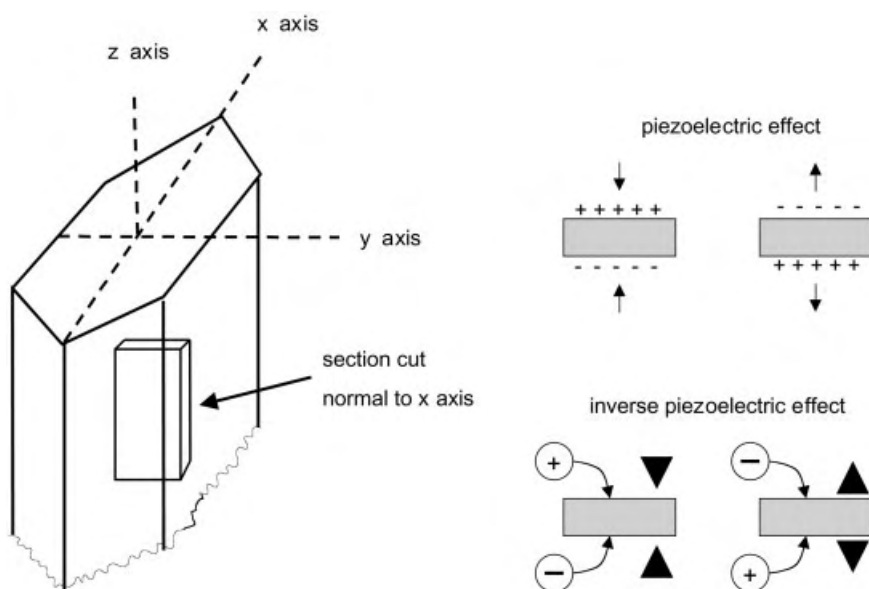


Fig. 7.3. The piezoelectric effect using x -cut quartz.

case of *x*-cut quartz a transducer of thickness 2.88 mm will have a natural frequency of 1 MHz whereas for 0.288 mm it is 10 MHz. This is why the conventional sonochemistry equipment (baths or probes) are of fixed frequency and why reports of comparative studies at widely differing frequencies cannot be performed using the same piece of equipment.

There are many piezoelectric materials besides quartz. The three which are commonly used in transducers are barium titanate (BaTiO_3), lead metaniobate (PbNb_2O_6) and the mixed crystal lead zirconate titanate. These are ferroelectric compounds i.e. they are spontaneously polarised and mechanical deformation causes a change in polarisation. These materials cannot be obtained as large single crystals and so, instead, they are ground with binders and sintered under pressure at above 1000°C to form a ceramic. The crystallites of the ceramic are then aligned by cooling slowly in oil in a magnetic field from above the ferroelectric transition temperature.

It is normal practise to clamp piezoelectric elements between metal blocks which serve both to protect the delicate crystalline material and to prevent it from overheating by acting as a heat sink. Usually two elements are combined so that their overall mechanical motion is additive although they are electrically opposed so that the blocks can be at earth potential. The blocks modify, by their sheer size, the nature of the ultrasonic vibrations generated. In this way a rugged reliable transducer is obtained. The construction of such a transducer is shown (Fig. 7.4). It is generally one half wavelength long (although multiples of this can be used) and it operates in the compressional mode. The peak to peak amplitudes generated by such systems are normally of the order of $10\text{--}20\text{ }\mu\text{m}$.

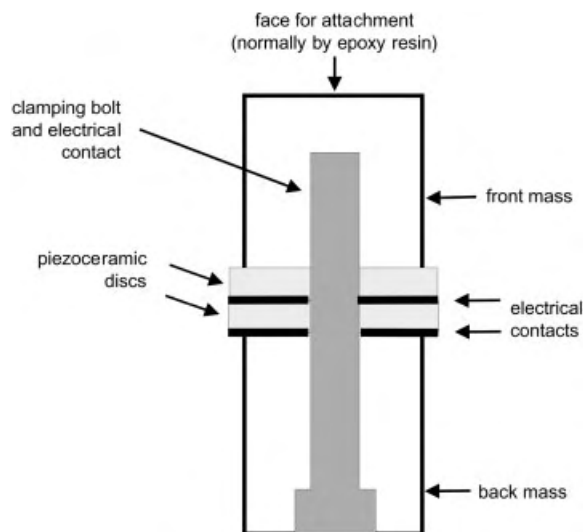


Fig. 7.4. Construction of a piezoelectric "sandwich" transducer.

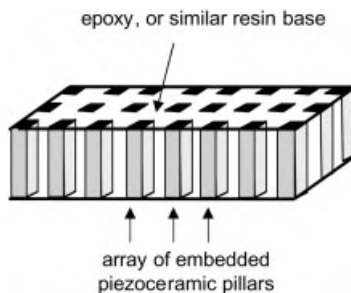


Fig. 7.5. Construction of a 1–3 composite transducer.

The use of such different types of piezoelectric materials permits the building of ultrasonic generators of different powers and frequencies for a range of applications.

New possibilities exist for the development of piezoelectric devices using so-called 1–3 composites. These consist of an array of piezoelectric pillars embedded in a pliable material providing a transducer in the form of a flexible sheet (Fig. 7.5) which can be moulded to fit the shape of a reactor. A particular advantage of such a system is that the emitting face is a combination of ceramic and plastic and can provide much better acoustic transmission into aqueous systems.

There is also a great deal of interest in the production of single crystal piezo material from a mixture of lead, zirconium and niobium compounds (from which they get the name PZN). Such single crystal transducers would provide low loss, high strain, low modulus and have high coupling coefficients. At the time of writing these materials are not yet commercially available.

Magnetostrictive transducers

Historically magnetostrictive transducers were the first to be used on an industrial scale to generate high power ultrasound. These are devices which use an effect found in some materials e. g. nickel which reduce in size when placed in a magnetic field and return to normal dimensions when the field is removed. This phenomenon, known as magnetostriction was discovered by Joule in 1847 [4]. When the magnetic field is applied as a series of short pulses the result is that the metal itself vibrates at the same frequency as the pulses are applied. In simple terms such a transducer can be thought of as a solenoid in which the magnetostrictive material (normally a laminated metal or alloy) forms the core with copper wire winding. To avoid magnetic losses two such solenoids are wound and connected in a loop (Fig. 7.6).

The major advantages of magnetostrictive systems are that they are of an extremely robust and durable construction and provide very large driving forces. This makes them an attractive proposition for heavy duty industrial processing. There are however

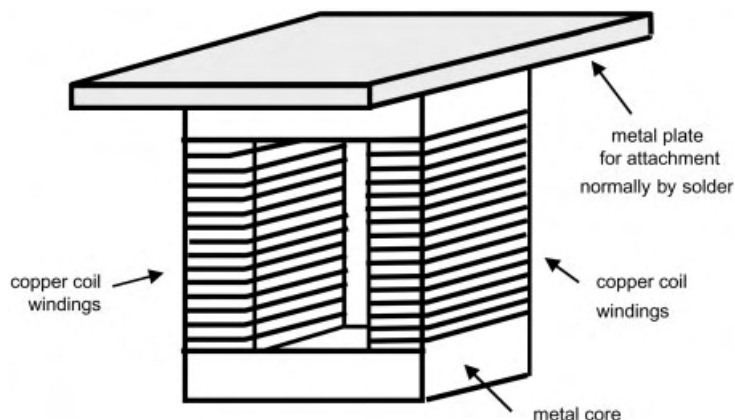


Fig. 7.6. Magnetostrictive transducer.

two disadvantages, firstly the upper limit to the frequency range is 100 kHz, beyond which the metal cannot respond fast enough to the magnetostrictive effect, and secondly the electrical efficiency is less than 60 % with significant losses emerging as heat. As a result of the second of these problems all magnetostrictive transducers subject to extended use are liquid cooled. This has meant that piezoelectric transducers (see below) which are more efficient and operate over a wider frequency range are generally considered to be the better choice in sonochemistry, especially in laboratory situations. However now that a range of industrial applications for sonochemistry are under consideration, particularly those requiring heavy duty continuous usage at high operating temperatures, the magnetostrictive transducer is coming back into consideration.

Many improvements in the operating efficiency of this type of transducer have been made all of which are based on finding a more efficient magnetostrictive core. The original nickel based alloys have been replaced by more electrically efficient cobalt/iron combinations and, more recently, aluminium/iron with a small amount of chromium. One of the latest developments in magnetostrictive technology has been the introduction of a new material called TERFINOL-D. This is an alloy of the rare earths terbium and dysprosium with iron which is zone refined to produce a material almost in the form of a single crystal. It can be produced in various forms, rods, laminates, tubes etc and has several major advantages over the more conventional alloys used. A magnetostrictive transducer based on this material can generate more power than a conventional piezoelectric transducer, it is compact (about 50 % smaller) and lighter than other magnetostrictives. It does have the same problem as other such devices in that it has an upper limit of frequency response – in this case 70 kHz.

The magnetically driven vibrating bar

This provides a significantly different system for large scale processing at audible frequencies. The source of vibrations for this is a large cylindrical steel bar. The bar is driven into a clover leaf type of motion by firing three powerful magnets in sequence which are located at each end of the bar [5]. The bar is supported by air springs so that the ends and the centre are then caused to rotate at a resonance frequency depending on its size (Fig. 7.7). One such unit, developed by Arc Sonics in Canada operates at a power of 75 kW, drives a bar which is 4.1 m long and 34 cm in diameter at its resonance frequency of 100 Hz. The bar itself weighs 3 t and produces a vibrational amplitude at each end of 6 mm considerably larger than the amplitudes available through sonochemical processing and hence better for the dispersal of materials in liquids. Material in the form of a liquid or slurry can then be pumped through the cells in order to perform operations such as mixing, grinding and the destruction of hazardous waste.

Hard spherical grinding balls are often added to the cells to assist in these processes. The combination of the large vibrational energy together with the motion of grinding balls appears to provide an extremely good alternative to conventional mixers and grinders. Other units using smaller sized bars operating at higher, though still audible, frequencies have also been built.

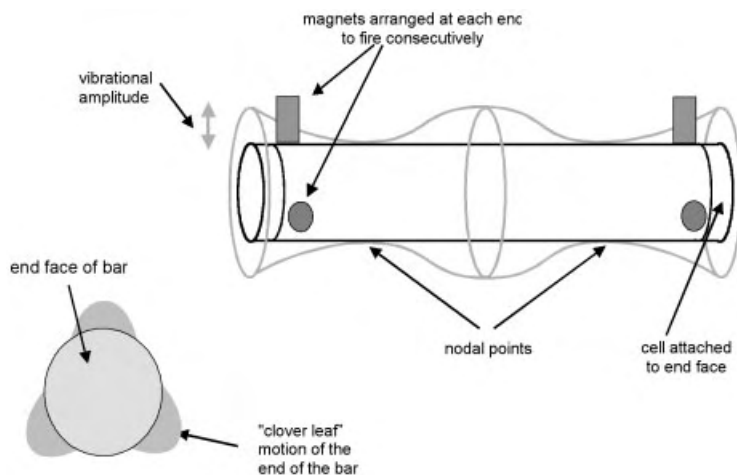


Fig. 7.7. Mode of operation of a vibrating bar transducer.

7.2

Ultrasonic Apparatus

The practising chemist has four types of laboratory ultrasonic apparatus which are commercially available. One of these, the whistle reactor, relies on mechanical generation of ultrasonic power whereas the other three – the bath, probe and cup-horn systems – are driven by electromechanical transducers. The construction of such systems is discussed below and a summary of their relative advantages (and disadvantages) in sonochemical usage are summarised in Tab. 7.1.

Tab. 7.1. A comparison of the types of electromechanical ultrasonic apparatus.

Ultrasonic cleaning bath

Advantages

- The most widely available laboratory source of ultrasonic irradiation.
- Fairly even distribution of energy through reaction vessel walls.
- No special adaptation of reaction vessels required.

Disadvantages

- Reduced power compared with probe system.
 - Fixed frequency (and different frequencies depending on type).
 - Poor temperature control.
 - Position of reaction vessel in bath effects intensity of sonication.
-

Ultrasonic probe (or horn) system

Advantages

- High powers available (no losses due to transfer through vessel walls).
- Probes can be tuned to give optimum performance at different powers.

Disadvantages

- Fixed frequency.
 - Difficult temperature control.
 - Radical species may be generated at the tip.
 - Tip erosion may occur leading to contamination by metallic particles.
-

The Cup-Horn

Advantages

- Better temperature control than a cleaning bath.
- Power control like a sonic horn but less intense.
- Little chance of radical formation in the reaction vessel.
- No fragmentation of metal into reaction from the horn tip.

Disadvantages

- Reduced power compared to horn.
 - Limited volume of reaction cell.
 - Fixed frequency.
-

7.2.1

Whistle Reactor

As noted above this type of mechanical transducer is predominantly used for homogenisation/emulsification. These devices differ markedly from the more usual bath and probe types in that they derive their power from the medium (by mechanical flow across the blade) rather than by the transfer of energy from an external source to the medium. The majority of the chemical effects observed on using whistle type transducers for the sonication of homogeneous reactions can be attributed mainly to the generation of very fine emulsions rather than the ultrasonic irradiation itself.

The use of the liquid whistle type of ultrasonic generators for homogenisation has increased dramatically since the Second World War. It was as far back as 1927 when Wood and Loomis reported that oil and water could be emulsified on sonication in the same beaker using quartz piezoelectric transducers [6]. However at that stage in the development of ultrasonic equipment it was quite difficult to see how transducers driven by quartz crystals could be employed on an industrial scale and so ultrasonic homogenisation remained a curiosity until 1948. In that year Janovski and Pohlmann highlighted the economic advantages to be gained from the use of a liquid whistle compared with magnetostrictive transducers of the type available at that time [7]. In 1960 a series of experiments was undertaken to compare four methods then in common usage for the emulsification of mineral oil, peanut oil and safflower oil [8]. The results proved that a homogeniser, which operated via a liquid whistle, was superior to three other types of apparatus namely a colloidal mill and two types of sonicator, one of which employed a quartz crystal and the other a barium titanate transducer. Subsequently the liquid whistle was adopted as an ideal method of homogenisation and it is this same design of instrument which has been used by Davidson to enhance the hydrolysis of fats and waxes (Fig. 7.2) [9].

An obvious benefit of such a system is that it can be used for flow processing and can be installed “on-line”. In this way large volumes can be processed as is the case in the manufacture of such items as fruit juices, tomato ketchup and mayonnaise.

7.2.2

Ultrasonic Cleaning Bath

This is probably the most accessible and cheapest piece of ultrasonic equipment available and it is for this reason that so many sonochemists begin their studies using cleaning baths.

The construction of a bath is very simple – it generally consists of a stainless steel tank with transducers clamped to its base (Fig. 7.8). One of the basic parameters in ultrasonic engineering is power density which is defined as the electrical power into

the transducer divided by the transducer radiating surface area. The low intensity (bath) system uses a power density at the transducer face of the order $1-2 \text{ W cm}^{-2}$ for a modern piezoelectric transducer. For small baths a single transducer may be sufficient but for larger systems an array of transducers are employed to introduce high power density into the liquid contained in tanks. The frequency and power of an ultrasonic bath depends upon the type and number of transducers used in its construction. The normal method of subjecting a chemical reaction to ultrasound using a bath is simply to dip the reaction vessel in the sonicated water. The sound energy must be intense enough to penetrate the walls of the vessel and cause cavitation in the reaction. Not all laboratory cleaning baths are sufficiently powerful to achieve this and so it is important to check any bath for power before attempting to use it for sonochemistry. The easiest test to apply involves dipping a piece of ordinary household aluminium foil into the sonicated bath water (containing detergent) for about 30 s. A bath which is suitable for sonochemistry will perforate the foil extensively in this time.

Once the bath has been chosen the correct design for the reaction vessel must be used. For normal chemical reactions, particularly those involving heat, round bottomed flasks are utilised but for sonochemistry in an ultrasonic bath the preferred vessel should be one with a flat-bottom e.g. a conical flask. The reason for this is that the energy is radiating vertically as sound waves from the base of the bath and this energy has to be transferred through the glass walls of the vessel into the reaction itself. The energy transference is much more effective when the sound impinges directly on the flat base of a conical flask

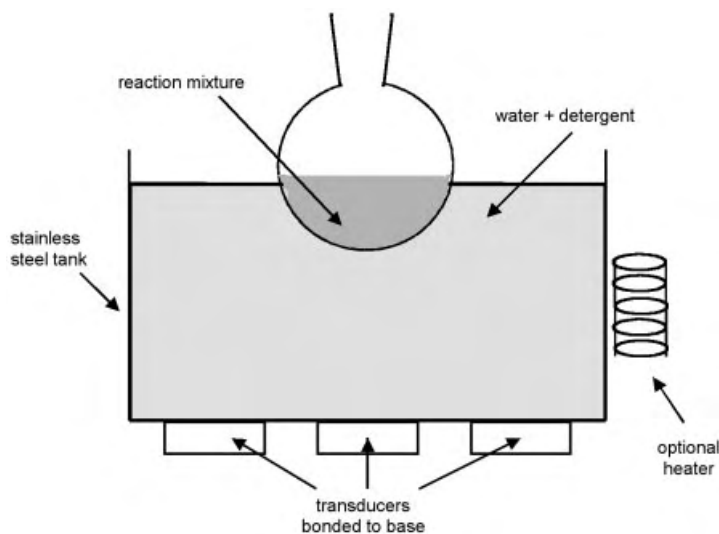


Fig. 7.8. The ultrasonic cleaning bath.

rather than hitting the underside of a spherical container at an angle since when this happens some energy will be reflected away.

Another important consideration when using baths to perform sonochemical reactions is that it may be necessary to stir the mixture mechanically to achieve the maximum effect from the ultrasonic irradiation. This is particularly important when using solid-liquid mixtures where the solid is neither dispersed nor agitated throughout the reaction by sonication alone and simply sits on the base of the vessel where it is only partially available for reaction. The reason that additional stirring is so important in such cases is that it ensures the reactant powder is exposed as fully as possible to the reaction medium during sonication.

Despite the advantages gained from the use of such a simple piece of apparatus there are a number of reservations which should be borne in mind when using this method of energy input.

- The amount of power dissipated into the reaction from the bath is not readily quantifiable because it will depend on the size of the bath, the reaction vessel type (and thickness of its walls) and the position of the reaction vessel in the bath.
- Temperature control is not easy. Most cleaning baths warm up during operation especially over a prolonged period of use. This is not a problem if a heater is used to establish thermal equilibrium but can lead to inconsistent results when working around room temperature or below. However two solutions are available. Either (1) operate for very short periods during which the temperature can be assumed to remain essentially constant or (2) circulate cooling water or adding ice. However if ice is used it must be remembered that solids will alter the characteristics of sonic wave transmission. Whatever method is chosen it must be emphasised that it is the temperature inside the reaction vessel which must be monitored as this is often a few degrees above that of the bath liquid.
- Cleaning baths do not all operate at the same frequency and this may well effect results particularly when attempting to reproduce those reported in the literature.

7.2.3

Laboratory Equipment Based on the Ultrasonic Cleaning Bath

Some of the problems associated with using a commercial cleaning bath can be overcome using an ultrasonic bath purpose built for sonochemistry. Typically these baths are designed with a large area transducer in the base and external cooling/thermostating (Fig. 7.9).

The reaction is performed in the bath itself and is therefore subjected to direct sonication. The acoustic field is more regular throughout the reacting system as a single flat emitting face is used. The vessel itself is enclosed and can be equipped with the

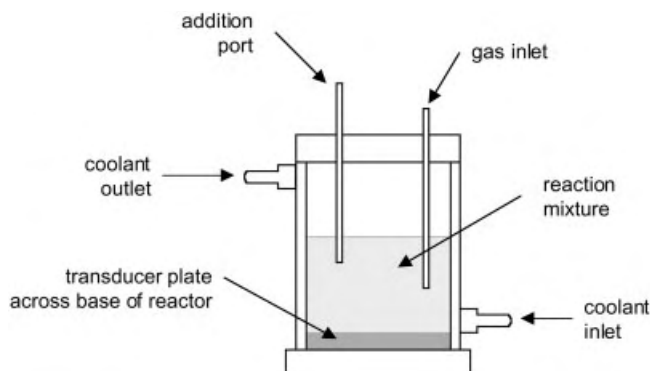


Fig. 7.9. Ultrasonic bath designed for sonochemistry.

normal facilities of gas bleed, addition funnels etc. Many of the more recent studies in sonochemistry, especially those involving higher frequencies, have been carried out with such equipment since the user can choose the particular transducer to be employed.

7.2.4

Direct Immersion Sonic Horn

A number of the disadvantages of the use of a simple cleaning bath in sonochemistry can be avoided using an ultrasonic probe. Originally these devices were simply adaptations of biological cell disrupters. These involve direct immersion of a metal probe into the reaction mixture. The probe – more correctly termed a sonic horn or velocity transformer – is driven by a transducer and ultrasound enters the reacting system *via* the probe tip. The intensity of sonication, the vibrational amplitude of the tip, can be controlled by altering the power input to the transducer and all sonicators have a power control. There is another technique for controlling power input to a system and this depends upon the design of probe used. Most modern systems are designed to operate with a range of detachable metal probes of differing tip diameters. Probe systems are undoubtedly the most efficient method of transmitting ultrasonic energy into a laboratory reaction (Fig. 7.10).

Horn design is a very important aspect of ultrasonic engineering. The vibrational amplitude of the piezoelectric crystal itself is normally so small that the intensity of sonication attainable by direct coupling of the transducer to the chemical system is not large enough to cause cavitation. The horn acts as an amplifier for the vibration of the transducer and the precise shape of the horn will determine the gain or mechanical amplification of the vibration. It is for this reason that it is sometimes referred to as a

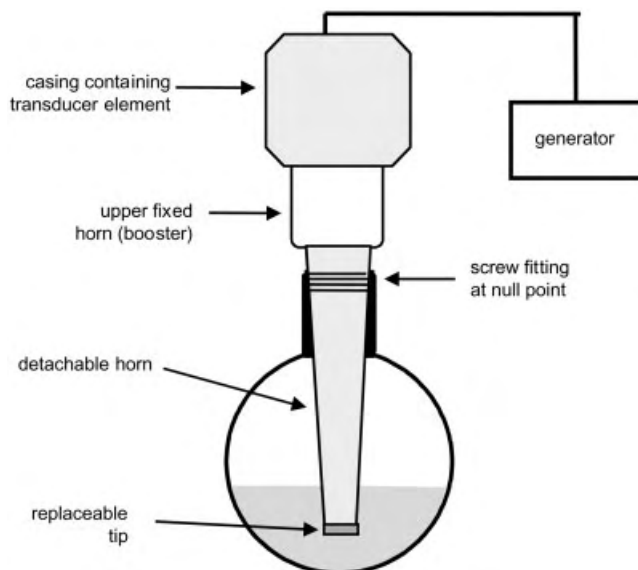


Fig. 7.10. The ultrasonic probe system.

velocity transformer. The material used for the fabrication of acoustic horns should have high dynamic fatigue strength, low acoustic loss, and resistance to cavitation erosion and chemical inertness. The most suitable material by far is titanium alloy.

7.2.4.1 Horn Design

Length

The wavelength of ultrasound in a material is determined by both the type of material and the frequency of the sound wave. In the case of the type of titanium alloy used for horns the wavelength for 20 kHz sound is about 26 cm and this defines absolutely the longitudinal dimension of titanium horns. Horns can be as short as half a wavelength but should the distance between the transducer and the sample being processed need to be increased, they can be designed in multiples of half wavelengths. This can also be achieved by screwing one horn into the other thereby building up the overall length.

Shape

A selection of differently shaped horns are shown in (Fig. 7.11).

Stepped

If a horn is fashioned in the shape of a uniform cylinder approximately 13 cm long and subjected to ultrasonic vibrations of frequency 20 kHz at one end there will be an exactly equal vibration produced at the other end. However there will be no vibration at the midpoint of the cylinder because this is the nodal point of the wave. If the cylinder was to be reduced in diameter at its midpoint to 0.5 of the original cross-sectional area then when vibrational energy is applied to the larger end the smaller end would automatically be subject to a doubling of energy density (energy applied at larger end now emerging through half the area at the smaller end). In order to deliver this increased intensity the tip, whose vibrational frequency is fixed at 20 kHz, must vibrate at an increased amplitude – hence the horn is behaving as a “velocity amplifier”. For a simple “stepped” design the amplification factor will always be the ratio of the cross sectional areas and such horns will easily accommodate gains of up to 16-fold.

The significance of the position at which the “step” is placed should be appreciated. It is always at the nodal point of the horn because at this point there is zero vibration (i. e. no stress). If the size reduction is not precisely at this null point stress will develop at this point. Fortunately however titanium has high tensile strength and so small errors in the position of constriction can be accommodated.

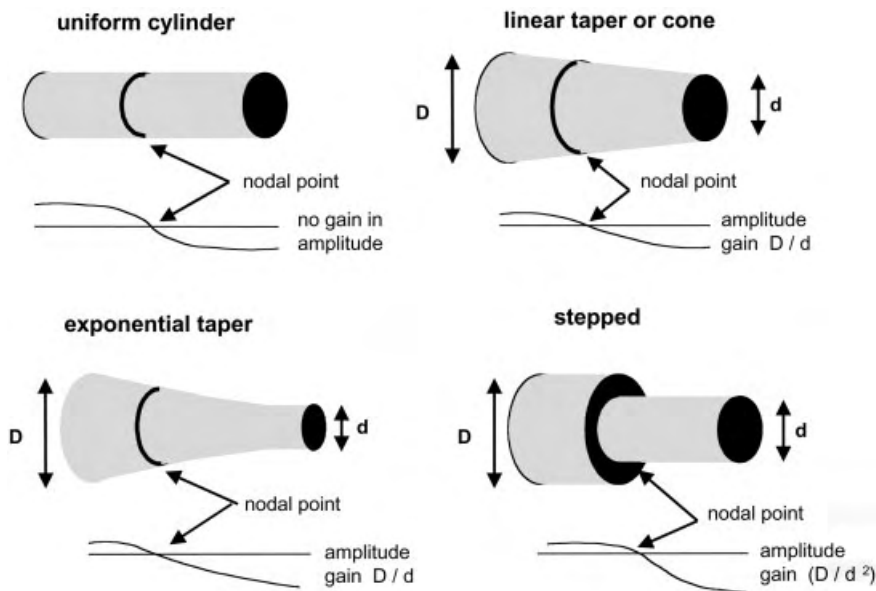


Fig. 7.11. The shapes of acoustic horns and magnification factors.

Linear and exponential taper

These designs avoid the possible stress developed in stepped horns. The amplification factor for either a linear or an exponential horn is the ratio of the end *diameters* (not areas as with stepped). The linear taper is the easier design to manufacture but its potential magnification is normally restricted to a factor of approx. 4-fold. The exponential taper offers higher magnification factors than the linear taper. Its shape makes it more difficult to manufacture but the small diameter of the working end and its length make it particularly suited to micro applications.

For the probe system, whatever design of horn is used, a large maximum power density can be achieved at the radiating tip. This can be of the order several hundred W cm^{-2} . The working frequencies are normally of the order 20–40 kHz. A number of probe devices are commercially available and, up to a few years ago (before the advent of sonochemistry) were referred to as cell disrupters. The majority operate at 20 kHz and utilise a wide range of different metal probes. The advantages of the probe method of energy input are threefold:

- Much higher ultrasonic powers can be used since energy losses during the transfer of ultrasound through the bath media and reaction vessel walls are eliminated.
- These devices can be tuned to give optimum performance in the reaction mixture for a range of powers.
- The ultrasonic intensity and size of sample to be irradiated can be matched fairly accurately for optimum effect.

However the probe, like the bath, does suffer from the same difficulty with respect to temperature control. This problem has been alleviated to some extent in modern instruments by the incorporation of a pulse mode of operation. Quite simply this consists of a timer attached to the amplifier which switches the power to the probe on and off repeatedly. The “off” time allows the system to cool between the pulses of sonication. The “on” time is represented as a fraction of the total time involved in the cycle (about 1 s) i.e. 100 % is continuous sonication while 50 % represents 0.5 s bursts of power every 0.5 s.

This type of pulse operation should not be confused with “duty cycle” as used in medical ultrasound. In medical parlance the duty cycle refers to the on/off ratio for scanning which involves the emission of pulse of extremely short duration (e.g. 10^{-5} seconds) involving only a few cycles of ultrasound in the MHz range. It is in the longer off period that the echoes are detected. By way of contrast a chemical sonicator pulse of 0.5 s involves 10 000 cycles at 20 kHz.

7.2.5

Laboratory Scale Reactors Involving Probe Systems

Although it is possible to simply dip the probe into a chemical reaction contained in a standard round bottomed flask or even a beaker, chemical reactions often require vapour tight apparatus, the slow addition of reagents or inert atmospheres. To cater for these constraints sonochemical apparatus has been developed and some of the simpler types are described below.

A so-called Rosett cell can be fitted with a flanged lid (Fig. 7.12). The design of the Rosett cell allows the irradiated reaction mixture to be sonically propelled from the end of the probe around the loops of the vessel and thus provides both cooling (when the vessel is immersed in a thermostatted bath) and efficient mixing. A PTFE sleeve provides a vapour tight fit between the probe and the glass joint.

As an alternative to this an ordinary reaction vessel can be adapted for sonic mixing by providing an indentation on its base to disperse the sonic waves as they are reflected from the base (Fig. 7.13).

In situations where elevated pressures need to be used a useful reactor has been described by Suslick (Fig. 7.14) [10].

A limitation of the reactors described above is that they are of the batch type. A favourite method of avoiding this is to use a flow-cell in a continuous or circulating system (Fig. 7.15).

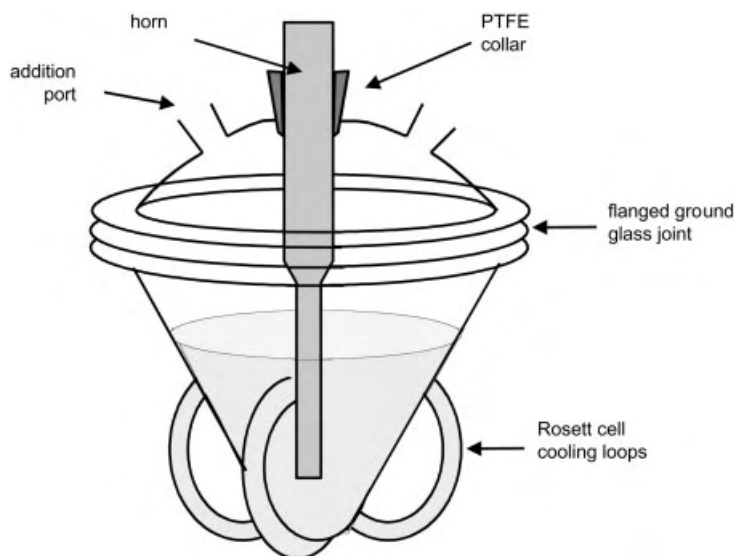


Fig. 7.12. Rosett cell.

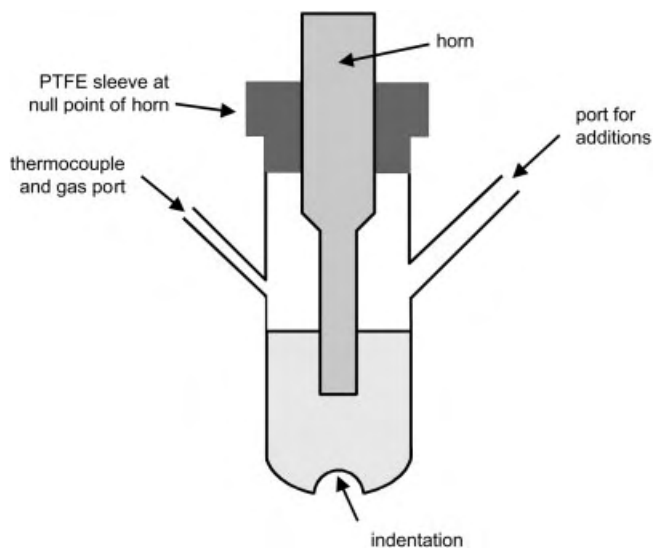


Fig. 7.13. Dimple cell.

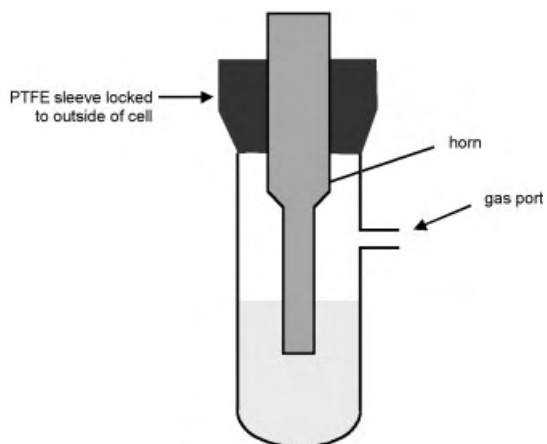


Fig. 7.14. Simple pressure cell.

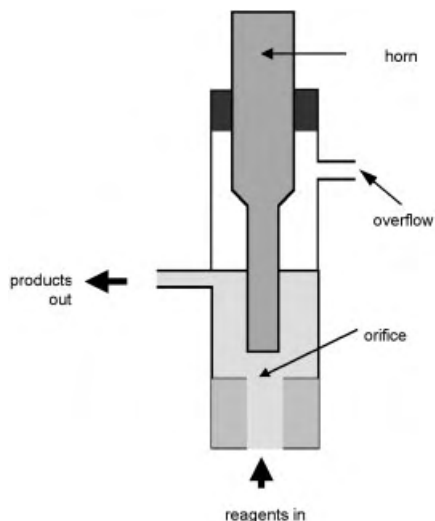


Fig. 7.15. Flow cell.

Although the use of a probe provides several advantages over the use of baths (*vide supra*), they do suffer from a common disadvantage – they are only capable of operating at single fixed frequency. There are however two additional problems peculiar to probe systems:

1. with direct sonication it is possible to generate radical species by the action of the probe tip on the solvent and
2. with prolonged use some erosion of the tip occurs which may mean contamination of the reaction under study by small metallic particles.

An apparatus which avoids tip erosion while still achieving the controllable power of a probe is the cup-horn (Fig. 7.16). This can be regarded as a small bath into which can be placed the vessel containing the reaction to be sonicated. Originally designed for controlled cell disruption, the use of such a system permits a more quantitative and reproducible study of sonochemical effects than either the cleaning bath or the probe system. The frequency is fixed but the power is tuneable and, unlike the direct immersion sonic horn, no fragments of metal are generated in the reaction itself.

The major disadvantages of the cup-horn are:

- a reduction in power compared with the direct immersion sonic horn and
- a restriction in size of the reaction vessel which can be placed inside the cup horn.

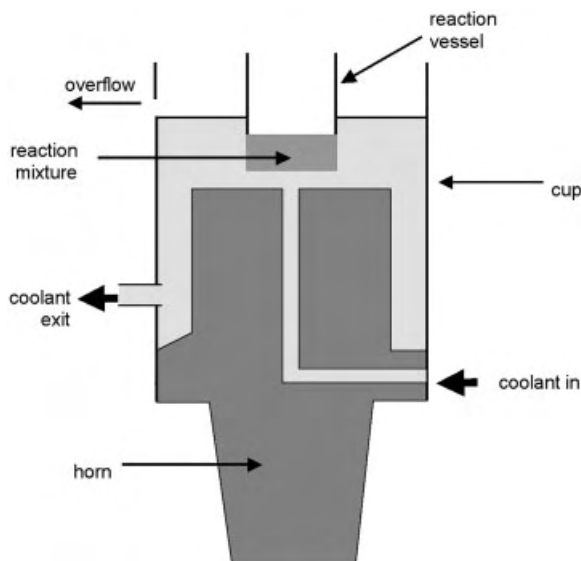


Fig. 7.16. The cup-horn.

7.3

Large Scale Applications

Solutions to the problem of the scale-up of sonochemical reactions do exist but they are not so simple as the use of bigger versions of laboratory equipment. In a production situation the volumes treated will be very much larger than those considered in the laboratory and the type of process will govern the choice of reactor design. It could well be that some processes would be more suited to low intensity sonication (e. g. using a bath type reactor) whereas others may need higher intensity irradiation (*via* a probe type system).

7.3.1

Whistle Systems

Reference has been made already to the use of whistle reactors for homogenisation. This system is already available for large scale processing since it is practical, robust and durable. It is ideal for liquid processing as long as the liquid can be pumped through the whistle at a sufficiently rapid rate. It can also be used for heterogeneous solid/liquid systems to deagglomerate material and cause extremely efficient mixing.

The production of polymeric resins involves heating acids and glycols to a high temperature then adding styrene as the temperature is reduced. It is the styrene which takes part in curing when the activator is added. In a process developed by Scott Bader at Wellingborough in the UK, the styrene is added and mixed with a traditional stirrer. After this stage some pyrogenic silica is stirred into the resin (the quantity depending upon the desired final specification of the resin). In order to obtain product uniformity it is now necessary to produce a completely even dispersion of the silica throughout the medium. This is achieved by passing the pre-mix through an ultrasonic homogeniser which is of the whistle type and capable of handling 12 000 L/h. This disperses the solid as a fine powder throughout the resin. The procedure ensures the correct thixotropic characteristics of each type of resin. Using this process, Scott Bader has been able to reduce the amount of pyrogenic silica required by some 40 % compared with conventional methodology. This obviously makes a considerable saving of a very expensive ingredient.

The underlying mode of action, involving as it does the flow induced vibration of a steel blade, immediately suggests the problem of erosion by particulate matter – the sand blasting effect. Despite this apparent drawback a whistle has been used in this Scott Bader process over several years without blade replacement.

7.3.2

Low Intensity Systems

In cases where low intensity irradiation is needed batch treatment could be as simple as using a large-scale ultrasonic cleaning bath as the reaction vessel. However the tank would need to be constructed of a material which was inert towards the chemicals involved. An appropriate grade of stainless steel might prove adequate or plastic tanks could be used. In the latter case however the transducer would need to be bonded onto a stainless or titanium plate and this assembly then bolted to the tank. A useful variant to this and indeed one which offers greater flexibility in use is the sealed, submersible transducer assembly (Fig. 7.17). With either system some form of additional (mechanical) stirring would almost certainly be needed.

Bath type reactors may also be used in a flow system. In this case the reacting liquids could be continuously fed into an ultrasonic tank with outflow over a weir to the next process. Such treatment could be intensified by recycling or by connecting a number of such sonicated tanks in line.

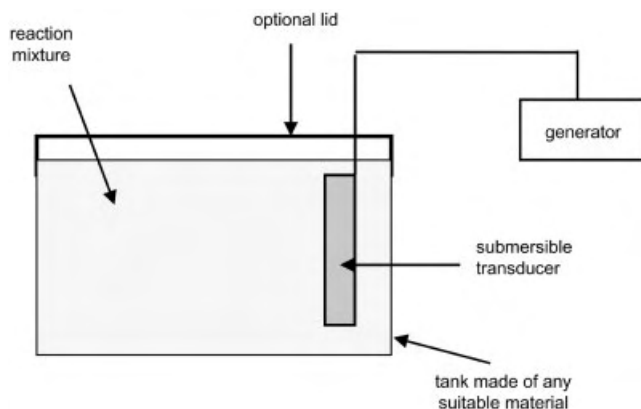


Fig. 7.17. Tank with submersible transducer assembly.

7.3.3

High Intensity Systems

One might expect that flow cells would be favourite for high intensity treatment of large volumes. The simple flow cell (Fig. 7.15) is an excellent means of processing relatively large volumes in a laboratory situation.

An alternative arrangement would involve a number of probes inserted through the walls of a vessel allowing a much larger sonochemical treatment zone. Such a system will suffer from the same problems as the individual flow cell except that it will continue to function even if one or two probe units fail (Fig. 7.18).

As an alternative to high power probe inserts it is also possible to use an array of transducers slotted into a plastic tube. In such a system the metal transducer face is emitting the energy and the plastic is simply providing the supporting tube. This is the approach used for the disintegration of sewage sludges with dry solid contents between 0.5 and 4% [11]. A reactor module was built using HDPE (high-density polyethylene) with a square channel (48×48 mm) with an overall length of 700 mm. This plastic was chosen for its high resistance to chemicals, low water absorption and also because it is highly impervious to water vapour and resistant to stress cracks. Some 60 transducers are used (15 transducers each 31 kHz on each face) affording an overall power of around 3.6 kW providing an acoustic intensity of about 7.5 W cm^{-2} in flow-through mode with a reactor volume of 1.6 L. The emitting face of each transducer is titanium in order to minimise wear and reduce chemical reactions at the liquid interface. In order to achieve uniform sonication the transducers are arranged in a spiral configuration. This is achieved by placing the transducers, in sequence on each face at

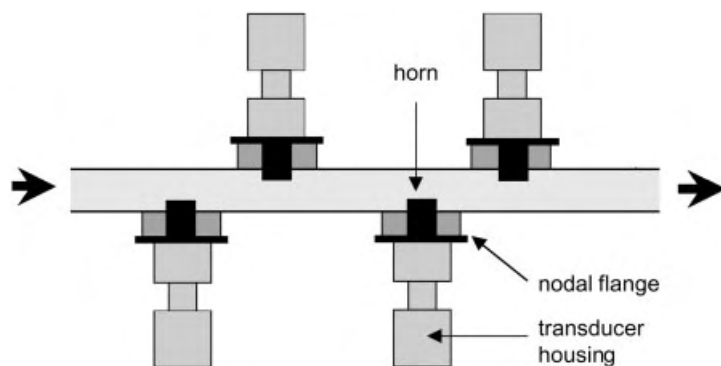


Fig. 7.18. Reaction tube with probe inserts.

a height difference of one quarter of the transducer diameter (Fig. 7.19). Using eight modules in series the treatment capacity lies between 0.2 and $2.5 \text{ m}^3 \text{ h}^{-1}$. The method of mounting transducers in different planes was first suggested as a means of producing focal ultrasound fields with spiral-shaped wave fronts [12].

If transducers are fixed to the external surface of a tube then the tube itself becomes the source of ultrasonic energy. The liquid to be processed can then be passed through the tube and receive sonication directly from the ultrasonically vibrating walls. Two design engineering problems are associated with this type of sonicator (1) the correct mounting of the transducers on the outer tube and (2) the length of the tube must be

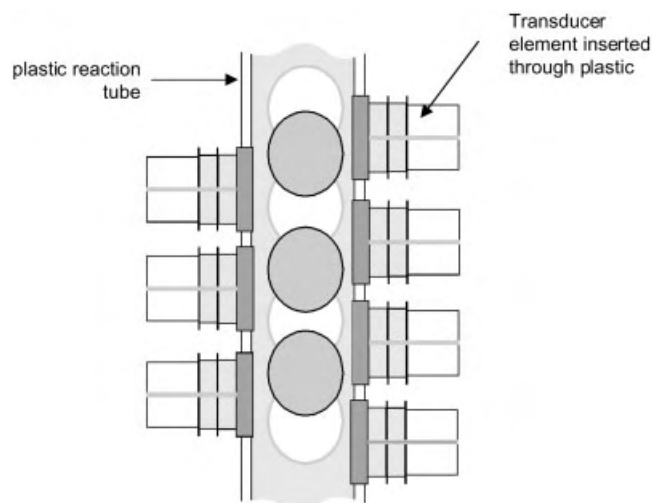


Fig. 7.19. Reaction tube with transducer inserts in a spiral configuration.

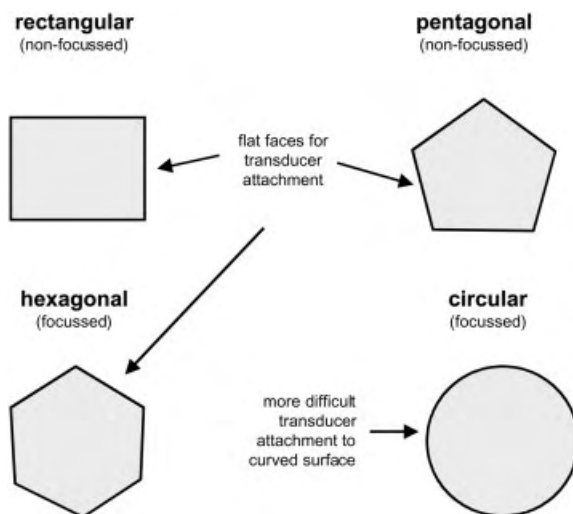


Fig. 7.20. Possible cross-section shapes for flow processors.

such that the ends are at a null point in the sound wavelength in the unit. This will eliminate vibrational problems associated with the coupling of the unit to existing pipework. The choices for pipe cross-section are generally one of four (Fig. 7.20) but in practice the current choices are predominantly rectangular or circular.

The vibrating faces are opposite each other in the rectangular cross-section geometry and so the possibility exists for the severe erosion of these faces. For this reason the design of such apparently simple flow reactors must be handled with care. Unless the pipe is seamless then high-powered ultrasonic vibration is also likely to find any weaknesses in the welded construction, particularly at corner joints.

To avoid this problem and to provide high power acoustic energy in a flowing system a parallel plate reactor has been developed by the Lewis Corporation in the U.S.A. and is known as the Nearfield Acoustic Processor or NAP (Fig. 7.21) [13]. This system can be visualised as two sonicated metal plates which enclose a flow system. In effect the plates can be regarded as the bases of two ultrasonic baths facing toward each other and separated by only a few centimetres. Under these conditions any liquid flowing between the plates is subject to an ultrasonic intensity greater than that expected from simple doubling of a single plate intensity. The ultrasound “reverberates” and is magnified in its effect. Already used for applications such as particle size reduction and the extraction of oil from oil shale it is clearly but a short step to using this system for chemistry. An additional benefit is that with vibrating plates the size of table tops the system can cope with very large throughputs of material.

To make a permanent bond for a high power transducer to the curved surface of a flow reactor of cylindrical cross-section is not as easy as to a flat surface but several

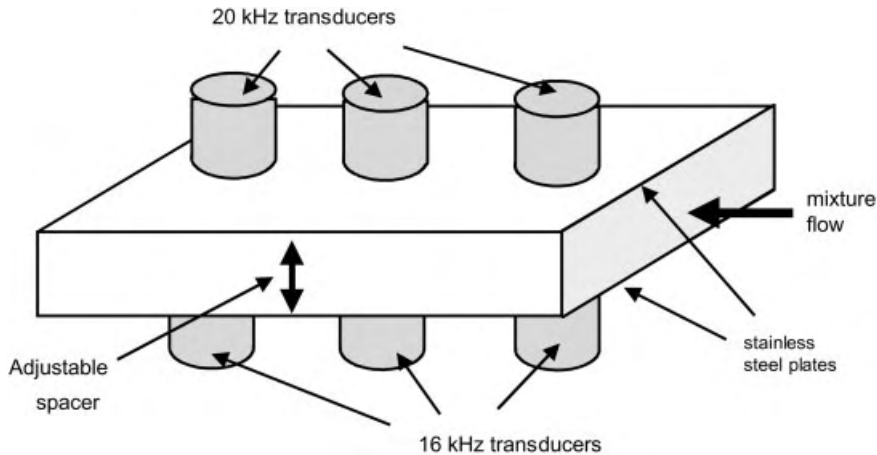


Fig. 7.21. Nearfield Acoustic Processor (NAP).

examples of this design exist. One important feature of the geometry of the tubular configuration is the intensification effect. When the walls are subjected to ultrasonic vibration the inner surface focuses the ultrasonic energy toward the middle of the tube. A resonating pipe of 6 inch diameter operating at 25 kHz has been developed and installed on offshore oil drilling rigs for the deagglomeration of drilling mud (Fig. 7.22) [14]. This process is required so that the jettisoned muds disperse with the movement of the sea and do not simply sink to the seabed under the platform. Accumulations of mud around the platform legs present a problem to sea life and eventually rig maintenance.

A neat method of introducing ultrasound into a medium flowing through a tube is via the coaxial insertion of a radially emitting bar into a pipe containing the flowing liquid. The vibrational energy is transferred from the longitudinal mode oscillations of a transducer at one end to vibrational motion directed perpendicular to the surface of the tube (radial). A number of systems are available for this purpose [15]. Two are illustrated a hollow tube driven by a single transducer (Telsonic tubular resonator) and a solid tube driven by a transducer at each end (Martin Walter Push-Pull system) (Fig. 7.23). In each case the tube is the source of radial ultrasound at half-wave-length distances along its length.

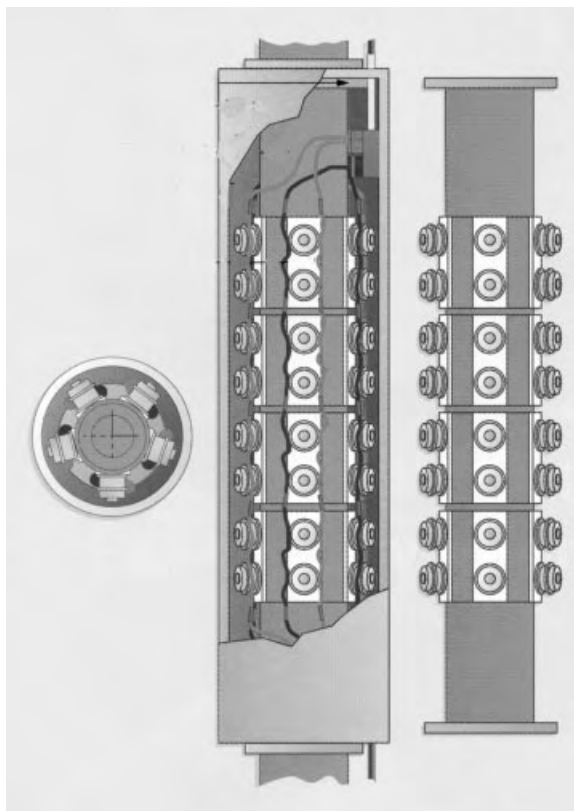


Fig. 7.22. Cylindrical tube processor with externally bonded transducers.

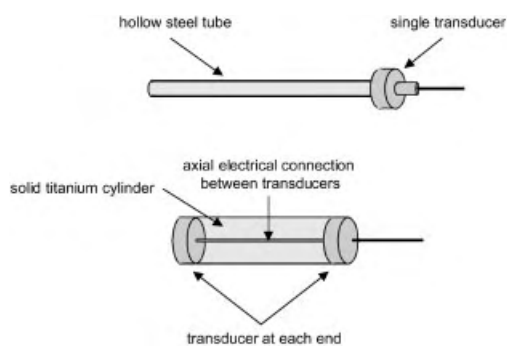


Fig. 7.23. Radial ultrasonic emitters for insertion in flow reactors.

References

1. F. Galton, *Inquiries into Human Faculty and Development*, MacMillan, 1883.
2. J.R. Frederick, *Ultrasonic Engineering*, John Wiley, 1965, Ch. 4.
3. J. Curie and P. Curie, *Compt. Rend.*, 1880, **91**, 294.
4. J.P. Joule, *Phil. Mag.*, 1847, **30**, 46.
5. J.P. Russell and M. Smith, Sonic energy in processing: Use of a large scale, low frequency sonic reactor, *Advances in Sonochemistry*, T.J. Mason (ed.), JAI Press, Stamford, USA, 1999, **5**, 279–302.
6. R.W. Wood and A.L. Loomis, *Phil. Mag.*, 1927, **4**, 417.
7. W. Janovski and R. Pohlmann, *Z. Angew. Phys.*, 1948, **1**, 22.
8. R.E. Singiser and H.M. Beal, *J. Am. Pharm. Assoc., (Scient. Ed.)*, 1960, **49**, 482.
9. R.S. Davidson, A. Safdar, J.D. Spencer, and D.W. Lewis, *Ultrasonics*, 1987, **25**, 35.
10. K.S. Suslick and R.E. Johnson, *J. Am. Chem. Soc.*, 1984, **106**, 6856.
11. D. Schneider, Construction of a high performance reactor, *Ultrasound in Environmental Engineering*, A. Tiehm and U. Neis (eds.), TUHH Reports on Sanitary Engineering, 1999, **25**, 101.
12. K. Kawabata and S. Umemura, *Ultrasonics*, 1993, **31**, 457.
13. R.L. Hunicke, *Ultrasonics*, 1990, **28**, 291.
14. N. Avern and P.A. Copernici, *World Oil*, 1997, 75.
15. T.J. Mason, *Sonochemistry*, Oxford University Primer Series No 70, Oxford Science Publications, 1999.